U.S. Department
of Commerce

Volume 114
Number 2
April 2016

Fishery Bulletin

Pacific Islands Fisheries
Science Center Library

Received on: 5/5/2016

U.S. Department of Commerce
Penny S. Pritzker
Secretary

National Oceanic and Atmospheric Administration
Kathryn D. Sullivan
NOAA Administrator

National Marine Fisheries Service
Eileen Sobeck
Assistant Administrator for Fisheries

The *Fishery Bulletin* (ISSN 0090-0656) is published quarterly by the Scientific Publications Office, National Marine Fisheries Service, NOAA, 7600 Sand Point Way NE, Seattle, WA 98115-0070.

Although the contents of this publication have not been copyrighted and may be reprinted entirely, reference to source is appreciated.

The Secretary of Commerce has determined that the publication of this periodical is necessary according to law for the transaction of public business of this Department. Use of funds for printing of this periodical has been approved by the Director of the Office of Management and Budget.

For Sale by the Superintendent of Documents, U.S. Government Printing Office, Washington, DC 20402. Subscription price per year: $32.00 domestic and $44.80 foreign. Cost per single issue: $19.00 domestic and $26.60 foreign. **See back for order form.**

Fishery Bulletin

Scientific Editor
Richard Langton

National Marine Fisheries Service
Northeast Fisheries Science Center
Maine Field Station
17 Godfrey Drive, Suite 1
Orono, ME 04473

Managing Editor
Sharyn Matriotti

National Marine Fisheries Service
Scientific Publications Office
7600 Sand Point Way NE
Seattle, Washington 98115-0070

Associate Editor
Kathryn Dennis

National Marine Fisheries Service
Office of Science and Technology
1845 Wasp Blvd., Bldg. 176
Honolulu, Hawaii 96818

Editorial Committee

Richard Brodeur	National Marine Fisheries Service, Newport, Oregon
John Carlson	National Marine Fisheries Service, Panama City, Florida
Kevin Craig	National Marine Fisheries Service, Beaufort, North Carolina
John Graves	Virginia Institute of Marine Science, Gloucester Point, Virginia
Rich McBride	National Marine Fisheries Service, Woods Hole, Massachusetts
Rick Methot	National Marine Fisheries Service, Seattle, Washington
Bruce Mundy	National Marine Fisheries Service, Honolulu, Hawaii
David Sampson	Oregon State University, Newport, Oregon
Michael Simpkins	National Marine Fisheries Service, Woods Hole, Massachusetts
Dave Somerton	National Marine Fisheries Service, Seattle, Washington
Mary Yoklavich	National Marine Fisheries Service, Santa Cruz, California

***Fishery Bulletin* web site: www.fisherybulletin.noaa.gov**

The *Fishery Bulletin* carries original research reports on investigations in fishery science, engineering, and economics. It began as the Bulletin of the United States Fish Commission in 1881; it became the Bulletin of the Bureau of Fisheries in 1904 and the *Fishery Bulletin* of the Fish and Wildlife Service in 1941. Separates were issued as documents through volume 46; the last document was no. 1103. Beginning with volume 47 in 1931 and continuing through volume 62 in 1963, each separate appeared as a numbered bulletin. A new system began in 1963 with volume 63 in which papers are bound together in a single issue. Beginning with volume 70, number 1, January 1972, *Fishery Bulletin* became a periodical, issued quarterly. In this form, it is available by subscription from the Superintendent of Documents, U.S. Government Printing Office, Washington, DC 20402. It is also available free in limited numbers to libraries, research institutions, state and federal agencies, and in exchange for other scientific publications.

U.S. Department of Commerce
Seattle, Washington

Volume 114
Number 2
April 2016

Fishery Bulletin

Contents

Short contribution

135–143 **Watson, William, Sharon R. Charter, and Cynthia A. Taylor Lawley**

Early larvae of the swordspine rockfish (*Sebastes ensifer*) identified by molecular methods

Articles

144–152 **Tagliafico, Alejandro, Nicolás Ehemann, María Salomé Rangel, and Néstor Rago**

Exploitation and reproduction of the bullnose ray (*Myliobatis freminvillei*) caught in an artisanal fishery in La Pared, Margarita Island, Venezuela

153–165 **Lewis, Leah A., David E. Richardson, Evgeny V. Zakharov, and Robert Hanner**

Integrating DNA barcoding of fish eggs into ichthyoplankton monitoring programs

166–178 **Lopez, Jon, Gala Moreno, Guillermo Boyra, and Laurent Dagorn**

A model based on data from echosounder buoys to estimate biomass of fish species associated with fish aggregating devices

179–185 **Demetras, Nicholas J., David D. Huff, Cyril J. Michel, Joseph M. Smith, George R. Cutter, Sean A. Hayes, and Steven T. Lindley**

Development of underwater recorders to quantify predation of juvenile Chinook salmon (*Oncorhynchus tshawytscha*) in a river environment

186–202 **Mathews, Elizabeth A., Laura A. Jemison, Grey W. Pendleton, Karen M. Blejwas, Kevin E. Hood, and Kimberly L. Raum-Suryan**

Haul-out patterns and effects of vessel disturbance on harbor seals (*Phoca vitulina*) on glacial ice in Tracy Arm, Alaska

The National Marine Fisheries Service (NMFS) does not approve, recommend, or endorse any proprietary product or proprietary material mentioned in this publication. No reference shall be made to NMFS, or to this publication furnished by NMFS, in any advertising or sales promotion which would indicate or imply that NMFS approves, recommends, or endorses any proprietary product or proprietary material mentioned herein, or which has as its purpose an intent to cause directly or indirectly the advertised product to be used or purchased because of this NMFS publication.

The NMFS Scientific Publications Office is not responsible for the contents of the articles.

203–219 **Yasumiishi, Ellen M., Keith R. Criddle, John H. Helle, Nicola Hillgruber, and Franz J. Mueter**

Effect of population abundance and climate on the growth of 2 populations of chum salmon (*Oncorhynchus keta*) in the eastern North Pacific Ocean

220–236 **Contente, Riguel F., and Carmen L. D. B. Rossi-Wongtschowski**

Fish assemblages on the southeastern Brazilian Bight, sampled by midwater trawl during spring and summer seasons: species composition, abundance, and environmental drivers

237–256 **Weijerman, Mariska, Ivor Williams, Jay Gutierrez, Shanna Grafeld, Brent Tibbatts, and Gerry Davis**

Trends in biomass of coral reef fishes, derived from shore-based creel surveys in Guam

257–260 **Guidelines for authors**

NOAA
National Marine
Fisheries Service

Fishery Bulletin
established 1881

Spencer F. Baird
First U.S. Commissioner
of Fisheries and founder
of *Fishery Bulletin*

Early larvae of the swordspine rockfish (*Sebastes ensifer*) identified by molecular methods

William Watson (contact author)[1]
Sharon R. Charter[1]
Cynthia A. Taylor Lawley[1, 2]

Email address for contact author: william.watson@noaa.gov

[1] Southwest Fisheries Science Center
National Marine Fisheries Service, NOAA
8901 La Jolla Shores Drive
La Jolla, California 92037-1508

[2] Scripps Institution of Oceanography
University of California, San Diego
9500 Gilman Drive, Mail Code 0203
La Jolla, California 92093-0203

Abstract—About 56 rockfish (*Sebastes*) species occur in Southern California, but the larvae of most of them are undescribed. Larval rockfishes collected off Southern California during the California Cooperative Oceanic Fisheries Investigations (CalCOFI) cruise in April 1999 and the Baseline Cowcod Conservation Area (CCA) cruise in February 2002 were identified by using mitochondrial cytochrome *b* genomic DNA to determine the abundances of individual species. About 27% of the larvae from the CalCOFI cruise and 16% of the larvae from the CCA cruise were *Sebastes ensifer*. Larval *S. ensifer* were undescribed for most of the size range identified here (2.6–8.4 mm, early preflexion through early postflexion stage). Larval S. ensifer are moderately deep-bodied and robust and have melanophores dorsally and ventrally on the gut, in a single ventral row on the tail, and on the pectoral fins. Starting at about 3.8 mm, melanophores form on the anterior part of the mandible. Larvae ≥6 mm have pigment in the mid- and hindbrain areas. Preflexion-stage larval *S. ensifer* are indistinguishable from the described larvae of sympatric species in the *Sebastes* subgenus *Sebastomus*, except perhaps *Sebastes rosaceus* and *S. umbrosus*. In later stages, *S. ensifer* may be distinguishable from *S. constellatus* and *S. helvomaculatus*.

Manuscript submitted 25 February 2015.
Manuscript accepted 16 December 2015.
Fish. Bull. 114:135–143 (2016).
Online publication date: 21 January 2016.
Doi: 10.7755/FB.114.2.1

The views and opinions expressed or implied in this article are those of the author (or authors) and do not necessarily reflect the position of the National Marine Fisheries Service, NOAA.

The rockfish genus *Sebastes* includes about 72 species in the eastern North Pacific Ocean; approximately 56 of these species occur in the Southern California Bight (Eschmeyer et al., 1983; Kendall, 1991), and many are important in sport and commercial fisheries (e.g., Lenarz, 1987; Leet et al., 1992, 2001). The swordspine rockfish, *Sebastes ensifer* Chen, 1971, is an abundant, small species (total length to about 25–30 cm) that ranges from northcentral California to the central Baja California Peninsula, Mexico (Love et al., 2002). Although not a preferred fishery species owing to its small size, *S. ensifer* contributes moderately to recreational fishery catches because of its abundance, and it is sold in Asian fish markets (Love et al., 2002).

Sebastes are live-bearers, and larvae are readily obtained from pregnant females and occur commonly in plankton samples, particularly during late winter and spring (Moser et al., 1993). Owing to this availability and to the use of larvae in providing fishery-independent estimates of spawning biomass (e.g., Moser and Butler, 1987; Moser et al., 2000; Ralston et al., 2003; Ralston and MacFarlane, 2010), considerable effort has been directed toward improving our ability to identify *Sebastes* larvae (Kendall, 1991; Moser, 1996b). However, the larvae are difficult to rear (e.g., Kendall, 1991), and there is considerable overlap among species in meristic, morphological, and pigment characters (Moser, 1996b). Therefore, to date, field-collected larvae of only 7 of the species that occur off Southern California have been visually identified with certainty (Moser et al., 2000).

Larvae of *S. ensifer*, a member of the Sebastes subgenus *Sebastomus*, are not readily identifiable. Differences among larvae of *Sebastomus* species are quite small (e.g., Moser, 1996b; Rocha-Olivares, 1998; Rocha-Olivares et al., 2000), and currently larvae of none of these species can be reliably identified with traditional morphological and pigment characters. Complete larval development for any *Sebastomus* species is still unknown; to date, extrusion larvae are known for 7 of the 15 species, and some later stages are known for 4 species, including the

cape redfish (*S. capensis*) of the Southern Hemisphere (e.g., Westrheim et al.[1]; Moser, 1967; Moser et al., 1977; Richardson and Laroche, 1979; Moser and Butler, 1987; Matarese et al., 1989; Sabatés and Olivar, 1990; Moser, 1996b; Rocha-Olivares et al., 2000). Larvae of another species, probably buccaneer rockfish (*S. exsul*) or spiny-eye rockfish (*S. spinorbis*), have been described through the postflexion stage (Moser et al., 1977). Early development of *S. ensifer* is known only from newly extruded larvae (Moser, 1967) and from large, transforming larvae (≥19.8 mm standard length) and pelagic juveniles (Rocha-Olivares et al., 2000). The purpose of this article is to describe external morphology and pigmentation of larval *S. ensifer* from the early preflexion stage through the early postflexion stage, nearly the full developmental range not previously described in the literature and a range that encompasses most of the rockfish larvae routinely collected in standard plankton tows (e.g., Moser, 1996b).

Materials and methods

This study was based on plankton samples collected with a bongo sampler that was equipped with 0.505-mm mesh nets and a flowmeter and towed obliquely through the upper 212 m of the water column during the quarterly California Cooperative Oceanic Fisheries Investigations (CalCOFI) survey in April 1999 (Ambrose et al., 2001) and during the Baseline Cowcod Conservation Area (CCA) survey in February 2002, both conducted in the Southern California Bight. Details of the CalCOFI sampling area, gear, and methods are available in the literature (Kramer et al., 1972; Ohman and Smith, 1995). Standard CalCOFI protocol was followed for collection of plankton in the CCA with the bongo sampler. A minor protocol revision, instituted in 1997, was the preservation of the sample from the port net of the bongo sampler in 95% tris-buffered ethanol to facilitate aging and genetics studies of selected species. All fish larvae were sorted from the ethanol-preserved samples, retained in 95% ethanol, and archived pending analysis.

Eight ethanol-preserved larval specimens of the genus *Sebastes* (4.1–8.4 mm, preflexion through early postflexion stage) from the CalCOFI survey were assigned tentatively to a unique unidentified type on the basis of similarities in morphological features and pigmentation pattern. All specimens were relatively robust; in specimens ≥6 mm long, there were large parietal and preopercular spines and melanophores on the lower jaw, on the margins of the pectoral fins, and on the ventral margin of the tail but they were absent on the upper jaw and snout and dorsally and laterally on the trunk and tail. Before molecular analysis, all 8 larvae were examined with a Wild M5 Stereomicroscope[2] (Wild Stereo Microscopes, now manufactured by Leica Microsystems Inc., Buffalo Grove, IL) equipped with an ocular micrometer, and the larvae best representative of a developmental sequence (Fig. 1) were drawn with the use of a camera lucida and the Wild microscope.

Pigmentation patterns, counts of myomeres, head spines, and fin rays, and various measurements were recorded. These measurements, including body length (BL), preanal length, head length (HL), snout length, length of the pectoral-fin blade, eye diameter, and body depth, are defined in Moser (1996a). Descriptions of body proportions (e.g., "short preanal length") follow those of Leis and Carson-Ewart (2000). Spines measured include the preopercular (APO1–4 and PPO2–4), parietal, nuchal, pterotic, postorbital, first lower infraorbital, and posttemporal. Spine terms follow those of Moser and Ahlstrom (1978). Larval lengths refer to BL of ethanol-preserved larvae, and descriptions of pigmentation refer to melanistic pigment. No adjustments were made in the measurements to account for shrinkage of the preserved larvae; larval fish shrinkage in ethanol, typically in the range of about 3–6%, has been reported in the literature (e.g., Theilacker, 1980; Porter et al., 2001; Moku et al., 2004; Fey and Hare, 2005).

All unidentified ethanol-preserved larvae of *Sebastes* from the CalCOFI cruise, including the descriptive series, were identified by using mitochondrial cytochrome *b* genomic DNA extracted from caudal-fin or muscle tissue as described by Taylor et al. (2004). Primers included GluRF and CB3RF (from Rocha-Olivares et al., 1999) and internal custom primers (CB306F 5′-TTACTACGGCTCVTACCT-3, Cb521R 5′-GTTGCATTGTCTACTGAG-3′ and CB364F, 5′-CTAGTTATAATAACTGCTTT-3′).

After molecular identifications of the *Sebastes* larvae from the CalCOFI survey were completed, identifications of larvae from the CCA cruise began, and it soon became apparent that an appreciable fraction of those larvae were *S. ensifer*. We decided to include specimens from both surveys to base the description of larval development on a larger sample size: the 8 CalCOFI larvae plus 41 larvae from the CCA survey were used for the full description, and another 36 larvae from the CCA survey supplemented the description of larval pigmentation. During the interval between completion of analysis of the CalCOFI sample set and the beginning of analysis of the CCA sample set, improvements were made to the chelex extraction and PCR protocols. Therefore, for larvae collected during the CCA survey, the revised protocols described by Hyde et al. (2005) were used to extract mitochondrial cytochrome *b* genomic DNA from an eyeball or caudal muscle tissue. Primers included GluRF2 5′ AAC CAT CGT TGT TAT TCA ACT ACA AGA ACC and CB3RF2

[1] Westrheim, S. J., W. R. Harling, D. Davenport, and M. S. Smith. 1968. Preliminary report on maturity, spawning season and larval identification of rockfishes (Sebastodes) collected off British Columbia in 1968, 28p. Fish. Res. Board Can., Manuscr. Rep. Ser. 1005.

[2] Mention of trades names or commercial companies is for identification purposes only and does not imply endorsement by the National Marine Fisheries Service, NOAA.

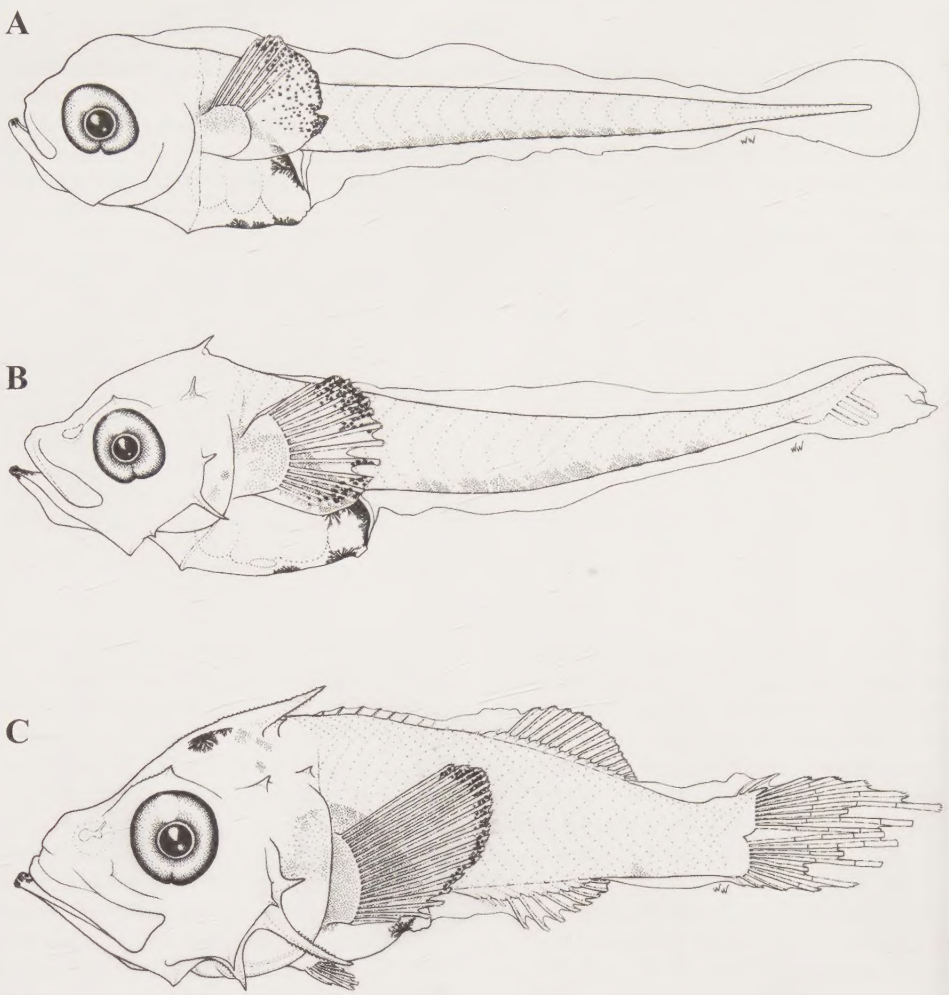

Figure 1

Larval swordspine rockfish (*Sebastes ensifer*) collected in the Southern California Bight during the California Cooperative Oceanic Fisheries Investigations survey during April 1999: (**A**) 4.4 mm (cruise 9904JD, station 90.30); (**B**) 6.2 mm (cruise 9904JD, station 90.53); (**C**) 7.7 mm (cruise 9904JD, station 90.37).

5′ CGA ACA GGA ART ATC AYT CTG G (Hyde and Vetter, 2009). In contrast to the protocols used for the CalCOFI specimens, this revised procedure provided a more robust amplification and saved both time and expense. Additionally, the use of only an eyeball, when possible, left the specimen otherwise intact for use in other studies.

Haplotype sequences from both the CalCOFI and CCA sample sets were compared with reference data of 374 independent haplotype sequences representing 67 *Sebastes* species (Hyde and Vetter, 2007) by using the software program PAUP*, vers. 4.0b10 (Sinauer Associates, Sunderland, MA; Swofford, 2000) with the optimality criterion set to distance (number of base-pair [bp] differences divided by total number of bp sequenced). Nonparametric bootstrapping was used (100 replications, MAXTREES set to 1000) to cluster each larval haplotype within a database of consensus haplotypes (i.e., most common haplotype from a database of known adults) for putative identification.

If the haplotype of a larva clustered with the single haplotype of a reference species with a bootstrap value ≥90%, the larva was identified as that species. Distances between reference haplotypes and the unknown were examined to confirm that the unknown fell within the intraspecific diversity as a secondary confirmation of identification. If a larva clustered with a single reference haplotype but the bootstrap value was <90%, a secondary analysis was performed that included all available haplotypes of at least the 3 nearest (in distance) species to the larval haplotype; the haplotype was identified by comparison with those of the reference species. Haplotype diversity for the reference species has a mean genetic distance of 0.0026 (correspond-

Table 1

Measurements of larval swordspine rockfish (*Sebastes ensifer*) collected in the Southern California Bight during the California Cooperative Oceanic Fisheries Investigations survey in April 1999 and Baseline Cowcod Conservation Area survey in February 2002, given as percentages of body length (BL): preanal length (PAL), body depth (BD), head length (HL), head width (HW), snout length (SnL), eye diameter (ED), length of the pectoral-fin blade (P_1L), and length of the pelvic fin (P_2L). For one specimen, an ED was not collected because the eyes were missing. *N*=number of specimens examined.

Stage	*N*	BL (mm)	PAL	BD	HL	HW	SnL	ED	P_1L	P_2L
Preflexion	2	2.6	39.0	20.6	21.9	9.2	3.6	9.6	6.9	0
Preflexion	3	2.8	39.5	19.9	21.7	8.6	5.0	9.3	7.1	0
Preflexion	2	2.9	39.5	18.4	19.5	9.0	5.5	8.6	5.5	0
Preflexion	3	3.0	36.4	18.6	18.3	7.4	5.2	9.9	5.6	0
Preflexion	3	3.1	34.4	17.8	21.3	10.0	6.5	9.5	8.8	0
Preflexion	3	3.2	35.2	18.1	21.8	8.2	5.6	8.8	6.7	0
Preflexion	3	3.3	34.3	19.7	21.8	7.3	4.9	8.2	6.7	0
Preflexion	2	3.4	28.5	17.9	19.3	6.9	4.9	7.9	5.9	0
Preflexion	2	3.5	38.6	16.7	17.7	9.9	5.7	8.9	8.4	0
Preflexion	3	3.6	35.0	18.9	17.1	8.9	6.5	9.4	6.9	0
Preflexion	1	3.8	41.3	21.1	27.6	11.3	8.2	–	9.7	0
Preflexion	2	3.9	39.5	19.7	19.7	8.7	7.9	9.0	9.5	0
Preflexion	1	4.1	33.0	15.0	13.6	7.3	2.9	6.8	5.8	0
Preflexion	2	4.2	33.6	18.3	21.1	11.3	5.7	8.1	8.9	0
Preflexion	3	4.3	41.9	24.9	25.3	11.5	6.5	9.5	12.2	0
Preflexion	1	4.4	36.4	20.9	20.0	12.7	4.5	8.6	10.0	0
Preflexion	1	4.5	45.1	21.8	19.1	8.9	5.6	8.2	10.9	0
Preflexion	3	4.6	34.8	20.3	25.4	8.5	6.7	8.7	9.7	0
Preflexion	1	4.9	35.9	18.2	21.4	8.8	6.9	7.6	13.9	0
Preflexion	1	5.1	34.5	23.5	20.6	9.6	4.9	9.0	13.3	0
Preflexion	1	5.2	36.4	21.7	22.5	10.9	5.4	7.8	7.8	0
Preflexion	1	5.4	38.7	20.6	25.0	9.1	5.7	8.0	14.8	0
Preflexion	1	6.0	37.4	23.8	25.2	15.2	7.3	8.8	11.3	0
Preflexion	1	6.2	41.6	23.7	25.0	13.6	8.4	8.4	11.0	0
Postflexion	2	7.7	52.5	32.9	38.2	22.8	13.5	11.6	17.9	6.0
Postflexion	1	8.4	53.6	33.8	33.8	20.0	8.6	11.2	18.6	6.2

ing to a 2-bp difference in the 782-bp sequenced) with a minimum of 0.0000 (e.g., *S. jordani*) and a maximum of 0.0066 (in *S. aleutianus*). Divergence among reference haplotypes for species of *Sebastomus* ranged from 0.0102 to 0.0204 (Hyde and Vetter, 2007).

Results

Identification of larvae

Respectively, 91 of 339 and 112 of 846 *Sebastes* larvae collected in the CalCOFI and CCA surveys were *S. ensifer*. Among the larval *S. ensifer* sequenced for this study, divergence from reference haplotypes ranged from 0.0000 to 0.0080. Of the 76 sequences submitted to GenBank (accession numbers KM974185–KM974260), 22 sequences were identical to haplotype references in the GenBank database, 20 sequences differed by 1 bp, 14 sequences differed by 2 bp, 18 sequences differed by 3 bp, 1 sequence differed by 4 bp; and 1 sequence differed by 5 bp.

Description

Moser (1967) illustrated a 4.2-mm early-stage larva as *Sebastodes rhodochloris*. The smallest larva described in our study, 2.6 mm, had no yolk or oil globule remaining. Notochord flexion begins soon after larvae reach 6.2 mm and is completed by about 7.7 mm. Transformation to the pelagic juvenile stage begins near 20 mm and is complete by about 27 mm (Rocha-Olivares et al., 2000).

Larvae are moderately deep-bodied and robust through much of their development, although they are initially somewhat elongate, have a rounded head and short snout, a short preanal length, and large, and slightly oval to round eyes (Fig. 1A, Table 1). Most body proportions increase gradually during development; more rapid increases in relative preanal length, body depth, HL, and eye diameter occur between preflexion and postflexion stages (Table 1). All larvae have 26 myomeres (6–8 preanal myomeres during the preflexion stage, shifting to 10–11 during the postflexion stage).

Table 2

Measurements of head and pectoral girdle spines of larval swordspine rockfish (*Sebastes ensifer*) collected in the Southern California Bight during the California Cooperative Oceanic Fisheries Investigations survey in April 1999 and the Baseline Cowcod Conservation Area (CCA) survey in February 2002, and given as percentages of head length (HL): posterior preopercular (PP01, PP03, PP04) and anterior preopercular (APO1 and AP04), parietal (PA), nuchal (NU), pterotic (PT), posttemporal (PST), postorbital (PSO), and first lower infraorbital (LIO1) spines. Lengths of larvae on which measurements were made are given as body length (BL).

BL (mm)	HL (mm)	Stage	PPO1	PPO3	PPO4	APO1	APO4	PA	NU	PT	PST	PSO	LIO1
4.2	0.6	Preflexion	0	0	0	0	0	0	0	0	0	0	0
4.4	0.9	Preflexion	0	0	0	0	0	0	0	0	0	0	0
5.2	1.2	Preflexion	0	0	0	0	0	0	0	0	0	0	0
6.0	1.5	Preflexion	9.2	30.3	5.3	0	0	17.1	0	10.5	0	2.6	0
6.2	1.6	Preflexion	7.8	20.8	0	0	0	13.0	0	7.8	0	3.9	0
7.7	2.8	Preflexion	14.1	29.6	15.5	2.8	8.5	26.8	0	7.0	1.8	3.5	0
7.7	3.0	Postflexion	13.2	27.6	14.5	5.3	5.9	26.3	3.9	2.6	2.6	3.9	2.0
8.4	2.8	Postflexion	14.1	35.9	18.3	5.6	7.0	32.4	2.1	8.5	7.7	4.9	0

Head and pectoral girdle spine formation begins during the preflexion stage between 5.2–6.0 mm, with the posterior preopercular, parietal, pterotic, and postocular spines. Posterior preopercular spine PPO3 and the parietal spine are large (Table 2). Anterior preopercular spines and a posttemporal spine are added by the early postflexion stage (~7.7 mm), and the nuccal and first lower infraorbital spine form soon after (Table 2). The margins of all spines and ridges are smooth through the preflexion stage, but by the early postflexion stage the parietal and supraocular ridges and their spines and preopercular spines PPO3, PPO4, and APO4 are serrate. By 8.4 mm, the posttemporal spine also is weakly serrate.

The first fin rays to form are the upper pectoral-fin rays, by 4.4 mm (Fig. 1A, Table 3). Rays are added ventrally, and the full complement of 16–18 rays is present by the early postflexion stage. Hypural development begins during the preflexion stage, by 5.2 mm, and principal caudal-fin rays begin to form late during this stage, by 6 mm. The full complement of 8+7 principal rays is present, and procurrent rays begin to form by the early postflexion stage (Table 3). Soft rays of the dorsal and anal fins are forming by early postflexion stage, and all (12–14 and 5–7, respectively) are present by ~7.7 mm. Pterygiophores of the dorsal- and anal-fin spines are discernible early during the postflexion stage. Dorsal-fin spines begin to form slightly later, and anal-fin spines form later still (Table 3); full complements of dorsal-fin and anal-fin spines were not present in the largest specimen (8.4 mm).

The principal elements of the larval pigment pattern are the presence of melanophores situated anteriorly on the lower jaw, dorsally and ventrally on the gut, in a single row on the ventral margin of the tail, and

Table 3

Counts of fin rays of larval swordspine rockfish (*Sebastes ensifer*) collected in the Southern California Bight during the California Cooperative Oceanic Fisheries Investigations survey in April 1999 and Baseline Cowcod Conservation Area (CCA) survey in February 2002. BL=body length. D=dorsal, A=anal, P_1=pectoral, P_2=pelvic, and C=caudal.

Stage	BL (mm)	D	A	P_1	P_2	Principal C	Procurrent C
Preflexion	4.1	0	0	0	0	0	0
Preflexion	4.4	0	0	6	0	0	0
Preflexion	5.2	0	0	4	0	(hypurals)	0
Preflexion	6.0	0	0	6	0	3 + 3	0
Preflexion	6.2	0	0	15	(buds)	2 + 2	0
Postflexion	7.7	11	8	18	I,5	8 + 7	1 + 1
Postflexion	7.7	VI,13	7	17	I,5	8 + 7	2 + 2
Postflexion	8.4	XI,13	I,7	16	I,5	8 + 7	2 + 2

Table 4

Pigmentation of larval swordspine rockfish (*Sebastes ensifer*) collected in the Southern California Bight during the California Cooperative Oceanic Fisheries Investigations survey in April 1999 and the Baseline Cowcod Conservation Area (CCA) survey in February 2002, given as percentages of the number of larvae examined that displayed the pigment character. Larvae ≤6.2 mm were in the preflexion stage; larvae ≥7.7 mm were in the postflexion stage. BL=body length, LJ=lower jaw, V margin=ventral margin of the tail, and P_1=pectoral fin. *N*=number of specimens examined.

BL (mm)	*N*	LJ	Brain	Nape	V margin	Blade (P_1)	Base (P_1)
2.6	3	0	0	0	100.0	0	0
2.7	1	0	0	0	100.0	0	0
2.8	8	0	0	0	100.0	0	0
2.9	3	0	0	0	100.0	0	0
3	8	37.5	0	0	100.0	0	0
3.1	3	33.3	0	0	100.0	0	0
3.2	10	10.0	0	0	100.0	0	0
3.3	12	25.0	0	0	100.0	8.3	0
3.4	5	20.0	0	0	100.0	0	0
3.5	3	66.7	0	0	100.0	66.7	33.3
3.6	4	50.0	0	0	100.0	37.5	37.5
3.8	1	100.0	0	0	100.0	100.0	0
3.9	2	100.0	50.0	50.0	100.0	100.0	0
4	1	0	0	0	100.0	0	0
4.1	1	100.0	0	0	100.0	100.0	0
4.2	2	50.0	0	0	100.0	50.0	0
4.3	4	100.0	25.0	25.0	100.0	100.0	25.0
4.4	1	100.0	0	0	100.0	100.0	0
4.5	1	100.0	100.0	100.0	100.0	100.0	100.0
4.6	3	100.0	33.3	0	100.0	100.0	66.7
4.9	1	100.0	100.0	0	100.0	100.0	100.0
5.1	1	100.0	100.0	0	100.0	100.0	100.0
5.2	1	100.0	0	0	100.0	100.0	0
5.4	1	100.0	100.0	0	100.0	100.0	100.0
6.0	1	100.0	100.0	0	100.0	100.0	100.0
6.2	1	100.0	0	0	100.0	100.0	100.0
7.7	2	100.0	100.0	100.0	100.0	100.0	100.0
8.4	1	100.0	100.0	100.0	100.0	100.0	100.0

on the pectoral fins, especially distally (Table 4, Fig. 1). Larvae ≥6 mm also have pigment in the mid- and hindbrain areas.

Pigmentation on the head initially is limited to 3–8 or more melanophores anteriorly on the lower jaw, primarily on the inner margin of the dentaries. This pigment increases and spreads posteriorly during the postflexion stage. Melanophores form over the midbrain area as early as 3.9 mm and always are present by 7.7 mm, covering much of the area dorsally and dorsolaterally. At the same time, 2–4 melanophores form internally on the hindbrain, usually anterolaterally on the cerebellum. There is no other pigmentation on the head through 8 mm.

Pigmentation on the gut in the smallest larva was largely limited to the dorsum and ventrum but melanophores expanded into the hindgut area to nearly surround it. Melanophores spread ventrally from the dorsum of the gut, beginning posteriorly at about 5 mm, and cover the upper 50–90% by postflexion stage. A melanophore forms internally on the peritoneum at the anterior margin of the liver by 4.4 mm, and more are added to cover much of the upper 50–90% by postflexion stage. There are about 1–5 ventral melanophores on the gut, commonly along the midline between the anterior midgut to near the anus.

Pigmentation of the trunk and tail is limited to the ventral margin of the tail. During the preflexion stage, a single row of 8–14 melanophores (mean: 11), usually elongate, extends from myomeres 10–11 to 20–24 (modal number: 10–21), at a spacing of about one melanophore per myomere, and appears as an almost continuous line of pigment. Most melanophores are primarily shallowly internal; the last 1–2 are primarily external. During the postflexion stage, the number of ventral melanophores decreases as the series becomes more deeply internal and begins to disappear from anterior to posterior.

The pectoral fins are pigmented in nearly all larvae, most densely at the margin and progressively more lightly toward the fin base. Early in the preflexion stage, melanophores occur on the distal ~50–60% of the pectoral fin but they become more concentrated near the margin with development and are only on the distal 10–20% of the fin during the postflexion stage. The pectoral fin base is unpigmented before 4.5 mm; afterward, melanophores form on its inner surface and densely cover it during the postflexion stage. Melanophores form on the distal ~25% of the pelvic fins during the postflexion stage, and pigmentation is densest at the margin between rays 1–2, sparser between rays 3–4, and little or none at ray 5. No other fin pigmentation was observed, except that the 8.4-mm specimen had one small melanophore each at the bases of anal-fin rays 2 and 3.

Discussion

Identification of larvae

It has only relatively recently become possible to identify to species all the *Sebastes* larvae that are collected during plankton surveys conducted in the vicinity of the California Current during peak parturition season (e.g., Chen, 1971; Wyllie Echeverria, 1987). Among the larval *S. ensifer* sequenced for this study, divergence from reference haplotypes (0.0000 to 0.0080) was well below the divergence between *Sebastomus* species (0.0102–0.0204 [Hyde and Vetter, 2007]). Haplotype diversity within *Sebastomus* species has a mean distance of 0.0046 (ranging from 0.000 in *S. oculatus* and *S. spinorbis* to 0.0115 in *S. rosaceus* [Hyde and Vetter, 2007]), comparable to the values found in this study for *S. ensifer*.

Distribution

Sebastes ensifer ranges along the Pacific coast from the central Baja California Peninsula, México, to central California; the highest abundance occurs off Southern California and northern Baja California (Love et al., 2002). Within the current CalCOFI domain (e.g., McClatchie, 2014), larval *S. ensifer* is the second most abundant rockfish species, accounting for about one-fifth of the total rockfish larvae collected in 1999 and 2002. Larval *S. ensifer* were collected primarily in the vicinity of the Southern California Eddy (SCE) (Taylor et al., 2004), a persistent feature in the Southern California Bight northwest of San Clemente Island.

Comparisons

Larval *Sebastomus* are more or less readily identifiable as a group on the basis of several shared characters, including a relatively robust body, with large parietal and preopercular spines present by about mid-preflexion stage and with melanophores usually present on the lower jaw, always present on the pectoral fins and ventral margin of the tail, absent on the upper jaw and snout, and absent dorsally and laterally on the trunk and tail until the latter part of the postflexion stage when a bar begins to form on the caudal peduncle. A dorsal saddle may form on the trunk as well, late during the postflexion stage or during transformation to the pelagic juvenile stage (e.g., Rocha-Olivares et al., 1999). On the basis of these characters, larval *Sebastomus* can be distinguished from larvae of most, but not all, *Sebastes* species described to date.

Within *Sebastomus* in the North Pacific, early-preflexion-stage larvae of all 6 species for which larvae are known share the pattern of melanophores dorsally and ventrally on the gut, on the ventral margin of much of the tail (but none dorsally on the trunk or tail), and melanophores present at birth or soon thereafter on the pectoral fins. Pectoral-fin melanophores are exclusively or most concentrated near the margin, but are more evenly distributed in the honeycomb rockfish (*Sebastes umbrosus*) (Moser et al., 1977; Moser, 1996b). All but the rosy rockfish (*S. rosaceus*) have pigment at the tip of the lower jaw (Moser et al., 1977; Matarese et al., 1989; Moser, 1996b). On the basis of morphological features and pigmentation early during the preflexion stage, larval *S. ensifer* are essentially indistinguishable from the other *Sebastomus* larvae, except perhaps *Sebastes rosaceus* and *S. umbrosus*.

Larvae older than the early preflexion stage are known for only 3 *Sebastomus* species in the North Pacific: the starry rockfish (*Sebastes constellatus*), known to the mid-flexion stage (Moser et al., 1977; Moser and Butler, 1987; Moser, 1996b) and the late postflexion to pelagic juvenile stages (Rocha-Olivares et al., 2000); the rosethorn rockfish (*S. helvomaculatus*), known from the late flexion to pelagic juvenile stages (Richardson and Laroche, 1979); and *S. ensifer*, illustrated at extrusion stage by Moser (1967) and described here through the early postflexion stage and by Rocha-Olivares et al. (2000) from the late postflexion to pelagic juvenile stages.

During the preflexion stage, *S. constellatus* and *S. ensifer* are nearly indistinguishable, although the pectoral fins may become more heavily pigmented in *S. constellatus* and *S. ensifer* may be somewhat deeper-bodied than *S. constellatus* (mean: 21% BL, range: 15–24% BL in *S. ensifer* versus mean: 16% BL, range: 15–17% BL in *S. constellatus*). Note that, although this comparison is between ethanol-preserved *S. ensifer* and formalin-preserved *S. constellatus*, shrinkage does not differ greatly between the 2 preservatives (typically about 3–6% in 80–95% ethanol and about 2–10% in 5% formalin solution).

By the late preflexion stage, *S. constellatus* has distinctly more evenly and heavily pigmented pectoral fins than *S. ensifer*, and it has melanophores on the snout and upper jaw, on the isthmus, and on the hypural margin, which are all lacking in *S. ensifer*. It should be noted that these comparisons are between field-collected *S. ensifer* and laboratory-reared *S. constellatus*; it is yet to be determined whether the differences

will be apparent in field-collected *S. constellatus*. By the late postflexion stage, field-collected specimens of both *S. constellatus* and *S. ensifer* are nearly identical in pigmentation and morphological features but can be distinguished by gill raker counts (34–40 on the first arch in *S. ensifer* versus 25–30 in *S. constellatus*), possibly by small differences in head spination, and by the longer dorsal- and anal-fin rays of *S. ensifer* (Rocha-Olivares et al., 2000).

Larval *S. ensifer* and *S. helvomaculatus* also are pigmented similarly, but *S. ensifer* apparently retains ventral pigment on the tail longer than ventral pigment on *S. helvomaculatus* (≥1 melanophore on the caudal peduncle to at least 8.4 mm versus none by 7.7 mm, respectively). The pectoral fin base apparently is more heavily pigmented in *S. helvomaculatus*: Richardson and Laroche (1979) reported (but did not show in their illustrations) that both the inner and outer surfaces of the fin base are pigmented by 7.7 mm in *S. helvomaculatus*. In contrast, *S. ensifer* has pigment only on the inner surface of the fin base through at least 8.4 mm. Larval *S. ensifer* may be slightly more slender than *S. helvomaculatus* (mean: 33% BL, range: 32–34% BL for *S. ensifer* 7.7–8.4 mm versus mean: 35% BL, range: 33–40% BL for *S. helvomaculatus* 7.7–8.8 mm), and have a slightly longer preopercular spine PPO3 (28–36% HL versus 27–31% HL for larvae within the size range of 7.7–8.8 mm).

Larval *Sebastes* of the subgenus *Sebastomus* are more or less readily identifiable as a group on the basis of traditional morphological and pigmentation characters, but the species within that group are not, perhaps reflecting the relatively recent origin and rapid radiation of this subgenus (Hyde and Vetter, 2007). Molecular techniques do allow for species identification and, coupled with visual pre-sorting to subgenus, do provide an efficient method for obtaining quantitative, species-specific data for these otherwise unidentifiable larvae. Development of microarrays and microbeads that allow automated reading of a fluorescent label after species-specific enzyme ligation may provide collection of real-time, species-specific abundance data aboard a ship during a survey.

Acknowledgments

We wish to thank the scientific and ship's crews of the NOAA Ship *David Starr Jordan* and Scripps Institution of Oceanography RV *New Horizon*. Our appreciation goes to A. Hays, D. Griffith, and R. Charter, who especially assisted in obtaining samples; L. Dunn for sorting the fish larvae from the plankton samples; H. Timms and A. Brooks for their assistance in the laboratory; and H. Moser, who contributed pertinent information during review. For his tutelage and review of this article, S. Charter is especially grateful to J. Hyde. We also thank the Oceanids Foundation and the Frieda Daum Urey scholarship committee for their endowment to CATL.

Literature cited

Ambrose, D. A., R. L. Charter, and H. G. Moser.
2001. Ichthyoplankton and station data for California Cooperative Oceanic Fisheries Investigations survey cruises in 1999. NOAA Tech. Memo. NOAA-TM-NMFS-SWFSC-311, 69 p.

Chen, L.-C.
1971. Systematics, variation, distribution, and biology of rockfishes of the subgenus *Sebastomus* (Pisces, Scorpaenidae, *Sebastes*). Bull. Scripps Inst. Oceanogr. 18, 115 p.

Eschmeyer, W. N., E. S. Herald, and H. Hammann.
1983. A field guide to Pacific coast fishes of North America, 336 p. Houghton Mifflin Co., Boston.

Fey, D. P., and J. A. Hare.
2005. Length correction for larval and early-juvenile Atlantic menhaden (*Brevoortia tyrannus*) after preservation in alcohol. Fish. Bull. 103:725–727.

Hyde, J. R., E. Lynn, R. Humphreys Jr., M. Musyl, A. P. West, and R. Vetter.
2005. Shipboard identification of fish eggs and larvae by multiplex PCR, and description of fertilized eggs of blue marlin, shortbill spearfish, and wahoo. Mar. Ecol. Prog. Ser. 286:269–277.

Hyde, J. R., and R. D. Vetter.
2007. The origin, evolution, and diversification of rockfishes of the genus *Sebastes* (Cuvier). Mol. Phylogen. Evol.

Kendall, A. W., Jr.
1991. Systematics and identification of larvae and juveniles of the genus *Sebastes*. Environ. Biol. Fish. 30: 173–190.

Kramer, D., M. J. Kalin, E. G. Stevens, J. R. Thrailkill, and J. R. Zweifel.
1972. Collecting and processing data on the fish eggs and larvae in the California Current region. NOAA Tech. Rep. NMFS Circ. 370, 38 p.

Leet, W. S., C. M. Dewees, and C. W. Haugen (eds.).
1992. California's living marine resources and their utilization. Univ. Calif. Sea Grant Ext. Pub. UCSGEP-92-12, 257 p.

Leet, W. S., C. M. Dewees, R. Klingbeil, and E. J. Larson (eds.).
2001. California's living marine resources: a status report, 593 p. Resources Agency, Calif. Dep. Fish Game, Sacramento, CA.

Leis, J. M., and B. M. Carson-Ewart (eds.).
2000. The larvae of Indo-Pacific coastal fishes: an identification guide to marine fish larvae, 850 p. Brill, Leiden, Netherlands.

Lenarz, W. H.
1987. A history of California rockfish fisheries. *In* Proceedings of the international rockfish symposium; Anchorage, AK, 20–22 October 1986, p. 35–41. Alaska Sea Grant Rep. 87-2, Univ. Alaska, Fairbanks.

Love, M. S., M. Yoklavich, and L. Thorsteinson.
2002. The rockfishes of the northeast Pacific, 404 p. Univ. Calif. Press, Berkeley, CA.

Matarese, A. C., A. W. Kendall Jr., D. M. Blood, and B. M. Vinter.
1989. Laboratory guide to early life history stages of northeast Pacific fishes. NOAA Tech. Rep. NMFS 80, 651 p.

McClatchie, S.
2014. Regional fisheries oceanography of the California Current System: the CalCOFI program. Springer. Dordrecht, Netherlands.

Moku, M., K. Mori, and Y. Watanabe.
2004. Shrinkage in the body length of myctophid fish (*Diaphus* slender-type spp.) larvae with various preservatives. Copeia 2004:647–651.

Moser, H. G.
1967. Reproduction and development of *Sebastodes paucispinis* and comparison with other rockfishes off Southern California. Copeia 1967:773–797.
1996a. Introduction. *In* The early stages of fishes in the California Current region (H. G. Moser, ed.), p. 1–72. CalCOFI Atlas 33.
1996b. Scorpaenidae: scorpionfishes and rockfishes. *In* The early stages of fishes in the California Current region (H. G. Moser, ed.), p. 733–795. CalCOFI Atlas 33.

Moser, H. G., and E. H. Ahlstrom.
1978. Larvae and pelagic juveniles of blackgill rockfish, *Sebastes melanostomus*, taken in midwater trawls off Southern California and Baja California. J. Fish. Res. Board Can. 35:981–996.

Moser, H. G., and J. L. Butler.
1987. Descriptions of reared larvae of six species of *Sebastes*. *In* Widow rockfish: Proceedings of a workshop, Tiburon, Calif., Dec. 11–12, 1980 (W. H. Lenarz and D. R. Gunderson, eds.), p. 19–29. NOAA Tech. Rep. NMFS 48.

Moser, H. G., E. H. Ahlstrom, and E. M. Sandknop.
1977. Guide to the identification of scorpionfish larvae (family Scorpaenidae) in the eastern Pacific with comparative notes on species of *Sebastes* and *Helicolenus* from other oceans. NOAA Tech. Rep. NMFS Circ. 402, 71 p.

Moser, H. G., R. L. Charter, P. E. Smith, D. A. Ambrose, S. R. Charter, C. A. Meyer, E. M. Sandknop, and W. Watson.
1993. Distributional atlas of fish larvae and eggs in the California Current region: Taxa with 1000 or more total larvae, 1951 through 1984. CalCOFI Atlas 31, 235 p.

Moser, H. G., R. L. Charter, W. Watson, D. A. Ambrose, J. L. Butler, S. R. Charter, and E. M. Sandknop.
2000. Abundance and distribution of rockfish (*Sebastes*) larvae in the Southern California Bight in relation to environmental conditions and fishery exploitation. CalCOFI Rep. 41:132–147.

Ohman, M. D., and P. E. Smith.
1995. A comparison of zooplankton sampling methods in the CalCOFI time series. CalCOFI Rep. 36:153–158.

Porter, S. M., A. L. Brown, and K. M. Bailey.
2001. Estimating live standard length of net-caught walleye pollock (*Theragra chalcogramma*) larvae using measurements in addition to standard length. Fish. Bull. 99:691–696.

Ralston, S., and B. R. MacFarlane.
2010. Population estimation of bocaccio (*Sebastes paucispinis*) based on larval production. Can. J. Fish. Aquat. Sci. 67:1005– 1020.

Ralston, S., J. R. Bence, M. B. Eldridge, and W. H. Lenarz.
2003. An approach to estimating rockfish biomass based on larval production, with application to *Sebastes jordani*. Fish. Bull. 101:129–146.

Richardson, S. L., and W. A. Laroche.
1979. Development and occurrence of larvae and juveniles of the rockfishes *Sebastes crameri*, *Sebastes pinniger*, and *Sebastes helvomaculatus* (Family Scorpaenidae) off Oregon. Fish. Bull. 77:1–46.

Rocha-Olivares, A.
1998. Multiplex haplotype-specific PCR: a new approach for species identification of the early life stages of rockfishes of the species-rich genus *Sebastes* Cuvier. J. Exp. Mar. Biol. Ecol. 231:279–290.

Rocha-Olivares, A., C. A. Kimbrell, B. J. Eitner, and R. D. Vetter.
1999. Evolution of a mitochondrial cytochrome *b* gene sequence in the species-rich genus *Sebastes* (Teleostei, Scorpaenidae) and its utility in testing the monophyly of the subgenus *Sebastomus*. Mol. Phylogen. Evol. 11:426–440.

Rocha-Olivares, A., H. G. Moser, and J. Stannard.
2000. Molecular identification and description of pelagic young of the rockfishes *Sebastes constellatus* and *Sebastes ensifer*. Fish. Bull. 98:353–363.

Sabatés, A., and M. P. Olivar.
1990. Early development and spawning of *Sebastes capensis* in the Southeast Atlantic. Mar. Biol. 107:389–395.

Swofford, D. L.
2000. PAUP*. Phylogenetic analysis using parsimony (*and other methods), vers. 4. Sinauer Associates Inc., Sunderland, MA.

Taylor, C.A., W. Watson, T. Chereskin, J. Hyde, and R. Vetter.
2004. Retention in larval rockfishes, *Sebastes*, near natal habitat in the Southern California Bight, as indicated by molecular identification methods. CalCOFI Rep. 45:152–166.

Theilacker, G. H.
1980. Changes in body measurements of larval northern anchovy, *Engraulis mordax*, and other fishes due to handling and preservation. Fish. Bull. 78:685–692.

Wyllie Echeverria, T.
1987. Thirty-four species of California rockfishes: maturity and seasonality of reproduction. Fish. Bull. 85:229–250.

NOAA
National Marine
Fisheries Service

Fishery Bulletin
established 1881

Spencer F. Baird
First U.S. Commissioner
of Fisheries and founder
of *Fishery Bulletin*

Exploitation and reproduction of the bullnose ray (*Myliobatis freminvillei*) caught in an artisanal fishery in La Pared, Margarita Island, Venezuela

Alejandro Tagliafico (contact author)[1,2]
Nicolás Ehemann[1]
María Salomé Rangel[1,2]
Néstor Rago[3]

Email address for contact author: tagliaficoa@gmail.com

[1] Escuela de Ciencias Aplicadas del Mar
Núcleo de Nueva Esparta
Universidad de Oriente
Calle La Marina
Boca de Río, 6304 Isla de Margarita, Venezuela

[2] National Marine Science Centre
Southern Cross University
2 Bay Drive
Coffs Harbour, New South Wales 2450, Australia

[3] Universidad Nacional de Costa Rica
Escuela de Biología
Avenida 1, Calle 9
Heredia 86-3000, Costa Rica

Abstract—Species of the genus *Myliobatis* have been poorly assessed because of a lack of available information regarding their capture and life history. We provide valuable data based on the commercial landings of the bullnose ray (*Myliobatis freminvillei*), which we studied during 2 separate time periods (October 2005–December 2007 and January–December 2013). A total of 187 individuals were analyzed: 85 females (24.0–96.0 cm in disc width [DW]) and 102 males (22.8–118.0 cm DW). There was no difference in the overall sex ratio (females to males: 4:5); however, differences were found between the annual sex ratio in 2005, 2006, and 2013. Estimated capture per unit of effort for this species was 0.8 individuals/trip (standard deviation [SD] 1.3) or 2.9 kg/trip (SD 5.5), showing an increase in effort through time and significant differences between years. Approximately 25% of both sexes were shorter than the estimated median DW at maturity. No pattern in the reproductive cycle was identified because of the lack of landings during several months; however, mature individuals were observed frequently throughout the study period; gravid females were observed on only 2 occasions. This study provides baseline biological information on the life history of the bullnose ray for necessary fishery management.

Manuscript submitted 14 January 2015.
Manuscript accepted 23 December 2015.
Fish. Bull. 114:144–152 (2016).
Online publication date: 21 January 2016.
doi: 10.7755/FB.114.2.2

The views and opinions expressed or implied in this article are those of the author (or authors) and do not necessarily reflect the position of the National Marine Fisheries Service, NOAA.

Elasmobranch overfishing has been documented since the late 1940s (Castro, 2013) and recent analyses have demonstrated that population diminution has occurred around the world, with at least one in 4 species being actually threatened with extinction (Dulvy et al., 2014). Nonetheless, numerous species of rays and skates have been poorly studied, preventing definition of their status and identification of threats (Molina and Lopez, 2015). Such is the case for the genus *Myliobatis*, which comprises 11 species (White, 2014). Of those species, 6 have been documented as data deficient by the International Union for Conservation of Nature (IUCN) in the IUCN Red List of Threatened Species, vers. 2015.4, available at website, accessed December 2015), 2 have been classified as species of least concern, and the remaining 3 species have been categorized as endangered, near threatened, or have not been assessed to date. The bullnose ray (*Myliobatis freminvillei*) is included within the data-deficient group, as a result of the lack of available information required to evaluate population trends; as a consequence, the need for further investigations of its biology and the fishery are required to re-assess the status of this species in the IUCN Red List (Stehmann, 2009).

The bullnose ray is a benthic–pelagic eagle ray widely distributed in the western Atlantic and captured mainly with artisanal long lines, gillnets, and industrial shrimp trawls (Cervigón et al., 1992; Stehmann, 2009; Froese and Pauly, 2015). In Brazil, a similar species, the southern eagle ray (*M. goodei*), is discarded as bycatch of beach seining (Velasco et al., 2011). However, in many Venezuelan coastal communities, the

bullnose ray is commercially valuable and is consumed fresh or salted (Cervigón et al., 1992; Cervigón and Alcalá, 1999). Between 2006 and 2007, 13,000 kg of bullnose ray were landed in the state of Nueva Esparta in Venezuela, representing 0.03% of the total landings from 176 commercially fished species (Marval and Cervigón, 2009). Although no fishery specifically targets this species, it is often landed as bycatch.

The results of this study provide insight on the life history and landings data of the bullnose ray captured as part of a small-scale, artisanal fishery in Margarita Island—baseline information that would be useful for management and conservation of this little known and potentially vulnerable species.

Materials and methods

La Pared is a small and isolated fishing community located on the northern coast of Macanao Peninsula, Margarita Island, in the state of Nueva Esparta in northeastern Venezuela (11°03′32.53″N, 64°18′47.25″W). At this place, fishermen manage the resources, rotating target species and using different gears depending on the time and abundance of fish (Tagliafico et al., 2013a).

All bullnose ray used in analysis for this study were sampled from fish landed with bottom gillnets at a site in this community. Descriptions of the boats and fishing gear of this fishery can be found in Méndez-Arocha (1963), Ginés et al. (1972), Iriarte (1997), Suárez and Bethencourt (2002), and González et al. (2006).

Sampling was carried out weekly from October 2005 through December 2007 and, 5 years later, from January through December 2013. The number of fishing boats, number of individual bullnose ray landed, and the total weight landed (kilograms) were recorded during each visit. Catch per unit of effort (CPUE) was defined as the number of individuals caught per trip and the total kilograms caught per trip. To identify statistical differences in the CPUE between years and months (except for 2005, because sample data were collected over only 3 months during that year), homogeneity of variances were tested with Levene's test, followed by 2-way fixed-effects analyses of variance (ANOVA), based on permutations; all of these analyses were conducted with Primer 6[1] (PRIMER-E Ltd., Ivybridge, U.K.; Clarke and Warwick, 2006) and PERMANOVA+ add-on software for Primer (Anderson et al., 2008). When statistical differences were detected, a Tukey's honestly significant difference (HSD) test was performed.

To determine the size-frequency distribution of the bullnose ray that were captured and analyzed, the disc width (DW), of each individual was measured in centimeters; therefore, all subsequent references to size in this article refer to DW. Sexes were differentiated by the presence of claspers in males and their absence in females (Conrath, 2005). Differences in the proportions of sexes were tested with a chi-square test (χ^2) (Zar, 1996).

Maturity was determined by macroscopic observation of reproductive organs at the landing site. Females were considered mature or immature on the basis of the presence or absence of fully developed ova in the ovaries. Gravid females were recognized by the presence of embryos in the uterus, and post-gravid females were recognized by the presence of a well-developed, large, and highly vascularized uterus (Conrath, 2005). For males, maturity was determined by inspecting and manipulating claspers. Organisms were considered mature when claspers were strongly calcified and could be easily rotated around the base (Conrath, 2005). They also had to have an extensible distal portion (Conrath, 2005) and show the presence of seminal fluid (Bizarro et al., 2007). Male bullnose ray that lacked these characteristics were considered to be immature.

The proportion of males to females at different reproductive stages was examined monthly to identify the reproductive cycles of the species in the study area. Other measurements, such as follicle diameter, uterus width, clasper length, gonad weight, and liver weight could not be obtained consistently because of the speed at which animals were cut and sold on arrival at the landing site.

The median size at maturity was estimated for males and females through the use of the logistic function:

$$M_f = 1/1 + \exp^{-a(L_i - b)}, \quad (1)$$

where M_f = the fraction of mature individuals;
a = the change in slope of M_f as a function of the size intervals (L_i); and
b = the DW at 50% maturity (DW_{50}).

Parameter estimates for a and b were obtained by using the least squares method with the statistical software R, vers 3.1.1 (R Core Team, 2014). A covariance analysis of these logistic regressions by sexes was performed.

Results

For this study, 187 bullnose rays were analyzed. General characteristics of these specimens are summarized in Table 1. The size ranges for all organisms analyzed were 22.8–118.0 cm DW and 0.2–19.0 kg. Both average DW and average weight increased slightly in recent years (Table 1). The size-frequency distribution shows that, although the fishery-captured specimens were of several size classes, the greatest number of individuals were between 55.0 and 60.0 cm DW (Fig. 1). The largest recorded individuals were males; however, only 4 males were larger than 75.0 cm DW, whereas 25 females were found above that size.

As summarized in Table 2, during the 39-month sampling period, 225 fishing trips were analyzed and

[1] Mention of trades names or commercial companies is for identification purposes only and does not imply endorsement by the National Marine Fisheries Service, NOAA.

Table 1

Biological measurements of the bullnose ray (*Myliobatis freminvillei*) caught by the artisanal fishery of La Pared, Margarita Island, Venezuela, during 2 periods: 2005–2007 and 2013. Average disc widths (DWs) and average weights are given with standard deviations (SDs). An asterisk (*) indicates statistical differences at level of significance (α) of 0.05.

Year	2005	2006	2007	2013	All years
n	14	33	91	49	187
Number of females (F)	2	10	42	31	85
Number of males (M)	12	23	49	18	102
Sexual ratio (F:M)	1:5*	2:5*	9:10	17:10*	4:5
DW intervals (F) (cm)	40.8–50.5	24.0–82.4	26.4–96.0	54.4–93.5	24.0–96.0
Weight intervals (F) (kg)	1.0–1.8	0.2–7.4	0.3–12.0	2.2–10.6	0.2–12.0
DW intervals (M) (cm)	42.0–56.4	45.0–60.2	22.8–118.0	37.6–86.5	22.8–118.0
Weight intervals (M) (kg)	1.0–2.8	1.3–3.0	0.2–19.0	0.6–8.6	0.2–19.0
Average DW (cm)	51.9 (SD 4.4)	56.2 (SD 10.0)	58.5 (SD 16.0)	69.4 (SD 13.3)	60.0 (SD 15.0)
Average weight (kg)	2.0 (SD 0.5)	2.7 (SD 1.7)	3.4 (SD 3.1)	5.1 (SD 2.8)	3.4 (SD 2.8)
First gravid (cm)	–	–	75.8	84.6	75.8
Immature (%)	50	33	18	10	25
Gravid (%)	0	0	1	1	1
DW 100% maturity (cm)	>54.0	>54.0	>54.0	>55.0	>55.0
Maximum fecundity	–	–	1	6	6
Maximum DW embryo (cm)	–	–	9.0	20.6	20.6

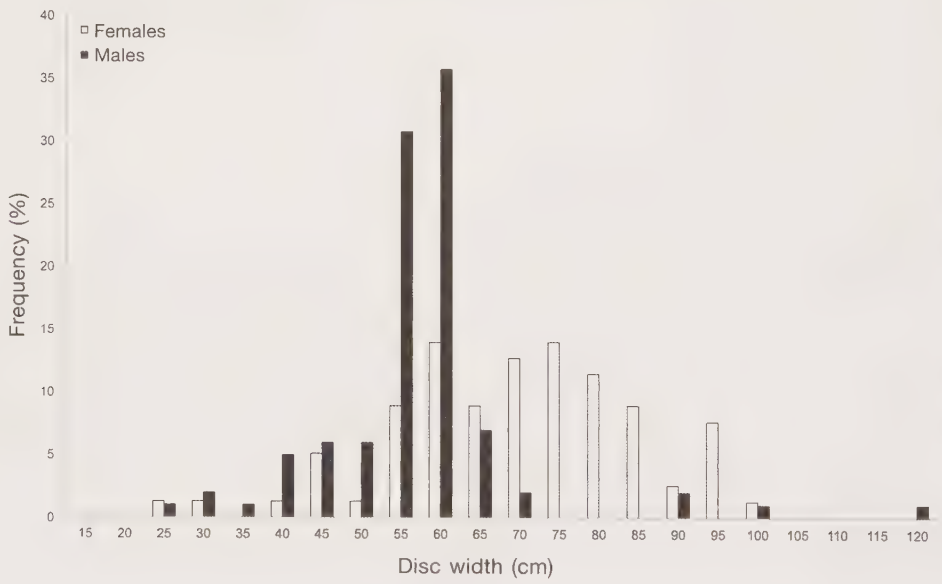

Figure 1

Frequency distribution of disc-widths of male and female bullnose ray (*Myliobatis freminvillei*) caught in the artisanal fishery of La Pared, Venezuela, during 2 periods: 2005–2007 and 2013.

provided a total yield of 648.1 kg of the bullnose ray. The estimated overall CPUE was 0.8 individuals/trip (standard deviation [SD] 1.3) or 2.9 kg/trip (SD 5.5). Differences in the number of trips, individuals, and kilograms of catch were observed over the years sampled. In 2013, the number of trips reached a maximum, but that peak occurred without a concomitant increase in the number of kilograms or animals captured. Monthly analysis showed a higher level of fishing effort during April–June 2013 in comparison with previous years, although there were high numbers of trips with no catches of the bullnose ray (Fig. 2A).

Table 2

Mean catch per unit of effort (CPUE), measured as individuals per trip and as kilograms per trip and given with standard deviations in parentheses, for bullnose ray (*Myliobatis freminvillei*) captured in La Pared, Venezuela, during 2 periods: 2005–2007 and 2013.

Year	Number of trips	Number of individuals	Catch (kg)	CPUE (individuals/trip)	CPUE (kg/trip)
2005	10	14	27.8	1.4 (1.8)	2.8 (3.7)
2006	48	33	87.3	0.7 (1.1)	1.8 (3.0)
2007	69	91	306.6	1.3 (1.4)	4.4 (5.5)
2013	98	49	226.4	0.5 (1.2)	2.3 (6.4)
All years	225	187	648.1	0.8 (1.3)	2.9 (5.5)

The highest monthly catch of 78.5 kg was registered in April 2013 (Fig. 2B).

A clear trend for estimated CPUE, expressed as both the number of individuals caught per trip and kilograms caught per trip, was not observed during the study period (Fig. 2, C and D). Variance between years was homogeneous (Levene's test: $P>0.05$). Statistical differences were observed in the number of individuals per trip and in the weight of the catches (kilograms per trip) between years but not between months (Tables 3 and 4). The posteriori Tukey's HSD test ($P<0.05$) revealed that both the average number of individuals per trip and kilograms per trip were significantly higher in 2007 than in 2006 or 2013 (Table 2). During the study period, 59% of trips resulted in no catch of bullnose ray.

Over the entire period of study, males occurred in slightly greater numbers than those of females, yet no significant difference was detected (χ^2 (1, n=187): 1.37, P=0.242). In contrast, when considering each year independently, differences were found in 2005 (χ^2 (1, n=14): 5.79, P=0.016), 2006 (χ^2 (1, n=33): 4.36, P=0.037), and 2013 (χ^2 (1, n=49): 4.00, P=0.046).

Results from covariance analysis of the logistic regressions indicated that sex had no significant effect (P=0.673), and, as a consequence, an average value of DW_{50} was estimated for both sexes at 53.3 cm DW, in which 95% confidence intervals ranged from 52.6 to 53.9 cm DW, whereas the slope of the regression was estimated at 0.42 with 95% confidence intervals from 0.35 to 0.51.

Immature females occurred less frequently (17%) than immature males (31%) in catches. Only 2 gravid specimens were reported during the entire study period: one in July 2007 (with 1 embryo of 9.0 cm DW) and the other in March 2013 (with 6 embryos: 2 females and 4 males between 19.7 and 20.6 cm DW). In addition, a postgravid female was captured in July 2007. Mature individuals were observed in almost all months for which landings were registered; however, a low number of gravid and postgravid females were recorded over the study period (Fig. 3).

Discussion

The maximum size of bullnose ray examined in this study (118.0 cm DW) exceeded the previous maximum size reported for this species in Venezuela (97.0 cm DW; Cervigón and Alcalá, 1999), in Brazil (100.0 cm DW; Bernardes et al., 2005), and in Argentina (106.0 cm DW; Refi, 1975). It is probable that the larger maximum size observed is due to the long duration of our study and the greater number of individuals analyzed, in comparison with other studies of the bullnose ray. Schwartz (2011), for example, reported the occurrence of a greater maximum DW (males: 165.0 cm, females: 147.0 cm) in Onslow Bay, North Carolina, over an extremely long time period (1972–2010) using 2 different capture methods (braided nylon long lines and otter trawls). On the other hand, Stehmann (2009) reported that 70.0 cm DW was the most common size for this species; in contrast, the most common size interval recorded in this study was between 55.0 and 60.0 cm DW. The average size of the bullnose ray observed (n=187) was 60.0 cm DW (SD 15.0 cm), similar to the mean size reported by Schmidt et al. (2012) for this species in Brazilian fisheries (63.8 cm DW [SD 7.0 cm], n=8); however, the average weight calculated in our study (3.4 kg [SD 2.8]) was slightly lower than that reported for bullnose ray in Brazil (3.6 kg [SD 1.3]).

Average DW of captured organisms increased from 51.9 cm (SD 4.4) in 2005 to 69.4 cm (SD 13.3) in 2013. In addition, the average recorded weight of captured organisms increased from 2.0 kg (SD 0.5) in 2005 to 5.1 (SD 2.8) in 2013 and weight increased steadily over the study period (average annual weights were 2.0, 2.7, and 3.4 kg per individual for 2005, 2006, and 2007, respectively). However, it is important to note that applied fishing effort was greater in 2013 than in previous years. Also, a total ban of the Venezuelan industrial trawling fishery occurred in 2008, a change that potentially may have increased food availability for bullnose ray, resulting in an increased size of bullnose ray and in a redirection of fishing effort. Both of these factors could explain the observed increase in

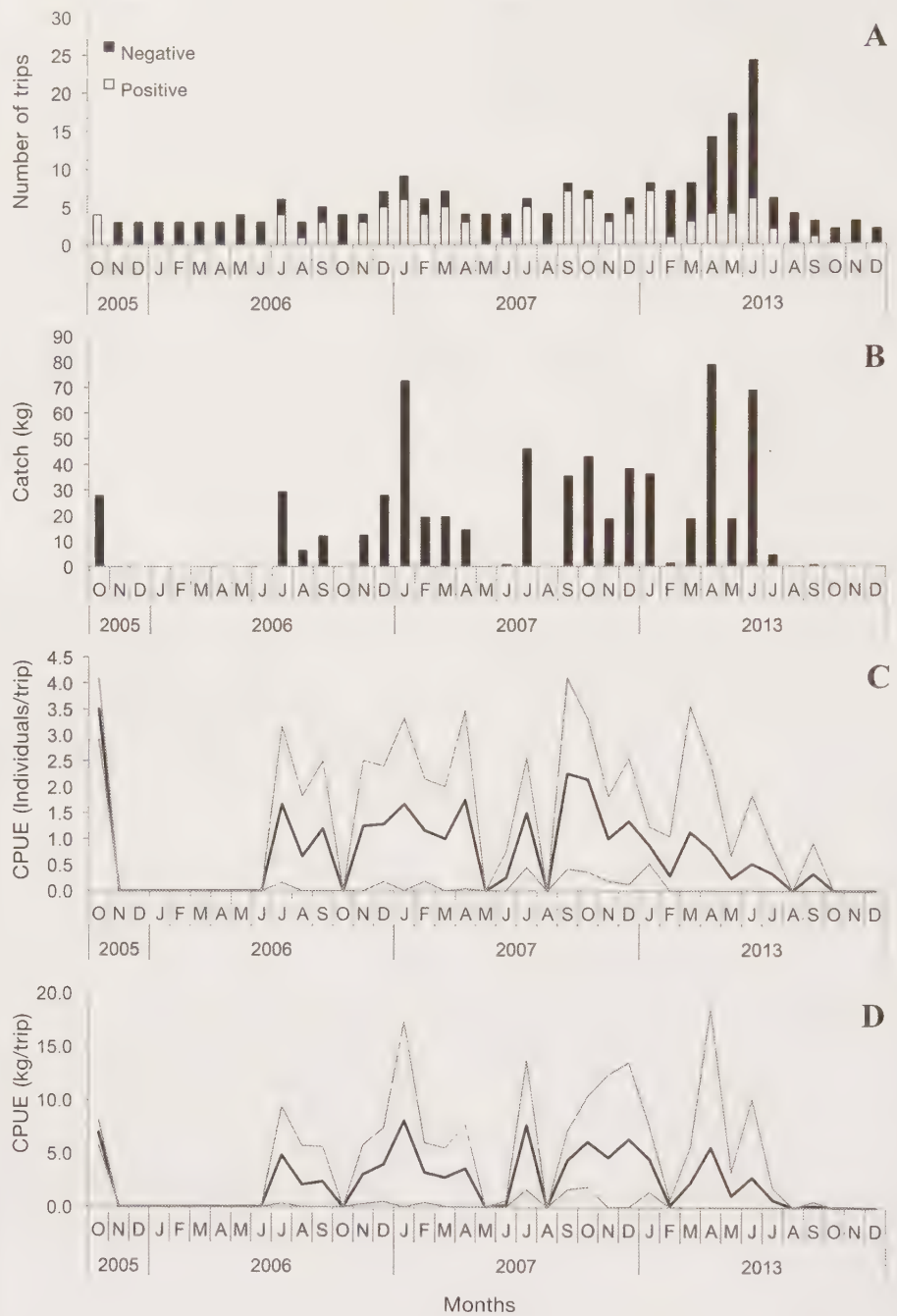

Figure 2

Monthly fishing effort in (**A**) number of trips and (**B**) catch by weight; and (**C**) monthly catch per unit of effort (CPUE) in individuals per trip and (**D**) weight per trip for bullnose ray (*Myliobatis freminvillei*) caught by the artisanal fishery of La Pared, Venezuela, during 2 periods, 2005–2007 and 2013. In panels C and D, thick lines represent mean values, and thin lines indicate the respective standard deviations of the means.

size and weight of captured specimens of bullnose ray in our study. Furthermore, fishing effort at La Pared can be influenced by the abundance of other species, such as tuna and deep sea sharks (Tagliafico et al., 2013a), as well as by natural events, such as strong wind, waves, or even local festivities, all of which can reduce landings, and with them, the data available for fishery-dependent research.

Table 3

Results of analysis of variance of catch per unit of effort, measured as individuals per trip of bullnose ray (*Myliobatis freminvillei*) captured in La Pared, Venezuela, during 2 periods, 2006–2007 and 2013, with the year and month used as sources of variation. An asterisk (*) indicates statistical difference at a level of significance (α) of 0.05. df=degrees of freedom; SS=sum of squares; MS=mean squares; *F*= *F*-test; CV=coefficient of variation.

Source	df	SS	MS	*F*	*P* (perm)	CV
Year	2	19.40	9.70	6.95	0.004*	0.16
Month	11	21.42	1.95	1.40	0.191	0.00
Year×Month	22	36.30	1.65	1.18	0.281	0.00
Residual	179	249.63	1.39			1.39
Total	214	336.16				

Table 4

Results of analysis of variance of CPUE, measured as kilograms per trip of the bullnose ray (*Myliobatis freminvillei*) captured in La Pared, Venezuela, during 2 periods, 2006–2007 and 2013, with the year and month used as sources of variation. An asterisk (*) indicates statistical difference at a level of significance (α) of 0.05. df=degrees of freedom; SS=sum of squares MS=mean squares; *F*= *F*-test; CV=coefficient of variation.

Source	df	SS	MS	*F*	*P* (perm)	CV
Year	2	240.7	120.4	3.948	0.025*	1.68
Month	11	296.6	27.0	0.884	0.514	0.00
Year×Month	22	534.9	24.3	0.797	0.641	0.00
Residual	179	5457.4	30.5			30.49
Total	214	6705.9				

Current literature on the sex ratio of bullnose ray comes from only a few studies: an 8-month study from Brazil, in which 6 females and 2 males were analyzed (Schmidt et al., 2012) and a 38-year study from North Carolina in which a 1:1 sex ratio was reported (Schwartz, 2011). For another species of this genus, the bat ray (*M. californica*), Hopkins and Cech (2003) found that females were more common than males (21:5) in California. The total sex ratio of all 187 organisms examined for our study was 4:5 (females to males), which indicates no significant difference between sexes and that spatial segregation by sex does not exist for the bullnose ray. However, when the data were analyzed over shorter time periods, significant differences occurred in sex ratios between different years (Table 1), highlighting the importance of collecting data over time periods greater than 1 year.

Future studies of the bullnose ray need to take into account the short, medium, and long-term population dynamics of this species. Our data, and previous work by Schmidt et al. (2012), indicate the likelihood of complex population dynamics and variable sex ratios, yet the data are not adequate to accurately describe the factors that affect sex ratios over different temporal scales or to provide information that is imperative for the management of this species. Additionally, it has been proposed that different sampling techniques can result in variable sex ratios (Hopkins and Cech, 2003). Therefore, bias from different sampling methods, biologically driven spatiotemporal segregation, and the overall mobility of elasmobranchs could hinder efforts to improve understanding of population-level attributes that create differences in the distribution of individual animals and observed sex ratios.

To our knowledge, only 2 reports describe size at sexual maturity for this species. McEachran and de Carvalho (2002) suggest that males reach maturity between 60.0 and 70.0 cm DW, yet they include no estimate for females. Gómez et al. (2010) indicate that females reach maturity when they are greater than 58.0 cm DW and males reach maturity when they are above 45.0 cm DW. By comparison, our data indicate that the average size at sexual maturity for this species occurs at a DW of 53.3 cm for both sexes—a size that is slightly lower than most of the previous estimates. Recently, Molina and Lopez (2015) estimated that the

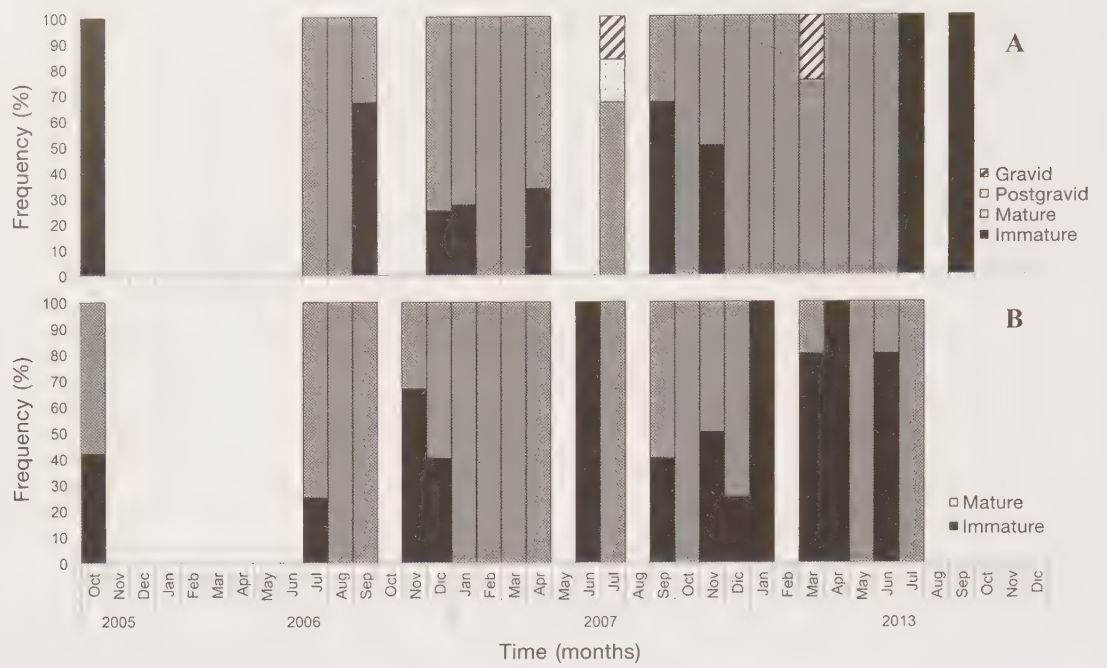

Figure 3

Monthly proportion of sexual maturity stages for (**A**) female and (**B**) male bullnose ray (*Myliobatis freminvillei*) captured by the artisanal fishery of La Pared, Venezuela, during 2 periods: 2005–2007 and 2013.

size at sexual maturity for the southern eagle ray in Northern Patagonia was 48.7 and 45.0 cm DW for females and males, respectively. In central California, for the bat ray, sexual maturity has been estimated to occur at 45.0–62.2 cm DW for males and 50% maturity of females has been reached at an estimated 88.1 cm DW (Martin and Cailliet, 1988). Differences in DW at sexual maturity for species occurring in diverse regions have also been reported for other species of Myliobatidae, and several factors may determine such disparities, such as real variations in populations, sample size, sampling bias, as well as errors in the assignation of maturity stages and the use of different estimation methods (Tagliafico et al., 2012).

No patterns were detected in the reproductive cycle of bullnose ray. As with our observations of gravid and postgravid females in July, Cervigón and Alcalá (1999) reported capture of gravid females in June and October. The low numbers of gravid females in our study may indicate a spatial segregation of the sexes, with females giving birth in waters outside the operational area of the fishery.

The maximum size of embryos registered in this study (20.6 cm DW) is similar to the previously reported range (21.5–21.7 cm DW; Cervigón and Alcalá, 1999) and to the size of neonates (25.0 cm, McEachran and de Carvalho, 2002; 22.0–23.0 cm, Gómez et al., 2010). Also, the maximum fecundity encountered in this study (n=6) is comparable to the previously reported numbers of 6–8 embryos (Cervigón and Alcalá, 1999; McEachran and de Carvalho, 2002). An outlier specimen, a female captured with a single embryo of 9.0 cm, is suspected to have aborted pups during its capture as a result of stress. Similar values for size and number of embryos have been indicated for the bat ray (n=2–5; size: 22.0–30.5 cm) (Martin and Cailliet, 1988).

Venezuelan fishery resources are showing signs of overexploitation (Mendoza[2]), and a lack of management for Myliobatiformes (i.e., the spotted eagle ray [*Aetobatus narinari*], southern stingray [*Dasyatis americana*], and longnose stingray [*D. guttata*]) has been reported previously (Tagliafico et al., 2012, 2013b). Precautionary management measures may be necessary to ensure ongoing population viability of the bullnose ray. In this study, we provide results regarding CPUE, DW at maturity, size structure by sex, and the sex ratio for this species, all of which are important parameters for demographic modeling and stock assessment that are necessary in order to develop management recommendations.

Previous studies have highlighted that most of the elasmobranchs accessible to the world's fisheries are under threat (Dulvy et al., 2014), and this group, with low resilience to fishing (Cheung et al., 2005) and a protracted period of 14 years for a stock to rebuild

[2] Mendoza, J. J. 2015. Rise and fall of Venezuelan industrial and artisanal marine fisheries: 1950–2010. Fish. Cent., Univ. British Columbia, Work. Pap. Ser. #2015-27, 16 p. [Available at website.]

(Froese and Pauly, 2015), may be considered highly vulnerable. However, the bullnose ray has shown signs of recovery since the implementation of shark-specific management strategies in the southeastern United States (Ward-Paige et al., 2012). Additional fishery-independent research is needed on the bullnose ray to develop effective conservation measures, particularly with regard to mortality, growth estimates, and migration patterns, and to detect temporal and spatial changes in abundance.

Currently, no law is in place to directly regulate catch of bullnose ray. However, this species was previously reported as bycatch in the industrial shrimp trawl fishery (Cervigón et al., 1992), and the total ban of this fishery in Venezuela that began in March 2009 (Article 23, Law of Fisheries and Aquaculture) may be contributing to the conservation of the bullnose ray. In addition, the fishing community in the area of our study has implemented self-management strategies, such as rotation of target species, fishing methods, and locations throughout the year (Tagliafico et al., 2013a). Such local adaptations of fishing practices can provide effective management strategies that would benefit fisheries and endemic marine populations.

Acknowledgments

We thank the fishermen of La Pared for their kind cooperation, allowing us to study their landings. We also appreciate the Instituto Nacional de Investigaciones Agrícolas (INIA) and A. Lárez for help with logistics, L. Gonzalez and J. Marin for their assistance during the field sampling in 2013, E. Guerra and J. Mendoza for statistical advice, and D. West, A. Arraez, J. Sippo, and anonymous referees for their valuable comments.

Literature cited

Anderson, M. J., R. N. Gorley, and K. R. Clarke.
2008. PERMANOVA+ for PRIMER: guide to software and statistical methods, 214 p. PRIMER-E Ltd., Plymouth, UK.

Bizarro, J. J., W. D. Smith, J. F. Márquez-Farías, and R. E. Hueter.
2007. Artisanal fisheries and reproductive biology of the golden cownose ray, *Rhinoptera steindachneri* Evermann and Jenkins, 1891, in the northern Mexican Pacific. Fish. Res. 84:137–146.

Bernardes, R. Á., J. L. deFigueiredo, A. R. Rodrigues, L. G. Fischer, C. M. Vooren, M. Haimovici, and C. L. D. B. Rossi-Wongtschowski.
2005. Peixes de Zona Econômica Exclusiva da Região Sudeste-Sul do Brasil: Levantamento com armadilhas, pargueiras e rede de arrasto de fundo, 295 p. Editora da Universidade de São Paulo, São Paulo.

Castro, J. I.
2013. Historical knowledge of sharks: ancient science, earliest American encounters, and American science, fisheries, and utilization. Mar. Fish. Rev. 75(4):1–26.

Cervigón, F., and A. Alcalá.
1999. Los peces marinos de Venezuela, vol. 5, 231 p. Fundación Museo del Mar, Caracas, Venezuela.

Cervigón, F., R. Cipriani, W. Fisher, L. Garibaldi, M. Hendrickx, A. J. Lemus, R. Márquez, J. M. Poutiers, G. Robaina, and B. Rodríguez.
1992. Guía de campo de las especies comerciales marinas y de aguas salobres de la costa septentrional de Sur América. Fichas FAO de Identificación de Especies para los Fines de la Pesca, 513 p. FAO, Roma.

Cheung, W. W. L., T. J. Pitcher, and D. Pauly.
2005. A fuzzy logic expert system to estimate intrinsic extinction vulnerabilities of marine fishes to fishing. Biol. Conserv. 124:97–111.

Clarke K. R., and R. M. Warwick.
2001. Change in marine communities: an approach to statistical analysis and interpretation, 2nd ed., 172 p. PRIMER-E Ltd., Plymouth, UK.

Conrath, C. L.
2005. Reproductive biology. *In* Management techniques for elasmobranch fisheries (J. Musick and R. Bonfill, eds.), p. 103–126. FAO Fish. Tech. Pap. 474. FAO, Rome.

Dulvy, N. K., S. L. Fowler, J. A. Musick, R. D. Cavanagh, P. M. Kyne, L. R. Harrison, J. K. Carlson, L. N. K. Davisdson, S. V. Fordham, M. P. Francis, C. M. Pollock, C. A. Simpfendorfer, G. H. Burgess, K. E. Carpenter, L. V. J. Compagno, D. A. Ebert, C. Gibson, M. R. Heupel, S. R. Livingstone, J. C. Sanciangco, J. D. Stevens, S. Valenti, and W. T. White.
2014. Extinction risk and conservation of the world's sharks and rays. eLIFE 2014;3:e00590

Froese, R., and D. Pauly (eds.).
2015. FishBase, vers. 10/2015. [World Wide Web electronic publication; available at website, accessed December 2015.]

Ginés, H., C. Angell, M. Méndez, G. Rodríguez, G. Febres, R. Gómez, J. Rubio, G. Pastor, and J. Otaola.
1972. Carta pesquera de Venezuela. I. Áreas del nororiente y Guayana. Monografía 16, 328 p. Fundación La Salle de Ciencias Naturales, Caracas, Venezuela.

Gómez, U. L., C. N. Signori, O. B. F. Gadig, and H. R. S. Santos.
2010. Guia para identificação de tubarões e raias do Rio de Janeiro, 1st ed., 234 p. Technical Books Editora Ltda., Rio de Janeiro.

González, L. W., N. Eslava, and F. Guevara.
2006. Catálogo de la pesca artesanal del estado Nueva Esparta, Venezuela, 222 p. Universidad de Oriente, Cumaná, Venezuela.

Hopkins, T. E., and J. J. Cech Jr.
2003. The influence of environmental variables on the distribution and abundance of three elasmobranchs in Tomales Bay, California. Environ. Biol. Fish. 66:279–291.

Iriarte, L. M.
1997. Embarcaciones, artes y métodos de pesca del estado Nueva Esparta. Monografía 42, 349 p. Fundación La Salle de Ciencias Naturales, Caracas, Venezuela.

Martin, L. K., and G. M Cailliet.
1988. Aspects of the reproduction of the bat ray, *Myliobatis californica*, in central California. Copeia 1988:754–762.

Marval, J. L., and F. Cervigón.
2009. Actividad pesquera en el estado Nueva Esparta, 122 p. Fundación Museo del Mar, Ex Libris, Boca de Río, Venezuela.

McEachran, J. D., and M. R. de Carvalho.
2002. Myliobatidae: eagle rays. *In* The living marine resources of the western central Atlantic. Volume 1: introduction, molluscs, crustaceans, hagfishes, sharks, batoid fishes and chimaeras (K. E. Carpenter, ed.), p. 578–582. FAO Species Identification Guide for Fishery Purposes and American Society of Icthyologists and Herpetologists Special Publication 5. FAO, Rome.

Méndez-Arocha, A.
1963. La pesca en la Isla de Margarita, Venezuela. Monografía 7, 267 p. Fundación La Salle de Ciencias Naturales, Caracas, Venezuela.

Molina, J., and A. Lopez.
2015. Biology of *Myliobatis goodei* (Springer, 1939), a widely distributed eagle ray, caught in northern Patagonia. J. Sea Res. 95:106–114.

R Core Team.
2014. R: a language and environment for statistical computing. R Foundation for Statistical Computing, Vienna, Austria. [Available at website, accessed July 2014.]

Refi, S. M.
1975. Myliobatidae y Dasyatidae del litoral bonaerense de la República Argentina y estudio comparado del mixopterigio (Chondrichthyes, Myliobatoidea). Physis, A 34:121–136.

Schwartz, F. J.
2011. Status of stingrays (Order Myliobatiformes) captured 1972–2010 at two sites in Onslow Bay, Atlantic Ocean, North Carolina. J. N. C. Acad. Sci. 127:35–37.

Schmidt, B. F., H. Harwalis, J. F. Santos-Domingos, A. N. Poscai, and A. F. Amorim.
2012. Ocorrência de *Myliobatis freminvillei* (Lesuer, 1824) na Pesca de parelha do sudeste e sul do Brasil. XV Simpósio de Biologia Marinha; São Paulo, 2–6 Julho, p. 193–195.

Stehmann, M.
2009. *Myliobatis freminvillii*. The IUCN Red List of Threatened Species 2009: e.T161568A5453661.

Suárez, M. M., and C. Bethencourt.
2002. La pesca artesanal en la costa Caribe de Venezuela, 2nd ed., 269 p. Fundación Bigott, Caracas, Venezuela.

Tagliafico, A., N. Rago, and M. S. Rangel.
2013a. Fishery and biology of *Rhinobatos percellens* (Rajiformes: Rhinobatidae) caught by the artisanal fishery at La Pared beach, Venezuela. Rev. Biol. Trop. 61:149–160.
2013b. Biological aspects of rays *Dasyatis guttata* and *Dasyatis americana* (Myliobatiformes: Dasyatidae) caught by the artisanal fishery in Margarita Island, Venezuela. Rev. Biol. Mar. Oceanogr. 48:365–373.

Tagliafico, A., N. Rago, M. S. Rangel, and J. Mendoza.
2012. Exploitation and reproduction of the spotted eagle ray (*Aetobatus narinari*) in the Los Frailes Archipelago, Venezuela. Fish. Bull. 110:307–316.

Velasco, G., M. C. Odonne, and R. P. Lopes.
2011. Records of selective fishing mortality of *Myliobatis goodei* on the southern Brazil coast by beach seine. Braz. J. Oceanogr. 59:397–400.

Ward-Paige, C. A., D. M. Keith, B. Worm, and H. K. Lotze.
2012. Recovery potential and conservation options for elasmobranchs. J. Fish Biol. 80:1844–1869.

White, W. T.
2014. A revised generic arrangement for the eagle ray family Myliobatidae, with definitions for the valid genera. Zootaxa 3860:149–166.

Zar, J.
1996. Biostatistical analysis, 3rd ed., 662 p. Prentice Hall, Upper Saddle River, NJ.

NOAA
National Marine
Fisheries Service

Fishery Bulletin
established 1881

Spencer F. Baird
First U.S. Commissioner
of Fisheries and founder
of *Fishery Bulletin*

Integrating DNA barcoding of fish eggs into ichthyoplankton monitoring programs

Leah A. Lewis[1]
David E. Richardson (contact author)[1]
Evgeny V. Zakharov[2]
Robert Hanner[2]

Email address for contact author: david.richardson@noaa.gov

[1] Northeast Fisheries Science Center
National Marine Fisheries Service, NOAA
28 Tarzwell Drive
Narragansett, Rhode Island 02882

[2] Biodiversity Institute of Ontario
University of Guelph
Guelph, Ontario, Canada N1G 2W1

Abstract—The data collected through ichthyoplankton monitoring surveys provide valuable insight into the spawning dynamics of multiple species. Fish eggs, more than larvae, offer a more precise evaluation of species-specific spawning characteristics; however, egg collections are greatly underused because of the limitations associated with morphology-based identifications. In recent years, a new means of molecular identification, termed *DNA barcoding*, has made species identification readily available across a broad range of taxa. We used DNA barcoding to identify ethanol-preserved fish eggs collected during 2002–2012 along the northeastern U.S. continental shelf. A subsampling protocol was used to select 1603 unidentified eggs for analysis. DNA sequences were successfully obtained from 1495 (93.26%) of these eggs, representing 50 species—many of which have either never before been identified to the species-level as eggs or have been identified previously only to a higher taxonomic level or during specific developmental egg stages. In comparison with past attempts at morphological identification, our molecular identifications comprise a broader diversity of eggs and provide a technique with high success rates of unambiguous identifications that is not sensitive to egg stage. Overall, this work shows that DNA barcoding of fish eggs is sufficiently advanced to be incorporated into long-term, regional-scale ichthyoplankton monitoring programs.

Manuscript submitted 6 April 2015.
Manuscript accepted: 20 January 2016.
Fish. Bull. 114:153–165 (2016).
Online publication date: 5 February 2016.
doi: 10.7755/FB.114.2.3

The views and opinions expressed or implied in this article are those of the author (or authors) and do not necessarily reflect the position of the National Marine Fisheries Service, NOAA.

Pelagic eggs and larvae, collectively referred to as ichthyoplankton, are the life-history stages of fish that are most abundant within the marine epipelagic zone. Because of this prominence, a number of long-term ichthyoplankton monitoring programs have been established worldwide. The data collected through large-scale surveys provide fisheries-independent information on the spawning locations, times, and intensities of multiple species simultaneously. Ichthyoplankton data have also been used to estimate spawning stock biomass (Zeldis, 1993) and to develop long-term indices of abundance (Richardson et al., 2010a). In contrast to larvae, fish eggs provide a more precise means of evaluating the distribution and abundance of spawning fish populations because of the reduced cumulative influence of egg transport and mortality (Ouellet et al., 1997; Richardson et al., 2009). However, the number of identifiable egg characteristics is far fewer than the number of morphological features available for larval identification. Consequently, the major prerequisite—accurate species-level identification from eggs—remains an obstacle for the use of fish eggs in long-term monitoring and management programs.

Historically, the identification of fish eggs has been limited; illustrative guides often reference a small subsample of eggs from known parents or a small quantity of eggs collected during surveys and reared through the larval and juvenile stages (Colton and Marak[1]; Ahlstrom and Moser, 1980; Berrien and Sibunka[2]). On a broad scale, identifications traditionally have been based on morphological characteristics, including egg shape and diameter; number, size, and position of oil globules; width of the perivitelline space; nature of the egg yolk and chorion surface; and embryonic pigmentation.

[1] Colton, J. B., Jr., and R. R. Marak. 1969. Guide for identifying the common planktonic fish eggs and larvae of continental shelf waters, Cape Sable to Block Island. Bur. Commer. Fish., Biol. Lab. Ref. 69-9, 43 p.

[2] Berrien, P. L., and J. D. Sibunka. 2006. A laboratory guide to the identification of marine fish eggs collected on the northeast coast of the United States. 1977–1994. U.S. Dep. Commer., NOAA, Northeast Fish. Sci. Cent. Ref. Doc. 06-21, 162 p.

Several of these features remain relatively constant throughout embryonic development; however, many characteristics are stage specific.

Overall, there are 4 significant limitations involved with morphological identifications. First, natural variation in morphological features of fish eggs, within a species, is common because of the effects of both maternal (Chambers and Leggett, 1996; Marteinsdottir and Steinarsson, 1998; Marteinsdottir and Begg, 2002) and environmental (Chambers and Leggett, 1996; Kucera et al., 2002) factors. Second, overlaps in morphological stages and similarities among the eggs of related and unrelated cryptic taxa can lead to incorrect identifications (Hyde et al., 2005; Berrien and Sibunka[2]; Gleason and Burton, 2012). Third, egg fixation in preservatives causes the loss of natural pigmentation and can obscure the developmental stage of an embryo (Valdez-Moreno et al., 2010). Finally, fixation can cause substantial egg shrinkage, a phenomenon that varies with preservative type and length of exposure (Hiemstra, 1962). In the Northwest Atlantic specifically, descriptions of eggs are lacking for more than 50% of fish species, and for those species for which there are descriptions, characteristics used to confidently identify field-collected specimens may be lacking for some or all stages of egg development (Kendall and Matarese, 1994).

Over the past decade, the use of molecular identification techniques has increased in response to the limitations associated with morphological identifications. For ichthyoplankton, these methods most frequently have involved the use of polymerase chain reaction (PCR) with species-specific primers and probes (Shao et al., 2002; Fox et al., 2005; Hyde et al., 2005; Carreon-Martinez et al., 2010) or the use of multiplex suspension bead arrays (Gleason and Burton, 2012); the former technique is even implemented onboard a research vessel (Hyde et al., 2005) and is used with formalin-preserved samples (Goodsir et al., 2008). Although these methods have been used successfully, the primary focus in these studies was to discriminate among a limited number of species. As a result, these methods rarely have proved versatile enough for use in fisheries monitoring programs or in large-scale egg surveys for which the identification of a wide diversity of species is necessary.

Around 2005, a new means of molecular identification was proposed with the goal of providing a universal approach to species identification. This concept, termed *DNA barcoding*, is based on the premise that the sequence diversity of a single mitochondrial gene, cytochrome *c* oxidase subunit 1 (COI), is suitable for identifying most animal species (Hebert et al., 2003a, 2003b). Concerns over the use of a single locus to discriminate between closely allied species have been stressed since the DNA barcoding movement began; however, multiple studies have concluded that COI analysis is sufficient for species-level diagnoses. For example, this approach has been used successfully to barcode many Australian fish species (Ward et al., 2005) and to reveal overlooked marine species in the Indian Ocean (Zemlak et al., 2009). The method of DNA barcoding has also been used to connect the egg and larval stages of marine species along the coastline of Yucatan, Mexico, to their adult counterparts (Valdez-Moreno et al., 2010) and for a large-scale larval fish study in the Straits of Florida (Richardson et al., 2007; Richardson et al., 2010b). To date, the DNA barcoding database for fishes (Barcode of Life Data System [BOLD], website, accessed March 2015) contains sequences of more than 175,000 specimens, representing more than 15,000 species (Ratnasingham and Hebert, 2007). These advances, coupled with a simultaneous decrease in cost (Richardson et al., 2007), have made it possible to consider the use of DNA barcoding for identification of fish eggs and to incorporate this approach into ecosystem monitoring programs.

In our study, we used DNA barcoding for the large-scale identification of fish eggs. We sequenced DNA from eggs that were selected from a 10-year, multiseasonal archive of 456 ethanol-preserved samples that exists within the Northeast Fisheries Science Center (NEFSC), National Marine Fisheries Service, NOAA. Before 2000, fish eggs were identified by using morphological criteria. Since 2000, fish eggs collected through the NEFSC Ecosystem Monitoring (EcoMon) program have been counted but not identified because of a lack of personnel. The goals of this study are 1) to compare the species identifications, those produced from morphological versus molecular analyses of eggs, in terms of species diversity and taxonomic resolution and 2) to evaluate the feasibility of incorporation of DNA barcoding into long-term, regional-scale ichthyoplankton monitoring programs.

Materials and methods

Sample collection and processing

The NEFSC since 1971 has conducted ichthyoplankton surveys multiple times annually along the northeastern U.S. continental shelf between Cape Hatteras, North Carolina, and Nova Scotia, Canada (Richardson et al., 2010a). During these surveys, ichthyoplankton was sampled throughout the water column (to a depth within 5 m of the seafloor or to a maximum depth of 200 m) with paired bongo samplers that had diameters of 61 cm and that were equipped with 333-μm mesh nets. These samples had been preserved in formalin and—because formalin fixation causes significant damage to DNA, inhibiting amplification of the target COI gene—therefore were not considered suitable for this project (Hajibabaei et al., 2005). However, an additional bongo net, with a 20-cm diameter, was included on the towing cable, just above the 61-cm bongo net at about 15–20% of the sampling stations. Samples collected in the smaller net had been fixed and preserved in 95% ethanol (EtOH).

For our study, we used an archive of 456 EtOH-preserved ichthyoplankton samples that were collected

during NEFSC surveys in the winter (January–February), late spring (May–June), late summer (August) and late autumn (November–December) over a 10-year period (2002–2012). Temperature and salinity profiles through the water column were collected with an SBE 19plus V2 SeaCAT[3] conductivity, temperature, and depth (CTD) profiler (Sea-Bird Electronics Inc., Bellevue, WA) attached to the tow wire above the bongo nets. Sea-surface temperatures (SSTs) were recorded during the upcast of the CTD profiler at the shallowest depth bin. Details on the collection localities and sampling dates were deposited within the publically available BOLD project file entitled "NIFEB: Fish Eggs Barcoding."

Ichthyoplankton samples preserved in EtOH were sorted manually for all fish eggs and larvae in the laboratory. Fish eggs were removed from a sample and transferred to 7-mL (2-dram) glass vials filled with 95% EtOH. No morphological identifications were attempted during or after the sorting procedure.

Subsampling of eggs for molecular identification

The total number of eggs collected in all of the samples exceeded our molecular processing capacity. For that reason, we implemented a 2-stage subsampling procedure designed to determine the diversity of eggs within each sample. For the first stage of subsampling, a maximum number of 10 eggs were randomly selected for identification from each sorted sample. Individual eggs were first digitally photographed and measured (in millimeters) with Nikon imaging software (NIS-Elements BR, vers. 2.3, Nikon Instruments Inc., Melville, NY) and a color digital camera (Nikon DXM-1200C) mounted on a stereo microscope (Nikon SMZ1500) under both reflected and transmitted light. Fish eggs were then placed in 96-well plates with one egg and one drop of 95% EtOH per well. A negative control well also was included on each plate.

Of the initial 456 samples, 73 contained >10 eggs and were subjected to a second round of subsampling that that was based on both egg measurements and the results from the initial round of molecular identifications. For this second round of subsampling, we measured the diameter of the remaining unidentified eggs in the samples. Histograms of egg diameters within 0.05-mm-diameter bins were developed for each sample, and additional eggs were chosen for molecular identification from any 0.05-mm-diameter bin that either did not include an egg identified during the first round of molecular identification or contained a high number of eggs and multiple species of eggs. The intent of this second round of subsampling was to ensure that the diversity of eggs within a sample was identified, while avoiding repeatedly sequencing the same species of egg at the same sampling station. As a result of the opaqueness of ethanol-preserved eggs, we did not use any other morphological feature (other than egg diameter) for subsampling.

To speed up the subsampling process, we developed an automated egg measuring graphical user interface with the Image Processing Toolbox in MATLAB, vers. R2012A (The MathWorks Inc., Natick, MA). Up to 40 eggs at a time were digitally photographed on an acrylic plate containing a rectangular well specifically sized for the digital image taken at 3× magnification (Fig. 1A). A black and white threshold was then manually applied to each image (Fig. 1B) and then the Hough transformation was applied to the thresholded image (Fig. 1C). The Hough transformation is designed to find circles within an image, including circles with a broken outer border. The interface that we developed contained slider bars that allow a user to optimize the black and white thresholding process for an individual picture, as well as the minimum circle quality used in the find circle algorithm. Finally, manual editing of the automatically measured circular egg was performed, and measurements of ovoid eggs were added (Fig. 1D). The result of this procedure was a text file that contained the diameters of each measured circular egg or the long axis and short axis of ovoid eggs.

Egg abundances are reported as the number of eggs per 10 m^2 of water. To account for the subsampling, each station's total egg abundance within each 0.05-mm egg-diameter bin was first calculated. For each diameter bin, species were assigned in proportion to the available molecular identifications within that bin with a procedure analogous to the use of age–length keys. Oval eggs, which corresponded to 1 of 3 anchovy species, were excluded from this process because they could be assigned to species based solely on shape (long axis:short axis) and size.

Molecular identification protocol

Prepared plates were sent by mail to the University of Guelph's Canadian Centre for DNA Barcoding, a molecular identification laboratory with a proven success rate and developed database capable of accommodating large data output associated with high-throughput DNA sequencing. Key sample data, including specimen collection information, voucher image files, and a plate record (sample array details for each plate) were sent electronically to the Canadian Centre for DNA Barcoding. This information was organized within the BOLD online database, and each COI barcode sequence was connected to its source specimen following DNA barcode analysis.

Standard DNA barcoding protocols were followed for all analytical steps, including DNA extraction, PCR, and DNA sequencing. Submitted samples were subjected to overnight lysis in a lysis buffer with proteinase K (Thermo Fisher Scientific Inc., Waltham, MA), followed by DNA extraction onto a glass fiber membrane (Pall Corp., Port Washington, NY) by using an automated protocol (Ivanova et al., 2006). A barcode region of 658

[3] Mention of trade names or commercial companies is for identification purposes only and does not imply endorsement by the National Marine Fisheries Service, NOAA.

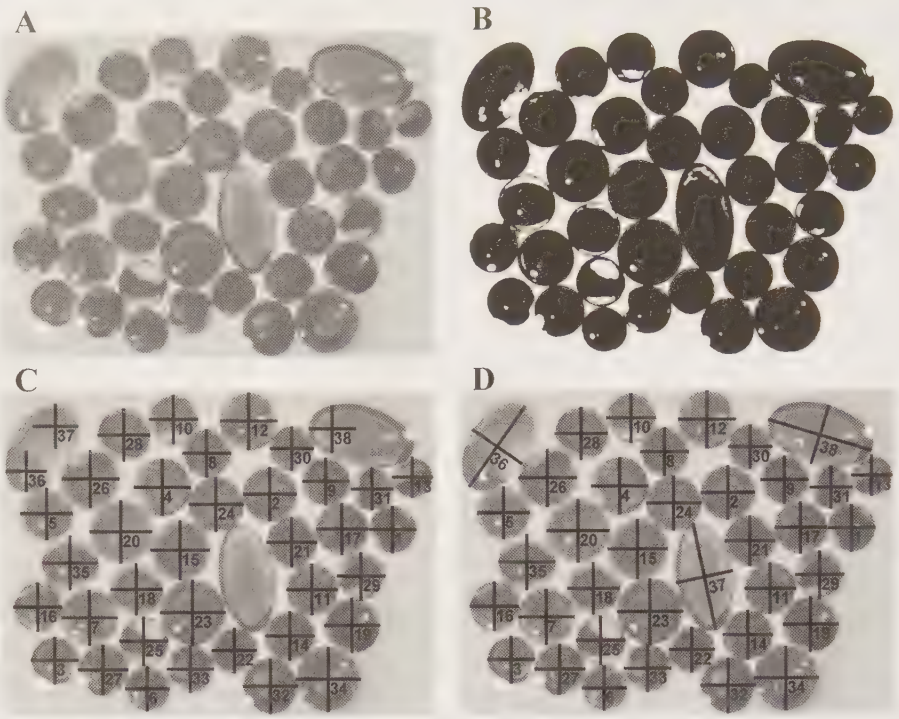

Figure 1

Depiction of the image analysis process for rapid egg measuring: (**A**) fish eggs are grouped and digitally photographed on a white background; (**B**) a black and white threshold is applied to the image; (**C**) after applying the Hough transformation to the black-and-white image, most eggs are found and accurately measured (mm); and (**D**) measured egg diameters then can be edited manually and oval anchovy egg measurements can be added. The center and diameters (or long and short axis of ovoid eggs) are indicated with the cross hair symbols. Egg numbers on the images are also indicated and can be linked back to the output text files.

base pairs (bp) of the mitochondrial gene COI was amplified with primer cocktails C_FishF1t1 + C_FishR1t1 and AquaF2 + C_VR1LRt1 (Ivanova et al., 2012). The PCR mix included 6.25 µL of 10% trehalose, 1.25 µL 10× PCR buffer, 0.625 µL (2.5 mM) $MgCl_2$, 0.125 µL (10 µM) forward and reverse primer cocktail, 0.625 µL (10 mM) deoxyribonucleotide triphosphates (dNTPs), 0.625 µL Platinum Taq polymerase (Thermo Fisher Scientific Inc.), 3 ul H_20 and 1 µL of DNA template.

The following cycle conditions were used to run PCRs: 1 min at 94°C followed by 5 cycles of 30 s at 94°C; 40 s at 55°C and 1 min at 72°C, followed by 35 cycles of 30 s at 94°C; 40 s at 55°C, and 1 min at 72°C, with a final extension of 10 min at 72°C. PCR products were visualized by using agarose gel electrophoresis with buffer-less precast E-Gel system (Thermo Fisher Scientific Inc.). Successful amplicons were cycle sequenced by using BigDye Terminator vers. 3.1 (Thermo Fisher Scientific Inc.) and the manufacturer's recommended protocols. Sequencing products with incorporated BigDye Terminator were purified with the bead cleanup method of *solid phase reversible immobilization* (SPRI; Agencourt Bioscience Corp., Beverly, MA) and were analyzed on an Applied Biosystems 3730xl DNA Sequencer (Thermo Fisher Scientific Inc.).

Applied Biosystems trace files for each specimen were assembled into contigs (contiguous sequences of DNA) with the use of Codon Code Aligner software (CodonCode Corp., Centerville, MA). Resulting consensus sequences and trace files were uploaded to the NIFEB project file on the BOLD data system.

Sequence analysis and species identification

For a comparison of sequences and species identification, we used the BOLD system and its analytical tools. Neighbor-joining taxonomic identification trees of Kimura 2-parameter distance were built on the basis of COI-5P (5′ region) nucleotide sequence data to provide a graphic representation of the pattern of divergence between species (Saitou and Nei, 1987). Regardless of bp length, medium- and high-quality COI sequences

were queried against the web-based BOLD database. We used a threshold of a 99% match to assign a match to species. For specimens for which the BOLD engine failed to find a match, sequences were applied directly to the Standard Nucleotide BLAST on GenBank (National Center for Biotechnology Information, website). Sequence data, electropherograms, and primer details for specimens are available within the completed NIFEB project file on BOLD. Sequence data was also submitted to GenBank (accession numbers: KP110771–KP112146). Low-quality sequences can often provide sufficient information to identify a sample to species; however, we chose to exclude them from subsequent analyses to ensure the reliability of our database.

Data analysis

Standard box plots were used to present the SST range and size range of each species of egg that we collected and barcoded. In addition, for species that were identified from at least 15 stations, we further sought to determine the correlation between egg measurement and the SST at sampling stations. The graphical and statistical tools available through RStudio (RStudio, Boston, MA) were used to perform linear regression analysis on the effects of SST on egg diameter. Notably, the process of measuring and photographing eggs did not occur for the first 2 plates (190 eggs) of samples; therefore, these eggs were excluded from the analyses where egg diameter was used.

For SST in our analyses, it was assumed that the eggs collected at a station were located above the thermocline or that the waters were well mixed. During the late fall (November–December) and winter (January–February), the water column in our region is well mixed and, therefore, the vertical distribution of eggs has little effect on the temperature they experience. The same is true year-round in the shallow areas on Georges Bank. However, during the late spring (May–June) and summer (August), the water column in our region is stratified. Typically, fish eggs collected in ichthyoplankton sampling are positively buoyant and concentrate in the upper water column, but there are exceptions (Conway et al., 1997). Because our sampling was not vertically stratified, we relied on SST as the best estimate of the temperature experienced by the eggs.

Results

In total, DNA was sequenced from 1603 unidentified fish eggs collected at 456 stations and that were processed as ethanol-preserved ichthyoplankton samples. Of these eggs, 93.26% (1495 eggs) were sequenced successfully, providing medium- or high-quality barcodes suitable for species-level identifications. Of the 108 unidentified eggs, 60 eggs (3.74%) failed both first- and second-round sequencing attempts, and 8 eggs (0.50%) were flagged because of contamination that occurred at an unknown point during the barcoding process. The remaining 40 eggs (2.50%) produced low-quality sequences. In many cases, identifications could be assigned to these low-quality sequences; however, we chose to be conservative and classify these eggs as unidentified. Sequence analysis revealed that the 1495 successfully sequenced fish eggs represented 50 identified species, 49 of which could be definitively matched to species-level barcodes, and 1 taxa with 12 eggs produced a match to a specimen identified previously only at the family level (Engraulidae) on GenBank (Table 1).

The number of identified eggs per species ranged from 1 to 196. The 4 most frequently identified eggs were those of silver hake (*Merluccius bilinearis*), fourspot flounder (*Hippoglossina oblonga*), Gulf Stream flounder (*Citharichthys arctifrons*), and red hake (*Urophycis chuss*); together, these 4 species accounted for more than 45% of all successful barcode identifications. In comparison with previous morphological attempts at fish egg identification in the northeastern United States (Colton and Marak[1]; Berrien and Sibunka[2]), the eggs of our barcoded species fit into 3 general categories: category I (6 of our 50 species) are eggs that have never before been identified to the species-level as eggs; category II (33 species) describes eggs that have historically been identifiable only at higher taxonomic levels (genus or family) or at the species level during specific stages of development (i.e., eggs at mid to late stages); and category III (11 species) contains eggs that are well described and can be identified confidently to species level through the use of morphological criteria at all stages of development (Table 1).

Overall, egg abundances varied significantly with sampling season (Fig. 2, A–D). In aggregate, the greatest abundances and diversity of eggs were found during the sampling periods of late summer (August) and late spring (May–June). The lowest abundance of eggs was encountered in late autumn (November–December), and the lowest diversity was found in the winter (January–February). Of the 50 species with eggs identified, 25 species had eggs collected during multiple seasons (indicative of cross-seasonal or elongated spawning). The most frequently observed cross-seasonal collection pattern was between late spring and late summer; however, the eggs of Atlantic cod (*Gadus morhua*) and pollock (*Pollachius virens*) were collected throughout late autumn and winter. The eggs of only 1 species, offshore hake (*Merluccius albidus*), were collected in all 4 sampling seasons. The 3 most abundant species of eggs identified, with all seasons combined, were red hake, Gulf Stream flounder, and silver hake (Table 1).

The successfully barcoded fish eggs were collected at a wide range of temperatures; recorded SSTs ranged from 3.11°C to 27.02°C (Table 1). In general, the SST range of an individual species was much narrower (Fig. 3). Eggs of haddock (*Melanogrammus aeglefinus*), American plaice (*Hippoglossoides platessoides*), and spotted pikeconger (*Hoplunnis tenuis*) were collected at the lowest average SSTs (4.63°C, 7.15°C, and 7.29°C,

Table 1

Results from the molecular identification of fish eggs with the use of DNA barcoding; number of identified eggs per species (*N*) and the number of stations (no. sta.) at which eggs of each species were found. Calculated abundances (number of eggs per 10 m^2 of water) by season for each species and the identification category (cat.) of the eggs for each species are also included: category I eggs have never before been identified to species-level as eggs; category II eggs have been identified previously only at higher taxonomic levels or to species-level at specific stages of development; and category III eggs are well-described and can be confidently identified to species-level at all stages of development. For each species, the mean egg diameter and size range are listed as well, along with the mean and range of collection-day sea-surface temperatures (SSTs).

					Calculated abundances						
Species	Family	Common name	*N*	No. sta.	Jan–Feb	May–Jun	Aug	Nov–Dec	Cat.	Mean diameter (mm)	Mean SST (°C)
Merluccius bilinearis	Merlucciidae	silver hake	196	59	0	18.2	92.3	2.1	III	0.92 *(0.73-1.06)*	15.3 *(8.6-23.2)*
Hippoglossina oblonga	Paralichthyidae	fourspot flounder	184	72	0	11.0	29.2	0	II	0.93 *(0.76-1.08)*	17.4 *(9.0-26.3)*
Citharichthys arctifrons	Paralichthyidae	Gulf Stream flounder	153	45	0	23.9	89.4	0	II	0.72 *(0.59-0.83)*	19.2 *(9.4-27.0)*
Urophycis chuss	Phycidae	red hake	144	53	0	4.7	210.2	0.3	II	0.73 *(0.62-0.81)*	18.0 *(10.9-26.3)*
		Unidentified	108	64	10	5.6	18.9	8.5		1.02 *(0.57-1.71)*	13.4 *(3.1-25.9)*
Scophthalmus aquosus	Scophthalmidae	windowpane	81	29	0	11.3	10.1	0.8	II	1.00 *(0.85-1.17)*	13.2 *(6.4-17.7)*
Limanda ferruginea	Pleuronectidae	yellowtail flounder	80	22	0	54.7	0.8	0	II	0.80 *(0.69-0.94)*	9.4 *(5.4-15.9)*
Peprilus triacanthus	Stromateidae	butterfish	52	22	0	14.7	10.3	0	II	0.73 *(0.57-0.85)*	18.6 *(11.9-25.9)*
Paralichthys dentatus	Paralichthyidae	summer flounder	50	16	0	0.7	0	16.0	III	0.96 *(0.76-1.10)*	15.0 *(11.9-17.5)*
Prionotus carolinus	Triglidae	northern searobin	49	10	0	0	22.7	0.4	II	0.98 *(0.87-1.11)*	24.7 *(16.1-26.8)*
Gadus morhua	Gadidae	Atlantic cod	47	15	15.5	0	0	9.1	II	1.34 *(1.15-1.71)*	8.6 *(3.1-11.0)*
Tautogolabrus adspersus	Labridae	cunner	45	17	0	23.3	1.6	0.0	II	0.88 *(0.77-1.00)*	13.8 *(9.0-20.4)*
Melanogrammus aeglefinus	Gadidae	haddock	44	10	41.0	1.5	0	0	II	1.46 *(1.25-1.62)*	4.6 *(3.1-10.2)*
Enchelyopus cimbrius	Lotidae	fourbeard rockling	35	19	0	14.1	1.0	0	II	0.75 *(0.65-0.83)*	11.0 *(7.6-15.3)*
Anchoa mitchilli	Engraulidae	bay anchovy	34	6	0	54.7	0	0	III	0.91 *(0.78-1.05)*	18.2 *(12.3-19.9)*
Pollachius virens	Gadidae	pollock	34	10	1.2	0	0	21.0	III	1.14 *(0.93-1.29)*	9.5 *(5.9-11.0)*
Etropus microstomus	Paralichthyidae	smallmouth flounder	23	9	0	4.5	2.0	0.0	II	0.65 *(0.57-0.73)*	19.8 *(16.2-26.7)*
Scomber scombrus	Scombridae	Atlantic mackerel	22	14	0	7.9	0.0	0.0	III	1.14 *(1.06-1.22)*	11.2 *(8.2-12.8)*
Merluccius albidus	Merlucciidae	offshore hake	19	9	0.4	2.0	2.9	0.6	III	1.13 *(1.08-1.24)*	17.9 *(11.1-25.1)*
Glyptocephalus cynoglossus	Pleuronectidae	witch flounder	18	12	0	3.2	2.1	0	II	1.14 *(1.06-1.29)*	11.0 *(8.2-16.7)*
Tautoga onitis	Labridae	tautog	17	7	0	5.5	0.4	0	II	0.99 *(0.86-1.07)*	15.0 *(9.4-24.8)*
Urophycis regia	Phycidae	spotted hake	16	7	1.0	0	0.9	1.8	II	0.74 *(0.67-0.82)*	17.0 *(7.3-25.1)*
Micropogonias undulatus	Sciaenidae	Atlantic croaker	15	2	0	0	19.3	0	II	0.72 *(0.65-0.77)*	26.0 *(25.9-26.0)*
Brosme brosme	Lotidae	cusk	15	7	0	6.4	0.5	0	II	1.25 *(1.08-1.42)*	9.5 *(5.4-12.9)*
Anchoa hepsetus	Engraulidae	striped anchovy	15	6	0	5.5	0	0	III	1.44 *(1.23-1.64)*	19.5 *(18.2-20.4)*
Astroscopus y-graecum	Uranoscopidae	southern stargazer	13	9	0	0	2.9	0	II	1.60 *(1.40-1.81)*	24.1 *(16.2-27.0)*
	Engraulidae	anchovy spp.	12	3	0	0	55.2	0	I	0.75 *(0.68-0.84)*	25.6 *(23.3-26.0)*
Prionotus evolans	Triglidae	striped searobin	11	5	0	2.4	0.2	0	II	1.10 *(1.01-1.18)*	16.4 *(12.3-25.1)*
Centropristis striata	Serranidae	black sea bass	7	5	0	0.5	1.4	0	II	0.86 *(0.77-0.97)*	23.4 *(20.1-26.8)*
Orthopristis chrysoptera	Haemulidae	pigfish	7	1	0	0	0	0	II	no data	19.5 *(19.5)*
Menticirrhus americanus	Sciaenidae	southern kingfish	7	3	0	0.9	0.1	0	I	0.77 *(0.76-0.79)*	19.8 *(18.7-24.1)*
Brevoortia tyrannus	Clupeidae	Atlantic menhaden	5	3	0.5	0.7	0	0	III	1.35 *(1.17-1.57)*	12.3 *(3.1-15.2)*
Trichiurus lepturus	Trichiuridae	Atlantic cutlassfish	5	1	0	0	0.9	0	I	1.63 *(1.57-1.66)*	26.8 *(26.8)*
Ophichthus cruentifer	Ophichthidae	margined snake eel	5	4	0	0	3.3	0	III	2.43 *(2.29-2.52)*	22.0 *(18.1-25.2)*
Sarda sarda	Scombridae	Atlantic bonito	4	1	0	0	0	0	II	1.26 *(1.26)*	19.0 *(19.0)*
Auxis rochei	Scombridae	bullet tuna	4	2	0	0	1.2	0	II	0.86 *(0.79-0.89)*	25.7 *(25.0-26.3)*
Hippoglossoides platessoides	Pleuronectidae	American plaice	3	3	0.4	0.7	0	0	III	2.05 *(2.00-2.13)*	7.1 *(3.1-12.9)*
Pomatomus saltatrix	Pomatomidae	bluefish	3	2	0	0	1.6	0	II	0.72 *(0.72)*	21.3 *(19.5-24.9)*
Symphurus diomedeanus	Cynoglossidae	spottedfin tonguefish	3	2	0	0	0	0.7	II	0.75 *(0.71-0.78)*	15.8 *(15.7-15.8)*
Cynoscion regalis	Sciaenidae	weakfish	3	1	0	2.6	0	0	II	0.80 *(0.76-0.82)*	19.9 *(19.9)*
Menticirrhus saxatilis	Sciaenidae	northern kingfish	2	1	0	0	0	0	II	no data	19.0 *(19.0)*
Engraulis eurystole	Engraulidae	silver anchovy	2	1	0	0	0	0	III	1.32 *(1.32)*	19.5 *(19.5)*
Lopholatilus chamaeleonticeps	Malacanthidae	tilefish	2	1	0	0	0.7	0	II	1.29 *(1.27-1.30)*	25.1 *(25.1)*
Urophycis tenuis	Phycidae	white hake	2	1	0	1.1	0	0	II	0.77 *(0.76-0.78)*	22.0 *(22.0)*
Symphurus plagiusa	Cynoglossidae	blackcheek tonguefish	1	1	0	0	0.9	0	II	0.57 *(0.57)*	26.0 *(26.0)*
Lepophidium profundorum	Ophidiidae	fawn cusk-eel	1	1	0	0	0	0.4	II	1.01 *(1.01)*	13.1 *(13.1)*
Caulolatilus microps	Melacanthidae	grey tilefish	1	1	0	0	0	0	I	no data	17.6 *(17.6)*
Sciaenops ocellatus	Sciaenidae	red drum	1	1	0	0	0.2	0.0	II	0.80 *(0.80)*	26.8 *(26.8)*
Archosargus probataocephalus	Sparidae	sheepshead	1	1	0	0	0	0	II	no data	19.5 *(19.5)*
Hoplunnis tenuis	Nettastomatidae	spotted pikeconger	1	1	0.5	0	0	0	I	2.19 *(2.19)*	7.3 *(7.3)*
Hemanthias aureorubens	Serranidae	streamer bass	1	1	0	0	0	0.3	I	0.72 *(0.72)*	15.8 *(15.8)*
		Grand total:	1603		70.2	282.3	583.2	61.9			

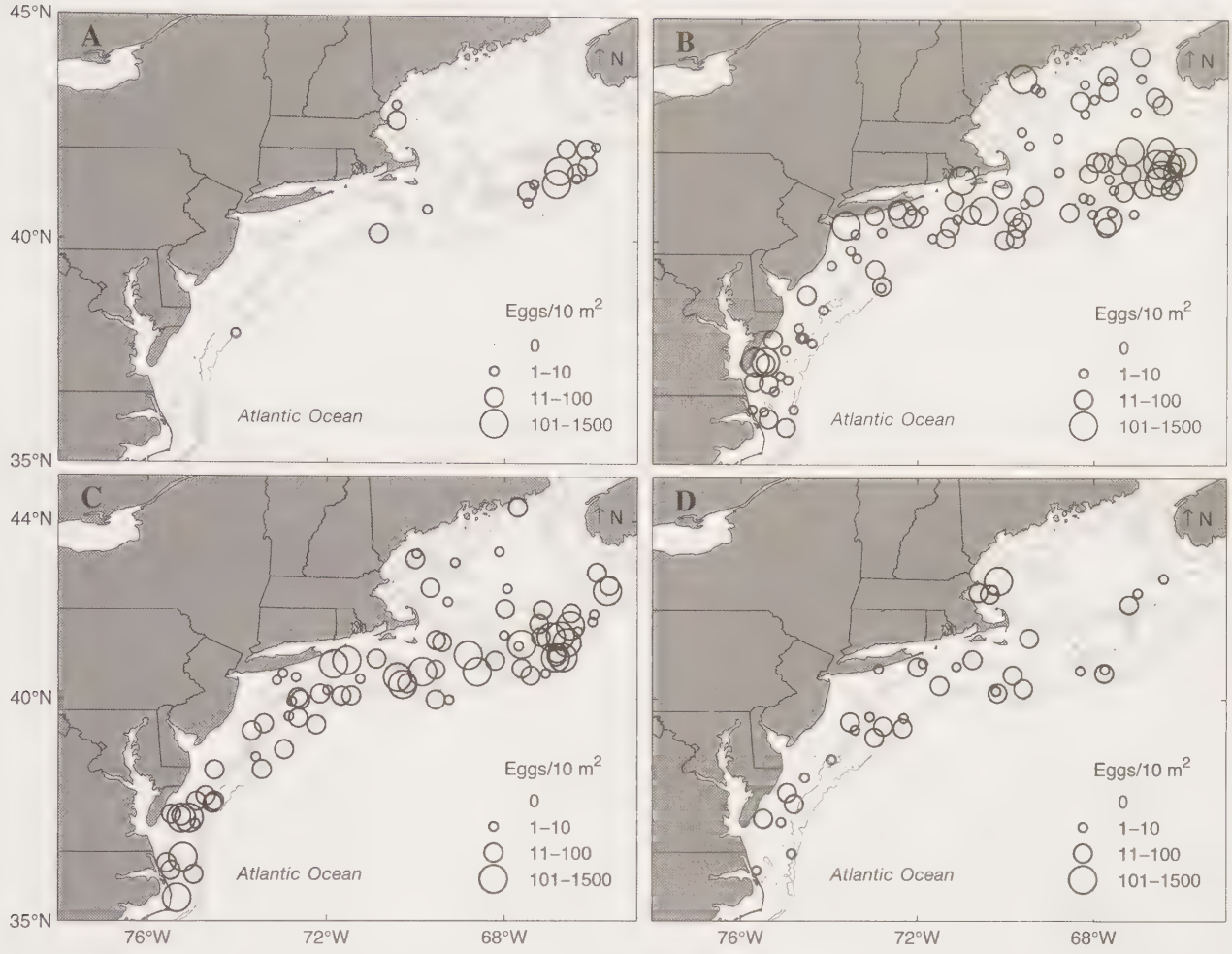

Figure 2

Maps showing the locations of calculated egg abundances, reported as the number of eggs per 10 m^2 of water, based on sort counts and station haul factor values from ichthyoplankton samples collected along the northeastern U. S. continental shelf during 2002–2012 by the NOAA Northeast Fisheries Science Center during its 4 sampling seasons of (**A**) winter (January–February), (**B**) late spring (May–June), (**C**) late summer (August), and (**D**) late autumn (November–December).

respectively), and the singular eggs of Atlantic cutlassfish (*Trichiurus lepturus*) and red drum (*Sciaenops ocellatus*) were each collected at the highest recorded temperature of 26.84°C.

Egg size also varied significantly between species; measured diameters of the successfully barcoded eggs ranged from 0.57 mm to 2.52 mm (Fig. 4). The eggs of blackcheek tonguefish (*Symphurus plagiusa*), smallmouth flounder (*Etropus microstomus*), and butterfish (*Peprilus triacanthus*) were smallest on average; each species had one egg with a measured diameter of 0.57 mm. On the opposite end of the scale, eggs of margined snake eel (*Ophichthus cruentifer*) were the largest, with an average egg diameter of 2.43 mm (N=5) (Table 1). The egg size range of Atlantic cod was the greatest with a difference of 0.56 mm separating the smallest and largest diameter measurements (N=47). Diameters for the various species of identified anchovies were based on long-axis measurements because eggs of these species are naturally ovoid in shape.

For barcoded species that were identified from at least 15 stations, egg measurement and collection data were further analyzed to determine correlations between egg size and SST. Of the 11 species that met the 15-station requirement and were tested, 5 species displayed significant trends (P<0.05 or 5%) between SST and average egg diameter (Table 2, Fig. 5, A–E), with yellowtail flounder (*Limanda ferruginea*) being the only species to illustrate a positive correlation between SST and egg diameter.

Discussion

One of the primary goals for this study was to compare our results from the molecular identification of

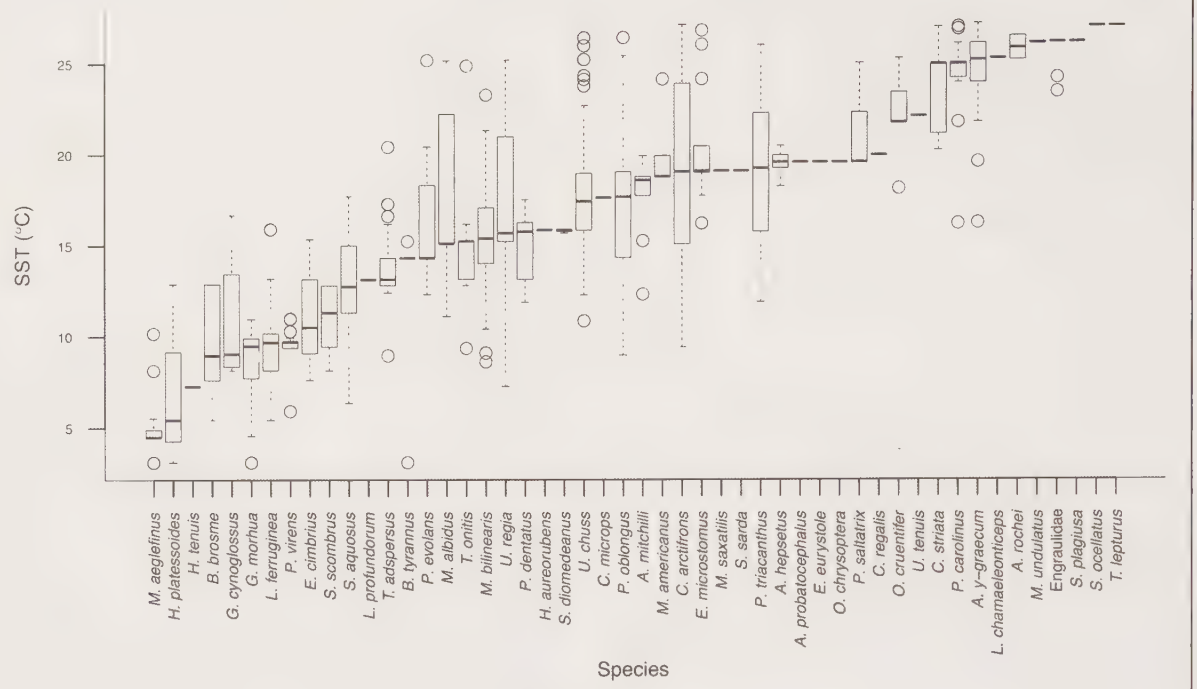

Figure 3

Box plot illustrating the ranges of sea-surface temperature (SST) (in degrees Celsius) for the collection day for each of the 50 species of eggs that were successfully identified by using DNA barcoding. For species with more than 1 identified egg a box is drawn to include SSTs within the first and third quartiles; dashed whisker lines extend from the box to the minimum and maximum SST observed. The median SST for the collection day for each species is marked by a thick, dark horizontal band, and outlying SSTs are indicated with open circles.

fish eggs with previous results from morphological identifications. Because of several inherent differences in methods, we were unable to conduct a direct comparison between morphological and molecular identification from the same specimens. Morphological egg identifications at the NEFSC were discontinued in the early 2000s because the involved individuals retired. Moreover, these identifications were performed on formalin-preserved eggs, which are less suitable for use in a DNA-barcoding approach. Specialized techniques have been developed to allow for the molecular identification of formalin-preserved material, but these procedures typically are more costly than our approach and use only very short DNA fragments. In contrast to formalin-preserved eggs, ethanol-preserved eggs can be readily identified with molecular techniques. However, ethanol denatures fish egg proteins, obscuring many of the internal morphological characters used for staging and identification. For this reason, the only morphological character we recorded for each molecularly identified egg was egg diameter; other characters could not clearly be resolved on all specimens. For some species, particularly those species with a large perivitelline space, such as Atlantic menhaden (*Brevoortia tyrannus*), egg shrinkage appears to differ between ethanol and formalin preservation, limiting comparisons of egg-size ranges among our data and historical data. Because of the impossibility of making direct specimen-by-specimen comparisons, we focused our analyses on broader patterns of species composition and diversity.

Overall, our molecular identifications represented a broader diversity of eggs than did the morphological identifications, including unexpectedly encountered taxa, such as white hake (*Urophycis tenuis*), which was not thought to spawn in the Gulf of Maine, as well as taxa that have previously been considered unidentifiable. In the past, many egg identifications were possible only to the genus level, whereas >93% of our barcoded fish eggs were identifiable to species; of our successfully barcoded eggs, 12 were identifiable only to the family level (Engraulidae) owing simply to the fact that this particular species has not yet been barcoded. Furthermore, our approach provides a technique with high success rates of unambiguous identifications and that is not sensitive to developmental egg stages. Historically, for morphological egg identifications, a large proportion of eggs was assigned to species in part by using nondiagnostic criteria, such as the presence of late-stage eggs of a species in the sample or the time and location of collection of the sample.

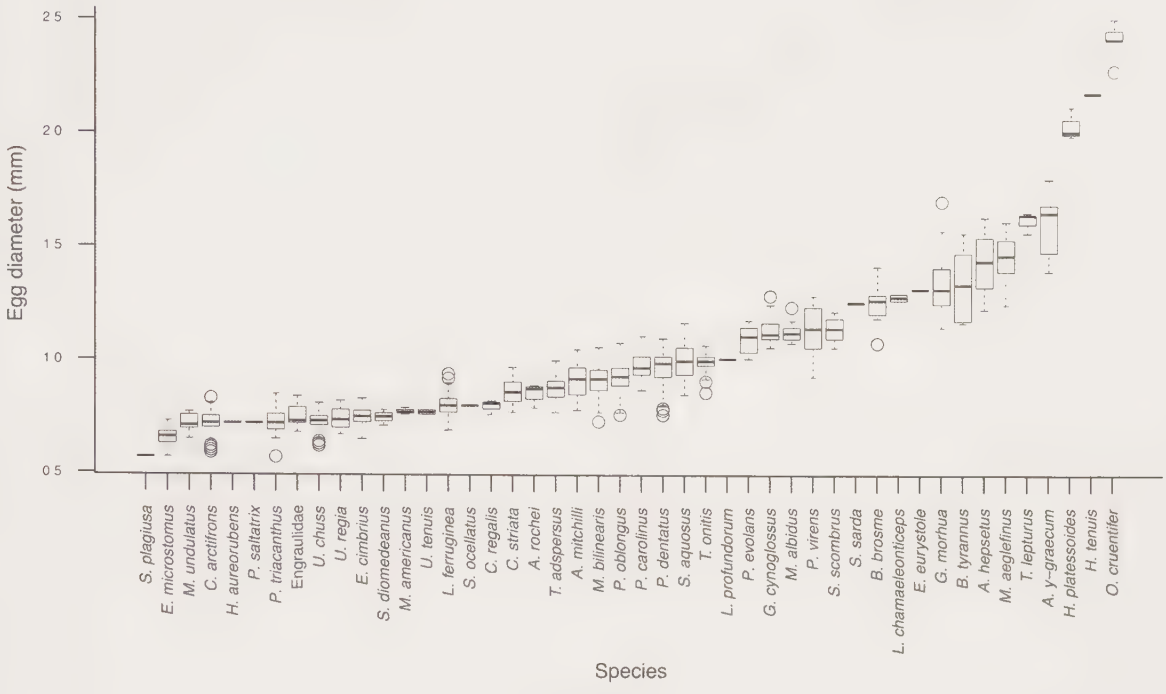

Figure 4

Box plot showing the measured egg diameter ranges (in millimeters) for 46 of the 50 species that were successfully identified by using DNA barcoding. Four species were excluded from the plot because of missing measurements of egg diameters. Egg diameters for the various identified species of anchovies (*Anchoa mitchilli*, *Engraulis eurystole*, and *Anchoa hepsetus*) were based on long-axis measurements because these eggs are naturally ovoid in shape

In general, the morphological identification of fish eggs has been problematic; therefore, the diversity of species subject to egg monitoring has been very limited. For example, the daily egg production method has been used successfully to estimate the biomass of a number of clupeoid fishes as well as Atlantic mackerel (*Scomber scombrus*) (Alheit, 1993; Priede and Watson, 1993; Stratoudakis et al., 2006). However, these successes have been limited taxonomically, and, for other species, substantial technical problems have emerged.

In an effort to compare 2 independent estimates of seasonal egg production and mortality for Atlantic cod and haddock on Georges Bank, Lough et al. (2008) stated directly that the early egg stages of both species are indistinguishable from one another and, furthermore, that estimates of early-stage egg abundance based on extrapolations of morphological identifications of late-stage eggs are likely inaccurate—stressing the need for improved spawning ground mapping with the development of DNA-based identification techniques. Similarly, in the Irish Sea, the use of TaqMan DNA technology confirmed the overestimation of cod egg abundance due to an extremely high rate of morphology-based misidentifications of "cod-like" eggs (Fox et al., 2005). In lower latitudes, where species diversity is much higher, the breadth of these problems is even more striking and the morphological identification of fish eggs is most often not even attempted (Kendall and Matarese, 1994).

Although the cost of DNA barcoding has decreased in recent years (Richardson et al., 2007), the cost per sample still presents an issue—especially for large-scale monitoring programs, such as ichthyoplankton surveys. For programs without any internal capabilities, the cost of having the molecular identification performed by an outside group is currently $14–20 per sample, for all steps in the process. For our program, performing this work internally would have required initial expenses to purchase equipment and set up laboratory space, reoccurring annual expenses to hire staff and maintain equipment, and the standard per sample expenses for reagents. The cost of doing the work internally would, therefore, have far exceeded the costs of working with an external partner—a pattern we expect would hold for most monitoring programs. The subsampling procedure we have developed is one means of reducing total barcoding cost. The development of an automated egg measuring tool based on image analysis software allowed us to optimize our sampling. Although we did not target a specific taxon in our sampling, such a direction is possible if DNA barcoding is combined with an efficient subsampling tool to target specific

Table 2

Results from the analysis of the effect of temperature on egg diameter for barcoded fish species that were identified from at least 15 stations in the northeastern U.S. continental shelf between Cape Hatteras, North Carolina, and Nova Scotia, Canada. Both *P*-values and the coefficient of determinations (r^2) were calculated with linear regression analysis of SST versus measured egg diameter (in millimeters). Species that displayed a significant trend between SST and egg diameter ($P<0.05$ or 5%) are indicated with an asterisk and are visually illustrated in Figure 5, A–E.

Species	*N*	Number of stations	*P*	r^2
Hippoglossina oblonga *	184	72	<0.0001	0.2335
Merluccius bilinearis	196	59	0.1901	0.0100
Urophycis chuss	144	53	0.3175	0.0070
Citharichthys arctifrons *	153	45	0.0438	0.0300
Scophthalmus aquosus	81	29	0.8347	0.0006
Peprilus triacanthus *	52	22	<0.0001	0.5083
Limanda ferruginea *	80	22	0.0012	0.1277
Enchelyopus cimbrius	35	19	0.1160	0.0732
Tautogolabrus adspersus	45	17	0.2615	0.0322
Paralichthys dentatus	50	16	0.0920	0.0580
Gadus morhua *	47	15	<0.0001	0.4951

species. This combination could make this approach a more cost-efficient one for small-scale projects.

Although other lower-cost techniques for molecular identification do exist, most of them are limited in regard to research scope. Hyde et al., (2005) successfully implemented multiplex PCR onboard a research vessel to identify fish eggs and larvae in real time; however, this approach is best-suited for identifications of 5–20 species at a time. Alternatively, the use of multiplex suspension bead arrays for the identification of fish eggs is lower in cost than DNA barcoding and similar in its high-throughput capability, but this technique can identify an egg only if a probe for that species is included in the array (Gleason and Burton, 2012)—a restriction that is not encountered with DNA barcoding. Where our specific approach to molecular identification falls short is that it is not suitable for use with formalin-preserved eggs, which are easier to stage than ethanol-preserved eggs. Applications, such as the daily egg production method, that require the ability to resolve egg stages, would benefit greatly with the ability to use formalin-preserved samples. Certain molecular identification approaches, targeted at specific species, have been successfully applied to formalin material (Goodsir et al., 2008), and techniques with DNA barcoding on shorter fragments and formalin-preserved material are being developed (Zhang, 2010).

Looking forward, a DNA-barcoding approach could be implemented in a wide range of ichthyoplankton studies in addition, and in relation, to the identification of fish eggs. In comparison with fish larvae, eggs provide a more precise documentation of spawning location and time. For Atlantic cod in particular, the potential use of DNA barcoding of fish eggs is notable. Atlantic cod in U.S. waters comprise at least 3 genetic stocks, each thought to have further substock diversity associated with specific spawning grounds and seasons (Kovach et al., 2010; Zemeckis et al., 2014). It also has been suggested that other spawning stocks in the eastern Gulf of Maine exist, although this area has been so depleted that it is unknown if spawning persists there (Ames, 2004). We found differences in egg size that were associated with temperature, which in turn was associated with season and region of collection. A more extensive sampling procedure would likely reveal further complexity.

Although DNA barcoding is insufficient for distinguishing among stocks, the laboratory procedures do provide an extensive time-series archive of DNA, allowing the identification of spawning components in future molecular studies. In regard to indices of spawning stock biomass, where problems have arisen in the past as a result of morphologically based misidentifications, DNA barcoding could be used to broaden the use of existing surveys, while bypassing the assumption of constant egg mortality that underlies the use of larval abundances as indices of spawning stock biomass.

Overall, we have shown that DNA barcoding of fish eggs is sufficiently advanced to be incorporated into long-term, regional-scale ichthyoplankton monitoring programs. Trial runs with unidentified, well-digested fishes obtained from stomach samples collected during an ongoing food habits monitoring program (Smith and Link, 2010) show similar promise (Lewis and

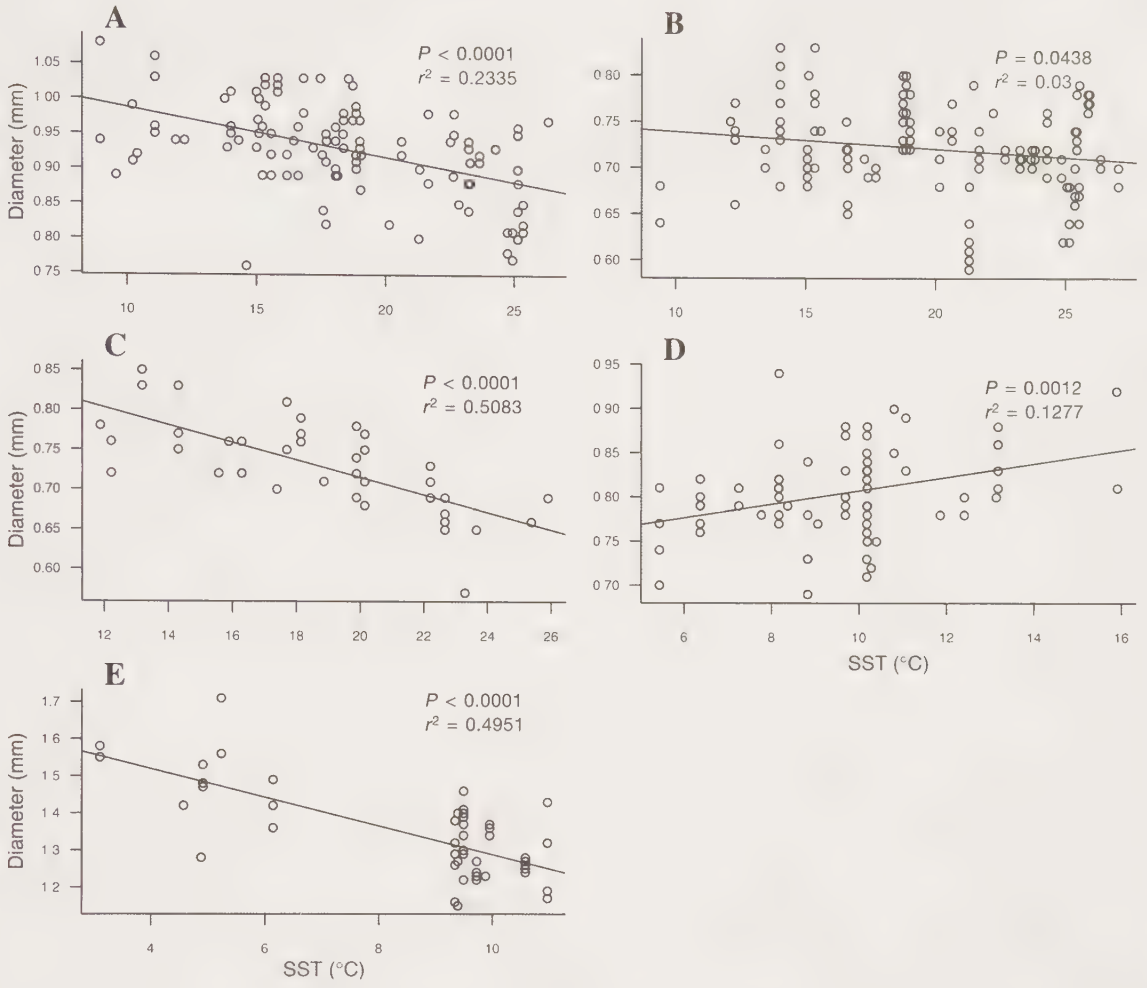

Figure 5

Scatter plots and linear regression analysis results for the 5 identified species, collected from at least 15 stations along the northeastern U. S. continental shelf during 2002–2012, for which a significant trend (P<0.05 or 5%) was observed between egg diameter (measured in millimeters) and sea-surface temperature (SST) of the collection day (in degrees Celsius): (**A**) fourspot flounder (*Hippoglossina oblonga*), (**B**) Gulf Stream flounder (*Citharichthys arctifrons*), (**C**) butterfish (*Peprilus triacanthus*), (**D**) yellowtail flounder (*Limanda ferruginea*), and (**E**) Atlantic cod (*Gadus morhua*). Each measured diameter is marked with an open circle, and a solid line illustrates the overall trend observed. The calculated P-value and the coefficient of determination (r^2) for each species are included in the top-right corner of each plot.

Smith[4]). Currently, many large organizations, such as the National Marine Fisheries Service, handle molecular identification on a program-specific basis, each of which may use a different technique. The consequence of this fractured approach is a substantial redundancy in cost, effort, and equipment across programs. Additionally, many smaller programs are unable to justify the start-up and reoccurring costs of a molecular laboratory and, therefore, continue to produce data with a substantial fraction of individual specimens not identified at the species level. The opportunity presented by DNA barcoding changes this fractured and inefficient approach to molecular identification into one unified method that can be shared across regions and types of sampling programs.

Acknowledgments

We thank the scientists and crew of the research vessels, too many to name individually, who contributed to the collection of ichthyoplankton samples over several decades, and in particular J. Prezioso, who ensured that additional ethanol-preserved samples were collect-

[4] Lewis, L., and B. Smith. 2013. Unpubl. data. Northeast Fish. Sci. Cent., Natl. Mar. Fish. Serv., NOAA, Narragansett, RI, and Woods Hole, MA.

ed over the past decade. We especially thank all the scientists and technicians at the Canadian Center for DNA Barcoding at the University of Guelph (Guelph, Ontario, Canada) for analytical support and A. Bucklin (University of Connecticut, Groton, Connecticut) and N. Copley (Woods Hole Oceanographic Institution, Woods Hole, Massachusetts) for the use of fish eggs from additional archived samples.

Literature cited

Ahlstrom, E. H., and H. G. Moser.
1980. Characters useful in identification of pelagic marine fish eggs. CalCOFI Rep. XXI:121–131.

Alheit, J.
1993. Use of the daily egg production method for estimating biomass of clupeoid fishes: a review and evaluation. Bull. Mar. Sci. 53:750–767.

Ames, E. P.
2004. Atlantic cod stock structure in the Gulf of Maine. Fisheries 29:10–28.

Carreon-Martinez, L. B., S. A. Holt, B. S. Nunez, C. K. Faulk, and G. J. Holt.
2010. The use of polymerase chain reaction for the identification of sciaenid eggs. Mar. Biol. 157:1889–1895.

Chambers, R. C., and W. C. Leggett.
1996. Maternal influences on variation in egg sizes in temperate marine fishes. Am. Zool. 36:180–196.

Conway, D. V. P., S. H. Coombs, and C. Smith
1997. Vertical distribution of fish eggs and larvae in the Irish Sea and southern North Sea. ICES J. Mar. Sci. 54:136–147.

Fox, C. J., M. I. Taylor, R. Pereyra, M. I. Villasana, and C. Rico.
2005. TaqMan DNA technology confirms likely overestimation of cod (*Gadus morhua* L.) egg abundance in the Irish Sea: implications for the assessment of the cod stock and mapping of spawning areas using egg-based methods. Mol. Ecol. 14:879–884.

Gleason, L. U., and R. S. Burton.
2012. High-throughput molecular identification of fish eggs using multiplex suspension bead arrays. Mol. Ecol. Resour. 12:57–66.

Goodsir, F., M. J. Armstrong, P. R. Witthames, D. L. Maxwell, and C. J. Fox.
2008. The use of species-specific TaqMan probes for identifying early stage gadoid eggs following formaldehyde fixation. ICES J. Mar. Sci. 65:1573–1577.

Hajibabaei, M., J. R. deWaard, N. V. Ivanova, S. Ratnasingham, R. T. Dooh, S. L. Kirk, P. M. Mackie, and P. D. N. Hebert.
2005. Critical factors for assembling a high volume of DNA barcodes. Philos. Trans. R. Soc. Lond., B 360: 1959–1967.

Hebert, P. D. N., A. Cywinska, S. L. Ball, and J. R. deWaard.
2003a. Biological identifications through DNA barcodes. Proc. R. Soc., B 270:313–321.

Hebert, P. D. N., S. Ratnasingham, and J. R. de Waard.
2003b. Barcoding animal life: cytochrome *c* oxidase subunit 1 divergences among closely related species. Proc. R. Soc., B 270(suppl 1):S96–S99.

Hiemstra, W. H.
1962. A correlation table as an aid for identifying pelagic fish eggs in plankton samples. J. Cons. Int. Explor. Mer 27:100–108.

Hyde, J. R., E. Lynn, R. Humphreys Jr., M. Musyl, A. P. West, and R. Vetter.
2005. Shipboard identification of fish eggs and larvae by multiplex PCR, and description of fertilized eggs of blue marlin, shortbill spearfish, and wahoo. Mar. Ecol. Prog. Ser. 286:269–277.

Ivanova, N. V., E. L. Clare, and A. B. Borisenko.
2012. DNA barcoding in mammals. Analytical protocols. *In* DNA barcodes: methods in molecular biology (W. J. Kress and D. L. Erickson, eds), p. 153–182. Humana Press, Totowa, NJ.

Kendall, A. W., Jr., and A. C. Matarese.
1994. Status of early life history descriptions of marine teleosts. Fish. Bull. 92:725–736.

Kovach, A. I., T. S. Breton, D. L. Berlinsky, L. Maceda, and I. Wirgin.
2010. Fine-scale spatial and temporal genetic structure of Atlantic cod off the Atlantic coast of the USA. Mar. Ecol. Prog. Ser. 410:177–195.

Kucera, C. J., C. K. Faulk, and G. J. Holt.
2002. The effect of spawning salinity on eggs of spotted seatrout (*Cynoscion nebulosus*, Cuvier) from two bays with historically different salinity regimes. J. Exp. Mar. Biol. Ecol. 272:147–158.

Lough, R. G., L. O'Brien, and L. J. Buckley.
2008. Differential egg mortality of Georges Bank cod and haddock inferred from two independent estimates of seasonal egg production. J. Northwest Atl. Fish. Sci. 41:119–128.

Marteinsdottir, G., and G. A. Begg.
2002. Essential relationships incorporating the influence of age, size and condition on variables required for estimation of reproductive potential in Atlantic cod *Gadus morhua*. Mar. Ecol. Prog. Ser. 235:235–256.

Marteinsdottir, G., and A. Steinarsson.
1998. Maternal influence on the size and viability of Iceland cod *Gadus morhua* eggs and larvae. J. Fish. Biol. 52:1241–1258.

Ouellet, P., Y. Lambert, and M. Castonguay.
1997. Spawning of Atlantic cod (*Gadus morhua*) in the northern Gulf of St. Lawrence: a study of adult and egg distributions and characteristics. Can. J. Fish. Aquat. Sci. 54:198–210.

Priede, I. G., and J. J. Watson.
1993. An Evaluation of the daily egg production method for estimating biomass of Atlantic mackerel (*Scomber scombrus*). Bull. Mar. Sci. 53:891–911.

Ratnasingham, S., and P. D. N. Hebert.
2007. BOLD: The Barcode of Life Data System (website). Mol. Ecol. Notes 7:355–364.

Richardson, D. E., J. D. Vanwye, A. M. Exum, R. K. Cowen, and D. L. Crawford.
2007. High-throughput species identification: from DNA isolation to bioinformatics. Mol. Ecol. Notes 7:199–207.

Richardson, D. E., J. K. Llopiz, K. D. Leaman, P. S. Vertes, F. E. Muller-Karger, and R. K. Cowen.
2009. Sailfish (*Istiophorus platypterus*) spawning and larval environment in a Florida Current frontal eddy. Prog. Oceanogr. 82:252–264.

Richardson, D. E., J. A. Hare, W. J. Overholtz, and D. L. Johnson.
2010a. Development of long-term larval indices for Atlantic herring (*Clupea harengus*) on the northeast US continental shelf. ICES J. Mar. Sci. 67:617–627.

Richardson, D. E., J. K. Llopiz, C. M. Guigand, and R. K. Cowen.
2010b. Larval assemblages of large and medium-sized pelagic species in the Straits of Florida. Prog. Oceanogr. 86:8–20.
Saitou, N., and M. Nei.
1987. The neighbor-joining method: a new method for reconstructing phylogenetic trees. Mol. Biol. Evol. 4:406–425.
Shao, K.-T., K.-C. Chen, and J.-H. Wu.
2002. Identification of marine fish eggs in Taiwan using light microscopy, scanning electric microscopy and mtDNA sequencing. Mar. Freshw. Res. 53:355–365.
Smith, B. E., and J. S. Link.
2010. The trophic dynamics of 50 finfish and 2 squid species on the northeast US continental shelf. NOAA Tech. Memo. NMFS-NE-216, 640 p.
Stratoudakis, Y., M. Bernal, K. Ganias, and A. Uriarte.
2006. The daily egg production method: recent advances, current applications and future challenges. Fish Fish. 7:35–57.
Valdez-Moreno, M., L. Vásquez-Yeomans, M. Elías-Gutiérrez, N. V. Ivanova, and P. D. N. Hebert.
2010. Using DNA barcodes to connect adults and early life stages of marine fishes from the Yucatan Peninsula, Mexico: potential in fisheries management. Mar. Freshw. Res. 61:655–671.
Ward, R. D., T. S. Zemlak, B. H. Innes, P. R. Last, and P. D. N. Hebert.
2005. DNA barcoding Australia's fish species. Philos. Trans. R. Soc. Lond., B 360:1847–1857.
Zeldis, J. R.
1993. Applicability of egg surveys for spawning-stock biomass estimation of snapper, orange roughy, and hoki in New Zealand. Bull. Mar. Sci. 53:864–890.
Zemeckis, D. R., D. Martins, L. A. Kerr, and S. X. Cadrin.
2014. Stock identification of Atlantic cod (*Gadus morhua*) in US waters: an interdisciplinary approach. ICES J. Mar. Sci. 71:1490–1506.
Zemlak, T. S., R. D. Ward, A. D. Connell, B. H. Holmes, and P. D. N. Hebert.
2009. DNA barcoding reveals overlooked marine fishes. Mol. Ecol. Resour. 9:237–242.
Zhang, J.
2010. Exploiting formalin-preserved fish specimens for resources of DNA barcoding. Mol. Ecol. Resour. 10: 935–941.

NOAA
National Marine
Fisheries Service

Fishery Bulletin
established 1881

Spencer F. Baird
First U.S. Commissioner
of Fisheries and founder
of *Fishery Bulletin*

A model based on data from echosounder buoys to estimate biomass of fish species associated with fish aggregating devices

Jon Lopez[1]
Gala Moreno[1,3]
Guillermo Boyra[1]
Laurent Dagorn[2]

Email address for contact author: jlopez@azti.es

[1] AZTI-Tecnalia
Herrera kaia
portualdea z/g
20110 Pasaia (Gipuzkoa), Spain

[2] Institut de Recherche pour le Développement
IRD, UMR EME 212
Avenue Jean Monnet
CS 30171
34203 Sète Cedex, France

[3] International Seafood Sustainability Foundation (ISSF)
805 15th Street NW
Washington, D.C. 20005

Abstract—Most of the drifting fish aggregating devices (DFADs) used in industrial tropical tuna purse-seine fisheries are equipped with satellite linked echosounder buoys, which provide fishing crews with remote, accurate geolocation information and rough estimates of FAD-associated tuna biomass. One of the most common brands of echosounder buoys (SATLINK, Madrid, Spain) is currently calibrated for the target strength of skipjack tuna (*Katsuwonus pelamis*) and provides biomass data on that species. Using that brand of echosounder buoy, we developed a new behavior-based approach to provide relative biomass estimates and a remote target classification of fish aggregations at FADs. The model is based on current knowledge of the vertical distribution of the main fish species associated with FADs, as well as on appropriate TS and weight values for different species and sizes, and is further based on parameter optimization against a set of fishing operations on DFADs. This model reduced the error variability in biomass estimates by about 60% and also reduced the ranges of underestimation and overestimation by 55% and 75%, respectively. Similarly, the original coefficients of correlation and determination were also considerably improved from 0.50 and 0.25 to 0.90 and 0.82, respectively. We discuss how this new method opens new opportunities for scientific studies and has implications for sustainable fishing.

Manuscript submitted 14 August 2015.
Manuscript accepted 29 January 2016.
Fish. Bull. 114:166–178 (2016).
Online publication date: 23 February 2016.
doi: 10.7755/FB.114.2.4

The views and opinions expressed or implied in this article are those of the author (or authors) and do not necessarily reflect the position of the National Marine Fisheries Service, NOAA.

Objects floating on the surface of the tropical and subtropical oceans attract a number of marine species, including tropical tunas (Castro et al., 2002; Taquet et al., 2007b). Taking advantage of this associative behavior, tropical tuna purse seiners regularly deploy drifting, man-made floating objects, also called drifting fish aggregating devices (DFADs), to facilitate their catch of skipjack (*Katsuwonus pelamis*), yellowfin (*Thunnus albacares*) and bigeye (*Thunnus obesus*) tunas. This fishing method is essential for the current operation of purse-seine fleets in all oceans; more than 50% of purse-seine sets (and greater than 70% of purse-seine sets during some years in the Indian and eastern Pacific Oceans) are made on floating objects. This method accounts for nearly half of the world's tropical tuna catch (Dagorn et al., 2013). Indeed, it has been estimated that 50,000–100,000 DFADs are deployed annually worldwide (Baske et al.[1]; Scott and Lopez[2]), which drift at sea on average for periods of over one or two months depending on the ocean (Maufroy et al., 2015). However, the increasing use of DFADs has led to concerns. Setting on floating objects contributes to the catch of small and undesirable sizes of bigeye and yellowfin tuna that are usually not caught by sets on free-swimming

[1] Baske, A., J. Gibbon, J. Benn, and A. Nickson. 2012. Estimating the use of drifting fish aggregation devices (FADs) around the globe, 8 p. PEW Environmental Group, 901 E Street NW, Washington, D.C. 20004. [Available at website.]

[2] Scott, G. P., and J. Lopez. 2014. The use of FADs in tuna fisheries. European Union, European Parliament, Policy Department B: Structural and Cohesion Policies, Fisheries IP/B/PECH/IC/2013-123, 70 p. [Available at website.]

schools (Fonteneau et al., 2013). In addition, while encircling tunas associated with a DFAD, purse seiners also enclose nontarget species that are associated with the object and thus increase the bycatch-to-catch ratio in comparison with ratios obtained from setting on free-swimming schools.

Today, many DFADs are equipped with satellite-linked echosounder buoys (Lopez et al., 2014), which provide fishermen with remotely collected rough estimates of the DFAD-associated tuna biomass, as well as accurate geolocation information. Fishing crews use the biomass estimates from the buoys, along with other information (e.g., environmental conditions from remote sensing data, catches by other vessels in the same area), to decide on the best DFAD to visit next. A biomass estimate provided by an echosounder buoy is represented by a single value and does not comprise information on species composition (tuna and nontuna) nor the size distribution of the aggregation. Fishermen obtain information only on the size and species composition of the aggregations after setting on the floating device and the catch is hauled on deck. Therefore, fishing crews cannot currently use echosounder buoys to remotely assess the catch composition (biomass of every species and size category) before deciding on which DFAD they will set a course.

On the other hand, scientists have been studying fish aggregations at DFADs using various observation techniques such as active acoustic tracking (Matsumoto et al., 2014), passive acoustic tracking (Taquet et al., 2007a; Filmalter et al., 2011; Schaefer and Fuller, 2013; Matsumoto et al., 2014), scientific acoustic surveys (Moreno et al., 2007), and underwater visual census (Taquet et al., 2007b). Clearly, scientific knowledge on the behavior of DFAD-associated aggregations is currently limited by the cost of accessing and working on remote DFADs. Developing autonomous observation tools that can be attached to DFADs for continuous direct long-term monitoring of fish aggregations has been a challenge in recent years (Dagorn et al., 2007a). Therefore, echosounder buoys used extensively by fishermen appear to be a powerful tool for observing fish aggregations at DFADs remotely in a cost-effective manner. However, there is currently no satisfactory buoy that can provide reliable information on the abundance and sizes of the different species that compose these fish aggregations. The lack of reliable information precludes gaining a better understanding of the behavioral processes involved in the dynamics of these aggregations.

The objective of this study was to develop a new processing method for data collected by one of the brands of echosounder buoys used by tropical tuna purse seiners, by using data on the vertical distribution of the different fish species and fish sizes at FADs, their corresponding target strength (TS, dB re 1 m^2; MacLennan et al., 2002) and weight values, and further parameter optimization against the data from a set of fishing operations on DFADs.

Materials and methods

The buoy

At the start of this study, three companies were manufacturing echosounder buoys for DFAD fishing. Echosounder specifications (frequency, beam width, depth range, etc.), and the algorithms used to convert acoustic backscatter into biomass values differ between companies. Twenty-four Spanish tropical tuna purse seine skippers were interviewed to collect data on echosounder buoy usage, display quality, and reliability of different brands. Manufacturers were also contacted to obtain technical information on their products. On the basis of all available information, the Satlink buoy (SATLINK,[3] Madrid, Spain, website) was selected for the purpose of the present study.

The buoy contains a Simrad ES12 echosounder, which operates at a frequency of 190.5 kHz with a power of 140 W (beam angle at –3dB: 20°). The sounder is programmed to operate for 40 seconds. During this period, 32 pings are sent from the transducer and an average of the backscattered acoustic response is computed and stored in the memory of the buoy's software program (hereafter called "acoustic sample"). Volume backscattering strength (S_v, dB re 1 m^{-1}; MacLennan et al., 2002) values smaller than –45 dB are automatically removed by the internal module of the buoy, as a precautionary measure to eliminate signals that likely correspond to organisms smaller than tuna (e.g., organisms of the sound scattering layers; Josse et al., 1998; Josse and Bertrand, 2000). The observation depth range extends from 3 to 115 m (with a blanking zone [a data exclusion zone to eliminate the near-field effect of the transducer; Simmonds and MacLennan, 2005] from 0 to 3 m depth) and is composed of 10 homogeneous layers, each with a resolution of 11.2 m (Fig. 1). Because echosounder buoys belonged to fishing crews, they were not calibrated at the deployment site; instead, they were calibrated by manufacturers in tanks before delivery.

Raw acoustic data are provided for each depth layer and were originally converted to biomass (in metric tons, [t]) by using an experimental algorithm developed by the manufacturer, which is based on the TS of skipjack tuna, the main target species of the fleet fishing around DFADs. This conversion is automatically executed in the internal module of the buoy for each integrated layer (n=1, 2, ..., 10) by means of a depth layer echo-integration procedure (Simmonds and MacLennan, 2005), with the assumption that there was the presence of only individuals of skipjack tuna of identical weight (for confidentiality reasons, authors of this article are not allowed to describe some of the proprietary technical information regarding the echosounder buoy. Readers interested in more technical de-

[3] Mention of trade names or commercial companies is for identification purposes only and does not imply endorsement by the National Marine Fisheries Service, NOAA.

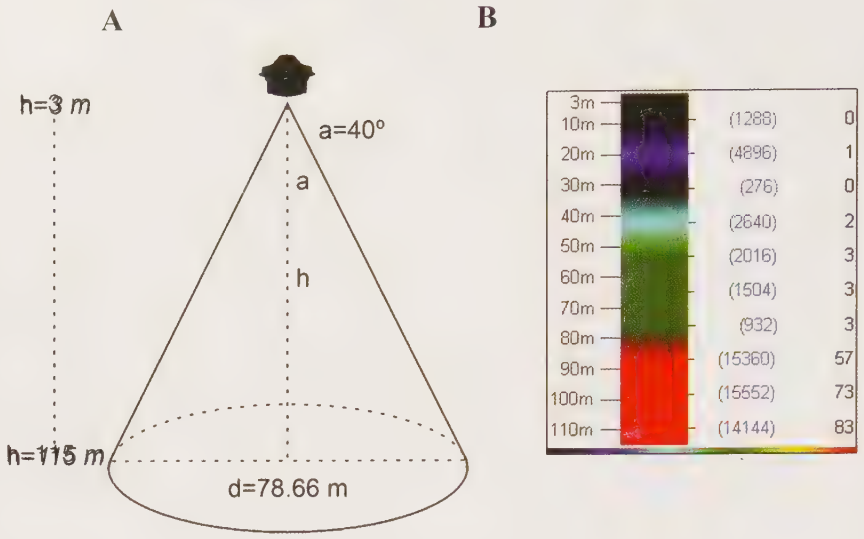

Figure 1

(**A**) Beam width [or angle] (a), depth range (h), and diameter (d) at 115 m of the Satlink echosounder buoy. (**B**) An example of the echogram display for the 10 depth layers (ranging from 3 m to 115 m): raw acoustic backscatter (numbers between parentheses) and their corresponding biomass estimates in metric tons (numbers in black) for skipjack tuna (*Katsuwonus pelamis*) based on the manufacturer's algorithms. The acoustic information used in this study was collected by a commercial Spanish purse seiner operating in the central and eastern Atlantic Ocean between 2009 and 2011.

tail about this process should contact the manufacturer directly).

The model

Because the manufacturer's method is not designed to provide abundance estimates for the different species and sizes of fish that usually compose fish aggregations at DFADs (Fonteneau et al., 2013), we proposed a new method consisting of developing specific algorithms by ocean or regional sites. The specificities of the regional algorithms would be based on 1) existing knowledge of the vertical behavior of fish at FADs, 2) appropriate TS and weight values for different species and sizes to perform a multispecies and size echo-integration, and 3) further parameter optimization against a set of fishing operations on DFADs of each region. In the present study, and as an example of application of the method, we developed a specific algorithm for DFADs in the Atlantic Ocean using a set of 21 fishing sets.

Assigning a species group to each depth layer Knowing the vertical distribution of species within the observational range of the buoy is essential for accurately converting acoustic backscatter into biomass of different fish groups. For that purpose, we reviewed all available scientific studies focused on the investigation of the behavior of tuna and nontuna species when associated with FADs (Brill et al., 1999; Musyl et al., 2003; Schaefer and Fuller, 2005; Matsumoto et al.[4]; Dagorn et al., 2007b; Dagorn et al., 2007c; Taquet et al., 2007a, 2007b; Babaran et al., 2009; Leroy et al., 2009; Govinden et al.[5]; Filmalter et al., 2011; Mitsunaga et al., 2012; Muir et al.[6]; Govinden et al., 2013; Schaefer and Fuller, 2013; Weng et al., 2013; Matsumoto et al., 2014; Forget et al., 2015), as well as on the spatial distribution of the echo-traces recorded around DFADs during scientific acoustic surveys (Moreno et al., 2007). Additional information was obtained from 25 echosounder buoys deployed in the Indian Ocean between 2009 and 2012 (a total of about 2000 acoustic samples). The plot

[4] Matsumoto, T., H. Okamoto, and M. Toyonaga. 2006. Behavioral study of small bigeye, yellowfin and skipjack tunas associated with drifting FADs using ultrasonic coded transmitter in the central Pacific Ocean. Scientific committee, second regular session. Western and Central Pacific Fisheries Commission Inf. Pap. WCPFC-SC2-2006/FT IP-7, 25 p. [Available at website.]

[5] Govinden, R., L. Dagorn, M. Soria, and J. Filmalter. 2010. Behaviour of tuna associated with drifting fish aggregating devices (FADs) in the Mozambique Channel. Indian Ocean Tuna Commission (IOTC), Working Party Tropical Tuna (WPTT) IOTC-2010-WPTT-25, 22 p. [Available at website.]

[6] Muir, J., D. Itano, M. Hutchinson, B. Leroy, and K. Holland. 2012. Behavior of target and non-target species on drifting FADs and when encircled by purse seine gear. Scientific committee, eigth regular session. Western and Central Pacific Fisheries Commission Inf. Pap. WCPFC-SC8-2012/EB-WP-13, 7 p. [Available at website.]

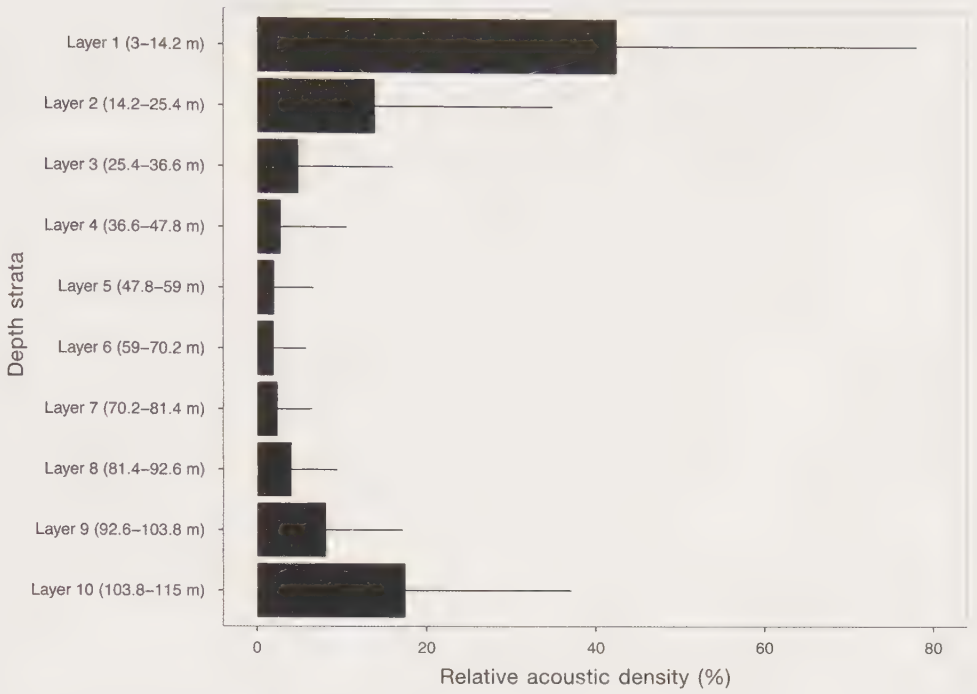

Figure 2

Average percentages of acoustic backscatter (black bars) and their standard deviations (lines) recorded at sunrise from about 2000 acoustic samples recorded by 25 Satlink echosounder buoys attached to drifting fish aggregating devices (DFADs) in the Indian Ocean between 2009 and 2012. This information was used as complementary information to define the preliminary depth limits between the different fish groups present at DFADs. The figure indicates a potential segregation of size increasing with depth and a greater likelihood of larger tuna occupying waters deeper than 80 m (individuals with swim bladders). The large amount of acoustic backscatter recorded in the first 25 m could be due to the presence of nontuna species, which also have swim bladders. Skipjack tuna, *Katsuwonus pelamis*, the main target species of the fleet fishing around DFADs is usually known to occupy medium depths and has no swim bladder. This potential segregation of size increasing with depth has also been found in previous works with conventional scientific echosounders around DFADs (Moreno et al., 2007).

of the average acoustic backscatter recorded by each echosounder buoy depth layer (Fig. 2), combined with the behavioral information in the references cited above, suggested a potential segregation of tuna size increasing with depth, indicating a greater likelihood of larger tuna occupying waters deeper than 80 m. This seems to be in agreement with previous findings obtained through conventional scientific echosounders around DFADs (Moreno et al., 2007).

From this accumulated information, the vertical boundary between nontuna species and small tunas was set at 25 m. Similar depth limits were adopted in previous studies with the use of the same echosounder buoys to separate bycatch from tuna (Lopez et al.[7]; Robert et al., 2013). Because vertical depth limits between small and large tunas may be vague, a preliminary limit was initially set at 80 m depth, and was then re-adjusted in agreement with a set of 21 purse seine fishing operations conducted on DFADs in the Atlantic Ocean (see *Parameter optimization* section).

Assigning TS and weights values to each species group Selecting appropriate TS and weight values for different species is also crucial for adequately converting acoustic backscatter into reliable biomass estimations, by species or fish groups. Because no specific TS/fork length (FL) relationship was available in the literature for nontarget species, we considered a TS value of –42 dB for the entire group based on previous field studies (Josse et al., 2000; Doray et al., 2006; Doray et al., 2007; Lopez et al.[7]). The mean weight used for the biomass characterization of this community was 1 kg/ind, which was estimated from the mean length of most

[7] Lopez, J., G. Moreno, M. Soria, P. Cotel, and L. Dagorn. 2010. Remote discrimination of by-catch in purse seine fishery using fisher's echo-sounder buoys. Indian Ocean Tuna Commission (IOTC), Working Party Ecosystem Bycatch (WPEB) IOTC-2010-WPEB-03, 14 p. [Available at website.]

Table 1

Target strength (TS), acoustic backscattering cross-section (σ_{bs}, TS in linear scale) and weight (w) parameters used by the proposed method to conduct the echo-integration for each group of fish considered in this study. Below are the coefficients of correlation (r) and determination (r^2) between the uncorrected predicted biomass and real catches depending on the depth limit that was set to separate small and large tunas.

	Non-tunas	Small tunas	Large tunas						
TS (dB re 1 m^2)	–42	–35.1	–29.9						
σ_{bs} (m^2)	$6.31\ 10^{-5}$	$3.09\ 10^{-4}$	$1.02\ 10^{-3}$						
W (kg)	1	2	21						
Depth limit (m)	25	36	47	59	70	80	92	104	115
r	0.85	0.84	0.84	0.84	0.74	0.74	0.75	0.76	0.85
r^2	0.73	0.70	0.71	0.71	0.54	0.54	0.57	0.58	0.73

represented nontuna species at DFADs, and their corresponding weights (i.e., 72 cm FL for dolphinfish [*Coryphaena hippurus*], 100 cm FL for wahoo [*Acanthocybium solandri*], 30 cm FL for triggerfish [*Canthidermis maculata*], and 54 cm FL for rainbow runner [*Elegatis bipinnulata*] [Forget[8]]).

Moreno et al. (2007) analyzed the spatial distribution of the TS of fish aggregations around DFADs. Because the study of Moreno et al. (2007) is the only study conducted around DFADs with conventional scientific echosounders, to determine our tuna depth layers we used the TS values found by Moreno et al. (2007) (–35.1 dB for acoustic structures found between 20 and 80 m; and –29.9 dB for acoustic structures found between 80 and 100 m), which fitted reasonably well with the range of observations we initially proposed for small and large tunas. According to the most common tuna sizes caught at DFADs (Delgado de Molina et al.[9]; IATTC, 2013; Chassot et al.[10]; Floch et al.[11]; Fonteneau et al., 2013; Harley et al.[12]), the depth range between 25 and 80 m was considered to be populated by skipjack, yellowfin and bigeye tuna of a mean mass of 2 kg/ind (about 50 cm FL), whereas the depth between 80 and 115 m was assumed to be populated by larger yellowfin and bigeye tuna individuals with a mean weight of 21 kg/ind (110–100 cm FL, for yellowfin and bigeye tuna, respectively).

Echo-integration Area backscattering coefficients (s_a, m^2/m^2; MacLennan et al., 2002) recorded in each of the ten echosounder buoy layers were converted into biomass following a depth layer echo-integration procedure. A specific acoustic backscattering cross-section value (σ_{bs} , m^2, TS in linear scale; MacLennan et al., 2002) was used to obtain the number of individuals for each of the integrated layer (n=1, 2, ..., 10) according to the presence of each group initially assigned in this study to each depth layer (i.e., nontuna [3–25 m], small tuna [25–80 m], large tuna [80–115 m]). The σ_{bs} and weight values used for the echo-integration of the acoustic backscatter are shown in Table 1. The number of fish per group and layer ($N[n, gr]$) were estimated as follows:

$$N(n,gr) = \frac{s_a(n)}{\sigma_{bs(gr)}} \cdot A(n) \quad (1)$$

where $s_a(n)$ = the TVG-corrected (time-varied-gain, a correction function to compensate the signal for spreading and absorption losses; Simmonds and MacLennan, 2005) area backscattering coefficient (Maclennan et al., 2002) in each layer (n);

$\sigma_{(bs(gr))}$ = the mean TS of a known group (i.e., of nontuna species, small or large tunas) in linear scale; and

$A(n)$ = the mean cross sectional area sampled by the beam of the cone for each layer (n).

Then, the total number of fish per group N(gr) were obtained by summing for all layers (2):

[8] Forget, F. 2012. Personal commun. Institut de Recherche pour le Développement (IRD), UMR EME 212, Ave. Jean Monnet, CS 30171, 34203 Sète Cedex, France

[9] Delgado de Molina, A., J. C. Santana, J. Ariz, and I. Sabaté. 2012. Estadísticas Españolas de la pesquería atunera tropical, en el Océano Atlántico, hasta 2010. Collect. Vol. Sci. Pap. ICCAT 68:1200–1220. [Available at website.]

[10] Chassot, E., A. Delgado de Molina, C. Assan, P. Dewals, P. Cauquil, J. J. Areso, D. M. Rahombanjanahary, and L. Floch. 2013. Statistics of the European Union and associated flags purse seine fishing fleet targeting tropical tunas in the Indian Ocean 1981–2012. Indian Ocean Tuna Commission (IOTC), Working Party Tropical Tuna (WPTT) IOTC-2013-WPTT15-44, 28 p. [Available at website.]

[11] Floch, L., A. Damiano, A. Tamegnon, P. Cauquil, P. Chavance, I. Terrier, and E. Chassot. 2014. Statistics of the French purse seine fishing fleet targeting tropical tunas in the Atlantic Ocean (1991–2012). Collect. Vol. Sci. Pap. ICCAT 70:2669–2692. [Available at website.]

[12] Harley, S., P. Williams, S. Nicol, and J. Hampton. 2013. The western and central Pacific tuna fishery: 2011 overview and status of stocks, 31 p. Secretariat of the Pacific Community, Noumea, New Caledonia. [Available at website.]

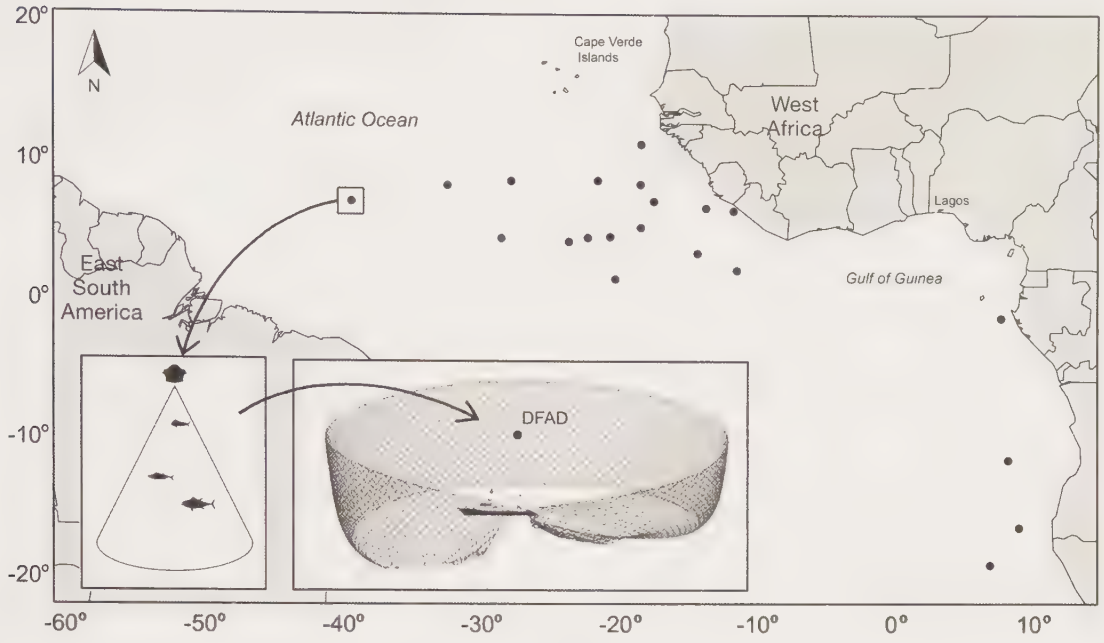

Figure 3

Map of the 21 locations (•) where echosounder buoy acoustic data and catch information were collected around drifting fish aggregating devices (DFADs). Acoustic samples were taken at sunrise and were followed by regular fishing sets to gather information on the size and composition of catch. Fishing sets were conducted by a commercial Spanish purse seiner in the central and eastern Atlantic Ocean between 2009 and 2011.

$$N(\mathrm{gr}) = \Sigma_n N(n, gr) \quad (2)$$

The estimated number of fish per group (N[gr]) was converted into biomass per group (B[gr], in t) by multiplying the total amount of individuals by their corresponding mean weight (w, in kg) and dividing by 1000.

$$B(gr) = \frac{N(gr) \cdot w(gr)}{1000} \quad (3)$$

where $B(gr)$ = the biomass estimated per fish group (in t);
$N(gr)$ = the number of individuals per group; and
$w(gr)$ = the average weight of an individual of a particular group (in kg) used to convert number of individuals in weight.

Finally, the total uncorrected predicted tuna biomass (B_u, in t) is the sum of the biomass estimated for the two tuna categories (corresponding to the sum of depth layers 3–10), whereas total biomass of nontuna species is the estimate obtained for that specific group (sum of layers 1–2).

Parameter optimization Because vertical limits (depth boundaries) previously set may vary depending on the regional site, we used a set of 21 fishing sets to optimize our method and evaluate the depth limit selected for the particular case of the Atlantic Ocean. Additionally, the same set of catches was used in a further stage to adjust and correct biomass estimates of the new method (see next section).

Twenty-one acoustic samples collected from echosounder buoys between 2009 and 2011 in the central and eastern tropical Atlantic Ocean were used, along with their corresponding catch data, to make a first assessment of the performance of the proposed method (Fig. 3). Acoustic samples were collected at sunrise (i.e., the time of the day at which, according to the belief of fishermen, fish are supposed to be more concentrated under the DFAD) and were followed by regular fishing sets. We assumed purse seine catch to be a proxy for the total associated fish biomass at DFADs. Fishing operations were conducted by a Spanish purse seiner during conventional commercial fishing trips. Information on the species composition of the aggregation was then obtained in t and as commercial categories for each tuna species from the skipper's logbook.

In order to investigate the effect of the changes in the selection of the depth limit between small and large tunas for final biomass estimates, the echo-integration procedure was conducted repeatedly by applying all possible combinations to the depth limit between small and large tunas within the entire depth range (i.e., changing the virtual limit from 80 m to 92 m, 104 m, 115 m, 70 m, 59 m, 47 m, 36 m, and 25 m), with the exception of the first 25 m, which were always considered inhabited mainly by nontuna species (Robert et al., 2013; Forget et al., 2015). For the

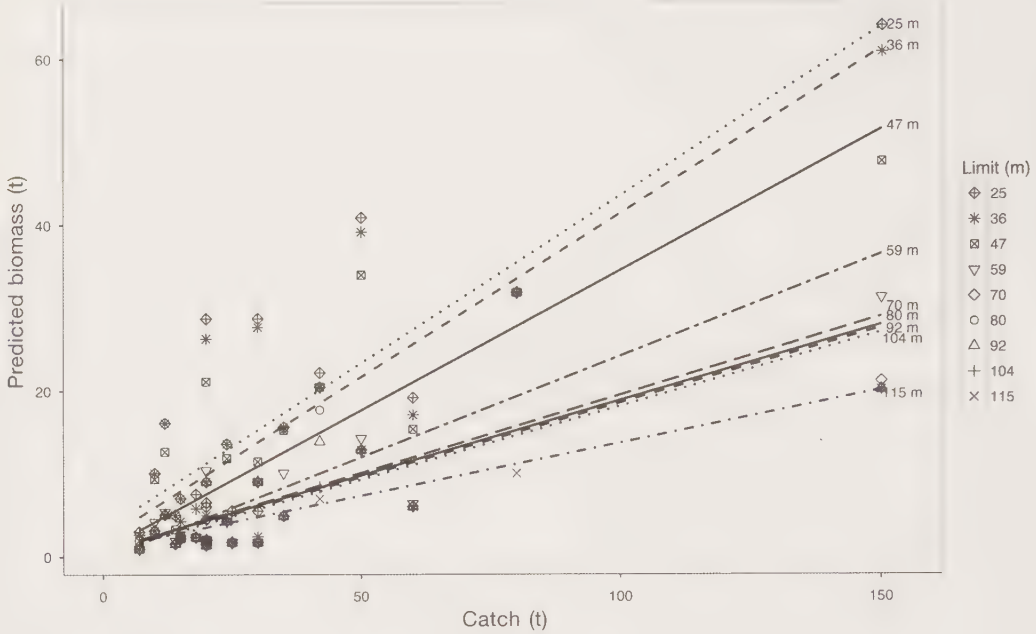

Figure 4

Linear relationships between uncorrected predicted biomasses, obtained from models with different depths to set the limits between small and large tunas, and the real catch for the 21 samples collected by a commercial Spanish purse seiner in the central and eastern Atlantic Ocean between 2009 and 2011. The coefficients of correlation and determination of these relationships were used to select the optimum depth limit between small and large tunas for the particular case of this study.

specific case of these 21 fishing sets in the Atlantic Ocean, the best values for coefficients of correlation (r) and determination (r^2) (r=0.85, r^2= 0.73; Table 1, Fig. 4) provided by the optimization process led us to reconsider and modify the original selection of vertical depth limits. Because of a known potential overlap between species and fish sizes in the vertical depth zones and the higher number of small tuna than large tuna individuals occurring at DFADs, we opted to keep only the TS and weight values of small tunas for the whole depth range (i.e., corresponding to a depth limit of 115 m (Table 1 and Fig. 4). This is the more ecologically coherent choice because the presence of small tunas at DFADs usually exceeds 95% of the catch (Fonteneau et al., 2013), which was also supported by the proportion of small tunas found in our 21 fishing sets.

Defining an error function In order to reduce uncertainty and improve the accuracy of biomass estimation with the new method, the uncorrected predicted biomass was compared and calibrated to the 21 real catches. Error (in t) of the new method was modeled with different regression models (polynomials of order 2 and 3, generalized linear models [GLM], and generalized additive models [GAM]; Hastie and Tibshirani, [1990]; Venables and Dichmont, [2004]; Wood, [2006]) (Fig. 5) as a function of the uncorrected predicted biomass, which was corrected as follows:

$$B_c = B_u - f(B_u) + \varepsilon, \quad (4)$$

where B_c = the corrected predicted biomass;
B_u = the uncorrected predicted biomass of the new method; and
$f(B_u)$ = the error modeled following different regression methods as a function of uncorrected predicted biomass ($f[B_u]$=–0.318 B_u^2+0.9951 B_u–17.598 for the polynomial of order 2; $f[B_u]$=–0.0346 B_u^3+0.7223 B_u^2–6.7657 B_u–5.5385 for the polynomial of order 3; $f[B_u]$=–4.7605 B_u–3.0981 for the GLM; and $f[B_u]$=absolute error of B_u~s(Bu) as a generic formula for the GAM. Note that no explicit expression for the estimated smooth terms (s) is available for GAMs (see Hastie and Tibshirani, 1990). For the GAM case, values used to correct B_u were extracted by using the predict.gam function of the mgcv package (vers. 1.7.29); and ε is the assumed error (0 in this case). All the regression models were fitted by using the mgcv package, vers. 1.7.29, for R software, vers.3.2.1 (R Core Team, 2015).

The prediction capacity of each model was measured by computing both r and r^2 between the corrected predicted biomass and the 21 real catches, and by using

the summary statistics of the absolute errors (Table 2).

Results

Accuracy of estimated tuna biomass

To evaluate the accuracy of both our methods and those of the manufacturer, corrected tuna biomass estimates obtained by each method were compared with the biomass estimates from the purse-seine catch on these 21 DFADs. The r and r^2 and the main statistics of the errors for each corrected biomass estimates obtained through the different correction functions are shown in Table 2. Results showed that all the methods performed similarly, significantly improving the accuracy of prediction values compared with the manufacturer's method. Despite the similar values obtained for all the corrected predicted biomasses from the different regression models, the GAM corrected model was selected as the potential main model selection of this study on the basis of its statistical robustness and consistency (Wood, 2006). Table 3 and Figure 6 show the final biomass estimates and the boxplot of the distribution of the error for the manufacturer's method and the GAM-corrected method developed by the authors. Maximum biomass estimation error ranged from –69 to 101 t (median and standard deviation [SD] of –4 ±33.9 t) for the manufacturer's method and from –30.12 to 24.80 t (with a median and SD of 1.23 ±13.74 t) for the GAM corrected method. Thus, the original error variability (SD=33.9) was significantly reduced by ~60% (SD=13.74) and the ranges of underestimation and overestimation were diminished by ~55% and ~75%, respectively. Additionally, the original r and r^2 values were also considerably improved from 0.50 and 0.25 to 0.90 and 0.82, respectively.

Nontuna biomass estimates

Because the crew was conducting regular fishing trips with no observer, we could not use catch data on in situ nontuna species to test the accuracy of the predicted biomass for this group. However, the average value of non-

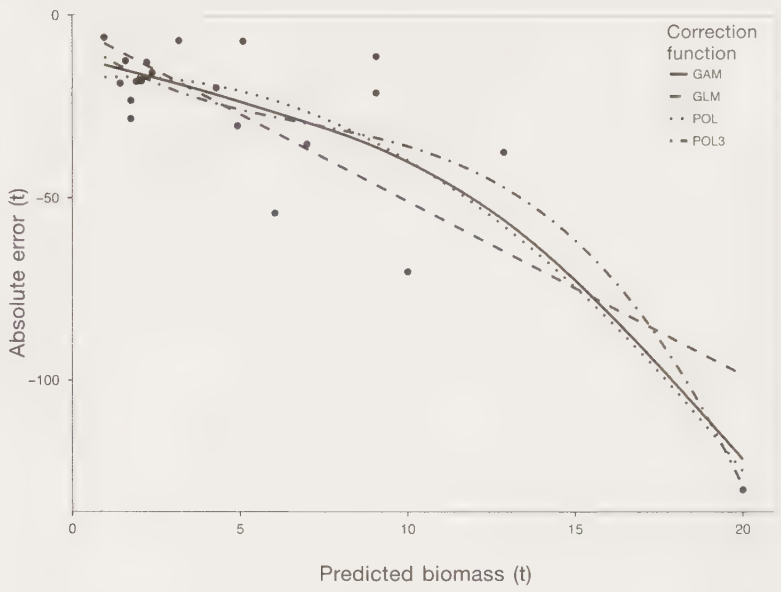

Figure 5

Regressions obtained through different methods (generalized additive model [GAM], generalized linear model [GLM], and polynomials of order 2 [POL] and 3 [POL3]) between uncorrected predicted biomass and absolute errors for the 21 samples collected by a commercial Spanish purse seiner in the central and eastern Atlantic Ocean between 2009 and 2011. Specific equations used in the present study are provided in the *Defining an error function* section. Regressions were used to correct and adjust the uncorrected biomass to the real catch.

Table 2

Summary statistics (med=median; min=minimum; max=maximum; SD=standard deviation) of the absolute errors (in metric tons [t]) for the final biomass estimations corrected through different regression models (GLM=generalized linear model; POL=polynomial of order 2; POL3=polynomial of order 3; GAM=generalized additive model) and the corresponding coefficients of correlation (r) and determination (r^2), when the statistics were compared with real catches.

Error	Before correction	Manufacturer	GLM	POL	POL3	GAM
med (t)	–18.57	–4	–1.18	0.54	2.18	1.23
min (t)	–130	–69	–31.67	–30.80	–34.43	–30.12
max (t)	–6	101	35.23	23.68	22.30	24.80
SD (t)	28.22	33.87	16.77	13.96	13.38	13.74
Parameter						
r	0.85	0.50	0.85	0.90	0.91	0.90
r^2	0.73	0.25	0.73	0.81	0.83	0.82

Table 3

Absolute error (in metric tons, t), for biomass estimates (t) and real catch (t), from each of the two methods analyzed in this study for 21 sets conducted by a commercial Spanish purse seiner in the Atlantic Ocean between 2009 and 2011. Shown also are the biomass estimates originally provided by the Satlink buoy (S) with the use of an algorithm based on skipjack (*Katsuwonus pelamis*) and the final biomass estimates obtained with the new method (NM) proposed in this study.

Buoy code	Catch (t)	Biomass estimate (t) (S)	Absolute error (t) (S)	Biomass estimate (t) (NM)	Absolute error (t) (NM)
23753	20	12	−8	17.66	−2.34
23728	24	8	−16	25.84	1.84
23737	10	20	10	21.90	11.90
23825	150	81	−69	141.58	−8.42
23737	20	121	101	44.88	24.88
23825	14	10	−4	16.60	2.60
23751	60	38	−22	32.43	−27.57
23750	50	84	34	68.60	18.60
28171	18	16	−2	19.23	1.23
23736	35	31	−4	28.21	−6.79
28179	25	11	−14	17.13	−7.87
28184	80	63	−17	49.88	−30.12
28643	42	106	64	36.09	−5.91
28471	30	17	−13	17.13	−12.87
28707	15	14	−1	18.71	3.71
28697	12	32	20	28.81	16.81
30528	7	2	−5	14.48	7.48
28390	20	11	−9	16.07	−3.93
28216	15	14	−1	18.71	3.71
28705	30	59	29	44.88	14.88
30530	20	16	−4	18.18	−1.82

tuna species biomass per set was estimated at 0.627 t (min=0; max=12.398; SD=2.37), which fitted reasonably well with the values found in the Atlantic Ocean for the European purse seine fleet (mean=0.79; min=0; max=22.06) (Amandé[13]).

Discussion

Echosounder buoys are widely employed by the industrial tropical tuna purse seine fishery and their use has rapidly increased since their introduction into the market in the mid-to-late 2000s (Lopez et al., 2014). In fact, Baske et al.[1] estimated an annual production of 50,000–70,000 satellite-tracked buoys by the major buoy-producing companies, of which most were fitted with echosounders. However, this source of information needs to be evaluated and validated before use in fisheries applications. We present a processing method that takes into account the multispecies and multisize nature of DFAD-associated aggregations. The method substantially improves the overall precision of the original biomass estimation (error variability and the ranges of underestimation and overestimation have been notably diminished) and also provides biomass data by major species groups, rather than a single information unit on the entire fish aggregation based only on one species of tuna (i.e., skipjack tuna).

Echosounder buoys for scientific studies

The method developed in the present study shows the potential for echosounder buoys as small autonomous tools that can provide information on fish aggregations at DFADs over weeks and months. Echosounder buoys attached to FADs could constitute ideal observational platforms, providing data on the fish community associated with floating objects. Monitoring of FAD buoy data could then provide a powerful tool for scientific evaluation of resource abundance and for improved knowledge of the associative behavior of the fish communities associated with FADs. In order to increase the sampling potential and data input, scientists should consider similar studies on the other echosounder buoy brands currently used by industrial purse-seine operators and which are not addressed in the present study.

[13]Amandé, M. J. 2012. Personal commun. Centre de Recherces Oceanologiques, CRO, 29, Rues des pecheurs, BP V 18, Abidjan, Cote d'Ivoire.

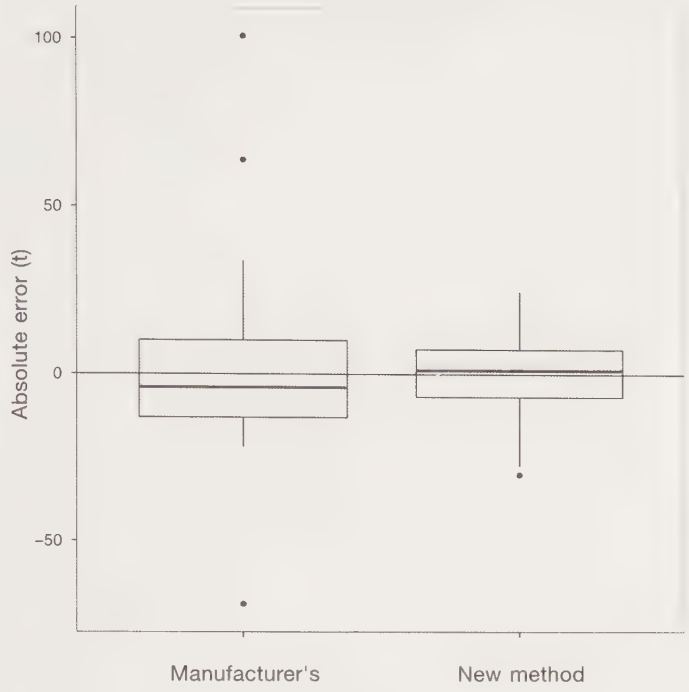

Figure 6

Error variability when converting acoustic backscatter into biomass by two different methods analyzed in the present work: the manufacturer's original method and the GAM corrected biomass estimations obtained with the new method developed in this study. Acoustic data and real catches were collected by a commercial Spanish purse seiner in the central and eastern Atlantic Ocean between 2009 and 2011 to illustrate the use of the new method. Black dots are outlier points. The box show the quartiles, with the bars extending to the most extreme data point which is no more than ±1.5 the interquartile range. The heavy line across the box is the median.

The new remote-target classification method opens a broad range of future lines of research in the area of FAD-related fish ecology and behavior. Because the model can group species, every acoustic sample given by the buoy could return specific biomass-index estimates for nontuna and tuna species. This raises the possibility of computing a wide range of statistical and mathematical analyses by fish group, such as modeling environmental preferences of each species and groups or estimating fish biomass fluctuations in relation to FAD trajectories, time of the day or soaking time, among other variables.

One of the most interesting and promising lines of investigation derived from this study is the possibility of obtaining fisheries-independent indices of relative abundance for tuna and nontuna species, a major and urgent challenge that would certainly complement current data on target and nontarget species populations. Significant effort has been recently conducted by fisheries scientists in this field, who have started to design the first promising steps to carry out this kind of study (Capello et al.[14]; Santiago et al.[15]).

Sustainable fishing practices with echosounder buoys

Nontuna biomass data provided by the new method, when validated by observational data in the specific regions of interest, may have at least two different applications for conservation issues. First, nontuna-to-tuna biomass ratios can be remotely estimated, helping fishing crews to avoid setting on undesirable DFADs with a high proportion of nontarget individuals. As Dagorn et al. (2012) suggested, the smaller the nontuna-to-tuna ratio, the lower are the impacts on nontarget species. In this context, echosounder buoys may contribute, from virtually unlimited distances, to the selection of the best DFAD to fish from a conservation point of view. Fishermen could benefit by saving fuel and time, optimizing their effort, catch and profits, by carefully planning their FAD-fishing routes in advance. Second, potential nontuna hotspots could be discovered, which could aid setting conservational measures, such as temporal or permanent marine protected areas or DFAD closures, if necessary. Hotspots obtained by this approach should be ground-truthed to those found through analysis of observer data, keeping in mind that the information of observers is based on fishing operations and hence, limited by fishing effort and fishing coverage constraints. Both sources of information should be, therefore, complementary. Although the nontuna biomass given by this study has not been specifically validated due to a lack of scientific biological sampling during the fishing operations used for testing the model, the results seem to be in accordance with values found by unpublished studies in the Atlantic Ocean (Amandé[13]). Future studies should take into account more detailed information on species composition (e.g., observers' data) to better understand the performance capability of this new method, especially in relation to nontuna species.

It is important to note that the original idea of this article was to include tuna size in the biomass estimation models, which would provide interesting informa-

[14]Capello, M., J.-L. Deneubourg, M. Robert, K. Holland, K. Schaeffer, and L. Dagorn.. 2013. A new fisheries independent method to estimate abundances of tropical tunas. Indian Ocean Tuna Commision (IOTC). Working Party Tropical Tuna (WPTT) IOTC–2013–WPTT15–12, 30 p. [Available at website.]

[15]Santiago, J., J. Lopez, G. Moreno, H. Murua, I. Quincoces, and M. Soto. 2015. Towards a tropical tuna buoy-derived abundance index (TT-BAI). International Council for the Conservation of Atlantic Tunas (ICCAT) SCRS/2015/90, 12 p. ICCAT, Corazón de María, 8, 28002 Madrid, Spain.

tion on the relative presence of both small and large tunas at DFADs. However, and likely due to the limited catch sample and the high numbers of small tunas occurring in those catches (i.e., ~95%), the optimization process led us to keep a single group of tuna sizes for the whole vertical range. We expect that, by tuning and refining this method, by ocean or regional site and with greater amounts of data in the future, this approach will be able to remotely provide fishing crews and scientists with the potential proportion of different tuna sizes under a particular DFAD, with consequent fishing advantages and conservation applications.

Model improvement

Although FADs tend to standardize the vertical behavior of fish (Matsumoto et al.[4]; Taquet et al., 2007b; Leroy et al., 2009; Govinden et al.[5]; Matsumoto et al., 2012; Schaefer and Fuller, 2013), it seems likely that the main depths occupied by fish of different sizes and species may differ between oceans or regional sites. Because vertical behavior is likely affected by the oceanography of an area, future tagging experiments should cover unsampled locations and couple both simultaneous in situ environmental data recorders (i.e., CTD profile recorders or acoustic surveys with scientific echosounders) and acoustic telemetry. High quality and high resolution data would contribute to a better understanding of the effect of biotic and abiotic factors on the vertical behavior of fish species when associated with floating objects—research that is necessary to improve the interpretation of data from echosounder buoys.

The present study employs the TS values obtained by Moreno et al. (2007), which fit reasonably well with the preliminary vertical depth layers defined in this work and with the results of other studies (Josse and Bertrand, 2000; Josse et al., 2000; Doray et al., 2006; Doray et al., 2007). As is widely recognized, knowing the TS value of a species is of primary importance to properly transform acoustic backscatter into species biomass. However, TS of many FAD-associated species remains elusive. Further ex situ or in situ investigations coupling acoustics with other supplementary technologies, such as video-cameras or ROVS (i.e., remotely operated vehicles) would permit obtaining precise TS values by species and thus improve the accuracy of estimates at species levels. Nonetheless, species-specific biomass conversion seems to be difficult to achieve in the current scenario. As Handegard et al. (2012) stated, one of the major challenges associated with acoustic measurements on autonomous platforms is the lack of biological sampling to verify the taxonomic composition. One possible solution to solve this situation is to explore catch variability and obtain spatiotemporal patterns of species composition at DFADs. Results could be used in future experiments to improve the performance of the method by postprocessing actual biomass estimates in cases where no biological sampling is available.

Although the echosounder buoys used in this study were developed for fishing purposes, there is still much room to improve the technical and technological features of current echosounder buoys. Ideally, some technical issues such as the lack of regular calibrations of the transducers or the characterization of their vertical and angular detection ranges should be solved. These are complicated issues due to the large number of echosounders (thousands of each brand) that are deployed with DFADs each year globally. A compromise solution could be the calibration of a limited number of transducers of each brand along an extended period of time, long enough to model a general calibration factor as a function of time. If consistent, the obtained brand-specific function could be then applied to all transducers, replacing the need to calibrate each transducer for every period of time. These calibrations could also include detectability functions at different depth ranges and angles in order to characterize the vertical and angular detection ranges of the transducer as a function of the TS of the targets. Then, the obtained detectability functions could be applied by using distance-sampling techniques (Buckland et al., 1993). Similarly, the range of the echosounder system, operation frequency, split beam technology, etc. should also be re-examined, optimized, installed, and adapted to the presence of different tropical tuna and accompanying nontuna species. Therefore, continuous improvements would be possible in the successive releases of new generations of transducers. For example, the recent inclusion of multifrequency transducers in two echosounder buoy brands could enable improved species discrimination in the near future, although those transducers would also require improved algorithms for analysis.

Due to confidentiality and sensitive issues, the flow of echosounder buoy data from vessel owners to research institutes is still rare. A data exchange system that preserves the privacy and ensures future bilateral advantages could help in effective industry and science collaboration. These kinds of initiatives should be endorsed by international bodies (e.g., tuna regional fisheries management organizations) to guarantee the viability of a project for both industry and science and to help promote such studies with an aim toward maintaining the long-term sustainability of fisheries.

Acknowledgments

The authors sincerely thank all the fishing masters from the Spanish tuna purse-seiner fleet who kindly agreed to answer our questions. We would like to thank the Spanish ship-owners and the associations that represent them (Asociación Nacional de Armadores de Buques Atuneros Congeladores [ANABAC] and Organización de Productores Asociados de Grandes Atuneros Congeladores [OPAGAC]). Of course we would like to thank the buoy manufacturers that provide us with technical data on their echosounder buoys. We sincerely thank G. P. Scott for revising the English and for useful comments that considerably improved this

article. This study was part of the European project MADE (Mitigating adverse ecological impacts of open ocean fisheries), funded by DG Research (Collaborative Project n° 210496). This article is contribution no. 751 from AZTI-Tecnalia. This study was partly funded by a PhD grant by the Fundación Centros Tecnológicos Iñaki Goenaga to Jon Lopez.

Literature cited

Babaran, R., C. Endo, Y. Mitsunaga, and K. Anraku.
2009. Telemetry study on juvenile yellowfin tuna *Thunnus albacares* around a payao in the Philippines. Fish. Eng. (Jpn) 46:21–28.

Brill, R. W., B. A. Block, C. H. Boggs, K. A. Bigelow, E. V. Freund, and D. J. Marcinek.
1999. Horizontal movements and depth distribution of large adult yellowfin tuna (*Thunnus albacares*) near the Hawaiian Islands, recorded using ultrasonic telemetry: implications for the physiological ecology of pelagic fishes. Mar. Biol. 133:395–408.

Buckland, S. T., D. R. Anderson, K. P. Burnham, and J. L. Laake.
1993. Distance sampling: estimating abundance of biological populations, 446 p. Chapman and Hall, London.

Castro, J. J., J. A. Santiago, and A. T. Santana-Ortega.
2002. A general theory on fish aggregation to floating objects: an alternative to the meeting point hypothesis. Rev. Fish Biol. Fish. 11:255–277.

Dagorn, L., K. Holland, J. Dalen, P. Brault, C. Vrignaud, E. Josse, G. Moreno, P. Brehmer, L. Nottestad, S. Georgakarakos, V. Trigonis, M. Taquet, R. Aumeeruddy, C. Girard, D. Itano, and G. Sancho.
2007a. New instruments to observe pelagic fish around FADs: satellite-linked acoustic receivers and buoys with sonar and cameras. *In* Cutting-edge technologies in fish and fisheries science. Australian Society for Fish Biology Workshop Proceedings; Hobart, Tasmania, Australia, 28–29 August 2006 (J. M. Lyle, D. M. Furlani, and C. D. Buxton, eds.), p. 37–43. Australian Soc. Fish Biol., Hobart, Tasmania, Australia.

Dagorn, L., K. N. Holland, and D. G. Itano.
2007b. Behavior of yellowfin (*Thunnus albacares*) and bigeye (*T. obesus*) tuna in a network of fish aggregating devices (FADs).

Dagorn, L., D. Pincock, C. Girard, K. Holland, M. Taquet, G. Sancho, D. Itano, and R. Aumeeruddy.
2007c. Satellite-linked acoustic receivers to observe behavior of fish in remote areas. Aquat. Living Resour. 20:307–312.

Dagorn, L., J. D. Filmalter, F. Forget, M. J. Amandè, M. A. Hall, P. Williams, H. Murua, J. Ariz, P. Chavance, and N. Bez.
2012. Targeting bigger schools can reduce ecosystem impacts of fisheries. Can. J. Fish. Aquat. Sci. 69:1463–1467.

Dagorn, L., K. N. Holland, V. Restrepo, and G. Moreno.
2013. Is it good or bad to fish with FADs? What are the real impacts of the use of drifting FADs on pelagic marine ecosystems? Fish Fish. 3:391–415.

Doray, M., E. Josse, P. Gervain, L. Reynal, and J. Chantrel.
2006. Acoustic characterisation of pelagic fish aggregations around moored fish aggregating devices in Martinique (Lesser Antilles). Fish. Res. 82:162–175.

Doray, M., E. Josse, P. Gervain, L. Reynal, and J. Chantrel.
2007. Joint use of echosounding, fishing and video techniq ues to assess the structure of fish aggregations around moored fish aggregating devices in Martinique (Lesser Antilles). Aquat. Living Resour.20:357–366.

Filmalter, J. D., L. Dagorn, P. D. Cowley, and M. Taquet.
2011. First descriptions of the behavior of silky sharks, *Carcharhinus falciformis*, around drifting fish aggregating devices in the Indian Ocean. Bull. Mar. Sci. 87:325–337.

Fonteneau, A., E. Chassot, and N. Bodin.
2013. Global spatio-temporal patterns in tropical tuna purse seine fisheries on drifting fish aggregating devices (DFADs): taking a historical perspective to inform current challenges. Aquat. Living Resour. 26:37–48.

Forget, F. G., M. Capello, J. D. Filmalter, R. Govinden, M. Soria, P. D. Cowley, L. Dagorn.
2015. Behaviour and vulnerability of target and non-target species at drifting fish aggregating devices (FADs) in the tropical tuna purse seine fishery determined by acoustic telemetry. Can. J. Fish. Aquat. Sci. 72:1398–1405.

Govinden, R., R. Jauhary, J. Filmalter, F. Forget, M. Soria, S. Adam, and L. Dagorn.
2013. Movement behaviour of skipjack (*Katsuwonus pelamis*) and yellowfin (*Thunnus albacares*) tuna at anchored fish aggregating devices (FADs) in the Maldives, investigated by acoustic telemetry. Aquat. Living Resour. 26:69–77.

Handegard, N. O., L. Buisson, P. Brehmer, S. J. Chalmers, A. De Robertis, G. Huse, R. Kloser, G. Macaulay, O. Maury, P. H. Ressler, N. C. Stenseth, and O. R. Godø.
2012. Towards an acoustic-based coupled observation and modelling system for monitoring and predicting ecosystem dynamics of the open ocean. Fish Fish. 4:605–615.

Hastie, T. J., and R. J. Tibshirani.
1990. Generalized additive models. Monogr. Stat. Appl. Probability 43, 335 p. Chapman and Hall/CRC, London.

IATTC (Inter-American Tropical Tuna Commission).
2013. Tunas and billfishes in the eastern Pacific Ocean in 2012. IATTC Fish. Status Rep. 11, 171 p. [Available at website.]

Josse, E., P. Bach, and L. Dagorn.
1998. Simultaneous observations of tuna movements and their prey by sonic tracking and acoustic surveys. Hydrobiologia 371:61–69.

Josse, E., and A. Bertrand.
2000. *In situ* acoustic target strength measurements of tuna associated with a fish aggregating device. ICES J. Mar. Sci. 57:911–918.

Josse, E., L. Dagorn, and A. Bertrand.
2000. Typology and behaviour of tuna aggregations around fish aggregating devices from acoustic surveys in French Polynesia. Aquat. Living Resour. 13:183–192.

Leroy, B., D. G. Itano, T. Usu, S. J. Nicol, K. N. Holland, and J. Hampton.
2009. Vertical behavior and the observation of FAD effects on tropical tuna in the warm-pool of the western Pacific Ocean. *In* Tagging and tracking of marine animals with electronic devices (J. L. Nielsen, H. Arrizabalaga, N. Fragoso, A. Hobday, M. Lutcavage, and J. Sibert,

eds.), p. 161–179. Springer Netherlands, Dordrecht, the Netherlands.

Lopez, J., G. Moreno, I. Sancristobal, and J. Murua.
2014. Evolution and current state of the technology of echo-sounder buoys used by Spanish tropical tuna purse seiners in the Atlantic, Indian and Pacific Oceans. Fish. Res. 155:127–137.

MacLennan, D. N., P. G. Fernandes, and J. Dalen.
2002. A consistent approach to definitions and symbols in fisheries acoustics. ICES J. Mar. Sci. 59:365–369.

Matsumoto, T., T. Kitagawa, and S. Kimura.
2012. Considerations on diving patterns of bigeye tuna *Thunnus obesus* based on archival tag data. Fish. Sci. 79:39–46.

Matsumoto, T., K. Satoh, and M. Toyonaga.
2014. Behavior of skipjack tuna (*Katsuwonus pelamis*) associated with a drifting FAD monitored with ultrasonic transmitters in the equatorial central Pacific Ocean. Fish. Res. 157:78–85.

Maufroy, A., E. Chassot, R. Joo, and D. M. Kaplan.
2015. Large-scale examination of spatio-temporal patterns of drifting fish aggregating devices (dFADs) from tropical tuna fisheries of the Indian and Atlantic Oceans. PLoS ONE. 10(5):e0128023.

Mitsunaga, Y., C. Endo, K. Anraku, C. M. Selorio Jr., and R. P. Babaran.
2012. Association of early juvenile yellowfin tuna *Thunnus albacares* with a network of payaos in the Philippines. Fish. Sci. 78:15–22.

Moreno, G., E. Josse, P. Brehmer, and L. Nøttestad.
2007. Echotrace classification and spatial distribution of pelagic fish aggregations around drifting fish aggregating devices (DFAD). Aquat. Living Resour. 20:343–356.

Musyl, M. K., R. W. Brill, C. H. Boggs, D. S. Curran, T. K. Kazama, and M. P. Seki.
2003. Vertical movements of bigeye tuna (*Thunnus obesus*) associated with islands, buoys, and seamounts near the main Hawaiian Islands from archival tagging data. Fish. Oceanogr. 12:152–169.

R Core Team.
2015. R: a language and environment for statistical computing. R Foundation for Statistical Computing, Vienna, Austria. [Available from website, accessed July 2015.]

Robert, M., L. Dagorn, J. Lopez, G. Moreno, and J.-L. Deneubourg.
2013. Does social behavior influence the dynamics of aggregations formed by tropical tunas around floating objects? An experimental approach. J. Exp. Mar. Biol. Ecol. 440:238–243.

Schaefer, K. M., and D. W. Fuller.
2005. Behavior of bigeye (*Thunnus obesus*) and skipjack (*Katsuwonus pelamis*) tunas within aggregations associated with floating objects in the equatorial eastern Pacific. Mar. Biol. 146:781–792.
2013. Simultaneous behavior of skipjack (*Katsuwonus pelamis*), bigeye (*Thunnus obesus*), and yellowfin (*T. albacares*) tunas, within large multi-species aggregations associated with drifting fish aggregating devices (FADs) in the equatorial eastern Pacific Ocean. Mar. Biol. 160:3005–3014.

Simmonds, J., and D. N. MacLennan.
2005. Fisheries acoustics: theory and practice, 2nd ed., 437 p. Blackwell Science, London.

Taquet, M., L. Dagorn, J.-C. Gaertner, C. Girard, R. Aumerruddy, G. Sancho, and D. Itano.
2007a. Behavior of dolphinfish (*Coryphaena hippurus*) around drifting FADs as observed from automated acoustic receivers. Aquat. Living Resour. 20:323–330.

Taquet, M., G. Sancho, L. Dagorn, J.-C. Gaertner, D. Itano, R. Aumeeruddy, B. Wendling, and C. Peignon.
2007b. Characterizing fish communities associated with drifting fish aggregating devices (FADs) in the Western Indian Ocean using underwater visual surveys. Aquat. Living Resour. 20:331–341.

Venables, W. N., and C. M. Dichmont.
2004. GLMs, GAMs and GLMMs: an overview of theory for applications in fisheries research. Fish. Res. 70:319–337.

Weng, J.-S., M.-K. Hung, C.-C. Lai, L.-J. Wu, M.-A. Lee, and K.-M. Liu.
2013. Fine-scale vertical and horizontal movements of juvenile yellowfin tuna (*Thunnus albacares*) associated with a subsurface fish aggregating device (FAD) off southwestern Taiwan. J. Appl. Ichthyol. 29:990–1000.

Wood, S.
2006. Generalized additive models: an introduction with R, 410 p. Chapman and Hall/CRC, London.

NOAA
National Marine
Fisheries Service

Fishery Bulletin
established 1881

Spencer F. Baird
First U.S. Commissioner
of Fisheries and founder
of *Fishery Bulletin*

Development of underwater recorders to quantify predation of juvenile Chinook salmon (*Oncorhynchus tshawytscha*) in a river environment

Nicholas J. Demetras (contact author)[1]
David D. Huff[2]
Cyril J. Michel[1]
Joseph M. Smith[3]
George R. Cutter[4]
Sean A. Hayes[5]
Steven T. Lindley[5]

Email address for contact author: nicholas.demetras@noaa.gov

[1] University of California, Santa Cruz
Affiliated with Southwest Fisheries Science Center
National Marine Fisheries Service, NOAA
110 Shaffer Road
Santa Cruz, California 95060

[2] Point Adams Research Station
Fish Ecology Division
Northwest Fisheries Science Center, NOAA
PO Box 155, Hammond, OR 97121

[3] School of Aquatic and Fishery Sciences
University of Washington
1122 NE Boat Street
Seattle, Washington 98105

[4] Fisheries Resource Division
Southwest Fisheries Science Center
National Marine Fisheries Service, NOAA
8901 La Jolla Shores Drive
La Jolla, California 92037-1508

[5] Fisheries Ecology Division
Southwest Fisheries Science Center
National Marine Fisheries Service, NOAA
110 Shaffer Road
Santa Cruz, California 95060

Abstract—Recent acoustic tagging of juvenile Chinook salmon (*Oncorhynchus tshawytscha*) in the southern portion of California's Sacramento–San Joaquin Delta has revealed extremely low survival rates (<1%), possibly due to predation by piscivorous fishes. We evaluated predation as a cause of low survival by designing and testing freely floating GPS-enabled predation-event recorders (PERs) baited with juvenile Chinook salmon. We estimated predation rates and identified predation locations within a 1-kilometer reach of the Lower San Joaquin River. We modeled the relationship between time to predation and environmental variables with a Cox proportional hazards analysis that accounts for censored data. Our results indicated that an increase of 1 m/s in water velocity elevated the minute-by-minute hazard of predation by a factor of 9.6. Similarly, each increase in median depth decreased the predation hazard by a factor of 0.5. The mean relative predation rate in the study area was 15.3% over 9 sampling events between March and May 2014. Waterproof video cameras attached to a subset (48 of 216) of PERs successfully identified predator species 25% of the time. Our GPS-enabled PERs proved to be an inexpensive and reliable tool, which quantified predation, identified predation locations, and provided complementary information for acoustic telemetry and predator diet studies.

Manuscript submitted 9 July 2015.
Manuscript accepted 3 February 2016.
Fish. Bull. 114:179–185 (2016).
Online publication date: 23 February 2016.
doi: 10.7755/FB.114.2.5

The views and opinions expressed or implied in this article are those of the author (or authors) and do not necessarily reflect the position of the National Marine Fisheries Service, NOAA.

Predation on juvenile Chinook salmon (*Oncorhynchus tshawytscha*) and other native fishes within California's Sacramento–San Joaquin Delta has raised considerable debate over the last several decades (Bennet and Moyle, 1996; Mount et al., 2012). Traditionally, juvenile Chinook salmon survival within this delta has been estimated by using acoustic tagging data or coded-wire tag recoveries from mid-water trawls (Brandes and McLain, 2001; Newman and Rice, 2002; Buchanan et al., 2013; Michel et al., 2013; Pyper et al., 2013; Newman, 2003; Newman[1]). It is currently not clear what proportion of juvenile salmonid mortality may be directly attributed to fish predation. It is also difficult to interpret results regarding population-level survivorship in the Delta because these data have limited spatial scales, used various tagging methodologies, and do not clearly connect tag loss or mortality to predation (Grossman et al.[2]). Be-

[1] Newman, K. B. 2008. An evaluation of the four Sacramento-San Joaquin River Delta juvenile salmon survival studies, 181 p. U.S. Fish Wildl. Serv., Stockton, CA. [Available at website, accessed October 2014.]

[2] Grossman, G. D., T. Essington, B. Johnson, J. Miller, N. E. Monsen, and T. N. Pearsons. 2013. Effects of fish predation on salmonids in the Sacramento River–San Joaquin Delta and associated ecosystems, 71 p. [Available at website, accessed October 2014.]

cause most survival data come from acoustic tagging studies, it is essential to improve our understanding of the underlying cause of mortality events (i.e. predation, environmental, or other) from these types of instruments. We developed a tool to address this research need by designing floating, baited, predation-event recorders (PERs). These recorders allow estimation of relative predation rates in various environments, and reveal information about mortality produced by different species of fish predators.

Our objectives were to investigate the feasibility of 1) developing and constructing a passive, baited, GPS-enabled PER, 2) evaluating relative risk of predation mortality and 3) observing and identifying individual predators and associated predation events. We estimated relative predation mortality and identified predation hot spots upon juvenile Chinook salmon to compliment ongoing acoustic telemetry surveys. We were able to accurately identify the location of individual predation events, reliably identify predators, and the recorder system was easily deployed and retrieved by a boat-based crew of 2 people.

Materials and methods

PER construction

PERs were constructed from an approximately 75 cm length of 76 mm diameter, schedule 40 polyvinyl chloride (PVC) pipe. The bottom end was fitted with a PVC cap which was glued in place and the top end was fitted with a two part threaded, removable cap. Attached to the top cap was a GARMIN® TT™10[3] GPS transponder (available at website) set to update and record its position every five seconds. A predation-activated timer was attached to the bottom cap. The design of the timer, similar to that of Somerton et al. (1988), is connected to a baited line attached to a magnet, which is slotted inline into a receptacle on the timer, housing a magnetic switch (Fig. 1). When the bait is pulled, the magnet is removed, activating the timer that records the precise timing of the predation event. All GPS trackers were controlled and their tracks recorded with a GARMIN® Alpha 100®[1] handheld base-station unit plugged into a laptop computer located on board the boat. Up to 20 GPS trackers may be tracked simultaneously in real-time with one Alpha 100® handheld unit, as long as all trackers are within approximately 14 kilometers line-of-sight. More trackers can be tracked if multiple base stations are used.

Attached to each predation timer was a 50 cm length of 3.6 kg breaking-strength fluorocarbon leader. A sub yearling fall-run juvenile Chinook salmon from the Mokelumne River fish hatchery was attached to the distal end of the fluorocarbon leader by means of a loop threaded through the mouth and operculum. A seven-gram split-shot style weight was placed approximately 10 cm above the fish. Approximately 2.25-kg of lead shot was placed inside the bottom of each PER as ballast, which served to keep PERs upright while submerging all but the upper most 10 to 15 cm, where the GPS receiver was attached. GoPro[3] underwater cameras, with 64 gigabyte storage SanDisk[3] memory cards (available at website), were attached to a subset of 3 PERs opposite the predation timer and aimed directly at the attached smolt (Fig. 1). PERs were spray painted in a green and brown camouflage pattern to reduce visibility and obtrusiveness in the upper water column, but the top 10 to 15 cm above the water line were painted a bright safety orange and marked with reflective tape for easier visual identification by passing watercraft. Onset® HOBO®[3] pendant temperature and light data loggers (available at website) were attached to each PER (Fig. 1) so that we could relate environmental variables to predation events.

Field trials

All field trials were conducted within a 1-km study site (lat. 37.806°N, long. 121.317°W, lat. 37.799°N, long. 121.313° W) on the lower San Joaquin River located approximately 1.5 km downstream from Mossdale, CA. The depth of the sampling site ranged from 3.65 m to 0.6 m and had a mean depth of 1.98 m; the minimum effective depth of the PERs was 0.6 m, which represented approximately 88% of the total wetted stream channel. Depth of the entire sampling site was measured and mapped with boat-mounted sonar. River velocities ranged from 0.49 m/s to –0.32 m/s (mean velocity: 0.27 m/s. Negative values denote a flood tide and reversal of flow going upstream. Channel width ranged from approximately 70 m to 90 m. The sinuosity index (SI) of the study reach was 1.21. SI is a measurement of a river or stream's deviation from the shortest possible downslope path. A value of 1.0 indicates a perfectly straight channel, whereas increasing values of 1 are representative of increased meandering (Mueller, 1968). Ten PERs were repeatedly deployed on 9 separate trials, either one hour before sunrise or one hour before sunset by a 2-person boat crew, all trackers remained within line of site of the boat while deployed. Each trial consisted of 2 separate deployments mid channel; if a tether became beached or fouled it was promptly retrieved and redeployed at mid-channel. Each re-deployment was considered a unique deployment on its own.

The procedure for deploying PERs was 1) activation of GPS transponders/GoPro cameras (30 sec/PER), 2) attachment of the salmon smolt to predation timers (1 min/timer), 3) release of PERs (1 min/PER), 4) transit of PER through study site (45 min. to 1 h. depending upon river velocity), 5) retrieval of PERs and recording of timer data (20–30 min). Digital predation timers were immediately recorded upon retrieval. The cumulative time spent preparing, deploying, fishing, and re-

[3] Mention of trade names or commercial companies for identification purposes only and does not imply endorsement by the National Marine Fisheries Service.

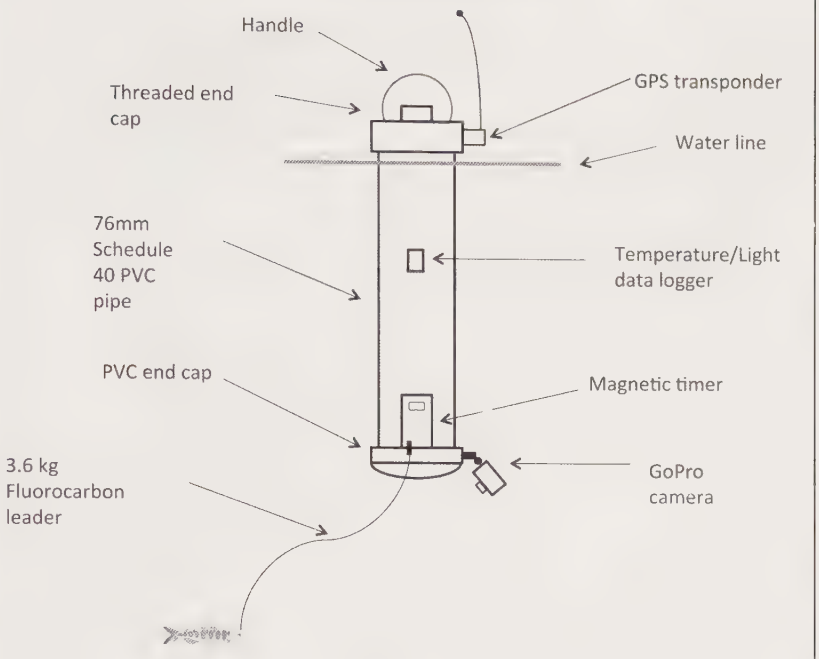

Figure 1

Schematic of a predation-event recorder (PER) with attached salmon smolt as bait. PERs were used to evaluate predation rates and environmental variables in the Sacramento–San Joaquin Delta, California from March through May of 2014.

trieving ten PERs by a 2-person boat crew ranged from 90 to 115 minutes.

Owing to extremely low flows during our study period in the spring of 2014, the lower San Joaquin River was under direct tidal influence over the course of the study and experienced a mixed, semidiurnal tidal pattern. The tidal nature of the San Joaquin River during this period required extra effort to determine the correct mid-channel placement of the PERs so that they would remain within the site for approximately 45 minutes or longer. If a PER did not remain within a study site for at least 45 minutes, or became beached or otherwise fouled, it was promptly retrieved, re-baited and redeployed within the study site.

Data processing and analysis

PER GPS transponders recorded a location every 5 seconds, whereas predation timers recorded the timing of predation events. By cross-referencing predation data from the predation timer (time of predation) with PER GPS data (time/latitude/longitude) we were able to obtain locations of each predation event. GoPro video footage was captured with a widescreen aspect ratio of 16:9, resolution 1920×1080 (1080p HD "Superview"), at 30 frames per second at the low light setting. Each camera produced on average approximately 12 to 20 gigabytes of data per deployment depending on individual PER sampling time. Video footage was later viewed to confirm predation events and to identify predator species.

The relationship between survival of tethered smolt, exposure time, and environmental factors was modeled with a Cox proportional-hazards regression for censored data (Cox, 1972) by using the OIsurv package, vers. 0.2 (Diez, 2013) in R statistical software, vers. 3.2.0 (R Core Team, 2015). Before model construction, we examined correlation coefficients of candidate covariate pairs to identify collinearity and only included one variable of a pairwise comparison that had correlations greater than 0.7 (Dormann et al., 2013). The candidate covariates for the model were total distance traveled (m), median light intensity (lux), median depth (m), standard deviation of depth (m), median water temperature (° C), and median water velocity (ms^{-1}). Akaike's information criterion (AIC; Burnham and Anderson, 2002) was used to select the most parsimonious model with the best fit to the data in a forward and backward step-wise fashion. Model residuals were examined to evaluate the model fit.

Results

We conducted 216 PER deployments between late March and late May 2014. Of the 216 deployments, we recorded 33 total predation events (15%), 12 of which were captured on video by the GoPro camera. Throughout the study we were able to easily combine the timer data with the corresponding GPS data to produce accurate maps of PER pathways and predation event locations within the study site (Fig. 2).

Water conductivity and water velocity were collinear at r=–0.75. Water conductivity was excluded, however, from the analysis because it was within the physiological range of both juvenile Chinook salmon and predators and was assumed to have minimal impact on their ability to forage. AIC model selection indicated that water velocity and median depth best explained variation in predation rate. The coefficient for water velocity was 2.3 and median depth was –0.7. The exponentiated coefficient for water velocity was 9.6 and median depth was 0.5. Exponentiated coefficients are interpretable as multiplicative effects on the hazard. For example, by holding the median depth constant, an additional meter per second increase in water velocity increases the minute-by-minute hazard of predation by a factor of 9.6. Similarly, each increase in median depth decreases the hazard by a factor of 0.5. The likelihood-ratio [LR]

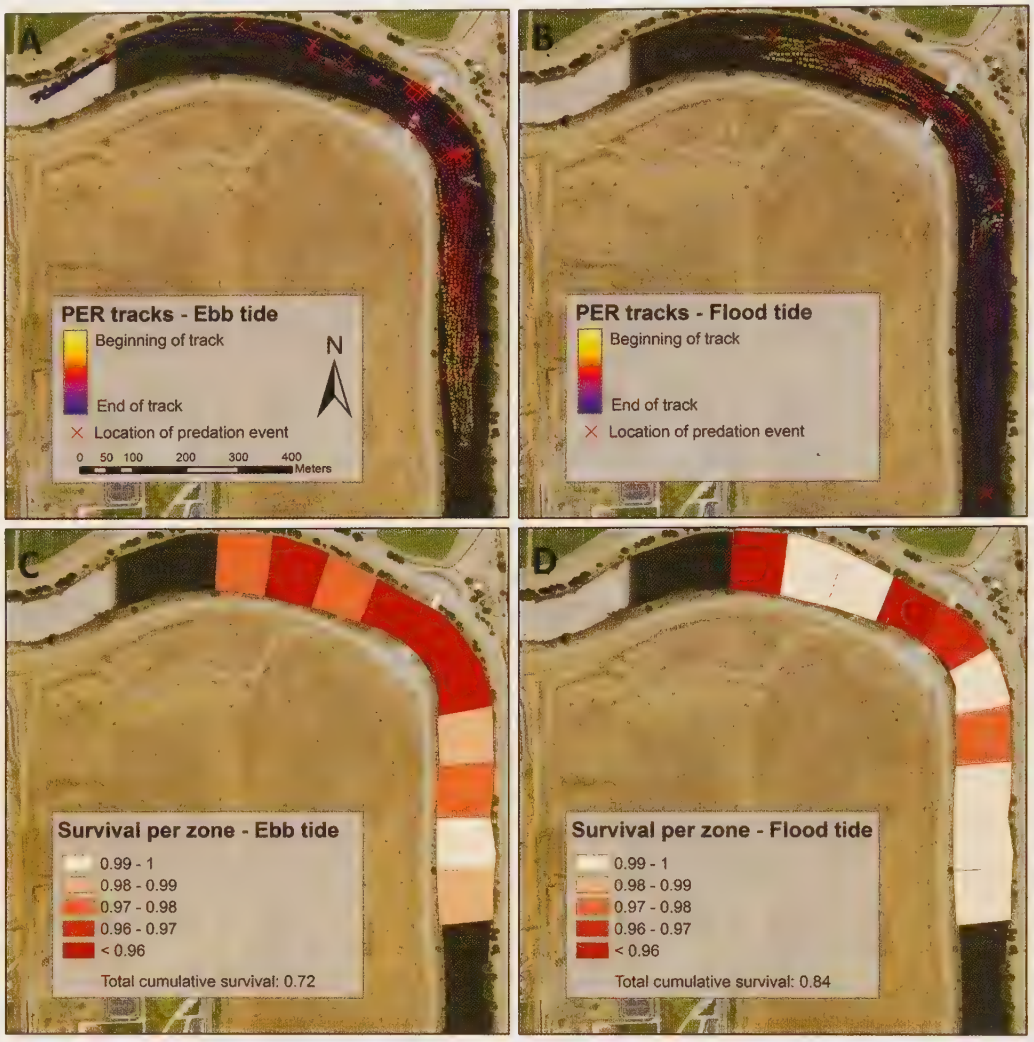

Figure 2

Multipanel aerial photograph of the study site. (**A**) Individual PER tracks during ebb tide conditions. Red ×'s denote individual locations of predation. (**B**) Individual PER tracks during flood tide conditions. Red ×'s denote individual locations of predation. (**C**) Study site segmented into 100-m sections. Color coding denotes survival per 100-m sections during ebb tide conditions. (**D**) Study site segmented into 100-m sections. Color-coding denotes survival per 100 m sections during flood-tide conditions.

test of the null hypothesis that the β's are zero was rejected (LR=11.3, 2 df, P=0.004). The estimated distribution of survival times was calculated at the mean values of the covariates (Fig. 3). These indicated that the proportion of salmon that were preyed upon increased sharply from 20 to 30 minutes of exposure to predators. We plotted the distribution of survival times as they varied from the minimum (negative) to the maximum (positive) water velocities by 0.1 m/s increments (Fig. 4). Predation was greatest with increasing positive water velocities and was lowest at the more negative water velocities.

From the PERs that were outfitted with cameras, we obtained 48 complete videos of individual deployments (22% of total) that resulted in approximately 800 gigabytes of raw data. Of these, tripped timers in combination with missing smolts indicated that 12 were predation events. Video analysis confirmed the predation and a fish was seen preying upon the smolt in each instance. Three of the events captured on video were confirmed to be predation by striped bass (*Morone saxatilis*), and the remaining 8 predators were not identifiable to species. Analysis of the video data revealed that if the timer was activated and the

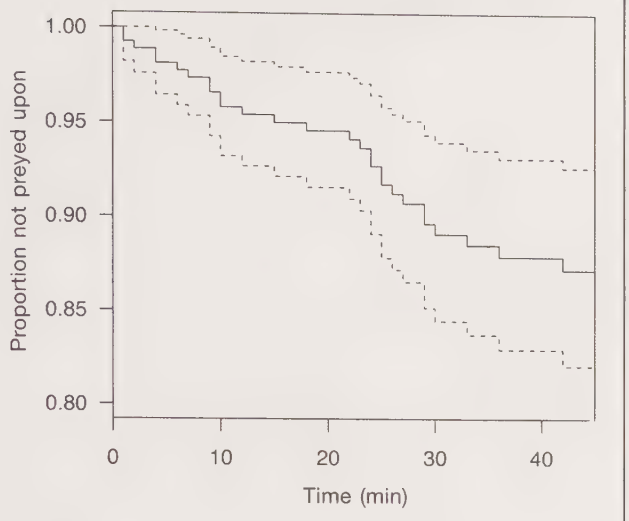

Figure 3

Estimated survival function for the Cox regression of time to predation on water velocity and median depth. Broken lines indicate a point-wise 95% confidence interval about the survival function.

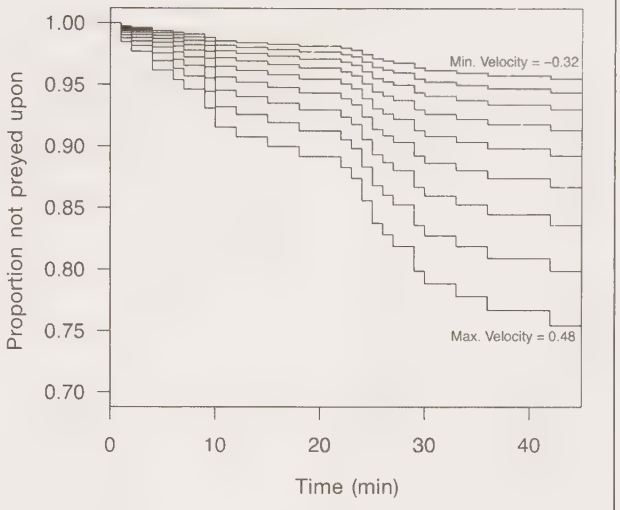

Figure 4

Estimated survival function for the Cox regression of time to predation over a series of water velocities from the minimum (negative) to the maximum (positive) water velocities by increments of 0.1 m/s.

smolt was missing, it was a confirmed predation event. Video analysis also indicated that the tethered smolts remained in an upright and active swimming position during deployments.

Discussion

Predation upon juvenile Chinook salmon in the Sacramento–San Joaquin Delta and resulting effects on population level has been a topic of debate. The presumption that predation may play a significant role in survival was investigated with the use of statistical models on winter-run Chinook salmon by Lindley and Mohr (2003) and Hendrix.[4] Neither analysis implied a substantial link between striped bass predation and Chinook salmon survival. However, the quality of the data used in statistical analyses is a major determinant of the strength of the results, and diet data for many piscine predators in the delta is lacking (Grossman et al.[2]). The addition of robust data from new methods for quantifying predation may help fill this crucial gap for future modeling efforts. Our results, that predation was greatest at maximum positive water velocities (outgoing tide) and lowest at more negative water velocities (incoming tide), are in contrast with those of Anderson et al. (2005), who found that survival of juvenile salmon was influenced more by travel distance than travel time or velocity. However, there are some important differences between studies. First, we conducted our study on a much smaller spatial and temporal scale that quantified individual predation events and therefore characterized more proximate, short-term processes. Secondly, our study system was strongly tidally influenced, to the extent that tidal water movements may have substantially affected predator behavior.

Acoustic tag technology for basin-scale studies has become the standard for assessing movement and survival of fish, particularly in salmonids (Perry et al., 2010; Michel et al., 2013). However, these studies are often expensive and do not reveal the mechanisms or locations of mortality. Although researchers are developing acoustic tags that report predation events through a change in tag ID code, it may be hours to days before the digestion-based processes trigger the predation event to be detected by a receiver (Afentoulis and Schultz, 2014). Furthermore, acoustic tags designed to report predation events do not identify predator species or distinguish the difference between predation events and the scavenging of tagged fish after some other cause of mortality. As such, alternative methods and instrumentation, such as PERs are needed to complement acoustic tagging studies to evaluate predation mortality.

Fishery and water managers often call for investigations of predator control along with predator habitat manipulation as a management tool, and some predator-reduction studies have been implemented (e.g., Porter, 2011). Evaluations of predator control and preda-

[4] Hendrix, N. 2008. A statistical model of Central Valley Chinook incorporating uncertainty: description of *Oncorhynchus* Bayesian analysis (OBAN) for winter run Chinook, 18 p. R2 Resource Consultants Inc., Redmond, WA. [Available at website, accessed November 2014.]

tor habitat manipulation require estimates of pretreatment predation rates and of how predation rates fluctuate with changes in predator abundance and habitat condition. These predation rates may be estimated in various ways. One method involves conducting coordinated studies of predator and prey distribution and abundance, in combination with predator diet studies (Rieman et al., 1991). However, this approach is labor intensive and time consuming, making it difficult to replicate in several different areas at once. Considering that the Sacramento–San Joaquin Delta has a complex suite of hydrological processes and geography (the south delta is especially affected by municipal and freshwater export processes), there is potential for substantial spatial heterogeneity in fish predation rates, thus requiring replication of predation rate studies in many different areas and habitats.

Diet-based predation studies lack statistical power when prey species of concern are rare and make up only a small part of a predator's diet. Predation-event recorders (PER) provide an alternative that has the advantage of being relatively inexpensive and also capable of being implemented over a broad spatial and temporal scale. The intent of this method is not to quantify absolute predation rates, but rather to provide a relative comparison of predation rates among study areas to substantiate predator density and environmental covariate hypotheses. Additionally, the identification of predation "hotspots" gives us insight into the underlying physical and biological mechanisms that contribute to observed mortality. By simultaneously collecting environmental data, we were able to construct and select appropriate statistical models to describe the contributing factors that affect predation.

Fish ecologists have used stationary tethers to study predation on fishes (Linehan et al., 2001; Adams et al., 2004; Chittaro et al., 2005). However, our free drifting PERs have features that are more useful in free-flowing rivers. Drifting PERs may be the preferred design under conditions where movements through a habitat feature are favored, resulting in a more natural presentation and larger area sampled. This is especially important when assessing interactive effects of variables such as water exports, flow rate, total discharge and tidal mechanics on the movement and survival of young fish. Alternatively, anchored PERs enable targeted sampling around specific habitat features like the lower water column in deeper river sections, littoral habitats, or around fixed structures. The PER design has the advantage that it may be altered (size, shape etc.) for sampling in different conditions. Owing to the tidal nature and relatively low current velocities in our study site, we designed our PERs to maximize the effect of subsurface current forces in order to counteract the effect of wind. PERs may also be adapted to study predation on other fish species, such as delta smelt (*Hypomesus transpacificus*) or steelhead (*Oncorhynchus mykiss*) that also occur in the Sacramento–San Joaquin Delta, and it may be modified for use in rivers, lakes, estuaries and coastal ocean environments.

Acknowledgments

We would like to thank the many people who assisted with fieldwork, particularly M. Sabal, V. Lo, T. Brown, B. Lehman, and M. Miller. In addition, M. Henderson and F. Cordoleani provided insightful comments on early drafts and three anonymous reviewers provided helpful suggestions during the review process. The California Department of Water Resources funded this work under agreement no. 46-10100 with the National Marine Fisheries Service. Material and logistical support was also provided by The National Marine Fisheries Service Southwest Fisheries Science Center, Santa Cruz, CA.

Literature cited

Adams, A. J., J. V. Locascio, and B. D Robbins.
2004. Microhabitat use by a post-settlement stage estuarine fish: evidence from relative abundance and predation among habitats. J. Exp. Mar. Biol. Ecol. 299:17–33.

Afentoulis, V., and A. Schultz.
2014. Efficacy test of a tag designed to signal when a fish has been consumed. *In* Challenges, collaboration, solutions. California-Nevada Chapter of the American Fisheries Society 48th Annual Conference; Sacramento, CA, 27–29 March, p. 29. Calif.-Nev. Chapter Am. Fish. Soc., Davis, CA. [Available at website.]

Anderson, J. J., E. Gurarie, and R. W. Zabel.
2005. Mean free-path length theory of predator–prey interactions: application to juvenile salmon migration. Ecol. Model. 186:196–211.

Bennett, W. A., and P. B. Moyle.
1996. Where have all the fishes gone: interactive factors producing fish declines in the Sacramento-San Joaquin estuary. *In* San Francisco Bay: the ecosystem, vol. 1 (J. T. Hollingbaugh, ed.), p. 519–542. Pacific Division, American Association for the Advancement of Science, San Francisco, CA

Buchanan, R. A., J. R. Skalski, P. L. Brandes, and A. Fuller.
2013. Route use and survival of juvenile Chinook salmon through the San Joaquin River Delta. North Am. J. Fish. Manage. 33:216–229.

Burnham, K. P., and D. R. Anderson.
2002. Model selection and multimodel inference: a practical information-theoretic approach, 2nd ed., 488 p. Springer, New York.

Brandes, P. L., and J. S. McLain.
2001. Juvenile Chinook salmon abundance, distribution and survival in the Sacramento-San Joaquin estuary. *In* Contributions to the biology of Central Valley salmonids, vol 2. Calif. Dep. Fish Game, Fish. Bull. 179 (R. L. Brown, ed.), p. 39–136. Calif. Dep. Fish Game, Sacramento, CA.

Chittaro, P. M., P. Usseglio, and P. F. Sale.
2005. Variation in fish density, assemblage composition and relative rates of predation among mangrove, seagrass and coral reef habitats. Environ. Biol. Fish. 72:175–187.

Cox, D. R.
1972. Regression models and life-tables. J. R. Stat. Soc., Ser. B 34:187–220.

Dormann, C. F., J. Elith, S. Bacher, S. Bachmann, G. Carl, G. Carré, J. R. García Marquéz, B. Gruber, B. Lafourcade, P. J. Leitão, T. Münkemüller, C. McClean, P. E. Osborne, B. Reineking, A. K. Skidmore, D. Zurell, and S. Lautenbach.
2013. Collinearity: a review of methods to deal with it and a simulation study evaluating their performance. Ecography 36(1):27–46.

Diez, D. M.
2013. OIsurv: survival analysis supplement to OpenIntro guide. [Available at website, accessed June 2015.]

Lindley, S. T., and M. S. Mohr.
2003. Modeling the effect of striped bass (*Morone saxatalis*) on the population viability of Sacramento River winter-run Chinook salmon (*Oncorhynchus tshawytscha*). Fish. Bull. 101:321–331.

Linehan, J. E., R. S. Gregory, and D. C. Schneider.
2001. Predation risk of age-0 cod (*Gadus*) relative to depth and substrate in coastal waters. J. Exp. Mar. Biol. Ecol. 263:25–44.

Michel, C. J., A. J. Ammann, E. D. Chapman, P. T. Sandstrom, H. E. Fish, M. J. Thomas, G. P. Singer, S. T. Lindley, A. P. Klimeley, and R. B. MacFarlane.
2013. The effects of environmental factors on the migratory movement patterns of Sacramento River yearling late-fall run Chinook salmon (*Onchorhynchus tshawytscha*). Environ. Biol. Fish. 96:257–2571.

Mueller, J. E.
1968. An introduction to the hydraulic and topographic sinuosity indexes. Ann. Assoc. Am. Geogr. 58:371–385.

Mount, J., W. Bennett, J. Durand, W. Fleenor, E. Hanak,. J. Lund, and P. Moyle.
2012. Aquatic ecosystem stressors in the Sacramento–San Joaquin Delta, 22 p. Public Policy Inst. California, San Francisco. [Available from website, accessed October 2014.]

Newman, K. B.
2003. Modelling paired release-recovery data in the presence of survival and capture heterogeneity with application to marked juvenile salmon. Stat. Model. 3:157–177.

Newman, K. B., and J. Rice.
2002. Modeling the survival of Chinook salmon smolts outmigrating through the lower Sacramento River system. J. Am. Stat. Assoc. 97:983–993.

Perry, R. W., J. R. Skalski, P. L. Brandes, P. L. Sandstrom, A. P. Klimley, A. Ammann, and B. MacFarlane.
2010. Estimating survival and migration route probabilities of juvenile Chinook salmon in the Sacramento-San Joaquin River Delta. North Am. J. Fish. Manage. 30:142–156.

Porter, R.
2011. Report on the predation index, predator control fisheries, and program evaluation for the Columbia River Basin Experimental Northern Pikeminnow Management Program, 124 p. U.S. Dep. Energy, Bonneville Power Administration, Portland, OR. [Available at website, accessed October 2014.]

Pyper, B. T., Garrison, and S. Cramer.
2013. Analysis of trawl efficiency at Chipps Island using coded-wire-tagged releases of juvenile Chinook salmon, 97 p.. Cramer Fish Sciences, Gresham, OR. [Available at website, accessed October 2014.]

R Core Team.
2015. R: a language and environment for statistical computing. R Foundation for Statistical Computing, Vienna, Austria. [Available at website, accessed March 2015.]

Rieman, B. E., R. C. Beamesderfer, S Vigg, and T. P. Poe.
1991. Estimated loss of juvenile salmonids to predation by northern squawfish, walleyes, and smallmouth bass in the John Day Reservoir, Columbia River. Trans. Am. Fish. Soc. 120:448–458. website

Somerton, D. A., B. S. Kikkawa, and C. D. Wilson.
1988. Hook timers to measure the capture time of individual fish. Mar. Fish. Rev. 50(2):1–5.

NOAA
National Marine
Fisheries Service

Fishery Bulletin
established 1881

Spencer F. Baird
First U.S. Commissioner
of Fisheries and founder
of *Fishery Bulletin*

Haul-out patterns and effects of vessel disturbance on harbor seals (*Phoca vitulina*) on glacial ice in Tracy Arm, Alaska

Elizabeth A. Mathews (contact author)[1]
Lauri A. Jemison[2]
Grey W. Pendleton[2]
Karen M. Blejwas[1,2]
Kevin E. Hood[3]
Kimberly L. Raum-Suryan[4]

Email address for contact author: BethAnnMathews@gmail.com

[1] Department of Natural Sciences
University of Alaska Southeast
11120 Glacier Hwy
Juneau, Alaska 99801
Present address: 1350-B Yulupa Avenue
Santa Rosa, California 95405

[2] Division of Wildlife Conservation
Alaska Department of Fish and Game
P.O. Box 115525
Juneau, Alaska 99811-5525

[3] Juneau Ranger District Wilderness Program
U.S. Forest Service
U.S. Department of Agriculture
8510 Mendenhall Loop Road
Juneau, Alaska 99801

[4] Sea Gypsy Research
928 NW Cottage Street
Newport, Oregon 97365-3337

Abstract—Tidewater glacial fjords provide important habitat for breeding harbor seals (*Phoca vitulina*) that rest, give birth, and nurse pups on icebergs. These fjords also attract tourist vessels that potentially disturb seals. In May and June during 2001–2006, we documented seal abundance, pupping phenology, and seal–vessel interactions in Tracy Arm, a glacial fjord in southeastern Alaska. We used randomized observations to determine the frequency at which seals entered the water in the presence and absence of vessels, and we estimated the reaction distances of seals to approaching vessels. Mean daily vessel counts varied from 10.2 (2001) to 2.0 (2006) (range: 1–33). Tour and power vessels were the most common types of vessels, but seals were most sensitive to cruise ships and kayaks. The odds of a seal entering the water were higher when vessels were present (>2 times) or within 100 m (3.7 times), and when a pup was present (1.3 times). The baseline, undisturbed, rate of seals entering the water was 0.06 (95% CI: 0.05–0.08) per 10 min. Seal births occurred during 30 May–25 June and peaked (4–8 per day) during 7–13 June. The maximum pup count (408) was observed on 24 June. Harbor seal fitness in Tracy Arm may be reduced by vessel disturbances during breeding and pupping.

Manuscript submitted 4 February 2015.
Manuscript accepted 28 January 2016.
Fish. Bull. 114:186–202 (2016).
Online publication date: 3 March 2016.
doi: 10.7755/FB.114.2.6

The views and opinions expressed or implied in this article are those of the author (or authors) and do not necessarily reflect the position of the National Marine Fisheries Service, NOAA.

Harbor seals (*Phoca vitulina*) are widespread throughout the temperate and subarctic waters of the North Pacific and North Atlantic and primarily inhabit coastal waters where they haul out on land or ice to rest, give birth, and molt (Hoover, 1983). In Alaska, tidewater glacial fjords provide important habitat for pupping and molting harbor seals (Bishop, 1967; Calambokidis et al., 1987; Mathews and Pendleton, 2006; Jansen et al., 2010; Hoover-Miller et al., 2011). The number of harbor seals that use glacial ice increases in the late spring and summer, when they give birth and molt on drifting ice (Calambokidis et al., 1987; Mathews and Kelly, 1996; Herreman et al., 2009; Blundell et al., 2011; Womble and Gende, 2013). Glacial ice may be preferable to terrestrial haul-out sites because of the reduced risk of terrestrial or marine predation and the availability of ice throughout the tidal cycle (Fay, 1974; Hoover, 1983; Calambokidis et al., 1987; Mathews and Adkison, 2010). Up to 73% of the several thousand seals in Glacier Bay National Park (GBNP), Alaska, use glacial habitat rather than land haul outs during breeding (Mathews and Pendleton, 2006).

Glacial fjords in Alaska also attract substantial numbers of tourists, most of whom visit these sites by boat during the summer. These visits introduce the potential for the disturbance of seals and other wildlife in these fjords. With dramatic increases in tourism in Alaska and worldwide over the past 2 decades, and the coincident high use of glacial fjords during summer by both harbor seals and tourists, the possibility for unintended harassment of seals increases—harassment that is in violation of the Marine Mammal Pro-

tection Act (Calambokidis et al.[1]; Allen[2]; Suryan and Harvey, 1999; Henry and Hammill, 2001; Johnson and Acevedo-Gutiérrez, 2007; Jezierski, 2009; Young, 2009; Jansen et al., 2010; Hoover-Miller et al., 2013). From May through September, approximately 850 cruise ship trips carrying a total of nearly 1 million passengers visit southeastern Alaska each year (Nuka Research and Planning Group[3]). Commercial and private vessels with overnight accommodations bring thousands of additional passengers into Alaskan fjords throughout the summer months (Nuka Research and Planning Group[3]).

Frequent exposure of harbor seals to vessel traffic, especially during the critical stages of pupping and nursing (May–July) and molting (July–September), can alter seal behavior (Allen et al., 1984) (e.g., increased vigilance, premature entry into the water). Such alterations might affect seal fitness and pup survival (Johnson, 1977; Renouf et al., 1983; Jemison, 1997; Osinga et al., 2012). Captive seals deprived of haulout access compensated later by hauling out to rest for longer periods, indicating a physiological need for resting out of water even when they were not molting or breeding (Brasseur et al., 1996). Before weaning, pups remain almost constantly with their mothers, especially when hauling out on moving glacial ice (Hoover, 1983). The first few hours after a pup is born are the most important for establishing the mother-pup bond (Johnson, 1977; Lawson and Renouf, 1987), and separation of mother and pup during the first 2–3 weeks after birth can result in permanent abandonment and starvation of a pup (Johnson, 1977; Renouf et al., 1983; Osinga et al., 2012).

Even disturbances that do not cause permanent separation may have negative consequences for pup survival, as seen with gray seals (*Halichoerus grypus*) (Robinson, 2014). In addition, harbor seal pups are born with a relatively thin insulative-blubber layer (Bigg, 1969; Newby, 1973; Pitcher, 1986; Hoover-Miller[4]). Given the cold surface-water temperatures in glacial fjords, repeated disturbances that cause pups to spend >50% of their time in frigid glacial waters could be detrimental; the energy deficit incurred by increased metabolism could reduce blubber deposition in pups and overall fitness (Jansen et al. 2010) or possibly increase energetic costs for lactating females to compensate for increased pup energy requirements.

Steep declines in harbor seal counts have been documented at 2 glacial sites in Alaska (Hoover-Miller[4]; Mathews and Pendleton, 2006; Womble et al., 2010; Hoover-Miller, 2011), highlighting the need for a better understanding of 1) the basic ecology of seals that use glacial habitat and 2) the potential benefits and costs of using glacial ice to give birth, breed, or molt (Blundell et al., 2011). In the 1980s, GBNP began partial and complete vessel closures in John Hopkins Inlet, a tidewater glacial fjord, in response to concerns about the disturbance of harbor seal pups (Calambokidis et al.[1]); those regulations remain in place (Glacier, 2006).

Research on harbor seals in glacial fjords in Alaska has been concentrated in GBNP (Streveler[5]; Calambokidis et al.[1]; Mathews and Kelly, 1996; Mathews and Pendleton, 2006; Young, 2009; Womble et al., 2010; Blundell et al., 2011; Womble and Gende, 2013), Kenai Fjords National Park (KFNP) (Hoover, 1983; Jezierski, 2009; Hoover-Miller et al., 2011, 2013), and Disenchantment Bay (Jansen et al., 2010, 2015). Tracy Arm is a glacial fjord that is used by more than 1000 harbor seals during the summer and that has high tourist visitation. However, other than aerial population assessment surveys and preliminary telemetry tagging (results not available), there has been no research before this study on harbor seals in Tracy Arm (Withrow and Jansen[6]). Blundell and Pendleton (2015) studied haul-out patterns by tracking harbor seals equipped with VHF-transmitters in Tracy Arm and neighboring Endicott Arm, but that study was conducted after the collection of data for this study.

The objectives of this study were 1) to determine the patterns of abundance of nonpup and pup harbor seals during the pupping season and investigate the potential effects of environmental factors and number of vessels on seal counts, 2) to document vessel traffic (numbers and type) in Tracy Arm during early–mid summer, and 3) to determine the effects of the presence, type (e.g., cruise ship, tour vessel), proximity of vessels, and environmental variables on the probability that hauled-out seals would enter the water.

Materials and methods

Study area

Tracy Arm–Fords Terror Wilderness within the Tongass National Forest comprises 2 deep and narrow fjords: Tracy Arm and Endicott Arm (Fig. 1; each fjord is >48 km long). The Sawyer and South Sawyer glaciers, located at the end of Tracy Arm, flow into tidewater, which creates icebergs; both glaciers are rapidly

[1] Calambokidis, J., L. E. Healy, and G. H. Steiger. 1985. Reaction of harbor seals (*Phoca vitulina*) to boats in Glacier Bay, Alaska, 23 p. [Unpubl. report.] Cascadia Research Collective, Olympia, WA.

[2] Allen, S. 1991. Harbor seal habitat restoration at Strawberry Spit, San Francisco Bay, 44 p. Final report for U.S. Marine Mammal Commission contract MM2910890-9, NTIS PB91-212332, Marine Mammal Commission, Bethesda, MD.

[3] Nuka Research and Planning Group. 2012. Southeast Alaska vessel traffic study, 21 p. Nuka Research and Planning Group, Seldovia, AK. [Available at website.]

[4] Hoover-Miller, A. A. 1994. Harbor seals (*Phoca vitulina*): biology and management in Alaska, 45 p. Report to the Marine Mammal Commission, Washington, D.C.

[5] Streveler, G. P. 1979. Distribution, population ecology and impact susceptibility of the harbor seal in Glacier Bay, Alaska, 49 p. [Available from Glacier Bay National Park and Preserve, P.O. Box 140, Gustavus, AK.]

[6] Withrow, D. E., and J. K. Jansen. 2015. Personal commun. Natl. Mar. Mamm. Lab., Alaska Fish. Sci. Cent., Natl. Mar. Fish. Serv., NOAA, Seattle, WA 98115-6349.

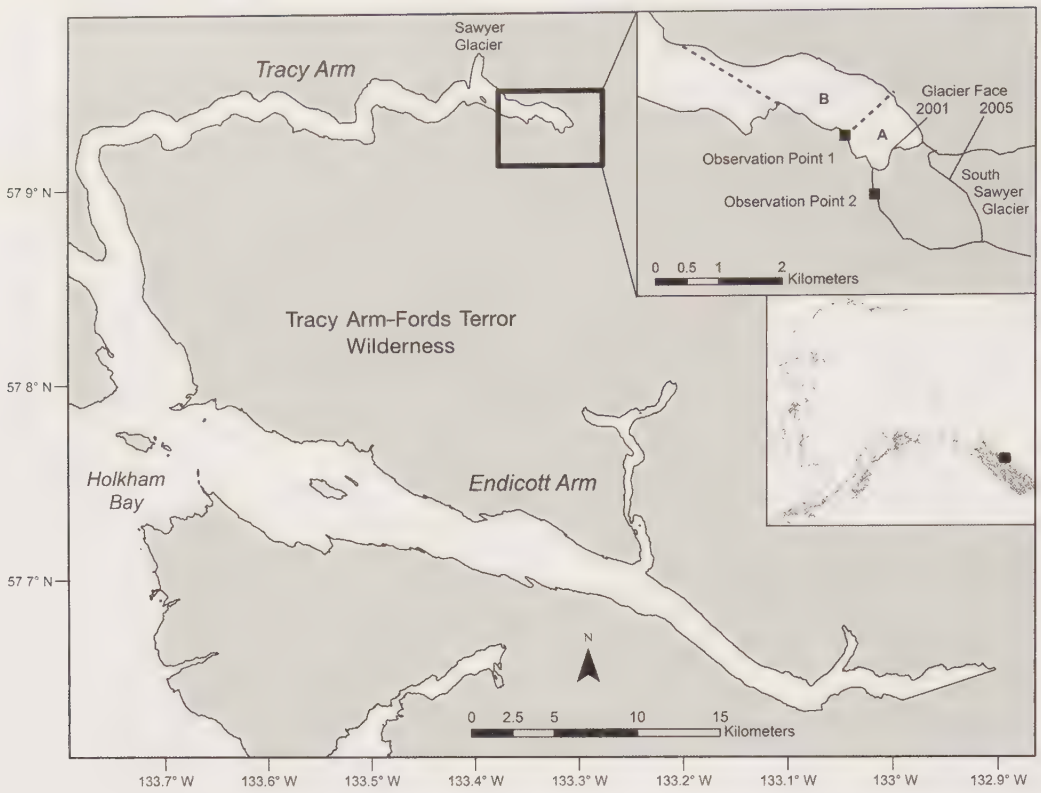

Figure 1

Map of the study area and its location within the Tracy Arm–Fords Terror Wilderness area in southeastern Alaska where harbor seals *(Phoca vitulina)* rest and nurse their pups on ice calved from glaciers. Observation point 1 (upper inset), from which seals were studied, is located at 57.857°N, 133.135°W. We recorded the time when boats entered and left sections A and B (upper inset). Observation point 2 was used beginning in 2005 after the South Sawyer Glacier had receded so far that observation point 1 no longer provided a good view of the seals.

thinning and retreating (Larson et al., 2007). Endicott Arm also has tidewater glaciers. Tracy Arm is 72 km south of Juneau, a major cruise ship port (CLAA[7]) and the capital of Alaska. The proximity of this fjord to Juneau results in hundreds of cruise ships (7 visits/week on average; Nuka Research and Planning Group[3]), tour boats, other commercial vessels, and private vessels visiting Tracy Arm each year. Unlike vessel traffic in GBNP, where numbers and speed are restricted, vessel traffic is currently unregulated in Tracy Arm.

We conducted our study in Tracy Arm from 2001 to 2006 and conducted more intensive sampling (e.g., more days of sampling and more types of data collected) in 2001 than in later years. We monitored seals and vessels from an elevated observation point (OP1) initially ~500 m from the face of the South Sawyer Glacier (Fig. 1). Tracy Arm is approximately 1 km wide at OP1, which afforded an unobstructed view of the areas of greatest seal and ice concentration (Fig. 1). From July 2004 through August 2005, the South Sawyer Glacier receded dramatically such that the face of the glacier was >1.6 km farther from OP1. Because of that change, a second observation point (OP2) was used late in the 2006 season (Fig. 1), but the use of OP2 had little direct effect on the type of data collected (i.e., counts from shore and from behavioral sampling) during this period. We refer to the area visible from OP1 and OP2 as "the study site" or "the inlet."

Seal counts

From 27 May through 30 June 2001, harbor seals were counted from OP1 with tripod-mounted 10×42 binoculars. Whenever possible, 2 observers counted simultaneously. Each day between 0700 and 2000 h, 3–6 counts (1–4 of which were paired counts) were made; the median time interval for conducting a count was 22 min (range: 7–39 min). Each day, we attempted to obtain at least 1 count before vessel disturbance (i.e., before vessels entered the study site).

[7] CLAA (Cruise Line Agencies of Alaska). 2015. Cruise ship calendar for 2016. CLAA, Ketchikan, AK. Available at website.]

Seals were categorized as nonpups or pups and as hauled out or in the water. We identified seals as pups by several criteria, including their small size, close association and positioning with an adult (presumed to be the mother), behavior (e.g., suckling, nuzzling), overall body shape, and pelage. In late June as pups approach or cease weaning, they typically are larger and more likely to be left unattended (Boness et al., 1994). Therefore, we distinguished pups and yearlings in late June by pelage differences if they were close enough for pelage to be seen clearly. It is likely that we underestimated pup abundance in late June because of difficulty in seeing pelage on unattended pups and yearlings far from our observation point, and that difficulty may have slightly reduced peak pup counts, slightly increased peak nonpup counts, and possibly caused a slight underestimate in the date of the peak pup count. In contrast, the estimated date of onset of pupping would not have been affected by these factors.

We recorded percent ice cover (visually estimated in 10% increments), weather variables, the number of vessels present, and incidences of disturbance (i.e., seals entering the water in response to vessel activity) during each count. Weather variables included sky condition (i.e., clear, partly cloudy, overcast), temperature, precipitation (i.e., none, mist or light rain, heavy rain), wind speed (Beaufort scale), and wind direction (i.e., up, down, or across the fjord). When there were 2 observers, we used the average of the estimates of ice cover. For 13 counts with ice cover recorded in 25% increments, we used the mid-point of each category for our estimate.

During each count, we also recorded the number of icebergs with evidence of fresh blood or the presence of bald eagles *(Haliaeetus leucocephalus)*, which we used as a proxy for the number of recent seal births. Bald eagles are attracted to fjords during seal pupping because they eat the seal afterbirth and stillborn pups (Calambokidis and Steiger, 1985). At the end of a count, each observer rated the quality of his or her count on a scale of 1–7, with 1 being excellent and 7 being poor. Counts with a quality rating of 7 were excluded from analyses.

We used generalized linear models (GLMs; Poisson error, log link) to estimate the relationships between seal counts (i.e., nonpups, pups, and all seals) and the following explanatory variables: count quality, day of year (DOY), time of day (TOD), percent ice cover, sky conditions, temperature, precipitation, wind speed and direction, and the presence of vessels in the count area. We included vessels as a variable in 1 of 2 forms: 1) presence or absence or 2) the number of vessels in the inlet; only 1 of these vessel-related variables was used in a single model. For this and all subsequent analyses, DOY was centered on the median DOY of all counts, and TOD was centered on solar noon. Centering predictors eliminates the correlation between linear and quadratic terms, facilitating model fitting (Draper and Smith, 1981). Quadratic terms for DOY and TOD were also included in initial models.

To account for over-dispersion, we included a scale parameter estimated as the Pearson chi-square value divided by the degrees of freedom. All variables were included in the initial model and deleted one at a time until all remaining variables had Wald chi-square-based *P*-values of approximately <0.05. Mean counts adjusted for the other variables in the model (i.e., least-squares means; Littell et al., 2006) were computed for the levels of categorical variables that remained in the final models.

Vessel traffic

We recorded all vessels that entered the inlet from the start of observations in the morning to the end of observations for that day. We recorded the time that each vessel entered (came into view) and departed (disappeared from view) from the inlet. Vessels that approached the glacier face were likely to have had greater effects on seals than vessels that did not; therefore, in 2001, we divided the study area into 2 sections (Fig. 1, inset map, A and B) by drawing a line between our observation point and a large waterfall across the inlet, and we recorded if and when a vessel entered and left section A. Because the South Sawyer Glacier was receding, the A and B section categorization was not used after 2001.

We categorized vessels into 6 types: 1) cruise ships (large, oceangoing vessels of 91 metric tons gross or more that carry passengers for hire; 2) tour boats (commercial vessels less than 91 metric tons gross that operate on a daily or weekly schedule); 3) power boats (chartered vessels and private vessels, including sailboats under power and nonskiff auxiliary vessels from cruise ships [these subcategories were pooled because it was not always possible to distinguish among them]); 4) inflatables (inflatable skiffs with an outboard motor), 5) skiffs (hard-hulled skiffs with an outboard motor), or 6) kayaks. For groups of inflatables, skiffs, or kayaks traveling together, the lead vessel was tracked if the group was monitored for seal disturbance, but each boat in the group was counted separately for vessel summaries. Because observations were concentrated during the day and vessels may have entered the inlet before or after observations, vessel counts were minimums; counts of tour boats likely were the most accurate because their times of daily entry and departure usually were within our observation periods.

Seal–vessel interactions

Randomized observations We conducted randomized observations of focal groups (Altmann, 1974) of seals to determine the rate at which seals entered the water—a rate that we modeled as a function of predictor variables, including the presence of vessels. We conducted 2–14 observations (median: 6 observations) of 10 min each per monitoring session. To spread sampling proportionately, the study site was divided into 10 zones. We used a computer-generated list to randomly select 1

zone for monitoring during each 10-min period. At the start of each 10-min period, the observer chose a general area within the selected zone as the initial search area for scans. We tried to vary the ice type (i.e., either dense, with icebergs packed together, or scattered, with much open space among icebergs) and the position of the initial search area in subsequent samples.

Once an initial search area was selected, the observer used binoculars or a spotting scope and the first seals to come into view became the focal seals for that period. If possible, we added additional seals in the immediate vicinity to try to bring the total number of focal seals to between 6 and 10. We recorded the size of the seal group, number of mother–pup pairs in each group, ice type, the position of the seals in relation to an overall patch of icebergs (e.g., interior versus near an edge next to a section with open water or less ice), and weather (i.e., sky condition, precipitation, and wind speed). During each 10-min observation period, we recorded the number of seals that entered the water and the number of vessels in the inlet. In 2001, we also recorded the vessel type of the nearest vessel and the closest approach (in the categories 0–50 m, 51–100 m, 101–300 m, >300 m) of that vessel to the focal seals. Observations were terminated early if any of the focal seals drifted out of view; these rare, incomplete observations were not used.

We used a generalized linear mixed model (GLMM; binomial error, logit link) to model how the probability of a seal entering the water was affected by external factors. The response variable was the number of seals that entered the water in the 10-min observation period in relation to the number of seals under observation. The predictors were DOY, TOD, seal position on the ice, number of mother–pup pairs, ice type, sky condition, precipitation, wind speed, number of vessels, vessel type, and distance to vessels. We included quadratic terms for DOY and TOD to allow for nonmonotonic associations. For several variables (e.g., sky condition, precipitation, wind speed, vessel distance), categories with few observations were combined with adjacent categories. The predictors mother-pup pairs and vessels were, in separate models, fitted as either continuous predictors (counts) or binary predictors (presence or absence). Vessel type was fitted as a single, multicategory predictor to determine whether responses differed by vessel type; then we fitted models for the presence of each vessel type separately to produce individually estimated odds ratios for each vessel type.

Initially, models included DOY, TOD, their quadratic terms, seal position on the ice, and all weather variables. Wald chi-square statistics (P>~0.05) were used to eliminate unimportant variables one at a time (Hosmer and Lemeshow, 2000). After this model fitting (i.e., after we determined useful environmental predictors), mother–pup pairs and vessel predictors were included and evaluated in the same way.

Vessel approaches To estimate the effect of vessel type and distance more directly on seal behavior (i.e., the probability that a seal will enter the water), in 2001 we observed a subset of the vessels entering Tracy Arm as they approached seals hauled out on icebergs. When seals are hauled out, they are in a temporary state that ends when the seal enters the water. As such, external factors, including the presence of boats, can only affect the timing of when a hauled-out seal enters the water, not the fact that the entry will occur. We used entry into the water as our response because it is an easily observed and unambiguous behavior with energetic and predator-exposure consequences, and it has been used as a measured response in most comparable studies (Calambokidis et al.[1]; Mathews, 1995; Jansen et al., 2010; Young et al., 2014).

Once a vessel was selected for observations of seal–vessel interaction, the observer selected one or more focal icebergs in the vessel's path and recorded the number of nonpups and pups on each iceberg. We estimated the distance between the vessel and seals and classified it into 1 of 4 distance classes: 0–50 m, 51–100 m, 101–300 m, and ≥300 m. When possible, we selected icebergs that were >300 m from the vessel at the start of an observation, but not all distance classes were observed for every vessel–iceberg combination. For each distance class transited by a vessel, we recorded the number of pups and nonpups that entered the water (which could be zero). We continued to monitor icebergs until shortly after the vessel made its closest approach to the seals, at which point observations were terminated and a new iceberg was selected for focus. We attempted to monitor a vessel during its entire inbound and outbound track, and we recorded both seal behavior and vessel activity (i.e., vessel moving or not moving) during these observations. Most observations were made within 1 km of the observation point.

We evaluated our visual distance estimates by comparing them with measurements made with laser rangefinder binoculars (Leica Vector IV[8], Vectronix, Inc., Bedford, NH), which allowed us to measure the distances to the vessel and to the seal(s) and the angle between them, automatically calculating the distance between the vessel and the seal(s); the rangefinder was calibrated according to the manufacturer's recommendations. For this effort, 2 observers simultaneously recorded distances between selected icebergs or an iceberg and a vessel; 1 observer estimated the distance visually, using the seal–vessel distance classes, and the other observer measured the distance with the laser rangefinder. The distance measurements made with the rangefinders were then converted to distance classes, and the visual estimates of distance were scored into 3 bins: classified correctly, overestimated by 1 or 2 classes, or underestimated by 1 or 2 classes.

Although we did not systematically monitor such behavior, we occasionally observed seals entering the water after the vessel had passed its point of closest

[8] Mention of trades names or commercial companies is for identification purposes only and does not imply endorsement by the National Marine Fisheries Service, NOAA.

approach to a seal or seal group because of wake effects or for other reasons (also reported by Calambokidis et al.[1]). If the seal entered the water when the vessel was still in the same distance class as the closest approach, we used the observation in the analyses, assuming that most such disturbances would have been observed. However, we did not use observations of disturbances when vessels had moved beyond the distance class of their closest approach because we were far less likely to observe them. Consequently, our estimates of the probability of disturbance are biased low but are comparable to those of other studies where seals were not tracked after vessels passed them (Jansen et al., 2010; Young et al., 2014) and comparable to counts of "visual reactions" (versus "wake reactions") reported by Calambokidis et al.[1]

We used a GLMM (binomial error, logit link) to estimate the effect of predictor variables on the probability of a seal entering the water. We used the following predictors: distance between the seal and vessel, seal age class (pup, nonpup), DOY, TOD, group size (the number of seals on an iceberg when the vessel entered each distance zone), percent ice cover in the area of the monitored iceberg, if ≥1 pup was on an iceberg when it was first observed, vessel activity (i.e., moving, not moving), sky condition, temperature, and precipitation. Encounter (i.e., individual vessel observed) and iceberg within an encounter were included in the model as random effects because observations within these units were not independent. We included quadratic terms for DOY and TOD to allow for nonlinear (on the logit scale) responses between the predictors and water-entry probability.

We also included the interaction terms *distance class*vessel type* and *distance class*age* to allow the effect of distance class to vary by vessel type or by seal age category. The effect of *age* and *distance class*age* were investigated by using a data set that separated observations of pups and nonpups; a data set that included both pups and nonpups was used to investigate all other predictors. For 2 *distance*vessel* categories (skiff: >300 m; kayak: >300 m), there were no observations of seals entering the water—a situation that prevented successful model fitting and estimation of parameters (Hosmer and Lemeshow, 2000). To overcome this problem and facilitate model fitting, we added 0.1 (i.e., added one-tenth of a water entry) to one observation in each category. Because of this adjustment, the estimates for these 2 categories are slightly positively biased, although they remain essentially zero.

Results

Seal counts and timing of pupping

In 2001, we counted seals in Tracy Arm 193 times on 34 days (range: 3–10 counts per day); 100 of these counts were paired (50 pairs), with counts differing by >10% in 8 of the 50 pairs. All counts were included in the analyses. Total counts (i.e., pups+nonpups) peaked during 24–26 June, with a high count of 1351 seals (Fig. 2A). Separate counts of both pups and nonpups peaked during this period, at ~400 pups and ~1000 nonpups (Fig. 2B). The average numbers of pups seemingly began to level off by about 25 June, with the maximum pup count of 408 observed on June 24; however, it is unclear whether the average nonpup numbers were still increasing or were at a peak on 30 June, the last day that we made observations in 2001 (Fig. 2B). We observed the first evidence of birth (blood on iceberg) on 30 May, the third day of our study, and we recorded the last on 25 June. Peak daily numbers of icebergs with evidence of recent births (4–8) were observed during 7–13 June.

For all 3 groupings of seals (nonpups, pups, and all seals), 6 variables (count quality, DOY, TOD*TOD, percent ice cover, sky condition, and temperature) were retained in the GLMs (Table 1). Mean counts were lowest for high count qualities and highest for intermediate count qualities (Table 1). The number of nonpups peaked at around 1300, whereas the number of pups showed no distinct diurnal pattern (Fig. 3). Seal counts, for both pups and nonpups, were positively related to ice cover (Table 1). More seals were counted under clear skies, more nonpups were counted when there was no precipitation, and more pups were counted when wind speed was intermediate among the conditions we observed (i.e., Beaufort 2) compared with the counts when there was more (i.e., Beaufort 3) or less (i.e., Beaufort 1) wind (Table 1). Counts of nonpups and pups increased with increasing temperatures (Table 1).

Vessel traffic

The mean numbers of vessels observed daily in Tracy Arm varied from 10.2 in 2001 to 2.0 in 2006 (Fig. 4). The maximum number of vessels recorded in a day was 33 on 26 June 2001. Also in 2001, the mean number of vessels per day on weekdays (10.25, n=24) was similar to that observed on weekend days (10.20, n=10); consequently, this factor (i.e., weekday versus weekend day) was not used in other analyses.

Tour boats were the most common type of vessel observed in most years, followed by power boats (Fig. 4), and these 2 types of boats accounted for 57–100% of the vessels observed in a day. The number of sampling days was small during the years 2004–2006, making the ranking of vessel types potentially imprecise for those years. The majority of inflatables, skiffs, and kayaks were launched from larger vessels.

In 2001, most vessels (87%) entered section A, the part of our study area closest to the glacier (Fig. 1, inset map). Individual vessels were in the study area an average of 1.2 h both in 2001 (n=269; 95% confidence interval [CI]: 1.10–1.30) and during 2002–2006 (n=193; 95% CI:1.12–1.30). Some estimates of mean lengths of stay were underestimated when vessels arrived or departed outside of our observation periods. The number of vessels per day in Tracy Arm declined over the period 2001–2006, both in total and for each vessel type

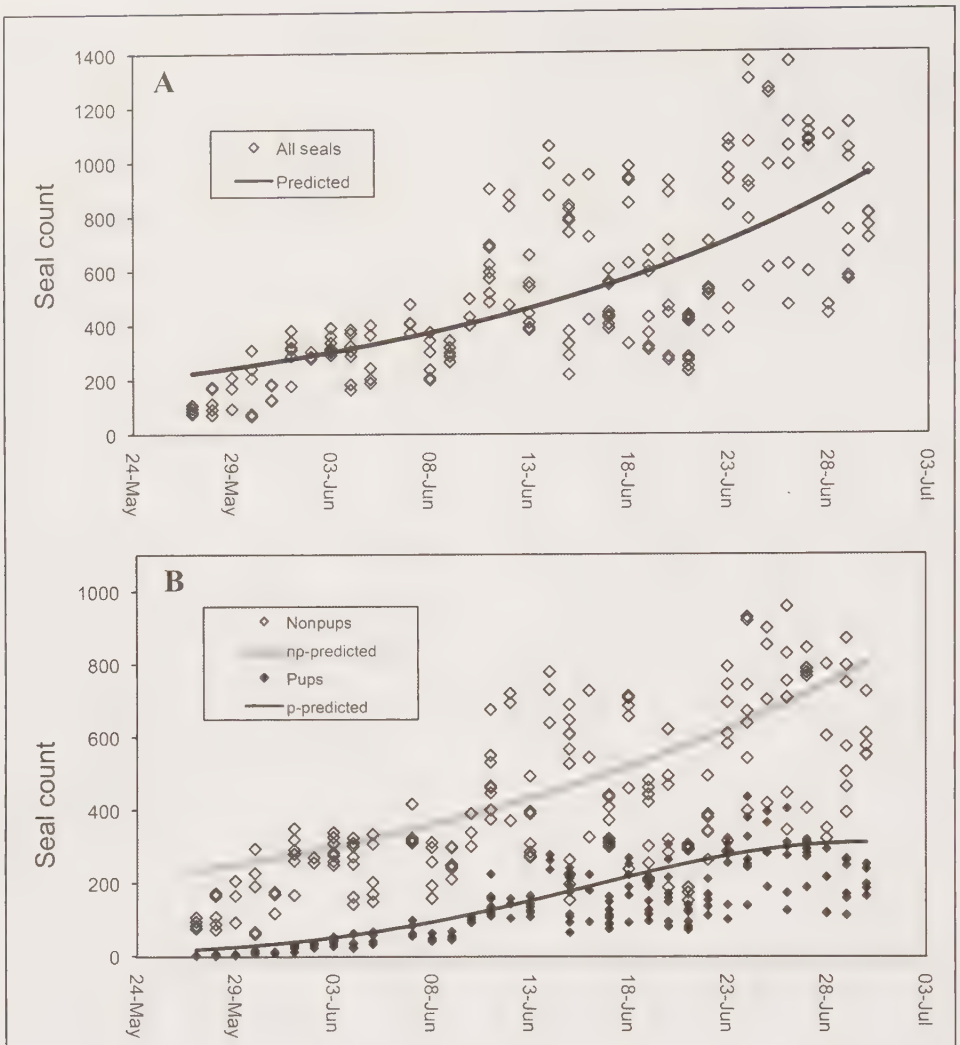

Figure 2

Counts of harbor seals (*Phoca vitulina*) in Tracy Arm, Alaska, including both seals that were hauled out and those in the water. Seals were counted from 27 May–30 June 2001 and are summarized as (**A**) all seals and (**B**) pups and nonpups separately. Lines are the predicted counts based on modeled functions of the mean counts in relation to day of year and are adjusted for other predictors in the models.

(Fig. 4). Although vessel traffic declined in Tracy Arm, the number of vessels counted in nearby Endicott Arm increased (U.S. Forest Service[9]; Fig. 4).

Seal–vessel interactions

Randomized focal observations We made 662 10-min observations of focal seal groups, and recorded the behavior of 3250 seals (group size: 1–24, median 4). The probability of a seal entering the water, during a 10-min period when no vessels were present—an undisturbed baseline level for the entering the water behavior—averaged across all other predictor variables, was 0.06 (95% CI: 0.05–0.08). In other words, every 10 minutes we would expect 6 of 100 undisturbed seals, on average, to enter the water. The odds of a seal entering the water was not related to DOY or TOD ($P>0.17$), to ice type (dense versus scattered), or to any of the weather predictors (Fig. 5). The presence of a pup, usually indicative of a mother–pup pair, and the number of pups were associated with reduced probability of a seal from those groups entering the water (Fig. 5, pup present).

Vessel type affected the probability of seals entering the water in different ways (Fig. 5, vessel type). The odds of seals entering the water were >2 times higher when vessels were present in the study area

9 U.S. Forest Service. 2002–2013. Unpubl. data. Juneau Ranger District Wilderness Program, U.S. Forest Service, Juneau, Alaska 99801.

Table 1

Analyses of counts of harbor seals (*Phoca vitulina*) recorded in Tracy Arm, Alaska in 2001. Means, adjusted for other variables in the model (i.e., least-squares means), are presented for categorical variables. For continuous variables, "%change" is the percentage increase in counts for a 1-unit increase in the predictor. Analyses were conducted separately for nonpups, pups, and total counts. For means and change percentages, 95% confidence intervals are given in parentheses.

	Nonpups		Pups		All seals	
Variable	*P*	Mean or %change	*P*	Mean or %change	*P*	Mean[1] or %change
Count quality	<0.01		<0.01		<0.01	
1.5		350.6 (301.0–408.5)		106.5 (90.8–128.2)		466.1 (401.4–541.2)
2		355.5 (303.4–416.6)		111.0 (94.4–130.6)		477.4 (408.6–557.7)
2.5		399.9 (348.7–458.6)		130.8 (114.0–150.0)		543.2 (474.9–621.4)
3		389.1 (342.3–442.3)		127.5 (113.4–144.4)		524.1 (462.0–594.4)
3.5		486.3 (408.9–578.4)		167.7 (142.5–197.1)		675.6 (570.6–800.0)
4		476.3 (417.7–543.0)		154.2 (136.6–174.0)		645.4 (567.4–723.3)
4.5		466.4 (352.7–616.9)		176.9 (134.3–233.1)		652.7 (497.5–856.3)
5		414.3 (318.9–538.4)		125.4 (92.0–171.6)		528.3 (404.9–689.2)
6		409.2 (301.6–555.2)		125.9 (88.7–179.1)		532.9 (391.2–725.8)
Day of year (DOY)	<0.01	[2]	<0.01	[2]	<0.01	[2]
DOY*DOY	0.28		<0.01	[2]	0.58	
Time of day (TOD)	0.17		0.16		0.19	
TOD*TOD	<0.01	[3]	<0.01	[3]	<0.01	[3]
Ice cover (%)	<0.01	0.80% (0.43–1.18)	<0.01	1.22% (0.80–1.63)	<0.01	0.93% (0.57–1.31)
Sky	<0.01		0.04		<0.01	
Clear		516.8(426.1–626.7)		164.7 (134.0–202.3)		698.9 (577.7–845.5)
Partly cloudy		369.4 (326.2–418.4)		119.1 (104.8–135.6)		492.9 (436.2–556.9)
Overcast		371.0 (335.2–410.7)		123.5 (109.7–139.8)		498.9 (451.7–551.0)
Temperature	0.05	1.27% (-0.01–2.57)	0.01	1.84% (0.45–3.24)	0.03	1.35% (0.08–2.63)
Precipitation	0.01		0.41		0.05	
None		470.5 (435.3–508.5)				612.8 (567.0–662.4)
Mist or light rain		391.6 (337.1–454.9)				523.6 (451.2–607.8)
Heavy rain		384.4 (303.1–487.6)				535.5 (426.7–672.1)
Wind speed	0.16		0.05		0.10	
Beaufort 1				127.6 (114.1–142.8)		
Beaufort 2				147.2 (127.9–169.8)		
Beaufort 3				129.0 (103.9–160.7)		
Wind direction	0.55		0.76		0.66	
Vessels	0.65		0.30		0.55	

[1]Because models were fitted separately for nonpups, pups, and all seals, the effect of the predictors differs, and the means for "all seals" are not the sum of the means for nonpups and pups.
[2]See Figure 2.
[3]See Figure 3.

than when they were not (Fig. 5, vessel type pooled). Randomly selected seals were more likely to enter the water when inflatables or kayaks were present in the study area (Fig. 5, vessel type). However, seals entered the water less often when there was a tour boat in the inlet than when there were none. The estimated effects of other vessel types were imprecise, either because of small sample sizes or variable seal responses for seals on randomly selected patches of ices. When all vessel types were pooled, both the number of vessels and the presence of at least one vessel were associated with an increased probability of a seal entering the water in relation to the probability of entry when no vessels were present (Fig. 5, vessel type pooled).

The odds of a seal from a randomly selected focal group entering the water were 3.7 times (95% CI :2.6–5.4) greater when vessels were in the 2 shortest distance classes (0–50 m or 51–100 m) than when they were within the longest distance class (> 300 m). The estimate for the remaining distance class (101–300 m), although imprecise, also indicated an increased likelihood of a seal entering the water than when boats were >300 m away (Fig. 5, vessel distance).

Vessel approaches In 2001, vessels entered the inlet on all 34 days when vessel entries were tabulated. We monitored 141 vessels (of 348 seen) and 1199 icebergs with 1755 harbor seals for disturbances of seals as ves-

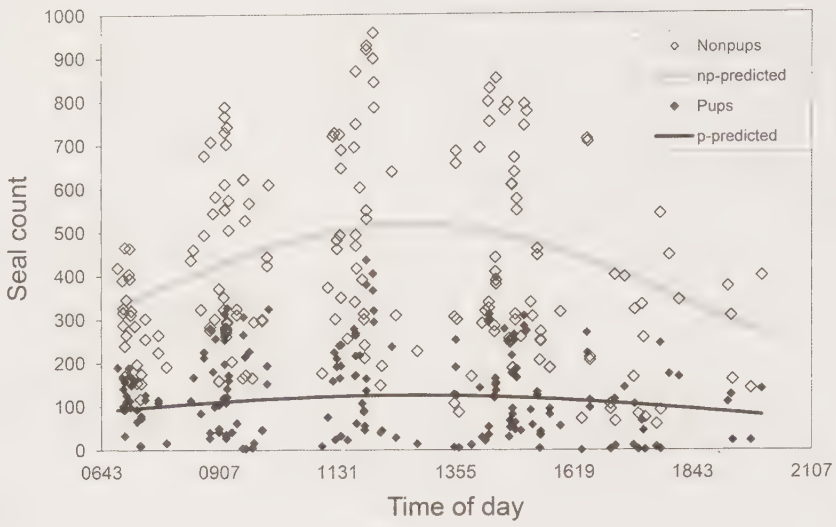

Figure 3

Counts of pup (p) and nonpup (np) harbor seals (*Phoca vitulina*), including seals that were hauled out and those in the water, in Tracy Arm, Alaska, from 27 May–30 June 2001 as a function of time of day (TOD). Lines are the modeled functions of the mean counts in relation to TOD and are adjusted for other predictors in the models.

sels approached. Vessels were observed for an average of 24 min (standard deviation=29 min). Individual icebergs had 1–15 nonpup seals and 1–5 pups; 725 icebergs (~60% of those observed) had at least 1 pup. Disturbances caused by monitored vessels occurred on all of the 32 days we observed vessel approaches.

Overall, 74% of visual estimates of distance were correctly classified by observers. Observers tended to estimate shorter distances more accurately than longer distances (93% of distances <50 m were classified correctly, but only 64% of distances >300 m were correctly categorized). Observers tended to underestimate rather than overestimate distances, and this bias increased with distance. Overall proportions of misclassification were similar for both observers, although variability between observers also increased slightly with distance.

Day of year and TOD were not related to the probability of a seal's entry into water (water entry [P>0.35]), nor were seal age category (including *age*distance class*), temperature, or precipitation (Fig. 6). Predictors associated with the probability of water-entry included seal group size, the presence of a pup at the start of the observation, percent ice cover, sky condition, vessel activity, and vessel distance, the latter 2 of which varied by vessel type (Figs. 6 and 7). Seals were more likely to leave an iceberg as ice cover decreased or under clear versus cloudy skies (Fig. 6). Seals were less likely to leave an iceberg with increasing group size but were much more likely (1.3 times [95% CI :1.0–1.8]) to enter the water if there was at least 1 pup present in the focal group of seals on an ice berg when the observation began (Fig. 6, pup present). However, pups were rarely the first seal in a group to enter the water. In 56 of the 278 (20%) instances when a seal entered the water when a pup was present, we recorded whether a pup or a nonpup entered the water first (in 222 instances, both entered at the same time or the order was not clear from the recorded data). For 43 of the 56 (77%) instances, a nonpup entered the water first.

The odds of a seal entering the water when a vessel was stopped were about 4 times as high as when a vessel was moving (Fig. 6, vessel activity). The probability that a seal entered the water increased dramatically as the distance between a seal and a vessel decreased, but the effect differed depending on vessel type (Table 2, Fig. 7). The probability of a seal responding to a vessel was higher for cruise ships and kayaks than for other vessel types (Fig. 7). The probability of a seal entering the water when vessels were within 50 m was >0.47 for every vessel type and almost 1 for cruise ships and kayaks. For vessel types other than cruise ships and kayaks, the probability of water entry by seals decreased to low levels for distances >100 m. Probabilities of water entry were uniformly low for all vessel types at distances >300 m (Fig. 7).

Discussion

Seal counts

In Tracy Arm in 2001, there were more seals (both nonpups and pups) hauled out with greater ice cover,

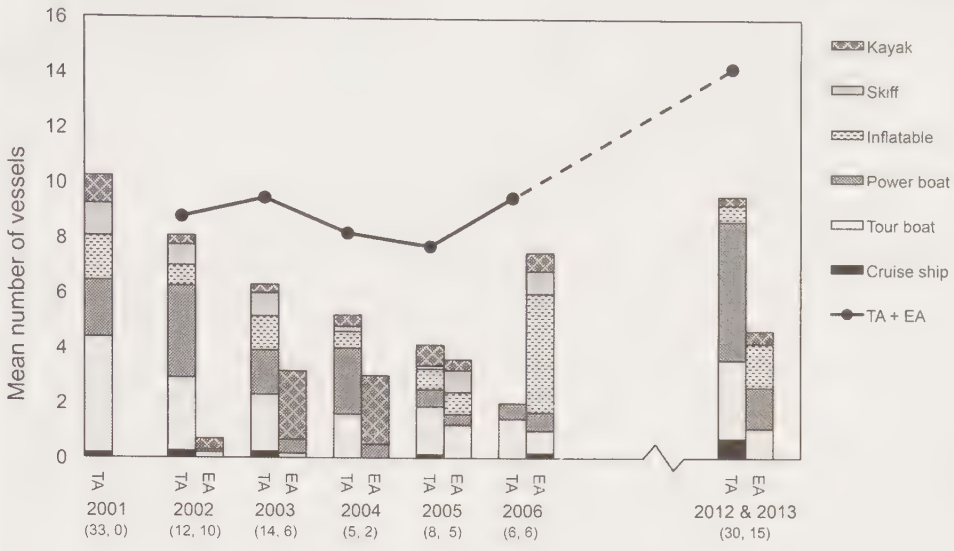

Figure 4

Mean daily counts of vessels, by type, for the period 2001–2006 in Tracy Arm (TA) and Endicott Arm (EA), Alaska, with counts for 2012 and 2013 (average for 2 years) included for comparison. The numbers of survey days in each inlet are listed (in parentheses) below year.

warmer temperatures, and clear skies; more nonpups hauled out when there was no precipitation, and more pups hauled out when wind speed was intermediate. Other studies also have found that harbor seal counts are affected by environmental factors, but such factors can be site specific or might not be detected in a study because of the limited range of conditions under which surveys were conducted (e.g., Boveng et al., 2003; Simpkins et al., 2003; Jemison et al., 2006, Jansen et al., 2015). Although harbor seal haul-out patterns on glacial ice typically are not affected by tide stage (Calambokidis et al., 1987; Boveng et al., 2003; Mathews and Pendleton, 2006; but see Hoover-Miller et al., 2011), they are affected by the availability of floating ice. Calambokidis et al. (1987) and Young et al. (2014), both working in GBNP, found that seal counts were positively related to percent ice cover, the proportion of seals counted in the water was negatively related to percent ice cover, and, when ice cover was low, hauled-out seals were concentrated on the few remaining icebergs. Jansen et al. (2015) reported that seals were most abundant with intermediate ice densities (5–7 tenths coverage).

As with other harbor seal studies in glacial fjords in southeastern Alaska, we found peak pup counts in late June (Mathews and Pendleton, 2006, Jansen et al., 2015). However, Hoover-Miller et al. (2011) reported peak pup counts in Aialik Bay, KFNP, in early- to mid-June, indicating regional variation in pup birth dates. The maximum proportion of pups from our counts (30–36%) was also similar to the high values reported for seals in other tidewater glacial fjords (KFNP: 21–34%, Hoover, 1983, Hoover-Miller et al., 2011; GBNP: 34–40%, Calambokidis et al., 1987, Mathews and Pendleton, 2006), but ~3 times greater than the proportion of pups in Disenchantment Bay (Jansen et al., 2015). Note also that the proportion of pups can be affected by immigration or emigration of nonpups in addition to changes in productivity.

Seal haul-out patterns

The number of nonpups that were hauled out peaked at around 1300 (Fig. 3)—a number similar to patterns seen with other ice-associated harbor seals (Calambokidis et al., 1987; Mathews and Pendleton, 2006; Hoover-Miller et al., 2011, Blundell and Pendleton, 2015). Using telemetry data, Blundell and Pendleton (2015) found that seals in Tracy Arm and Endicott Arm had the highest haul-out probabilities in the middle of the day, especially during the pupping season. Our randomized observations indicated that the probability of a seal entering the water was not related to TOD, but the time span of our observations might have been too narrow to detect a pattern if the afternoon peak was broad. Blundell and Pendleton (2015) found seals more likely to end haul-out bouts (i.e., enter the water) later in the day.

In contrast to the pattern observed for nonpups, the predicted number of pups hauled out in Tracy Arm, after accounting for other predictors, showed no distinct diurnal pattern (Fig. 3), although the observed counts indicate a slight peak. In Aialik Bay, mother-pup pairs also were less influenced by environmental

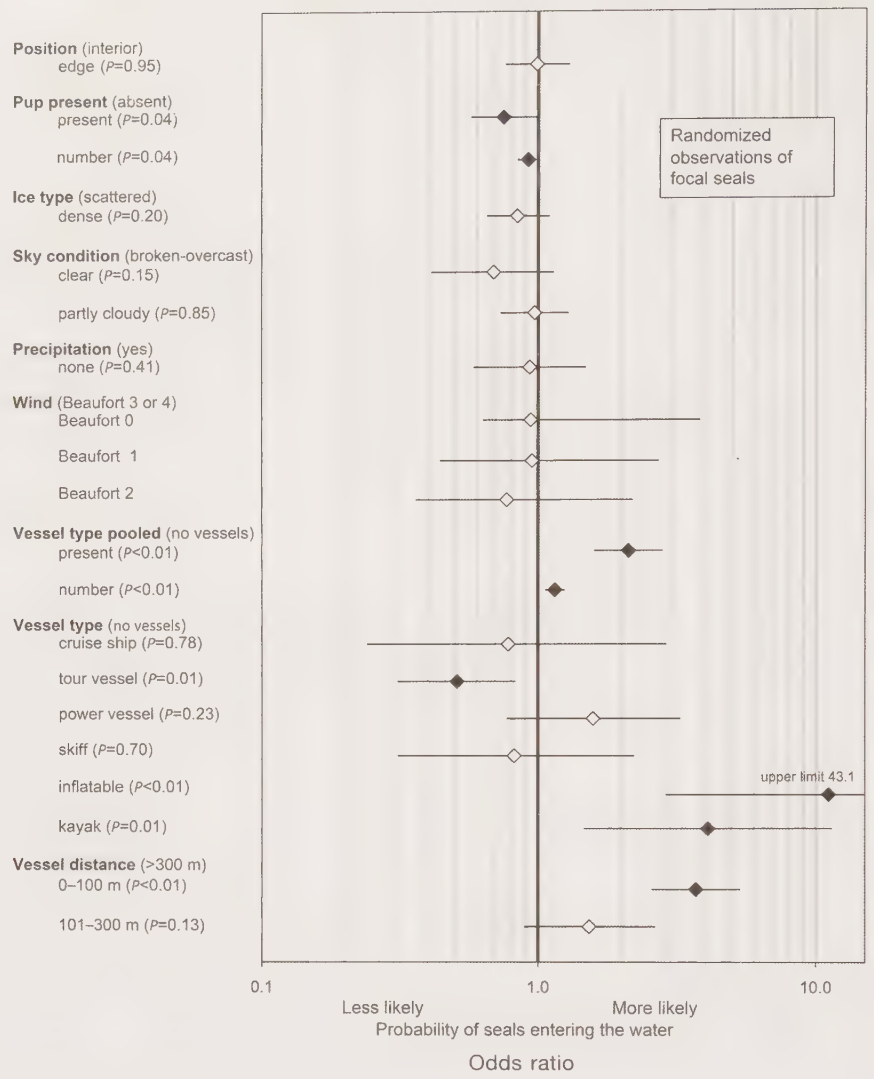

Figure 5

Odds ratios of a harbor seal (*Phoca vitulina*) entering the water during randomized, focal seal observations (2001–2006). Bars indicate 95% confidence intervals (CIs). Solid black symbols indicate factors that were statistically significant (i.e., where the CI does not cross 1). The odds ratios are relative to what we used as the comparison category for each variable (in parentheses). Position=seal's position in relation to the overall patch of ice (e.g., interior versus near an edge next to a section with open water or less ice). Vessel type and vessel distance results are based on 2001 data only. Vessel distance=distance from the focal seal or group.

conditions than nonpups, but they did show a midday peak in counts (Hoover-Miller et al., 2011). Because pups suckle when they are hauled out, the haul-out cycles of lactating females may be influenced by the needs of their pups. We found that, when >1 mother-pup pair was present, seals were less likely to enter the water during a random 10-min observation than were seals in groups without a pup present (Fig. 5), which also suggests longer haul-out bouts by mother-pup pairs. In Johns Hopkins Inlet, GBNP, in June, the TOD also was not associated with counts of either nonpups or pups or with the proportion of hauled-out seals that were pups (Mathews and Pendleton, 2006). Our analyses of our randomized observations did not reveal any relationship between seals entering the water and local ice dispersion (i.e., scattered or dense) (Fig. 5). In contrast, Young et al. (2014) observed a pattern in which seals were more likely to enter the water when an ice cover index (a combination of cover and density) was high.

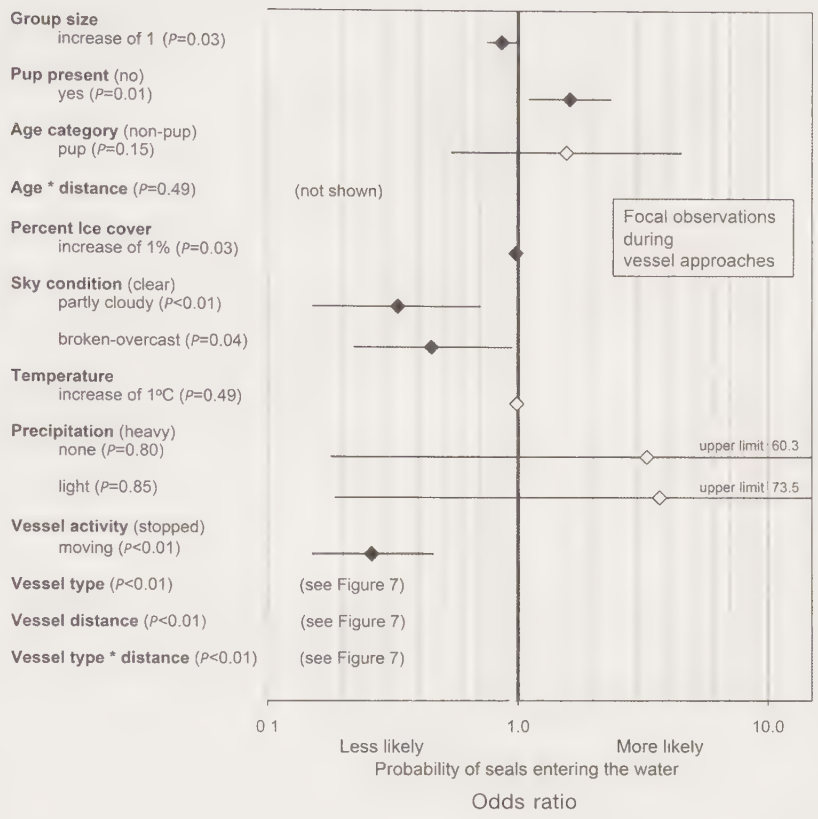

Figure 6

Odds ratios of a harbor seal *(Phoca vitulina)* entering the water in response to vessels approaching or remaining near an iceberg where the seal was hauled out. Bars indicate 95% confidence intervals (CIs). Solid black symbols indicate factors that were statistically significant (i.e., where the CI does not cross 1). The odds ratios are relative to what we used as the comparison category for each variable (in parentheses). Observations were made from 27 May through 30 June 2001.

Vessels and seals

Vessel traffic We documented high levels of vessel activity in Tracy Arm in 2001 (10.2 vessels/day (maximum 33 vessels/day) during 32 days of observation), compared with Johns Hopkins Inlet in GBNP during months when vessels could enter the inlet (3.7 vessels/day, 1994–2001, E. A. Mathews, unpubl. data; 2.8 vessels/day, 178 vessels during 64 days of observation in July 2007 and 2008, Young et al., 2014). After 2001, vessel traffic decreased in Tracy Arm, whereas it increased in nearby Endicott Arm (Fig. 4), likely because of the rapid recession of South Sawyer Glacier that increased the number of icebergs in the water, making maneuvering boats and ships in Tracy Arm more difficult and potentially hazardous. From 2001 through 2013, the combined vessel traffic in Tracy Arm and Endicott Arm remained high and may have increased (Fig. 4).

Seal counts and vessel numbers Higher vessel counts were not associated with reduced seal counts in 2001 (Table 1), a pattern also noted by Jansen et al. (2015) in Disenchantment Bay. However, our total counts included seals in the water, and therefore they were less sensitive to vessel disturbance. Furthermore, there could have been an effect of vessels on seal counts that we were unable to detect because of the constant daily presence of boats. In Muir Inlet in GBNP, peak counts of seals on days with no vessels were, on average, 15% higher than counts when vessels were present (Calambokidis et al.[1]).

Seal–vessel interactions All of our analyses of seal–vessel interactions (i.e., randomized focal observations and direct observations of vessel approaches) revealed increased probabilities that seals would enter the water in response to at least some types of boats (Tables 1, Figs. 5–7). We also found that the probability of a seal

Table 2

Predicted probabilities of a harbor seal (*Phoca vitulina*) entering the water when vessels of various types approached within 4 distance classes. Confidence intervals (95%) are given in parentheses below their associated point estimates. Data were collected during 27 May–30 June 2001; sample sizes are listed in parentheses in the first 2 rows of this table.

Distance class	Cruise ship	Tour boat	Power boat	Skiff	Inflatable	Kayak
No. of vessels	(5)	(77)	(25)	(12)	(14)	(8)
No. of ice bergs	(103)	(694)	(147)	(81)	(110)	(64)
0–50 m	0.99	0.62	0.47	0.66	0.77	0.98
	(0.96–1.00)	(0.50–0.73)	(0.24–0.71)	(0.39–0,85)	(0.54–0.90)	(0.92–1.00)
51–100 m	0.50	0.16	0.10	0.01	0.12	0.62
	(0.23–0.76)	(0.11–0.24)	(0.04–0.23)	(0.00–0.11)	(0.05–0.26)	(0.32–0.85)
101–300 m	0.22	0.05	0.01	0.06	0.02	0.18
	(0.08–0.49)	(0.03–0.08)	(0.00–0.04)	(0.02–0.22)	(0.00–0.10)	(0.06–0.44)
>300 m	0.02	0.02	0.00	0.00	0.11	0.00
	(0.00–0.08)	(0.01–0.04)	(0.00–0.04)	(0.00–0.53)	(0.01–0.70)	(0.00–0.57)

entering the water increases with decreasing seal–vessel distance (Figs. 5 and 7)—a finding that agrees with those of other studies (Calambokidis et al.[1]; Jezierski, 2009; Jansen et al., 2010; Hoover-Miller et al., 2013, Young et al., 2014). However, seals in Tracy Arm during our study appeared to be less responsive to vessels at a given distance than seals in Disenchantment Bay, where only cruise ships were monitored (Jansen et al., 2010), and in Muir Inlet in GBNP where all vessel types were monitored (Calambokidis et al.[1]), and they were far less sensitive than seals in Johns Hopkins Inlet in GBNP (Young et al., 2014), even when accounting for vessel type.

For our visual estimates, we tended to underestimate distances between seals and vessels, especially for longer distances, and we did not adjust assigned distance classes used in other analyses. Our underestimates of distance could possibly explain some of the weaker distance response in Tracy Arm than that in other glacial fjords where seal-to-vessel distances were measured.

Independent of distance, we found that seals were more sensitive to the presence of cruise ships than to other vessel types, except kayaks. Other studies in which multiple vessel types were monitored also reported this pattern (Calambokidis et al.[1]; Calambokidis et al.,1987; Young et al., 2014; Blundell and Pendleton, 2015). Calambokidis et al.[1] found that cruise ships in GBNP disturbed seals on ice at an average distance of 277 m, Jansen et al. (2010) reported seal disturbances by cruise ships at distances of up to 500 m, and Young et al. (2014) reported disturbances by cruise ships at distances >800 m. In contrast, we found the probability of disturbance by cruise ships approached 1 for ships within 50 m of a seal, but the response probability declined rapidly to 0.02 when the distance between the seal and ship was >300 m (Fig. 7)—a more rapid decline in response than was observed by Jansen et al. (2010).

For all of our analyses by vessel type, kayaks also had high probabilities of causing seal disturbance, with a disturbance response pattern similar to that caused by cruise ships (Table 2). Some other studies had also noted that kayaks disturb seals at greater distances than those of motorized vessel types (e.g., power boats) (Jezierski, 2009; Hoover-Miller et al., 2013), but Calambokidis et al.[1] found that harbor seals were equally sensitive to kayaks and tour boats (and less sensitive to pleasure boats [i.e., private vessels in our study]) and Young et al. (2014) found seals were less sensitive to kayaks than any type of power vessel.

It is possible that harbor seals can habituate to the noise of power boats and can determine a boat's approximate location by the sound of its engine. Kayaks, on the other hand, travel more slowly and quietly and may go undetected by seals until they are in close proximity, or until they make a noise, causing the seals to startle and flee into the water. The lower sensitivity to kayaks reported by Young et al. (2014) could be a function of the behavior of kayakers at that specific site, possibly a function of regulations or boater education, which have been shown to reduce kayak-related disturbance elsewhere (Hoover-Miller et al., 2013). Also, kayakers frequently travel in groups, which could account for the higher probabilities of kayaks causing disturbance. Further, differences among sites in the sizes of kayak groups could be a factor in the variability among sites in patterns of harbor seal response to kayaks. We had too few observations of kayak groups to estimate the effect of kayak group size on disturbance probability.

We found responses of seals to tour boats, skiffs, inflatables, and power boats generally similar, although there was some variation in results from our study methods (i.e., randomized focal observations vs. vessel approaches) and analyses (Figs. 5–7). Analyses of the randomized observations indicated that seals were less likely to enter the water when a tour boat was present than when there were no tour boats present in the

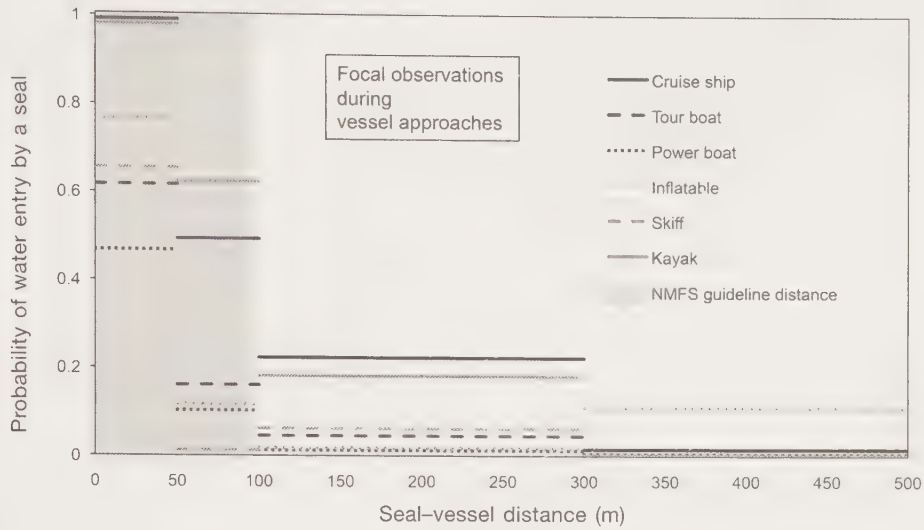

Figure 7

Estimated probabilities of hauled-out harbor seals (*Phoca vitulina*) entering the water when approached by a vessel as a function of seal–vessel distance and vessel type. Bars span the widths of the categorical distance bands used in this study. The National Marine Fisheries Service recommends that vessels remain beyond 100 yds (=91 m) from seals on haulouts (NMFS guideline avoidance area is blocked out in gray). Confidence intervals are presented in Table 2. Data were collected in Tracy Arm fjord in Alaska in 2001.

study area. Although we do not have a direct explanation for this pattern, possibilities include the predictable nature of tour boats in terms of arrival times and vessel maneuvering, the skill of experienced vessel captains, and seal habituation to specific boats. Some tour boats typically approach more slowly than other vessel types and then deploy motorized inflatables or skiffs to dispatch passengers, after which they continue slowly toward the glacier. Thus, another possible explanation is that the auxiliary craft preceding the tour boat may displace seals, functionally buffering the mother ship from producing disturbance. In addition, this could be a spurious result in which there was no actual tour boat effect, but because tour boats were always present at midday when seal haul-out probability was also highest, these two variables could end up being correlated without any cause and effect relationship, as suggested by Blundell and Pendleton (2015) and Jansen et al. (2015).

The number of vessel-caused disturbances is a function of the number of vessels of each type, how they are distributed, and the probability of disturbance at specific distances. Tour and private power vessels were the majority of vessels observed in our study; therefore, they almost certainly caused more of the total disturbances, a function of both disturbance risk and the number of encounters, than did the less commonly observed cruise ships or kayaks, even though the probability that tour and private power vessels caused a disturbance at a given distance was considerably lower. Consistent and predictable vessel speed after vessels pass harbor seals is also important in minimizing disturbance. Hoover-Miller et al. (2013) found that, although vessel captains were careful in approaching and passing seals, once the seals were behind the boat and out of view, some vessels accelerated, alerting the seals and occasionally causing them to flee into the water. We found that vessels that were stopped, often at their closest approach to the glacier—where there are typically lots of icebergs and seals—were more likely to cause disturbance than were vessels in motion. This pattern is consistent with the observations of Johnson and Acevedo-Gutiérrez (2007), where stopped power boats caused disturbances of hauled out harbor seals at distances of up to 10 times those of boats that passed by at steady speeds, even if the speed was fast.

Habituation and tolerance There were no days of our study at Tracy Arm without vessels. We recorded up to 33 vessels in one day and the minimum number of vessels we recorded was close to, or exceeded, the average numbers from other studies in glacial fjords (Calambokidis et al., 1987; Jansen et al., 2010; Young et al, 2014). Tracy Arm is only ~1 km wide (Fig. 1), which is 2–3 times narrower than Disenchantment Bay and Johns Hopkins Inlet, and most seals are clustered near the glacier face where vessels typically stop to view the glacier. Thus, it is likely that most seals in Tracy Arm were exposed to vessel traffic because they would likely have been within the diameter of a potential dis-

turbance swath as boats traversed the inlet. The difference in response distance in our study and the distances at other study sites with less vessel traffic, wider fjords, or both, could, therefore, result from higher levels of seal habituation to vessels. Alternatively, seals less tolerant of vessels might have left Tracy Arm for sites with less disturbance, leaving more tolerant seals or those seals incapable of dispersing (e.g., in poor condition) (Gill et al., 2001; Frid and Dill, 2002; Bejder et al. 2009). Individual habituation and selection for disturbance-tolerant individuals could yield similar patterns of lower levels of seal responses to vessels in Tracy Arm compared with other areas with less vessel traffic. Additional research, however, would be needed to address whether habituation or tolerance is more likely in glacial fjords with higher vessel traffic.

Harbor seal pups in Tracy Arm

The seasonal summer increase in vessel activity in Tracy Arm (Nuka Research and Planning Group[3]) coincides with the harbor seal pupping and nursing periods (late May–mid-July). The timing of harbor seal births in Tracy Arm (peak births occurred during 7–13 June and the maximum pup count occurred in late June) was similar to patterns in other glacial fjords in Alaska (Muir Inlet, Calambokidis et al., 1987; Johns Hopkins Inlet, Mathews and Pendleton, 2006; Aialik Bay Hoover-Miller et al., 2011).

Our analyses of observations of vessels approaching hauled-out seals showed that seal groups on icebergs that included a pup (and presumably its mother) were 1.6 times more likely to have at least 1 seal enter the water in response to the approach of a vessel than a seal in a group that did not include a pup (Fig. 6). The first seal, however, to enter the water usually was not a pup, which also was noted by Calambokidis et al.[1] and is consistent with observations of harbor seal mother–pup pairs at a terrestrial site (Renouf et al., 1983). Similarly, Suryan and Harvey (1999) and Henry and Hammill (2001) found that seal groups at a haul out with the highest proportion of pups were significantly more likely to show disturbance reactions to boats than seals hauled out at 2 other sites with lower proportions of pups.

Disturbances that do not cause permanent separation of the mother and her pup can have negative consequences for pup survival. Harbor seals have short lactation periods (Muelbert and Bowen, 1993; Thompson and Wheeler, 2008), and repeated disruption of nursing bouts could reduce pup growth and, consequently, pup survival (Harding et al., 2005). Repeated disturbances that increase the amount of time a young pup remains in cold glacial waters can increase its metabolism (Jansen et at., 2010), presumably having a negative impact on pup fitness. In addition, oxytocin, an endocrine hormone released during and shortly after birth, has been linked to maternal behavior in mothers (Pedersen and Prange, 1979; Pedersen et al., 1982; Keverne and Kendrick, 1992) and identified as an indicator of maternal success in phocid seals (Robinson, 2014). Gray seal females displaying abnormal maternal behavior were found to have lower plasma oxytocin concentrations than successful mothers that raised their pups to weaning age, and it is hypothesized that one cause of low oxytocin concentrations is disturbance of the mother-pup pair shortly after birth (Robinson, 2014). Because dependent pups are present in Tracy Arm during the summer tourist season, the potential exists for reduced pup fitness.

In 1996, the National Marine Fisheries Service (NMFS[10]), NOAA, published voluntary guidelines for viewing marine mammals in Alaska. These guidelines recommended that viewers stay at least 91 m (100 yards) from pinniped haul-out locations. In 2012, increasing concerns about disturbance to harbor seals in glacial fjords, including specific concerns about high levels of vessel traffic in Tracy Arm, led NMFS to consider regulations that would limit vessel disturbance of seals that use glacial sites (Federal Register, 2013). Because of public comment and other relevant information, NMFS decided to publish new voluntary guidelines that recommend that vessels stay 457 m (500 yards) from seals (NMFS[11]) and to distribute educational materials to vessel operators in 2015 (NMFS[12]).

Limiting access to these glacial habitats during the most critical life history stages of pup birth and nursing could reduce disturbance during critical mother-pup bonding, but it also could make seals more sensitive after closures are lifted because of potentially reduced habituation to vessel traffic. Better education of vessel operators could also help reduce seal disturbance, but the narrow configuration of Tracy Arm and the desire by vessel operators to closely approach the glacier face, and hence the seals, are problematic, especially in regard to the documented increase in marine-mammal–related tourism and the inevitable effect that such tourism will have on seal behavior.

Acknowledgments

This project was supported by NMFS grants to the Alaska Department of Fish and Game and by a National Science Foundation Research Experiences for Undergraduates Grant to the University of Alaska, Southeast. Logistical support was provided by the U.S. Forest Service (USFS), Juneau Ranger District, and by the captains of the MV *Keet*. B. Nielsen (Alaska Department of Fish and Game), T. Lydon and J. Neary

[10]National Marine Fisheries Service (NMFS). 2000 NOAA Fisheries proposes extra protection for humpback whale. [News release available at website, accessed January 2016]

[11]National Marine Fisheries Service (NMFS). 2015. NOAA Fisheries revises approach guidelines for vessels in Alaska glacial fjords, accessed January 2016.

[12]National Marine Fisheries Service (NMFS). 2015. Alaska harbor seal: approach guidelines in glacial fjords. [Available at website.]

(USFS) provided field leadership, and we thank the many field assistants for careful data collection. Research was conducted under NMFS research permits 358-1585 and 358-1787.

Literature cited

Allen, S. G., D. G. Ainley, G. W. Page, and C. A. Ribic.
1984. The effect of disturbance on harbor seal haul out patterns at Bolinas Lagoon, California. Fish. Bull. 82:493–500.

Altmann, J.
1974. Observational study of behavior: sampling methods. Behaviour 49(3):227–267. [Available at website.]

Bejder, L., A. Samuels, H. Whitehead, H. Finn, and S. Allen.
2009. Impact assessment research: use and misuse of habituation, sensitisation and tolerance in describing wildlife responses to anthropogenic stimuli. Mar. Ecol. Prog. Ser. 395:177–185.

Bigg, M. A.
1969. The harbour seal in British Columbia. Fish. Res. Board Can., Bull. 172, 33 p.

Bishop, R. H.
1967. Reproduction, age determination and behavior of the harbor seal, *Phoca vitulina* L. in the Gulf of Alaska. M.S. thesis, 121 p. Univ. Alaska Fairbanks, Fairbanks, AK.

Blundell, G. M., J. N. Womble, G. W. Pendleton, S. A. Karpovich, S. M. Gende, and J. K. Herreman.
2011. Use of glacial and terrestrial habitats by harbor seals in Glacier Bay, Alaska: costs and benefits. Mar. Ecol. Prog. Ser. 429:277–290.

Blundell, G. M., and G. W. Pendleton.
2015. Factors affecting haul-out behavior of harbor seals (*Phoca vitulina*) in tidewater glacier inlets in Alaska: can tourism vessels and seals coexist? PLoS ONE 10(5): e012486.

Boness, D. J., W. D. Bowen and O. T. Oftedal.
1994. Evidence of a maternal foraging cycle resembling that of otariid seals in a small phocid, the harbor seal. Behav. Ecol. Sociobiol. 34:95–104.

Boveng, P. L., J. L. Bengtson, D. E. Withrow, J. C. Cesarone, M. A. Simpkins, K. J. Frost, and J. J. Burns.
2003. The abundance of harbor seals in the Gulf of Alaska. Mar. Mamm. Sci. 19:111–127.

Brasseur, S., J. Creuwels, B. V. D. Werf, P. Beijnders, and Inst. For. Nat. Res.
1996. Deprivation indicates necessity for haul-out in harbor seals. Mar. Mamm. Sci. 12:619–624.

Calambokidis, J., and G. H. Steiger.
1985. Bald eagle (*Haliaeetus leucocephalus*) consumption of harbor seal (*Phoca vitulina*) placenta in Glacier Bay, Alaska. J. Raptor Res. 19:145.

Calambokidis, J., B. L. Taylor, S. D. Carter, G. H. Steiger, P. K. Dawson, and L. D. Antrim.
1987. Distribution and haul-out behavior of harbor seals in Glacier Bay, Alaska. Can. J. Zool. 65:1391–1396.

Draper, N. R., and H. Smith.
1981. Applied regression analysis, 2nd ed., 709 p. John Wiley & Sons, New York

Fay, F. H.
1974. The role of ice in the ecology of marine mammals of the Bering Sea. *In* Oceanography of the Bering Sea with emphasis on renewable resources. Occas. Publ. 2 (D. W. Hood and E. J. Kelley, eds.), p 383–399. Alaska Inst. Mar. Sci., Univ. Alaska Fairbanks, Fairbanks, AK.

Federal Register.
2013. Marine mammals: Alaska harbor seal habitats. Federal Register 78:15669–15672. [Available at website.]

Frid, A., and L. Dill.
2002. Human-caused disturbance stimuli as a form of predation risk. Conserv. Ecol. 6:11.

Gill, J. A., K. Norris, and W. J. Sutherland.
2001. Why behavioural responses may not reflect the population consequences of human disturbance. Biol. Conserv. 97:265–268.

Glacier Bay National Park and Preserve.
2006. 36 C.F.R. Sect. 13.65 (2006). [Available at website.]

Harding, K. C., M. Fujiwara, Y. Axberg, and T. Härkönen.
2005. Mass-dependent energetics and survival in harbour seal pups. Funct. Ecol. 19:129–135.

Henry, E., and M. O. Hammill.
2001. Impact of small boats on the haulout activity of harbour seals (*Phoca vitulina*) in Métis Bay, Saint Lawrence Estuary, Québec, Canada. Aquat. Mamm. 27.2:140–148.

Herreman, J. K., G. M. Blundell, D. B. McDonald, and M. Ben-David.
2009. Asymmetrical male-mediated gene flow between harbor seal (*Phoca vitulina*) populations in Alaska. Can. J. Zool. 87:498–507.

Hoover, A. A.
1983. Behavior and ecology of harbor seals (*Phoca vitulina richardsi*) inhabiting glacial ice in Aialik Bay, Alaska. M.S. thesis, 133 p. Univ. Alaska Fairbanks, Fairbanks, AK.

Hoover-Miller, A., S. Atkinson, S. Conlon, J. Prewitt, and P. Armato.
2011. Persistent decline in abundance of harbor seals *Phoca vitulina richardsi* over three decades in Aialik Bay, an Alaskan tidewater glacial fjord. Mar. Ecol. Prog. Ser. 424:259–271.

Hoover-Miller, A., A. Bishop, J. Prewitt, S. Conlon, C. Jezierski, and P. Armato.
2013. Efficacy of voluntary mitigation in reducing harbor seal disturbance. J. Wildl. Manage. 77:689–700.

Hosmer, D. W., Jr., and S. Lemeshow.
2000. Applied logistic regression, 2nd ed., 375 p. John Wiley & Sons, New York.

Jansen, J. K., P. L. Boveng, S. P. Dahle, and J. L. Bengston.
2010. Reaction of harbor seals to cruise ships. J. Wildl. Manage. 74:1186–1194.

Jansen, J. K., P. L. Boveng, J. M. Ver Hoef, S. P. Dahle and J. L. Bengston.
2015. Natural and human effects on harbor seal abundance and spatial distribution in an Alaskan glacial fjord. Mar. Mamm. Sci. 31:66–89.

Jemison, L. A.
1997. Recent history and demography of harbor seals on Tugidak Island, Alaska. M.S. thesis, 82 p. Univ. Alaska Fairbanks, Fairbanks, AK.

Jemison, L. A., G. W. Pendleton, C. A. Wilson, and R. J. Small.
2006. Long-term trends in harbor seal numbers at Tugidak Island and Nanvak Bay, Alaska. Mar. Mamm. Sci. 22:339–360.

Jezierski, C.
2009. The impact of sea kayak tourism and recreation on harbor seal behavior in Kenai Fjords National Park: integrating research with outreach, education, and tour-

ism. M.S. thesis, 69 p. Univ. Alaska Fairbanks, Fairbanks, AK.

Johnson, B. W.
1977. The effects of human disturbance on a population of harbor seals. *In* Environmental assessment of the Alaskan continental shelf, Annu. Rep. 1:422–432. Outer Continental Shelf Environmental Assessment Program, Boulder, CO.

Johnson, A., and A. Acevedo-Gutiérrez.
2007. Regulation compliance by vessels and disturbance of harbour seals (*Phoca vitulina*). Can. J. Zool. 85:290–294.

Keverne, E. B., and K. M. Kendrick.
1992. Oxytocin facilitation of maternal behavior in sheep. Ann. N. Y. Acad. Sci. 652:83–101.

Larson, C. F., R. J. Motyka, A. A. Arendt, K. A. Echelmeyer, and P. E. Geissler.
2007. Glacier changes in southeast Alaska and northwest British Columbia and contribution to sea level rise. J. Geophys. Res. 112:F01007.

Lawson, J. W., and D. Renouf.
1987. Bonding and weaning in harbor seals, *Phoca vitulina*. J. Mamm. 68:445–449.

Littell, R. C., G. A. Milliken, W. W. Stroup, R. D. Wolfinger, and O. Schabenberger.
2006. SAS for mixed models, 2nd ed., 828 p. SAS Institute, Cary, NC.

Mathews, E. A.
1995. Long-term trends in abundance of harbor seals *(Phoca vitulina richardsi)* and development of monitoring methods in Glacier Bay National Park, southeast Alaska. *In* Proceedings of the Third Glacier Bay Science Symposium; Gustavus, AK, 15–18 September 1993 (D. R. Engstrom, ed.), p. 254–263. U.S. Government Printing Office, Washington, D.C.

Mathews, E. A., and B. P. Kelly.
1996. Extreme temporal variation in harbor seal (*Phoca vitulina richardsi*) numbers in Glacier Bay, a glacial fjord in southeast Alaska. Mar. Mamm. Sci. 12:483–488.

Mathews, E. A., and G. W. Pendleton.
2006. Declines in harbor seal (*Phoca vitulina*) numbers in Glacier Bay National Park, Alaska, 1992–2002. Mar. Mamm. Sci. 22:167–189.

Mathews, E. A., and M. D. Adkison.
2010. The role of Steller sea lions in a large population decline of harbor seals. Mar. Mamm. Sci. 26:803–836.

Muelbert, M. M. C., and W. D. Bowen.
1993. Duration of lactation and postweaning changes in mass and body composition of harbour seal, *Phoca vitulina*, pups. Can. J. Zool. 71:1405–1414.

Newby, T. C.
1973. Changes in Washington State harbor seal population, 1942–1972. Murrelet 54:4–6.

Osinga, N., S. B. Nussbaum, P. M. Brakefield, and H. A. Udo de Haes.
2012. Response of common seals (*Phoca vitulina*) to human disturbances in the Dollard estuary of the Wadden Sea. Mamm. Biol. 77:281–287.

Pedersen, C. A., and A. J. Prange Jr.
1979. Induction of maternal behavior in virgin rats after intracerebroventricular administration of oxytocin. Proc. Natl. Acad. Sci. U.S.A. 76:6661–6665.

Pedersen, C. A., J. A. Ascher, Y. L. Monroe, and A. J. Prange Jr.
1982. Oxytocin induces maternal behavior on virgin female rats. Science 216:648–650.

Pitcher, K. W.
1986. Variation in blubber thickness of harbor seals in southern Alaska. J. Wildl. Manage. 50:463–466.

Renouf, D., J. Lawson, and L. Gaborko.
1983. Attachment between harbour seal (*Phoca vitulina*) mothers and pups. J. Zool. 199:179–187.

Robinson, K. J.
2014. The role of oxytocin in the maternal behaviour of the grey seal (*Halichoerus grypus*). Ph.D. thesis, 238 p. Univ. St Andrews, St. Andrews, U.K.

Simpkins, M. A., D. E. Withrow, J. C. Cesarone, and P. L. Boveng.
2003. Stability in the proportion of harbor seals hauled out under locally ideal conditions. Mar. Mamm. Sci. 19:791–805.

Suryan, R. M., and J. T. Harvey.
1999. Variability in reactions of Pacific harbor seals, *Phoca vitulina richardsi*, to disturbance. Fish. Bull. 97:332–339.

Thompson, P. M., and H. Wheele.
2008. Photo-ID-based estimates of reproductive patterns in female harbor seals. Mar. Mamm. Sci. 24:138–146.

Womble, J. N., and S. M. Gende.
2013. Post-breeding season migrations of a top predator, the harbor seal (*Phoca vitulina richardii*), from a marine protected area in Alaska. PLoS ONE 8(2): e55386.

Womble, J. N., G. W. Pendleton, E. A. Mathews, G. M. Blundell, N. M. Bool, and S. M. Gende.
2010. Harbor seal (*Phoca vitulina richardii*) decline continues in the rapidly changing landscape of Glacier Bay National Park, Alaska, 1992–2008. Mar. Mamm. Sci. 26:686–697.

Young, C.
2009. Disturbance of harbor seals by vessels in John Hopkins Inlet, Glacier Bay, AK. M.S. thesis, 120 p. San Jose State Univ., San Jose, CA.

Young, C., S. M. Gende, and J. T. Harvey.
2014. Effects of vessels on harbor seals in Glacier Bay National Park. Tourism Mar. Environ. 10:5–20.

NOAA
National Marine
Fisheries Service

Fishery Bulletin
established 1881

Spencer F. Baird
First U.S. Commissioner
of Fisheries and founder
of Fishery Bulletin

Effect of population abundance and climate on the growth of 2 populations of chum salmon (*Oncorhynchus keta*) in the eastern North Pacific Ocean

Ellen M. Yasumiishi (contact author)[1,2]
Keith R. Criddle[1]
John H. Helle[1,3]
Nicola Hillgruber[1,4]
Franz J. Mueter[1]

Email address for contact author: ellen.yasumiishi@noaa.gov

[1] University of Alaska Fairbanks
School of Fisheries and Ocean Sciences
17101 Point Lena Loop Road
Juneau, Alaska 99801

2 Auke Bay Laboratories
Alaska Fisheries Science Center
National Marine Fisheries Service, NOAA
Ted Stevens Marine Research Institute
17109 Point Lena Loop Road
Juneau, Alaska 99801-8626

[3] 2427 O'Day Drive
Juneau, Alaska 99801

[4] Thünen-Institute of Fisheries Ecology
Wulfsdorfer Weg 204
22926 Ahrensburg, Germany

Abstract—Seasonal and annual marine growth of chum salmon (*Oncorhynchus keta*) from Fish Creek, Alaska, during 1972–2004 and from Quilcene River, Washington, during 1973–2004 were examined in relation to abundances of chum salmon and pink salmon (*O. gorbuscha*) and climate indices from that period. Pink salmon abundance indices were included in the analysis because of evidence for density-dependent effects on chum salmon growth and survival. In linear regression models, growth was negatively related to abundance of chum salmon or to the combined abundance of pink and chum salmon during the middle juvenile (July–Sept), 1st immature, 2nd immature, and maturing stages for the Fish Creek chum salmon and the 1st immature, 2nd immature, and maturing stages for Quilcene River chum salmon, indicating possible density-dependent effects on growth. Mid-juvenile and maturing growth models for the Fish Creek chum salmon and the maturing growth model for Quilcene River chum salmon performed well in model validation, when model predictions were tested against 20% of the data that were not used for model specification, and provided insight into the effects of climate and abundance on growth of chum salmon from 1972 to 2004.

Manuscript submitted 30 June 2015.
Manuscript accepted 5 February 2016.
Fish. Bull. 114:203–219 (2016).
Online publication date: 3 March 2016.
doi: 10.7755/FB.114.2.7

The views and opinions expressed or implied in this article are those of the author (or authors) and do not necessarily reflect the position of the National Marine Fisheries Service, NOAA.

Over the last century, the quantity of chum salmon (*Oncorhynchus keta*) and pink salmon (*O. gorbuscha*) available for harvest in North America has fluctuated on a multidecadal scale with harvest peaks in the 1930s and the 1990s and lows in the 1950s, 1960s, and 1970s (Eggers et al.[1]; Ruggerone et al. 2010). From the mid1970s to the mid-1990s, increases in salmon production were attributed to a combination of causes: namely of hatchery supplementation (Eggers, 2009), increased survival of wild stocks due to favorable ocean conditions (Beamish and Bouillon, 1993; Francis and Hare 1994; Hare and Francis, 1995; Hilborn and Eggers, 2000; Morita et al., 2006), and improved management of wild stocks (Wertheimer, 1997).

Concurrent with increases in salmon production from the mid-1970s to the mid-1980s and 1990s, reductions in the average body size were observed in Pacific salmon from North America and Asia (Bigler et al., 1996; Helle and Hoffman, 1998; Bugaev et al., 2001), indicating possible density-dependent effects on growth in the ocean. Based on these correlations, a hypothesis was formulated that there might be a finite carrying capacity for Pacific salmon in the North Pacific Ocean, limited by the amount of food available to support fish growth (Helle and Hoffman, 1998).

Density-dependent influences on growth have been well documented for salmon in the Pacific Ocean. Juvenile pink and chum salmon have a high degree of overlap in diet off southeast Alaska and within Prince William Sound in the Gulf of Alaska (GOA) (Auburn and Ignell, 2000). The marine survival of chum salmon and stomach fullness of juvenile chum

[1] Eggers, D. M., J. R. Irvine, M. Fukuwaka, and V. I. Karpenko. 2005. Catch trends and status of North Pacific salmon. NPAFC Doc. 723, Rev. 3, 35p.

Table 1

Hypothesized mechanisms and effects (positive [+] and negative [–]) of selected climate indices on the marine growth of chum salmon (*Oncorhynchus keta*) in the North Pacific Ocean. Locations are the Gulf of Alaska (GOA), central subarctic North Pacific (CNP) and eastern subarctic North Pacific (ENP) oceans, and Washington (WA). Abbreviations include the mixed layer depth (MLD), Pacific Decadal Oscillation (PDO), and sea surface temperature (SST).

Stage	Location	Index	Mechanism	Effect
Fish Creek, southern Southeast Alaska (saltwater entry from February through May)				
Early juvenile	GOA shelf	Spring wind	Plankton bloom	–
Midjuvenile	GOA shelf	Winter MLD	Nutrients availability	+
Late juvenile	GOA shelf	Fall wind	Fall bloom	–
Immature/maturing	CNP ENP	Winter PDO	Cool, high nutrients+	
Immature/maturing	CNP ENP	Summer SST	Warm	+
Quilcene River, Washington (saltwater entry in May)				
Early juvenile	WA coast	Upwelling index	Nutrient upwelling	+
Early juvenile	WA coast	Spring transition	Later upwelling	–
Midjuvenile	GOA shelf	Winter MLD	Nutrients availability	+
Late juvenile	GOA shelf	Fall wind	Plankton bloom	–
Immature/maturing	CNP ENP	Winter PDO	Cool, high nutrients	+
Immature/maturing	CNP ENP	Summer SST	Warm	+

salmon was negatively correlated with the number of fry releases from the hatcheries in coastal waters of Japan (Fukuwaka and Suzuki, 2000). Chum salmon switched from eating crustacean to gelatinous zooplankton when pink salmon were more abundant (Tadokoro et al., 1996). For chum salmon in the eastern Bering Sea, a significant negative relationship was observed between catch-per-unit-of- effort of chum salmon and the mean growth rate for age 0.2 and age 0.3 chum salmon (Azumaya and Ishida, 2000). These observations of prey switching, diet overlap, reduced feeding, and survival success at higher salmon population levels all provide support for the hypothesis that a carrying capacity may exist for salmon in the North Pacific Ocean.

During their marine life, chum salmon from Oregon to the Alaska Peninsula are found primarily in the Alaska Gyre of the eastern North Pacific Ocean (Myers et al., 2007). In the first year at sea, juvenile chum salmon migrate with the counterclockwise Alaska Coastal Current along the Alaska coastline above the continental shelf (Hartt and Dell, 1986). At a velocity of 10 cm/s, we estimated that the Alaska Coastal Current is able to transport juvenile salmon over 1000 km in about 4 months, the approximate distance from Washington (WA) to southern Southeast Alaska (Reed and Schumacher, 1986); however this estimate was based on limited data. During the fall, juvenile pink and chum salmon migrate west and southwest along the Alaska Peninsula where they enter the swift westward flowing Alaska Stream (40 cm/s) (Reed and Schumacher, 1986). During their second through penultimate years at sea, immature northeastern Pacific chum salmon were primarily distributed to the north and east of the western (160°W) and southern (50°N) boundaries of the GOA in the eastern North Pacific Ocean (Myers et al., 2007). During their final year at sea, maturing salmon migrate through oceanic and continental shelf habitats to return to freshwater to spawn. In some years, immature and maturing southern North American stocks of chum salmon move into the Bering Sea in late summer and fall (Seeb et al., 2004). Because chum salmon occupy different regions of the North Pacific Ocean during their ontogenetic migration after first entering the marine realm until their return to their natal streams, it should be possible to develop habitat-specific growth models that could be used to explain variations in growth at each life stage.

Various hypotheses and mechanisms for climate to affect habitat-specific marine growth of chum salmon in the North Pacific Ocean are listed in Table 1. We expected an increase in growth of chum salmon in the eastern North Pacific Ocean to be associated with increased ocean productivity due to a stronger spring phytoplankton bloom as indexed by reduced wind speed (Spies and Weingartner, 2007). Growth was also expected to increase with the occurrence of a fall bloom, increased coastal upwelling, and an earlier timing of spring coastal upwelling (Logerwell et al., 2003). During summer, growth was expected to increase with a deeper mixing layer in the northern GOA during winter that enhances mixing of nutrients and a stronger spring bloom and enhanced summer feeding for juvenile salmon (Sarkar, 2007). Offshore, growth was expected to increase with warmer ocean temperatures (Martinson et al., 2008, 2009) and increased productivity offshore as indexed by the winter Pacific Decadal Oscillation (Mantua et al., 1997).

For this study, we attempt to explore density-dependent and climate limitations on growth for different life stages of chum salmon by examining the effects

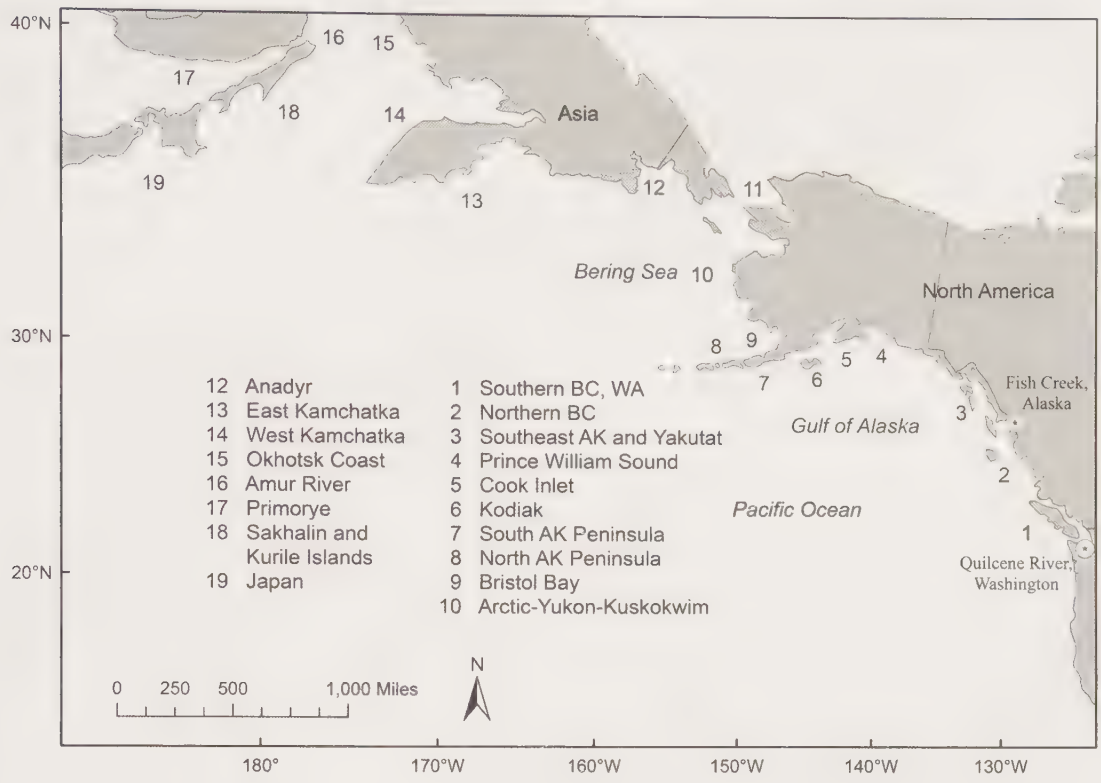

Figure 1

Map showing the regions used to estimate chum salmon (*Oncorhynchus keta*) and pink salmon (*O. gorbuscha*) abundances (from Ruggerone et al. [2010]) and locations of Fish Creek, Alaska, where biological data were collected from 1972 to 2007, and Quilcene River, Washington, where biological data were collected from 1973 to 2007.

of pink and chum salmon abundance and climate on stage-specific growth of these fish in those portions of the North Pacific Ocean that they occupy. The null hypothesis was that growth was not negatively related to an index of pink and chum salmon abundance and therefore chum salmon production was not limited by density-dependent growth in the North Pacific Ocean. The alternative hypothesis was that growth was negatively related to pink and chum salmon abundance—an indication that chum salmon production was limited by density-dependent growth in the North Pacific Ocean. Our objectives were 1) to determine the existence and magnitude of density-dependent growth, 2) to describe differences in density-dependent growth for chum salmon from WA and southern southeast Alaska, 3) to evaluate the influence of pink and chum salmon abundances on chum salmon growth, 4) to evaluate the influence of local and regional abundances on growth, and 5) to determine the influence of climate on growth.

Material and methods

Data, sample size, and assumptions

The National Marine Fisheries Service, Auke Bay Laboratories scientists collected biological data from summer chum salmon in Fish Creek near Hyder, Alaska, from 1972 to 2007 and from fall chum salmon from the Quilcene River and U.S. Fish and Wildlife's Quilcene National Fish Hatchery near Quilcene, WA, from 1973 to 2007 (Fig. 1). Fish Creek chum salmon were sampled from mid- to late-August, the peak of the summer run. Quilcene River chum salmon were typically sampled during the first two weeks of December, the peak of the fall run. Although Fish Creek chum salmon returned to spawn earlier in the year, they were larger at maturity than Quilcene River chum salmon.

Scales, body lengths, and sex data were collected from up to 300 chum salmon carcasses per year from both stocks. The aim was to obtain 50 samples for each sex and for the dominant age classes: age-0.2, age-0.3, and age0.4. Salmon ages were denoted with the decimal method ($x.y$), where x is the number of winters spent in freshwater after spending a winter in the gravel and y is the number of winters spent in the marine environment. For this study, we used only age0.3 male chum salmon to reduce variation in growth because of differences in growth between sexes and ages, and because of data availability. Only age-0.3 chum salmon were sampled in some years and we have larger sample sizes for males than females. We sampled during the peak of the spawning migration and the samples represented the dominant age class at that time. Typi-

cally, the growth and size of male and female salmon covary over time, although at different scales; therefore inclusion of models and discussion for both sexes would be redundant. Body length (nearest 1.0 mm) measurements were from the middle of the eye to the posterior edge of the hypural plate (MEHP). MEHP measurements were converted to fork length (FL) by using a conversion formula from male Fish Creek chum salmon carcasses measured in 1974: (FL=1.21($MEHP$)+32.8; n=51; r^2=0.923; P<0.001). Annual sample sizes for a given stock varied from 6 to 86 scales. Years with no data included 1995, 1997, and 2001 for Fish Creek and 1980 for Quilcene River.

Scale processing and scale measurements

Scales were processed for age and growth determination according to Arnold (1951). The acetate impressions were scanned at 24× magnification and stored in JPEG file format at 300 dpi. The electronic images were then imported into the digitizing software program Image Pro[2] with ringed structure macros developed by Media Cybernetics (Bethesda, MD). Scales were screened and those showing evidence of resorption or regeneration were not used in the growth analysis. Each scale was measured along a reference line drawn along the longest axis of the posterior portion of the scale from the center of the focus to the leading edge of the 9th circulus (Sa), 21st circulus (Sb), 1st annulus (Sc), 2nd annulus (S2), 3rd annulus (S3), and to the edge of the scale (S4). We use the terms annulus and annuli in a restricted sense to mean those groups of circuli that represent growth from 1 year to the next.

Growth during specified time periods during the first year at sea was estimated from intercirculus spacings in the first ocean zone on the scale (Fukuwaka and Kaeriyama, 1997). We estimated and assumed that circuli formed at an approximately constant rate (1 circulus/7–10 days) on the basis of the total number of circuli in the first ocean zone and the length of the growing season (time of fry out-migration to the time of formation of the first marine annulus on the scale). Fish Creek chum salmon fry leave their native streams from March through May (Heinl, 2005) and form an average of 30 to 35 (mean=32) circuli during the first year at sea. Quilcene River chum salmon fry that are released into the Quilcene River from the hatchery in early May form an average of 33 to 40 circuli (mean=36) during the first year at sea. Although the Quilcene River chum salmon left freshwater later and had more circuli, this southern stock likely endured a longer growing season. *Sa* represented the first 2–3 months (63–90 days) at sea (April–May/June for Fish Creek and May–June/July for Quilcene River). *Sb* represented the next 3–4 months (84–120 days) at sea (June–August/Sept or July–Sept/Oct for Fish Creek and July–Sept/Oct or Aug–Oct/Nov for Quilcene River). *Sc* represented the remaining time through the end of the first growing season, before formation of the first winter annulus on the scale.

Growth indice

For each stock, saltwater growth (SW) in body length (mm) was back-calculated for the early juvenile ($SW1a$), middle juvenile ($SW1b$), late juvenile ($SW1c$), 1st immature ($SW2$), 2nd immature ($SW3$), and maturing ($SW4$) life stages by using the Fraser-Lee back-calculation equation (Lee, 1920). With this method, fish length is assumed to be directly proportional to scale radius (Dahl, 1909; Kaeriyama, 1998). The equation was given as

$$\bar{L}_{t,i} = 40 + (\bar{L}_{t,total} - 40) \cdot (\bar{S}_{t,i} / \bar{S}_{t,total}), \quad (1)$$

where t = year;
40 = length of the fish at the time of scale formation (mm);
$\bar{L}_{t,i}$ = mean total body length at stage i;
$\bar{L}_{t,total}$ = mean total body length of the carcass samples;
$\bar{S}_{t,i}$ = mean radius from the focus to the mark on the reference line on the scale; and
$\bar{S}_{t,total}$ = mean total radius of the scale.

We set the intercept to 40 mm, the length at the time of formation of the scale for chum salmon (Kobayashi, 1961; Helle, 1979). Finally, SW indices were calculated as the differences in the back-calculated lengths (L) for each life stage: early juvenile ($SW1a$=La), middle juvenile ($SW1b$=Lb–La), late juvenile ($SW1c$=Lc–Lb), 1st immature year ($SW2$=$L2$–Lc), 2nd immature year ($SW3$=$L3$–$L2$), and maturing ($SW4$=$L4$–$L3$).

Salmon abundance indices

Chum and pink salmon abundance indices for early juvenile (SW1a), middle juvenile (SW1b), late juvenile (SW1c), 1st immature (SW2), 2nd immature (SW3), and maturing (SW4) stages were back-calculated from the numbers of pink and chum salmon returns (harvest and escapement) of North America by management region, time series of age composition of chum salmon, and marine mortality schedules for pink and chum salmon.

The pink and chum salmon abundance indices N for year t were estimated with the following equation:

$$N_t = \Sigma\left(p_{a,t+a} R_{a,t+a} \frac{1}{\Pi S_a}\right), \quad (2)$$

where p = the proportion of chum salmon of each age class for samples taken in-river;
a = age class;
R = returns (catch and escapement); and
ΠS = the product of daily survival rates from the middle of the life stage to the end of life.

Abundance indices were based on estimates of returns (harvest and escapement) of pink and chum salmon from Ruggerone et al. (2010). For each life

[2] Mention of trade names or commercial companies is for identification purposes only and does not imply endorsement by the National Marine Fisheries Service, NOAA.

stage, combined and separate indices for chum and pink salmon abundance were calculated for WA and southern BC (SBC), northern BC (NBC), southern and northern British Columbia (BC), southeast Alaska and Yakutat (SE), SE to the Alaska Peninsula (AP) (SE–AP), BC through AP (BC–AP) and Asia (AS) owing to overlap in the distribution and diets of juvenile and adult pink and chum salmon (Fig. 1) (Orsi et al.[3]; Davis et al.[4], 2009). Chum salmon abundance indices were calculated by age (0.0, 0.1, 0.2, 0.3) to match each age during the growth period (SW1, SW2, SW3, SW4). For this study, SW1a, SW1b, and SW1c were related to age 0.0 pink and chum salmon abundances, SW2 was related to age 0.1 pink and chum salmon abundances, SW3 was related to age 0.1 pink salmon and age 0.2 chum salmon abundances, and SW4 was related to age 0.1 pink salmon and age 0.3 chum salmon abundances. Three chum and pink salmon abundance indices were calculated for SW1 growth during age-0.0, the first year at sea. Maturing pink salmon were combined with the immature and maturing chum salmon because of spatial and dietary overlaps (Davis et al.[4]).

Each juvenile growth variable was related to three salmon abundance indices (chum salmon, pink salmon, and chum and pink salmon combined) from various regional groupings. For Fish Creek chum salmon, SW1a was related to SE salmon abundance indices (3 indices), SW1b was related to SE and BC–SE salmon abundance (6 indices), and SW1c was related to SE, BC–SE, SE–AP salmon abundance (9 indices). For Quilcene River chum salmon, SW1a was related to SBC salmon abundance (3 indices), SW1b was related to BC and BC–SE salmon abundance (6 indices), and SW1c was related to SE, BC–SE, SE–AP salmon abundance (9 indices). For the immature and maturing stages, chum salmon growth was related to two salmon abundance indices (chum salmon and chum and pink salmon combined) from various regional groupings. For Fish creek chum salmon, SW2, SW3, and SW4 were related to SE, BC–SE, SE–AP, BC–AP, BC–AS, and AS (12 indices). For Quilcene River chum salmon, SW2, SW3, and SW4 were related to BC, BC–SE, SE–AP, BC–AP, BC–AS, and AS (12 indices).

Age composition for chum salmon in Alaska and Asia was assumed to be well characterized by the time series of age composition from the Fish Creek stock, whereas the age composition for the BC stocks was assumed to be characterized by age composition from the Quilcene River stock.

Marine mortality rates were calculated from fry to maturity. Marine mortality rates were approximately 97% for chum and pink salmon (Kaeriyama, 1998). Approximately 70% of the total mortality occurs within the first 40 days at sea (Parker, 1968) and pink salmon experience a mortality of 2–4% (we used 3%) mortality per day for the first 40 days and 0.4–0.8%/d (we used 0.6%/d) thereafter (Parker, 1968). These daily mortality rates were used to develop a survival rate schedule by life stage for pink and chum salmon. The products of the daily survival rates were used to expand returns to reflect abundance during the middle of each life stage in our study.

Climate indices

The six climate indices used in this study were mean late spring (May–June) wind speed (m/s), mean fall (Sept–Oct) wind speed (m/s), deepest winter (Dec–Feb) mixed layer depth (m), spring transition index (day of year), mean summer/fall (July–Oct) SST (°C), and the winter (Dec–Feb) Pacific Decadal Oscillation (PDO) index.

Wind speed index Surface wind speed data were accessed from the website of the NOAA Fisheries Southwest Fisheries Science Center's Environmental Research Division (website, accessed Sept 2009). Indices were derived from data sets of atmospheric pressure fields at 6-hour intervals from the Fleet Numerical Meteorology and Oceanography Center. The spring wind (WS) index was calculated as the values for April 16 or 17 at Dixon Entrance off southern SE Alaska (56.5°N, 134.5°W). The fall wind (WF) index was calculated as the average of the September and October monthly wind index values at the surface east of Kodiak Island (58.5°N, 150.0°W).

Mixed layer depth index A mixed layer depth (MLD) index for winter was available for the mouth of Resurrection Bay (60°N, 149°W) in the northern GOA (Sarkar, 2007). The Freeland et al. (1997) algorithm was used to calculate the deepest winter MLD (m).

Spring upwelling transition index The spring transition index (STI) represents the timing (day of year) of the transition from downwelling to upwelling off the coast of WA and OR (Logerwell et al., 2003). The STI values ranged from 48 in 1985 to 161 in 1993. The transition occurs between March and June.

Upwelling magnitude index The monthly magnitude of upwelling ($m^3 \cdot s^{-1} \cdot 100\ m^{-1}$ of coastline) off WA was accessed from NOAA's Pacific Fisheries Environmental Laboratory website (website, accessed Sept 2008). The location of the upwelling index (UI) was 23 nautical miles (nmi) south and 13 nmi west of Cape Flattery at the tip of the Olympic peninsula off the WA coast (125°W and 48°N). A spring UI was calculated as the sum of the May and June indices.

[3] Orsi, J., A. Wertheimer, M. Sturdevant, E. Fergusson, and B. Wing. 2009. Insights from a 12-year biophysical time series of juvenile Pacific Salmon in southeast Alaska: the Southeast Alaska Coastal Monitoring Project (SECM). NOAA Alaska Fisheries Science Center AFSC Q. Res. Rep., 8 p. [Available at website.]

[4] Davis, N. D., K. W. Myers, and Y. Ishida. 1998. Bering Sea salmon diet overlap in fall 2002 and potential for interactions among salmon. North Pacific Anadromous Fish Commission (NPAFC) Doc. 779, 30 p.

Sea temperature Sea temperature data for the eastern North Pacific Ocean were available from NOAA's Earth System Research Laboratory's Physical Sciences Division website (website, accessed April 2012). The NCEP/NCAR re-analyzed SST data set was used (Kalnay et al., 1996) to derive average monthly SST for a region east of 157.5°W and north of 52.4°N. Averages were computed for 3 grids of equal area (52.4°N–48.6°N×148.1°W–157.5°W, 52.4°N–48.6°N×148.1°W–138.7°W, and 58.1°N–52.4°N×148.1°W–138.7°W) and the 3 areas were then averaged for each year from 1972 to 2004. An index was constructed from the average of the monthly SST from July 1 through Oct 31 to encompass the warmest months of the year.

Pacific Decadal Oscillation index The PDO was calculated as the leading principle component of the Reynolds optimally interpolated monthly SST anomalies poleward from 20°N (Zhang et al., 1997). Data were available from the website of Steven Hare and Nathan Mantua at the University of Washington Joint Institute for the Study of the Atmosphere and Ocean (Hare and Mantua, 2000). The mean winter PDO was calculated as the average of the monthly Dec (in year t–1), Jan (in year t), and Feb (in year t) PDO values. The correlation coefficient between the winter PDO and the summer SST time series was not statistically significant.

Analytical techniques

Scatter and line plots were used to assess temporal variation in the average length at maturity and growth during each life stage by stock. For the models, each time series was scaled and centered by subtracting the mean and dividing by the standard deviation. This allowed for interpretation of the model coefficients as the number of standard deviations of change in growth for each 1 standard deviation change in the predictor variable. For example, a coefficient of –0.500 (0.500) indicates a 50% decrease (increase) in 1 standard deviation of the dependent variable (growth) with an increase of 1 standard deviation in the predictor variable (abundance, length, or climate).

We used a transfer function-noise model introduced for fisheries by Noakes et al. (1987) to explain variation in growth. The growth dynamic model was a regression equation with an error correction equation. The regression equation based on a generalized least squares (GLS) method was used to describe growth as a function of chum and pink salmon abundance and body length at the start of the growing season. The error correction model was used to capture additional variation in growth due to multicollinearity among climate and salmon production. The GLS regression equation was given as

$$SW_{i,t} = \beta_1(Abundance_t) + \beta_2(Abundance_t)^2 + \beta_3 Length_{t-1} + \varepsilon_t, \quad (3)$$

where t = year or season;
$SW_{i,t}$ = growth variable at stage i in year t;
stage i = 1a, 1b, 1c, 2, 3, 4;
$Abundance_t$ = a chum and/or pink salmon abundance index in year t;
$Length_{t-1}$ = the length of the fish at the end of the previous growing season;
β = the coefficient; and
ε_t = the residuals.

The process encompasses contemporaneous and serially correlated sample, observation, and model specification error. To test for domeshaped or asymptotic relationships between growth and abundance and climate, we added variables for the square of the abundance. Degrees of freedom were calculated for the GLS model (n–k) from the number of observations in a time series (n) and the number of coefficients in model (k).

The error correction equation (Eq. 4) was used to extract signal from the noisy residuals from the regression equation (Eq. 3). A vector autoregression (VAR) equation was used to relate contemporaneous values of the regression model residuals with lagged values of the regression model residuals and lagged values of climate indices. In a system of two equations, the single VAR equation for two variables was given as

$$\varepsilon_t = B_{1,\varepsilon}\varepsilon_{t-1} + \ldots + B_{i,\varepsilon}\varepsilon_{t-j} + \ldots + B_{p,\varepsilon}\varepsilon_{t-p} + B_{1,x}X_{t-1} + \ldots + B_{i,x}X_{t-j} + B_{p,x}X_{t-p} + e_t, \quad (4)$$

where X_t = a climate index;
ε_t = a vector time series of the growth dynamic equation residuals for the two equations;
$B_{i,j}$ = coefficients to be estimated;
X_t = a vector of climate indices in time t;
p = the maximal lag length; and
e_t = the residuals.

For the equation, the maximum likelihood estimator for the matrix coefficient B was $B = Y'Z'(Z'Z)^{-1}$ where Z was a matrix composed of the elements of ε and X. Because the estimated coefficients of the VAR were conditional on the residuals of the growth model and because the estimated coefficients of the growth model were inefficient when serial correlation was present, it was necessary to iterate with equations 3 and 4 until the coefficient estimates of the both equations converged to stable values. The degree of freedom for the GLS and VAR integrated model were (n·m–k–p·m), where p was the number of lag years and m was the number of time series in the VAR equation. We limited the maximum lag to 4 years to account for the possible direct or indirect effect of generation cycles on growth.

To test the performance of the models, data were partitioned into two sets (*in-sample* set and *reserved observations* set). The insample set was used for coefficient estimation and model specification. The reserved observations set was used for model validation. The insample set consisted of the first approximately 80% of the observations. The remaining 20% of the observations, reserved observations, were reserved to generate outofsample predictions by using coefficients obtained for the insample model. Various software programs were used in the exploration of the time series, the

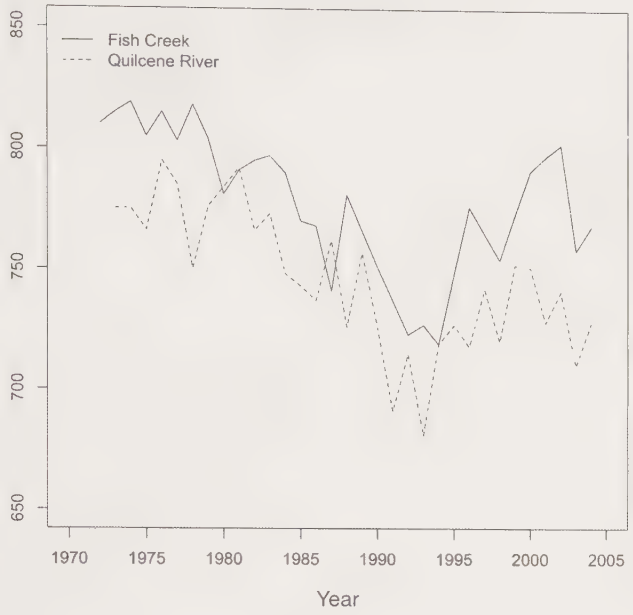

Figure 2

Average body length of age-0.3 male chum salmon (*Oncorhynchus keta*) carcasses at Fish Creek, Alaska from 1972 to 2007 and Quilcene River, Washington, from 1973 to 2007.

GLS regression modeling, and VAR modeling (Simetar, Simetar Inc., College Station, TX; Excel 2013, Microsoft Corp., Redmond, WA).

Model specification and selection was based on a Bonferonni correction factor and the lowest Schwarz information criterion (SIC) for each of the 12 growth variables. The SIC was applied to add a penalty for the number of predictor variables in the model. Abundance indices were added separately to GLS models because of multicollinearity. A Bonferroni correction factor was applied to the *P*-value of the coefficients for abundance to account for the number of abundance indices used in each model (α=0.05/number of possible predictors variables). The final GLS/VAR models were tested for heteroscedasticity of the residuals (Goldfeld-Quandt test, absolute residuals vs. fitted values plot), normality of the residuals (qq plots, studentized residuals vs. fitted values, and Shapiro test), and serial correlation of the residuals (autocorrelation test). Selection of the final GLS model and a comparison of the GLS and the GLS/VAR model were based on the SIC.

To test model performance, an *F*-test was used to determine whether the mean squared error was significantly greater for reserved observations and estimates than for in-sample observations and estimates. If the test statistic exceeded the critical value, model performance was judged to have deteriorated over the reserved observations, indicative of model misspecification. Lehmann's correlation was used to determine whether the mean squared error was reduced by integrating the climate and residuals using the VAR models and for determining model performance (Lehmann, 1959).

To compare our findings with other observational data, we examined the mean body length of juvenile chum salmon and the surface trawl catch of juvenile pink and chum salmon from continental shelf waters off Icy Point in the GOA from 1997 to 2011 (courtesy of the SE Coastal Monitoring Program, Alaska Fisheries Sciences Center, Juneau, Alaska).

Results

Trends in body size and growth

Trends in annual mean body length at maturity for age-0.3 male chum salmon were similar for the Fish Creek and Quilcene River stocks but on different scales (Fig. 2). From the 1970s to the early 1990s, mean length decreased by about 11.6% (99 mm) for Fish Creek chum salmon (from 815 to 720 mm) and by 8.6% (60 mm) for Quilcene River chum salmon (from 780 to 720 mm). The decline was followed by an increase in body length in both populations, but the increase from the early 1990s to 2000 was much larger for Fish Creek chum salmon (9.7%) than for Quilcene River chum salmon (2.8%). However, neither stock had regained body lengths observed in the 1970s.

Trends in SW2 and SW3 incurred offshore were similar for Fish Creek and Quilcene River chum salmon (Fig. 3). SW2 and SW3 declined from the mid-1970s to the mid-1990s and increased from the mid-1990s to the mid-2000s. Declines in growth from the mid-1970s to the mid-1990s also occurred in SW1a, SW1b, and SW4 for Fish Creek chum salmon but remained low from the mid-1990s to the mid-2000s. No trends were observed in SW1c for Fish Creek chum salmon and in SW1a, SW1b, SW1c, and SW4 for Quilcene River chum salmon.

Growth models

Growth was linearly and inversely related to both chum and pink salmon abundance indices. Growth was inversely related to chum or pink salmon abundance (or both abundances) for SW1b, SW2, SW3, and SW4 for chum salmon from Fish Creek and for SW2, SW3, and SW4 for chum salmon from Quilcene River. Only one growth variable was more strongly correlated with climate than chum and pink salmon abundance. SW1c for Fish Creek chum salmon was inversely related to the magnitude of fall wind speed in the northern GOA (Table 2).

Models for Fish Creek chum salmon

SW1b was significantly and negatively correlated with the estimated abundance of juvenile pink salmon from

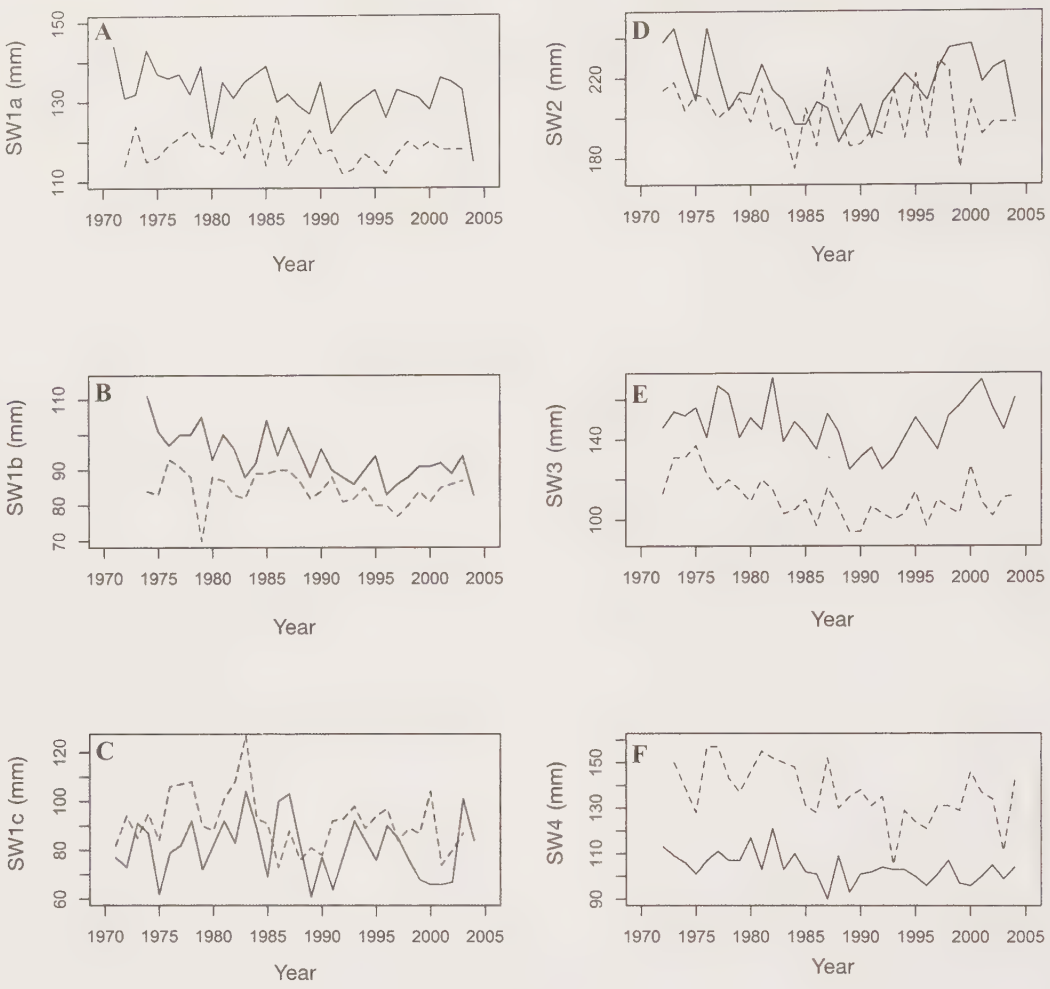

Figure 3

Average ocean growth (mm) of age-0.3 male chum salmon (*Oncorhynchus keta*) from Fish Creek (FC) Alaska and Quilcene River (QR), Washington. Time series data include (**A**) early juvenile growth SW1a (FC: 1971–2004 and QR:1972–2004), (**B**) middle juvenile growth SW1b (FC: 1974–2004; QR: 1974–2003), (**C**) late juvenile growth SW1c (FC: 1971–2004, (**D**) 1st immature year growth SW2 (FC: 1972–2004 and QR: 1972–2004), (**E**) 2nd immature year growth SW3 (FC: 1972–2004 and QR: 1972–2004), and (**F**) maturing growth SW4 (FC: 1972–2004 and QR: 1973–2004). Solid lines represent FC and dashed lines represent QR.

SE Alaska to the AP management-region harvests and was positively related to length at the start of the growing season (La) (Table 2). Seventy percent of the variation in SW1b was explained by La and pink salmon abundance (r^2=0.70; P<0.001).

SW1c was negatively correlated with the velocity of fall winds, but not correlated with pink and chum salmon abundance. Fall winds explained 39% of the variation in SW1c.

SW2 was inversely related to the combined abundances of immature age-0.1 chum salmon and maturing pink salmon on the basis of abundance data from BC to the south of the AP (Table 2). The SIC was further reduced by including lagged values of SST, PDO, and growth in the error correction model. SW2 was positively correlated with summer SST 2 years earlier and negatively correlated with the winter PDO 4 years earlier. The variables in the GLS/VAR model explained an additional 27% of the variation in SW2 in comparison with the GLS model. Performance measures indicated no change in the coefficients of variation when the error correction term was included in the SW2 model.

SW3 was negatively correlated with the abundance of immature age-0.2 chum salmon from BC to SE Alaska and maturing pink salmon from BC to SE Alaska (Table 2). Abundance explained 35% of the variation in SW3. Growth was also significantly and negatively cor-

Table 2

Insample generalized least squares (GLS) models and the integrated GLS and vector autoregression error correction models for the growth of age0.3 male chum salmon (*Oncorhynchus keta*) from Fish Creek, Alaska. Growth indices include middle juvenile growth (SW1b), late juvenile growth (SW1c), 1st immature year growth (SW2), 2nd immature year growth (SW3), and maturing growth (SW4). Length indices include early juvenile length (La) and total juvenile length (L1). $J_{SE\text{-}APt,Pink,t}$=juvenile pink salmon abundances from southeast Alaska to the Alaska Peninsula. $I_{SEAP,t}$=immature chum salmon and maturing pink salmon from southeast Alaska to the Alaska Peninsula. $I_{BC\text{-}SE,t}$=immature chum salmon and maturing pink salmon from British Columbia to southeast Alaska. $M_{AS,Chum,t}$=maturing chum salmon from Asia. WF=fall wind speed. SST=sea surface temperature. PDO=the Pacific Decadal Oscillation index. Model statistics included coefficient estimates (coeff.), *P*-values of the coefficients (*P*-value), the coefficient of determination (r^2), *P*value of the *F*statistic, coefficient of variation (CV), and Schwarz information criterion (SIC).

Variables		Model statistics					
Response	Predictors	Coeff.	*P*-value	r^2	*P*-value	CV	SIC
SW1b	La_{t-1}	0.618	<0.001	0.70	<0.001	0.039	165
	$J_{SEAP,Pink,t}$	–0.538	<0.001				
SW1c	WF_t	–0.571	<0.001	0.39	<0.001	0.111	205
SW2	$L1_{t-1}$	–0.582	<0.001	0.50	<0.001	0.049	218
	$I_{SEAP,t}$	0.741	<0.001				
SW2	$L1_{t-1}$	–0.582	<0.001	0.77	<0.001	0.031	193
	$I_{SEAP,t}$	–0.741	<0.001				
	SST_{t-2}	0.438	<0.001				
	PDO_{t-4}	–0.321	0.001				
SW3	$I_{BC\text{-}SE,t}$	–0.605	0.001	0.35	0.001	0.066	208
SW4	$M_{AS,Chum,t}$	0.602	0.0016	0.34	0.002	0.052	178
SW4	$M_{AS,t,Chum,t}$	0.556	0.0016	0.46	<0.0001	0.047	175
	SST_{t-1}	0.388					
	PDO_{t-3}	–0.302					

related with SST, but the SIC was lower than for the model with abundance.

SW4 was most strongly and inversely correlated with the abundance of maturing chum salmon from Asia (r^2=0.34; *P*=0.002). SW4 was not significantly related to other abundance or with SST and PDO during the year of growth. The SST at a 1 year lag and the PDO at a 3 year lag explained additional variation in SW4 and were both significant in the VAR model (r^2=0.46; *P*<0.001).

Quilcene River chum salmon models

Quilcene River chum salmon growth was inversely related to chum and pink salmon abundance during immature and maturing life stages, but not during the juvenile stage (Table 3). All sets of residuals passed the tests for normality, homoscedasticity, and serial correlation.

SW2 was inversely correlated with the abundance of immature age-0.1 chum salmon from Asia. Abundance explained 35% of the variability in growth in the GLS model (r^2=0.35; *P*<0.001) (Table 3).

SW3 was inversely correlated with the abundance of maturing age-0.1 pink salmon and immature age-0.2 chum salmon from BC to southern AP (r^2=0.52; *P*<0.001) (Table 3). The GLS/VAR model explained an additional 21% in growth (r^2=0.73; *P*<0.001) and reduced the SIC. Similar to the 1st immature year growth models for Fish Creek, growth was positively correlated with SST and negatively correlated with the PDO at a 2-year lag.

SW4 was negatively correlated with the abundance of maturing chum salmon from Asia (r^2=0.52; *P*<0.001) (Table 3). Maturing growth was not correlated with the climate indices in this study.

Model validation

For the reserved observations, the growth models did not perform well in the model validations (Tables 4 and 5). Positive r^2 values occurred for SW1b and SW4 Fish Creek and SW4 Quilcene River models. Negative r^2 values indicated that the mean of the growth time series performed better in model validation, when model predictions were tested against 20% of the data that were not used for model specification, than did the fitted values for the juvenile and immature models. Significant model deterioration occurred for the SW2 GLS and GLS/VAR and SW3 GLS models for Fish Creek and for the SW2 GLS and SW3 GLS/VAR models for Quilcene River as indicated by the *F*-statistic for model dete-

Table 3

Insample generalized least squares (GLS) models and the integrated GLS and vector autoregression error correction models for the growth of age0.3 male chum salmon (*Oncorhynchus keta*) from Quilcene River, Washington. Growth indices included 1st immature year, 2nd immature year (SW3), and maturing (SW4) life stages. SST=sea surface temperature. PDO=the Pacific decadal oscillation index. $I_{AS,Chum,t}$=immature Asian chum salmon. $I_{BC\text{-}SE,t}$ =immature chum and pink salmon abundance from British Columbia to southeast Alaska. $M_{AS,Chum,t}$=maturing chum salmon abundances from Asia. Model statistics included coefficient estimates (coeff.), *P*-values of the coefficients (*P*-value), the coefficient of determination (r^2), *P*-value of the *F*-statistic, coefficient of variation (CV), and Schwarz information criterion (SIC).

Variables		Model statistics					
Response	Predictors	Coeff.	*P*-value	r^2	*P*-value	CV	SIC
SW2	$I_{AS,Chum,t}$	–0.562	<0.001	0.35	<0.001	0.054	214
SW3	$I_{BC-SE,t}$	–0.797	<0.001	0.52	<0.001	0.070	196
SW3	$I_{BC-SE,t}$	–0.835	<0.001	0.73	<0.001	0.052	183
	SST_{t-2}	0.450	<0.001				
	PDO_{t-2}	–0.434	<0.001				
SW4	$M_{AS,Chum,t}$	0.718	<0.001	0.52	<0.0001	0.063	202

rioration (*F*-det.). The growth model for maturing fish did not deteriorate, but the coefficient of determination was close to zero.

According to the results of the Lehmann's correlation test (Table 6), the mean squared errors were significantly reduced for both insample regression equations when integrating the error correction equation. However, the mean squared error was not significantly reduced for any model when applied to the reserved observations.

From the SECM survey, at the station with the highest annual catch of juvenile pink salmon and chum salmon (>250 fish), we found an inverse relationship between the interannual mean length of chum salmon and catch of juvenile pink and juvenile chum salmon.

Discussion

Our study advances the understanding of potential factors influencing marine growth of chum salmon in the North Pacific Ocean. With this study, we have contributed two more chum salmon populations, 1 from the southeast Alaska and 1 from Washington state, to an

Table 4

Validation statistics based on the application of the growth models for age-0.3 male chum salmon (*Oncorhynchus keta*) from Fish Creek, Alaska to the reserved observations. GLS=the generalized least squares regression model. Growth indices included middle juvenile (SW1b), late juvenile (SW1c), 1st immature year, 2nd immature year (SW3), and maturing (SW4) life stages. GLS/VAR was the GLS and vector autoregression-integrated model. Statistics include sample size (*n*), coefficient of variation (CV), coefficient of determination (r^2), *F*-statistic, *P*-value of the *F*-statistic, *F*-statistic of model deterioration (*F*-det.), *P*-value of *F*-det. (*P*-det.), and the Schwarz's information criterion (SIC). Negative r^2 values and associated *F* and *P* values were not shown for the SW1c, SW2, SW3 and SW4 GLS models.

	SW1b	SW1c	SW2	SW2	SW3	SW4	SW4
	GLS	GLS	GLS	GLS/VAR	GLS	GLS	GLS/VAR
n	6	7	7	7	7	7	7
CV	0.05	0.14	0.07	0.07	0.12	0.05	0.04
r^2	0.25						0.27
F	1.01						1.32
P	0.44						0.36
F-det.	1.47	1.41	2.38	6.10	3.64	0.77	0.69
P-det.	0.23	0.25	0.05	<0.0001	0.008	0.61	0.68
SIC	34	51	56	63	58	39	41

Table 5

Validation statistics based on the application of the growth models for age-0.3 male chum salmon (*Oncorhynchus keta*) from Quilcene River, Washington to the reserved observations. GLS was the generalized least squares regression model. Growth indices included 1st immature year (SW2), 2nd immature year (SW3), and maturing (SW4) life stages. GLS/VAR was the GLS and vector autoregression-integrated model. Statistics include sample size (n), coefficient of variation (CV), coefficient of determination (r^2), F-statistic, P-value of the F-statistic, F-statistic of model deterioration (Fdet.), P-value of Fdet. (P-det.), and the Schwarz's information criterion (SIC). Negative r^2 values and associated F and P values were not shown for the SW2, SW3 and SW4 models.

	SW2	SW3	SW3	SW4
	GLS	GLS	GLS/VAR	GLS
n	7	7	7	6
CV	0.09	0.07	0.11	0.09
r^2				0.06
F				0.18
P				0.98
F-det.	2.52	1.14	4.13	1.79
P-det.	0.04	0.37	0.001	0.14
SIC	57	47	56	44

Table 6

Lehmann's correlation coefficients to test the difference among the mean square errors of the growth models for age-0.3 male chum salmon (*Oncorhynchus keta*) from Fish Creek and the Quilcene River. Growth indices included 1st immature year growth (SW2) and 2nd immature year growth (SW3). GLS=the generalized least squares regression model. GLS/VAR=the GLS and vector autoregression-integrated model. Models were not statistically significant at a 5% level of significance.

		Stock and life stage	
		Fish Creek SW2	Quilcene River SW3
Sample method		GLS	GLS
Insample	GLS/VAR	0.44	0.41
Outsample	GLS/VAR	–0.08	–0.50

increasing body of growth studies on chum salmon populations from southcentral Alaska (Helle, 1979), western Alaska (Agler et al., 2013), Russia (Zavolokin et al., 2009), Japan (Kaeriyama et al., 2007), and Korea (Seo et al., 2006). Contrary to growth in the Asian populations, juvenile and maturing growth did not increase in the mid-1990s, indicating that productivity on the North American continental shelf remained relatively lower than that in the western Pacific Ocean. In addition, we back-calculated indices of chum and pink salmon abundance using harvest data, age composition, and mortality schedules; therefore, this index was more likely to accurately represent the actual abundance of chum salmon than estimates based on harvest alone. We found that size of the adult chum salmon was primarily related to growth in oceanic waters during the immature life stage on the basis of data from the early 1970s to the mid-2000s and that immature growth was related to population abundance and to climate in prior years. Further research needs to focus on identifying and better understanding factors influencing immature growth in order to allow for more accurate predictions of size-at-maturity for returning chum salmon in a given year.

Trends in size and growth

Size at maturity was essential for determining fecundity, breeding success, and survival of progeny in salmon (Helle, 1979, 1989; Schroder, 1982). Therefore, it was important to understand factors influencing growth. Largebodied female salmon can dig deeper redds (van de Berghe and Gross, 1984), produce more eggs (Helle, 1989), produce larger eggs and fry (Koski, 1975), and have progeny with higher survival probability (Helle, 1979; 1989). Larger males are more aggressive and are more successful in competing for a mate than smaller males (Schroder, 1982). In the ocean, larger salmon consume more prey, more energy-rich prey, and more diverse prey than smaller salmon (Davis et al., 2009) and therefore have a competitive advantage for larger fish. Because a growth advantage once gained has a high likelihood of being maintained throughout the life of a fish, these factors highlight the significance of understanding the impacts of climate and population abundance on the marine growth and ultimately on the size at maturity of salmon.

In this study, the temporal trends in the body size at maturity of chum salmon from the two stocks from the early 1970s to early 1990s were similar to decreases in early juvenile, middle juvenile, immature, and maturing growth for Fish Creek chum salmon and to decreases in the immature and maturing growth for Quilcene River chum salmon. Our results are comparable to observed declines in body size of Hokkaido chum salmon in the mid-1980s that were linked to reduced growth during the 2nd immature and maturing stages for years 1970–1994 (Kaeriyama, 1998). Similarly, the reduction in the adult (mature) body size of chum salmon from the Anadyr River in Russia during the mid-1980s was linked to reduced growth in the immature and maturing stages (Zavolokin et al., 2009). Although the general trends in size at maturity from the 1970s to the 1990s were similar for different populations around the Pacific Ocean, the changes in adult size were linked to different developmental stages, namely the imma-

ture and maturing life stages in the western Pacific and the juvenile, immature, and maturing life stages in the eastern Pacific. From the mid-1990s to the mid-2000s, increases in body size of adult chum salmon in our study were related to increases in growth during the immature life stage in offshore waters.

Juvenile and maturing growth of chum salmon from the two populations in our study did not recover from the size reductions of chum salmon from the early 1970s to the early 1990s. Conversely, juvenile chum salmon released from Japan into the Sea of Okhotsk had lower growth from the late 1960s to the mid-1980s and higher growth from the mid-1980s to the mid-1990s, possibly because of reduced ice cover and warmer sea temperatures during summer and fall (Kaeriyama et al., 2007). Farther north in Russia, juvenile growth of chum salmon departing the Anadyr River was relatively stable from the early 1960s to the late 2000s, but slightly higher in the late 1990s (Zavolokin et al., 2009). The difference in the patterns in juvenile growth of chum salmon between the eastern and western Pacific Ocean populations indicates that conditions in the 1990s were more favorable for juvenile chum salmon in the western North Pacific than in the eastern North Pacific Ocean. Declines in zooplankton biomasses were documented in both regions of the North Pacific Ocean from the mid-1970s to the early 1990s but remained 50% to 300% higher in the western North Pacific (Sugimoto and Tadokoro, 1997). Lower ocean productivity in the eastern Pacific may have accounted for the lower juvenile growth of the two chum salmon populations in our study during the 1980s and 1990s. We could not include indices of zooplankton biomass in our models because sufficient data were not available.

In our study, increases in size at maturity in the 1990s were linked to increases in immature growth. However, in the validations with reserved data, our models did not capture the entire increase in the 1st and 2nd immature years of growth for Fish Creek and Quilcene River chum salmon. Alternative conditions may exist that can explain the increase in immature growth in the mid-1990s. For example, the annual growth during age-0.1, 0.2, and 0.3 immature stages measured on the scales of adult chum salmon from Korea was positively correlated with zooplankton biomass in the Bering Sea (Seo et al., 2006), thus establishing a potential pathway for climate-induced changes in growth. Helle and Fukuwaka (2009) found a strong positive correlation between body size of maturing chum salmon from the eastern North Pacific and Japan and the spring and summer sea temperatures in the southeastern Bering Sea for the period 1977–1994, but weak and often negative correlations during the 1960–1976 and 1995–2006 periods. Decadal-scale changes in growth of N. American chum salmon may be related to shifts in their ocean distribution, e.g., northwestward shifts into the Bering Sea during summer in warm periods vs. remaining in the GOA during cool periods. Additional factors, such as zooplankton biomass and prey diversity, need to be investigated to determine the cause of increases in body size in the mid-1990s.

Growth and abundance

Evidence of density-dependent growth was detected in the juvenile chum salmon from Fish Creek, but not in those from Quilcene River. One explanation for this discrepancy in growth patterns may be the much higher abundance of pink and chum salmon in SE in comparison with WA and OR during our study period. In fact since 1995, the harvest of pink and chum salmon has been 5 to 12 times higher in the GOA region than in WA, OR, and BC combined (Eggers et al.[1]). Annually, Alaska hatcheries release approximately 1.5 billion juvenile salmon into the Pacific Ocean (Alaska Department of Fish and Game, available at website, data obtained in September 2012) and the primary species released are pink and chum salmon. Pink salmon are primarily released from Prince William Sound hatcheries, whereas chum salmon are the primary species released from hatcheries in SE. In the waters along the Japan Sea coast of Honshu, Japan, where hatcheries release 100–300 million juvenile chum salmon annually, the relative weight of juvenile chum salmon stomach contents decreased as their density increased—a finding that was postulated to be the result of juvenile chum salmon depleting prey abundances (Fukuwaka and Suzuki, 2000). Similarly, early marine growth of Atlantic salmon (*Salmo salar*) from the Miramichi River in eastern Canada was inversely related to subsequent recruitment (Friedland et al., 2009). We found an inverse relationship between the mean body length of juvenile chum salmon and the surface trawl catch of juvenile pink and chum salmon from continental shelf waters off Icy Point in the GOA from 1997 to 2011 indicating density-dependent effects on growth. However, these surface-trawl-caught juvenile salmon were the length of the chum salmon in our study during the early juvenile stage and may not represent processes affecting growth later in life while chum salmon in the GOA.

Pink salmon abundance consistently influenced the immature growth of both populations of chum salmon, except in the 1st immature year of Quilcene River chum salmon. This finding was consistent with that of previous studies of the influence of pink salmon on the growth of chum salmon (Ivankov and Andreyev, 1971; Salo, 1991; Bugaev et al., 2001; Kaeriyama et al., 2007; Agler et al., 2013). This observation was not surprising because pink salmon are the most abundant North American species of Pacific salmon (Eggers et al.[1]). However, chum salmon mature at multiple ages within a brood and are likely more abundant as immature individuals than the maturing pink salmon. Other studies have documented the effects of pink salmon abundance on the feeding of chum salmon. In oddyears of higher pink salmon abundances in the ocean, chum salmon were observed to consume less prey (Ivankov and Andreyev, 1971; Salo, 1991), shift their diet to less

nutritious prey (Salo, 1991), and switch from eating crustacean zooplankton to eating gelatinous zooplankton (Tadokoro et al., 1996). From these studies it appears that the influence of pink salmon abundance may be greater than that of chum salmon because of their high population levels, fast growth rates, high degree of diet overlap with other salmon species, as well as their preference for lower trophic level prey, and their early migration to sea (Ruggerone and Nielsen, 2004).

Differences in the influence of pink salmon population abundances on growth of the 1st immature stage of chum salmon from the 2 populations investigated may be the result of differences in the migration and distribution of age0.1 chum salmon. The SW2 of Fish Creek chum salmon was inversely related to the abundance of maturing pink salmon and age-0.1 chum salmon from SE to AP, whereas Quilcene River chum salmon were more significantly correlated with the abundance of immature age-0.1 chum salmon from Asia. Chum salmon from WA and SE reside primarily in the eastern North Pacific and GOA (Urawa et al., 2009). However, 70% of the age-0.1 chum salmon along the 145°W longitude from 48°N to 53°N during February were of SE origin and less than 1% were of WA origin (Beacham et al., 2009). Pink salmon are more abundant farther north in Prince William Sound than in SE or WA. That is, the southern-origin chum salmon were not likely distributed as far west or north as their northern conspecifics at age-0.1.

For both stocks, growth during the 2nd immature stage was inversely related to chum and pink salmon abundance from British Columbia to Southeast Alaska, and growth during the maturing life stage was inversely related to maturing chum salmon from Asia. These results indicate possible co-occurrence of these 2 North American chum salmon populations in the ocean during their 2nd immature life stage. To address similarities and differences in the migration routes of summer and fall chum salmon, a comparison of marine growth could be made between summer and fall chum salmon from the same river or area.

Several direct and indirect mechanisms exist that cause salmon to compete for resources in the ocean, particularly because the different species of Pacific salmon have a high degree of overlap in prey and habitat (Myers et al., 2007). Physical and biological conditions in the marine environment have direct and indirect influences on density-dependent growth through their influences on feeding and metabolic rates (Davis et al.[4]). In salmon, behavioral responses to competition or interference include reduced feeding, prey switching, and migration (Azumaya and Ishida, 2000; Davis et al., 2009). In addition to direct interaction, there may also be indirect density-dependent interactions among pink and chum salmon that could affect growth of chum salmon. For example, while although the density of pink salmon was higher in odd-numbered years in the Bering Sea, the growth of chum salmon was also higher (Azumaya and Ishida, 2000). This may be explained by the observation that in odd years, chum salmon are more likely to move from the Bering Sea to the eastern North Pacific Ocean (Azumaya and Ishida, 2000)—a behavior that we interpret as a response to avoid interaction with Asian-origin pink salmon. In the eastern North Pacific Ocean, chum salmon were more abundant and consumed lower quality prey (gelatinous zooplankton) in odd-numbered years, whereas in even-numbered years chum salmon abundance was lower and they consumed higher quality prey (squid and fish; Tadokoro et al., 1996), indicating an indirect effect of pink salmon abundance in the Bering Sea on the intra-specific competition of chum salmon in the eastern North Pacific Ocean. The ability of chum salmon to display plasticity in migration and feeding patterns may also be an adaptive response to more effectively reduce the impact of density on growth.

Growth and climate

Contrary to our hypotheses, a shallower mixed layer depth in the previous winter at the inner continental shelf of the northern GOA was not associated with an increase in growth. An early and stronger stratification of depth in the spring favors primary production in the middle shelf of the GOA (Henson, 2007). Therefore, water column stability during spring rather than deeper mixing during winter may influence prey densities in the surface layers where juvenile chum salmon feed and may favor their growth.

As anticipated, a fall phytoplankton bloom, which was generally followed by a peak in secondary productivity, as indexed by lower wind speed in September and October, was associated with an increase in the late juvenile growth of Fish Creek chum salmon. However, the index was not correlated with the late juvenile growth of Quilcene River chum salmon. In the GOA, a bloom of phytoplankton can occur during September and October but does not occur every year (Cooney, 2005). The fall bloom is initiated when fall winds deepen the mixed layer and resupply nutrients to the photic zone. Once nutrients are added to surface waters, a stratification of the water column is required before a fall bloom can occur (Cooney, 2005). Thus, a fall bloom is only possible in those years when wind speeds in September and October are not excessive.

Cooler late summer and fall SSTs were associated with an increase in growth during the 2nd immature stage for the Fish Creek chum salmon, but growth was more strongly correlated with population abundance. Immature growth of western Alaska chum salmon was negatively correlated with GOA SSTs from 1965 to 2006 (Agler et al., 2013). This pattern might be explained by the fact that salmon in the eastern North Pacific Ocean and eastern Bering Sea are consuming higher quality prey in cool years (Aydin et al., 2000; Coyle et al., 2011). Specifically, in the eastern Bering Sea, chum salmon consumed primarily euphausiids in cold years and walleye pollock (*Gadus chalcogrammus*) in warm years (Coyle et al., 2011). Similarly, during the cold years 1996 and 1998 chum salmon were larger,

and their diets consisted of proportionately more gonatid squid (*Berryteuthis anonychus*) (Aydin et al., 2000). In addition, it has also been suggested that differences in diet and growth of chum salmon may have been the result interannual variations in the summer latitudinal sea surface temperature minimum (warmer north and cooler south of the boundary) in the North Pacific Ocean. Salmon in the high seas adapt to climate-induced changes in their prey resources by switching their diets either within or between trophic levels (Kaeriyama et al. 2004).

After accounting for density-dependent effects, growth was positively related to SST. Different possible mechanisms exist for immature growth to increase with warmer summer SSTs and negative PDO events (cooler than average winters) in earlier years. For example, different physical phenomena (e.g., eddies, wind patterns, El Niño events) may transport nutrients into oceanic water of the North Pacific Ocean. Predominant among such phenomena are eddies, which form in waters above the continental shelf and slope in the eastern North Pacific Ocean (Ladd et al., 2005). In the cores of these eddies, iron and nitrate are transported from the sea floor to surface waters (Johnson et al., 2005) and these transported nutrients result in phytoplankton blooms inside the eddies as they move into oceanic waters at a rate of a few months to 5 years (Ladd, 2007). Zooplankton species are similarly transported from the shelf into the GOA (Mackas and Galbraith, 2002a). These eddies form more frequently in warmer years and during El Niño events (Crawford and Whitney, 1999). In a winter with a negative PDO, there is a northerly wind pattern in the eastern North Pacific (Mantua et al., 1997) and these winds may push these eddies off the shelf and into oceanic waters. Brodeur and Ware (1992) documented positive correlations between the intensity of the winter winds and subsequent summer zooplankton biomass in the subarctic gyre within the 1956-1962 and 1988-1989 year periods. In addition to the effect of eddies and wind on the productivity of oceanic waters, El Niño events can lead to a transport of heat and zooplankton from the equator that can reach the subarctic waters of the North Pacific Ocean in 1 year and remain for 2 years (Mackas and Galbraith, 2002b). These events of increased ocean productivity may initiate and perpetuate a strong year class of a given prey taxon with a two-year life span. Finally, climate may also have a lag effect on growth through the lag effects of climate on mortality, bioenergetics, predation, competition, prey switching, distribution, and recruitment that influence growth, abundance, or the relationship of growth and abundance. Uncertainties in regard to the true mechanisms driving the annual variation in the growth of chum salmon support the use of a model with an error correction time series (Noakes et al. 1987).

No climate-related changes in growth were detected during the maturing life stage for the Quilcene stock. Our index of growth in length may not capture the total effects of climate or population abundance on growth. The lack of a significant relationship between maturing growth and climate indices in this study may be explained by the fact that during this stage, salmon growth favors an increase in body weight rather than length (Aydin et al., 2000), making it less possible for our length-based models to capture changes in growth. Alternatively, at larger body sizes, chum salmon switch from feeding on zooplankton to feeding on fish and gelatinous zooplankton not used by the other salmon species (Davis et al., 2009). This feeding plasticity may reduce the effects of intra- and interspecific competition for the larger, maturing chum salmon.

Caveats

Our model with the error correction that incorporated the lag structures of the model residuals and climate did not adequately predict the values of the reserved observations for SW2 of the Fish Creek chum salmon and SW3 of the Quilcene River chum salmon. The error correction component may have been incorrectly specified, the growth and abundance relationships may have undergone temporal change, or the time series may have been too variable or too short to provide reliable coefficient estimates. The error correction did not account for the total increase in growth in the late 1990s and early 2000s. Helle et al. (2007) suggested that the increase in body size of chum salmon in the mid-1990s during a period of high population abundance was due to an increase in the carrying capacity for salmon in the North Pacific Ocean. This question merits further investigation.

Although uncertainty exists regarding whether back-calculated abundance indices that are based on the numbers of returning salmon, marine mortality, and age composition are good indices for abundance earlier in life, the assumption that back-calculated salmon abundance was a metric of salmon abundance earlier in life was supported by a strong correlation between the abundances of juvenile pink salmon and the returns of adult pink salmon in the following year (Orsi et al.[3]). However, correlation does not imply causation. Nonetheless, it would have been preferable to base our analysis on a time series of actual abundance of juvenile and immature salmon at sea. This was not possible, because very few such time series exist and those that do exist were too short to be used for this study. Alternatively, at-sea estimates of abundance would likely be subject to large sampling uncertainty; hence the indices based on harvest and assumed mortality rates may actually be better.

Implications for management

During the first year at sea, size was considered a critical factor affecting marine mortality rates of salmon (Parker, 1971; Holtby et al., 1990). Size attained by the first winter at sea was also considered important in determining year-class strength (Beamish and Mahnken, 2001). We found that an increase in the abundance of ju-

venile pink salmon from SE has the potential to reduce growth of Fish Creek chum salmon. Therefore, fishery and hatchery managers may wish to consider adjusting the number of pink salmon fry released from hatcheries into coastal waters in order to increase early growth and subsequent survival of juvenile chum salmon.

Climate during the first year at sea was strongly correlated with survival in salmon (Mueter et al., 2002; Martinson et al., 2009). We found that the late juvenile growth of chum salmon from Fish Creek increased as the velocity of surface winds decreased in the fall—an indicator of the occurrence of fall phytoplankton blooms. Therefore, the wind velocity index in the northern GOA may be a useful predictor for the marine survival of chum salmon from the GOA.

This research provides insight into factors that affect growth and size-at-maturity of chum salmon for different life stages of 2 geographically separated stocks in the eastern North Pacific Ocean. We found evidence for density-dependent growth during the juvenile, immature, and maturing life stages, indicating that density-dependent influences on growth at sea influence final size at maturity of chum salmon. Results of our correlation study were viewed with caution but as possible mechanisms for changes in growth and final size-at-maturity of chum salmon.

Acknowledgments

Funding and support for this project was received from the Alaska Fisheries Science Center in Juneau, Alaska and the Advanced Studies Program, Professional Development program of the National Oceanic and Atmospheric Administration. We greatly appreciate the assistance of all the people that helped with field collection throughout the years and the assistance of the Alaska Department of Fish and Game in Ketchikan and the U.S. Fish and Wildlife Service at the Quilcene National Fish Hatchery in Quilcene, Washington. We appreciate the constructive comments from Phil Mundy, Ed Farley, and Lisa Eisner. We also thank the anonymous reviewers for their thoughtful suggestions that greatly improved the manuscript.

Literature cited

Agler, B. A., G. T. Ruggerone, L. I. Wilson, and F. J. Mueter.
2013. Historical growth of Bristol Bay and Yukon River, Alaska chum salmon (*Oncorhynchus keta*) in relation to climate and inter- and intra-specific competition. Deep-Sea Res., II 94:165–177.

Arnold, E. L., Jr.
1951. An impression method for preparing fish scales for age and growth analysis. Prog. Fish-Cult. 13:11–16.

Auburn, M. E., and S. E. Ignell.
2000. Food habits of juvenile salmon in the Gulf of Alaska July–August 1996. N. Pac. Anadr. Fish Comm. Bull. 2:89–97.

Aydin, K., Myers, K., and R. Walker.
2000. Variation in summer distribution of the prey of Pacific salmon *Oncorhynchus* spp. in the offshore Gulf of Alaska in relation to oceanographic conditions, 1994–98. N. Pac. Anadr. Fish Comm. Bull. 2:43–54.

Azumaya, T., and Y. Ishida.
2000. Density interactions between pink salmon (*Oncorhynchus gorbuscha*) and chum salmon (*O. keta*) and their possible effects on distribution and growth in the North Pacific Ocean and Bering Sea. N. Pac. Anadr. Fish Comm. Bull. 2:165–174.

Beacham, T. D., J. R. Candy, S. Sato, S. Urawa, K. D. Le, and M. Wetklo.
2009. Stock origins of chum salmon (*Oncorhynchus keta*) in the Gulf of Alaska during winter as estimated with microsatellites. N. Pac. Anadr. Fish Comm. Bull. 5:15–23.

Beamish, R. J., and C. Mahnken.
2001. A critical size and period hypothesis to explain natural regulation of salmon abundance and the linkage to climate and climate change. Prog. Oceanogr. 49:423–437.

Beamish, R. J., and D. R. Bouillon.
1993. Pacific salmon production trends in relation to climate. Can. J. Fish. Aquat. Sci. 50:1002–1016.

Bigler, B. S., D. W. Welch, and J. H. Helle.
1996. A review of size trends among North Pacific salmon (*Oncorhynchus* spp.). Can. J. Fish. Aquat. Sci. 53:455–465.

Brodeur, R. D., and D. M. Ware.
1992. Long-term variability in zooplankton biomass in the subarctic Pacific Ocean. Fish. Oceanogr. 1:32–39.

Bugaev, V. F., D. W. Welch, M. M. Selifonov, L. E. Grachev, and J. P. Eveson.
2001. Influence of the marine abundance of pink salmon (*Oncorhynchus gorbuscha*) and sockeye salmon (*O. nerka*) on growth of Ozernaya River sockeye. Fish. Oceanogr. 10:26–32.

Cooney, R. T.
2005. Biological and chemical oceanography. *In* The Gulf of Alaska: biology and oceanography (P. R. Mundy, ed.), p. 49–58. Alaska Sea Grant College Program, Univ. Alaska, Fairbanks, AK.

Coyle, K. O., L. B. Eisner, F. J. Mueter, A. I. Pinchuk, M. A. Janout, K. D. Cieciel, E. V. Farley, and A. G. Andrews.
2011. Climate change in the southeastern Bering Sea: impacts on pollock stocks and implications for the oscillating control hypothesis. Fish. Oceanogr. 20:139–156.

Crawford, W. R., and F. A. Whitney.
1999. Mesoscale eddy swirl with data in the Gulf of Alaska. EOS Trans. Am. Geophys. Union 80:365–370.

Dahl, K.
1909. The assessment of age and growth in fish: a short account of the development of present methods and main litterature on the subject. Int. Rev. Gesamten Hydrobiol. Hydrogr. 2:758–769.

Davis, N. D., A. V. Volkov, A. Y. Efimkin, N. A. Kuznetsova, J. L. Armstrong, and O. Sakai.
2009. Review of BASIS salmon food habits studies. N. Pac. Anadr. Fish Comm. Bull. 5:197–208.

Eggers, D. M.
2009. Historical biomass of pink, chum, and sockeye salmon in the North Pacific Ocean. Am. Fish. Soc. Symp. 70:267–306.

Francis, R. C, and S. R. Hare.
1994. Decadal-scale regime shifts in the large marine ecosystems of the North-east Pacific: a case for historical science. Fish. Oceanogr. 3:279–291.
Freeland, H., K. Denman, C. S. Wong, F. Whitney, and R. Jacques.
1997. Evidence of change in the winter mixed layer in the northeast Pacific Ocean. Deep-Sea Res. Oceanogr. 4:2117–2129.
Friedland, K. D., D. Moore, and F. Hogan.
2009. Retrospective growth analysis of Atlantic salmon (*Salmo salar*) from the Miramichi River, Canada. Can. J. Fish. Aquat. Sci. 66:1294–1308.
Fukuwaka, M., and M. Kaeriyama.
1997. Scale analyses to estimate somatic growth in sockeye salmon *Oncorhynchus nerka*. Can. J. Fish. Aquat. Sci. 54:631–636.
Fukuwaka, M., and T. Suzuki.
2000. Density-dependence of chum salmon in coastal water of the Japan Sea. N. Pac. Anadr. Fish Comm. Bull. 2:75–81.
Hare, S. R., and R. C. Francis.
1995. Climate change and salmon production in the northeast Pacific Ocean. Can. Spec. Publ. Fish. Aquat. Sci. 121:357–372.
Hare, S. R., and N. J. Mantua.
2000. Empirical evidence for North Pacific regime shifts in 1977 and 1989. Prog. Oceanogr. 47:103–145.
Hartt, A. C., and M. B. Dell.
1986. Early oceanic migration and growth of juvenile Pacific salmon and steelhead trout. Int. N. Pac. Fish. Comm. Bull. 46, 105 p.
Heinl, S. C.
2005. Chum salmon stock status and escapement goals in southeast Alaska. *In* Stock status and escapement goals for salmon stocks in southeast Alaska 2005. Alaska Dep. Fish Game, Spec. Publ. 05-22 (J. A. Der Hovanisian and H. J. Geiger, eds.), p. 191–209. Alaska Dep. Fish Game, Anchorage, AK.
Helle, J. H.
1979. Influence on marine environment on age and size at maturity, growth, and abundance of chum salmon, *Oncorhynchus keta* (Walbaum), from Olsen Creek, Prince William Sound, Alaska. Ph.D. thesis, 118 p. Oregon State Univ., Corvallis, OR.
1989. Relation between size-at-maturity and survival of progeny in chum salmon, *Oncorhynchus keta* (Walbaum). J. Fish Biol. 35(suppl. A):99–107.
Helle, J. H., and M. Fukuwaka.
2009. Body size of maturing salmon in relation to sea surface temperatures in the eastern Bering Sea. N. Pac. Anadr. Fish Comm. Bull. 5:303–319.
Helle, J. H., and M. S. Hoffman.
1998. Changes in size and age at maturity of two North American stocks of chum salmon (*Oncorhynchus keta*) before and after a major regime shift in the North Pacific Ocean N. Pac. Anadr. Fish Comm. Bull. 1:81–89.
Helle, J. H., E. C. Martinson, D. M. Eggers, and O. Gritsenko.
2007. Influence of salmon abundance and ocean conditions on body size of Pacific salmon. N. Pac. Anadr. Fish Comm. Bull. 4:289–298.
Henson, S. A.
2007. Water column stability and spring bloom dynamics in the Gulf of Alaska. J. Mar. Res. 65:715–736.
Hilborn, R., and D. Eggers.
2000. A review of the hatchery programs for pink salmon in Prince William Sound and Kodiak Island, Alaska. Trans. Am. Fish. Soc. 129:333–350.
Holtby, L., B. Andersen, and R. Kadowaki.
1990. Importance of smolt size and early ocean growth to interannual variability in marine survival of coho salmon *Oncorhynchus kisutch*. Can. J. Fish. Aquat. Sci. 47:2181–2194.
Ivankov, V. N., and V. L. Andreyev.
1971. The South Kuril chum (*Oncorhynchus keta* (Walb.)): ecology, population structure and the modeling of the population. J. Ichthyol. 11:511–524.
Johnson, W. K., L. A. Miller, N. E. Sutherland, and C. S. Wong.
2005. Iron transport by mesoscale Haida eddies in the Gulf of Alaska. Deep-Sea Res. Part II, 52:933–953.
Kaeriyama, M.
1998. Dynamics of chum salmon, *Oncorhynchus keta*, populations released from Hokkaido, Japan. N. Pac. Anadr. Fish Comm. Bull. 1:90–102.
Kaeriyama, M., M. Nakamura, R. Edpalina, J. R. Brower, H. Yamaguchi, R. V. Walker, and K. W. Myers.
2004. Changes in feeding ecology and trophic dynamics of Pacific salmon (*Oncorhynchus* spp.) in the central Gulf of Alaska in relation to climate events. Fish. Oceanogr. 13:197–207.
Kaeriyama, M., A. Yatsu, M. Noto, and S. Saitoh.
2007. Spatial and temporal changes in the growth patterns and survival of Hokkaido chum salmon populations in 1970–2001. N. Pac. Anadr. Fish Comm. Bull. 4:251–256.
Kalnay, E., M. Kanamitsu, R. Kistler, W. Collins, D. Deaven, L. Gandin, M. Iredell, S. Saha, G. White, J. Woollen, Y. Zhu, M. Chelliah, W. Ebisuzaki, W. Higgins, J. Janowiak, K. C. Mo, C. Ropelewski, J. Wang, A. Leetmaa, R. Reynolds, M. Chelliah, W. Ebisuzak, W. Higgans, J. Janowiak, K. C. Mo, C. Ropelewski, J. Wang, R. Jenne, and D. Joseph.
1996. The NCEP/NCAR 40-year reanalysis project. Bull. Am. Meteorol. Soc. 77:437–471.
Kobayashi, T.
1961. Biology of chum salmon, *Oncorhynchus keta* (Walbaum), by the growth formula of scale. Sci. Rep. Hokkaido Fish Hatch. 16:1–102. [In Japanese, English summary.]
Koski, K V.
1975. The survival and fitness of two stocks of chum salmon (*Oncorhynchus keta*) from egg deposition to emergence in a controlled-stream environment at Big Beef Creek. Ph.D. thesis, 213 p. Univ. Washington, Seattle, WA.
Ladd, C.
2007. Interannual variability of the Gulf of Alaska eddy field. Geophys. Res. Lett. 34, L11605.
Ladd, C., N. B. Kachel, C. W. Mordy, and P. J. Stabeno.
2005. Observations from a Yakutat eddy in the northern Gulf of Alaska. J. Geophys. Res. 110, C03003.
Lee, R. M.
1920. A review of the methods of age and growth determination in fishes by means of scales. Fish. Invest., II 4:1–32.
Lehmann, E. L.
1959. Testing statistical hypotheses, 369 p. John Wiley and Sons, New York.
Logerwell, E. A., N. Mantua, P. W. Lawson, R. C. Francis, and V. N. Agostini.
2003. Tracking environmental processes in the coastal

zone for understanding and predicting Oregon coho (*Oncorhynchus kisutch*) marine survival. Fish. Oceanogr. 12:554–568.

Mackas, D. L., and M. D. Galbraith.
2002a. Zooplankton distribution and dynamics in a North Pacific eddy of coastal origin: I. Transport and loss of continental margin species. J. Oceanogr. 58:725–738.
2002b. Zooplankton community composition along the inner portion of Line P during the 1997–1998 El Niño event. Prog. Oceanogr. 54:423–437.

Mantua, N. J., S. R. Hare, Y. Zhang, J. M. Wallace, and R. C. Francis.
1997. A Pacific interdecadal climate oscillation with impacts on salmon production. Bull. Am. Meteorol. Soc. 78:1069–1079.

Martinson, E. C., J. H. Helle, D. L. Scarnecchia, and H. H. Stokes.
2008. Density-dependent growth of Alaska sockeye salmon in relation toclimate–oceanic regimes, population abundances, and body size, 1925 to 1998. Mar. Ecol. Prog. Ser. 370:1–18.
2009. Growth and survival of sockeye salmon (*Oncorhynchus nerka*) from Karluk Lake and River, Alaska, in relation to climatic and oceanic regimes and indices, 1922–2000. Fish. Bull. 107:488–500.

Morita, K., S. H. Morita, and M. Fukuwaka.
2006. Population dynamics of Japanese pink salmon (*Oncorhynchus gorbuscha*): are recent increases explained by hatchery programs or climate variation? Can. J. Fish. Aquat. Sci. 63:55–62.

Mueter, F. J., R. M. Peterman, and B. J. Pyper.
2002. Opposite effects of ocean temperature on survival rates of 120 stocks of Pacific salmon (*Oncorhynchus* spp.) in northern and southern areas. Can. J. Fish. Aquat. Sci. 59:456–463.

Myers, K. W., N. V. Klovach, O. F. Gritsenko, S. Urawa, and T. C. Royer.
2007. Stock-specific distributions of Asian and North American salmon in the open ocean, interannual changes, and oceanographic conditions. N. Pac. Anadr. Fish Comm. Bull. 4:159–177.

Noakes, D., D. W. Welch, and M. Stocker.
1987. A time series approach to stock recruitment analysis: transfer function noise modeling. Nat. Resour. Model. 2:213–233.

Parker, R. R.
1968. Marine mortality schedules of pink salmon of the Bella Coola River, central British Columbia. J. Fish. Res. Board Can. 25:757–794.
1971. Size selective predation among juvenile salmonid fishes in British Columbia inlet. J. Fish. Res. Board Can. 28:1503–1510.

Reed, R. K., and J. D. Schumacher.
1986. Physical oceanography. *In* The Gulf of Alaska: physical environment and biological resource (D. W. Hood and S. T. Zimmerman, eds.), p. 57–75. Alaska Office, Ocean Assessment Division, NOAA, Anchorage, AK.

Ruggerone, G. T., R. M. Peterman, B. Dorner, and K. W. Myers.
2010. Magnitude and trends in abundance of hatchery and wild pink salmon, chum salmon, and sockeye salmon in the North Pacific Ocean. Mar. Coast. Fish. 2:306–328.

Ruggerone, G. T., and J. L. Nielsen.
2004. Evidence for competitive dominance of pink salmon (*Oncorhynchus gorbuscha*) over other salmonids in the North Pacific Ocean. Rev. Fish Biol. Fish. 14:371–390.

Salo, E. O.
1991. Life history of chum salmon (*Oncorhynchus keta*). *In* Pacific salmon life histories. (C. Groot and L. Margolis, eds.), p. 231–309. UBC Press, Vancouver, Canada.

Sarkar, N.
2007. Mixed layer dynamics along the Seward line in the northern Gulf of Alaska. Ph.D. thesis, 71 p. Old Dominion Univ., Norfolk, VA.

Schroder, S. L.
1982. The influence of intrasexual competition on the distribution of chum salmon in an experimental stream. *In* Proceedings of the salmon and trout migratory behavior symposium; 3–5 June 1981 (E. L. Brannon and E. O. Salo, eds.), p. 275–285. School Fish., Univ. Washington, Seattle, WA.

Seeb, L. W., P. A. Crane, C. M. Kondzela, R. L. Wilmot, S. Urawa, N. V. Varnavskaya, and J. E. Seeb.
2004. Migration of Pacific Rim chum salmon on the high seas: insights from genetic data. Environ. Biol. Fish. 69:21–36.

Seo, H., S. Kim, K. Seong, and S. Kang.
2006. Variability in scale growth rates of chum salmon (*Oncorhynchus keta*) in relation to climate changes in the late 1980s. Prog. Oceanogr. 68:205–216.

Spies, R. B., and T. Weingartner.
2007. Long-term change. *In* Long-term ecological change in the northern Gulf of Alaska (R. B. Spies, ed.), p. 259–418. Elsevier, Oxford, UK.

Sugimoto, S., and K. Tadokoro.
1997. Interannual-interdecadal variations in zooplankton biomass, chlorophyll concentration and physical environment in the subarctic Pacific and Bering Sea. Fish. Oceanogr. 6:74–93.

Tadokoro, K., Y. Ishida, N. D. Davis, S. Ueyanagi, and T. Sugimoto.
1996. Change in chum salmon (*Oncorhynchus keta*) stomach contents associated with fluctuation of pink salmon (*O. gorbuscha*) abundance in the central subarctic Pacific and Bering Sea. Fish. Oceanogr. 5:89–99.

Urawa, S., S. Sato, P. A. Crane, B. Agler, R. Josephson, and T. Azumaya.
2009. Stock-specific ocean distribution and migration of chum salmon in the Bering Sea and North Pacific Ocean. N. Pac. Anadr. Fish Comm. Bull. 5:131–146.

van de Berghe, E. P., and M. R. Gross.
1984. Female size and nest depth in coho salmon (*Oncorhynchus kisutch*). Can. J. Fish. Aquat. Sci. 41: 204–206.

Wertheimer, A. C.
1997. Status of Alaska salmon. *In* Pacific salmon and their ecosystems: status and future options (D. J. Stouder, P. A. Bisson, and R. Naiman, eds.), p. 179–199. Springer Science+Business Media, Dordrecht, Netherlands.

Zavolokin, A. V., E. A. Zavolokin, and Y. N. Khokhlov.
2009. Changes in size and growth of Anadyr chum salmon (*Oncorhynchus keta*) from 1962–2007. N. Pac. Anadr. Fish Comm. Bull. 5:157–163.

Zhang, Y., J. M. Wallace, and D. S. Battisti.
1997. ENSO-like interdecadal variability: 1900–93. J. Clim. 10:1004–1020.

NOAA
National Marine
Fisheries Service

Fishery Bulletin
established 1881

Spencer F. Baird
First U.S. Commissioner
of Fisheries and founder
of *Fishery Bulletin*

Fish assemblages on the southeastern Brazilian Bight, sampled by midwater trawl during spring and summer seasons: species composition, abundance, and environmental drivers

Riguel F. Contente (contact author)
Carmen L. D. B. Rossi-Wongtschowski

Email address for contact author: riguel@usp.br

Instituto Oceanográfico
Universidade de São Paulo
Praça Oceanográfico, 191
05508-120, São Paulo, SP, Brazil

Abstract—We provide an overall description of the species composition and abundance of pelagic fish assemblages sampled with midwater trawls at depths <100 m in the southeastern Brazilian Bight (SBB, south-southeastern Brazil) during the spring–summer period from 1995 through 2010. We also investigated the effect of 1) 3 water masses, the South Atlantic Central Water (SACW), Coastal Water (CW), and Mixed Water (M), and 2) a set of environmental and spatial variables on the SBB pelagic fish assemblages. The aggregations comprising 43 species, were dominated by highly abundant mid-trophic-level schooling species. The Argentine anchoita (*Engraulis anchoita*), rough scad (*Trachurus lathami*), Atlantic cutlassfish (*Trichiurus lepturus*), and Brazilian sardinella (*Sardinella brasiliensis*) were the dominant species by biomass. They were distributed widely over the SBB and occurred in all years. Results from multivariate analyses indicate that SACW and the combination of CW and M affected the SBB pelagic assemblage structure and that each contained a specific species grouping, whose abundance changed in relation to depth within the water column and to distance from shore of both SACW and CW+M. This pattern is consistent with the hydrographically complex structure of the SBB in spring and summer.

Manuscript submitted 1 February 2015.
Manuscript accepted 23 February 2016.
Fish. Bull. 114:220–236 (2016).
Online publication date: 15 March 2016.
doi: 10.7755/FB.114.2.8

The views and opinions expressed or implied in this article are those of the author (or authors) and do not necessarily reflect the position of the National Marine Fisheries Service, NOAA.

The dramatic increase of human activities in coastal ecosystems worldwide has caused unprecedented losses of biodiversity and changes in the structure, resilience, resistance, and services of ecosystems (Möllmann et al., 2015). Many ecological consequences of these disturbances remain largely unclear because consistent ecological data are lacking, especially in the tropics. High biodiversity, combined with the high diversity of habitats and oceanographic dynamics in tropical and subtropical areas, induces complex spatiotemporal patterns in fish assemblages (Longhurst and Pauly, 2007). Such complexity makes traditional fishery management based on monospecific population models inadequate and emphasizes the need to control tropical fisheries on the basis of an ecosystem-based fisheries management (EBFM) perspective (Vasconcellos and Gasalla, 2001; Curtin and Prellezo, 2010). The first step toward achievement of strong EBFM is to know how fish species respond to the oceanographic environment and its dynamism (Longhurst and Pauly, 2007; Curtin and Prellezo, 2010; Harding et al., 2011; Litz et al., 2014).

The largest fish aggregations (defined here as a large multispecific group of fishes that gather together, for behavioral or other reasons) on continental shelves are generally dominated by small pelagic fish species, such as sardines and anchovies, that are usually short-lived, planktivorous fishes frequently associated with areas of high productivity (Brodeur et al., 2005; Harding et al., 2011; Litz et al., 2014). These species are ecologically and economically important, exerting bottom-up, top-down, and wasp-waist control in shelf food webs (Cury et al., 2000; Speckman et al., 2005) and supporting valuable fisheries (Vasconcellos and Gasalla, 2001). The presence and abundance of small pelagic fishes are particularly sensitive indicators of changing oceanographic and climatic conditions, migrating quickly into their preferred habitat or responding with pronounced recruitment fluctuations over relatively short time intervals (Brodeur et al., 2003; Brodeur et al., 2005; Longhurst and Pauly, 2007).

In spite of being a western boundary system, the large marine ecosystem of the southeast South American shelf (SSAS; sensu Bisbal, 1995) presents productivity hotspots comparable to those of eastern bound-

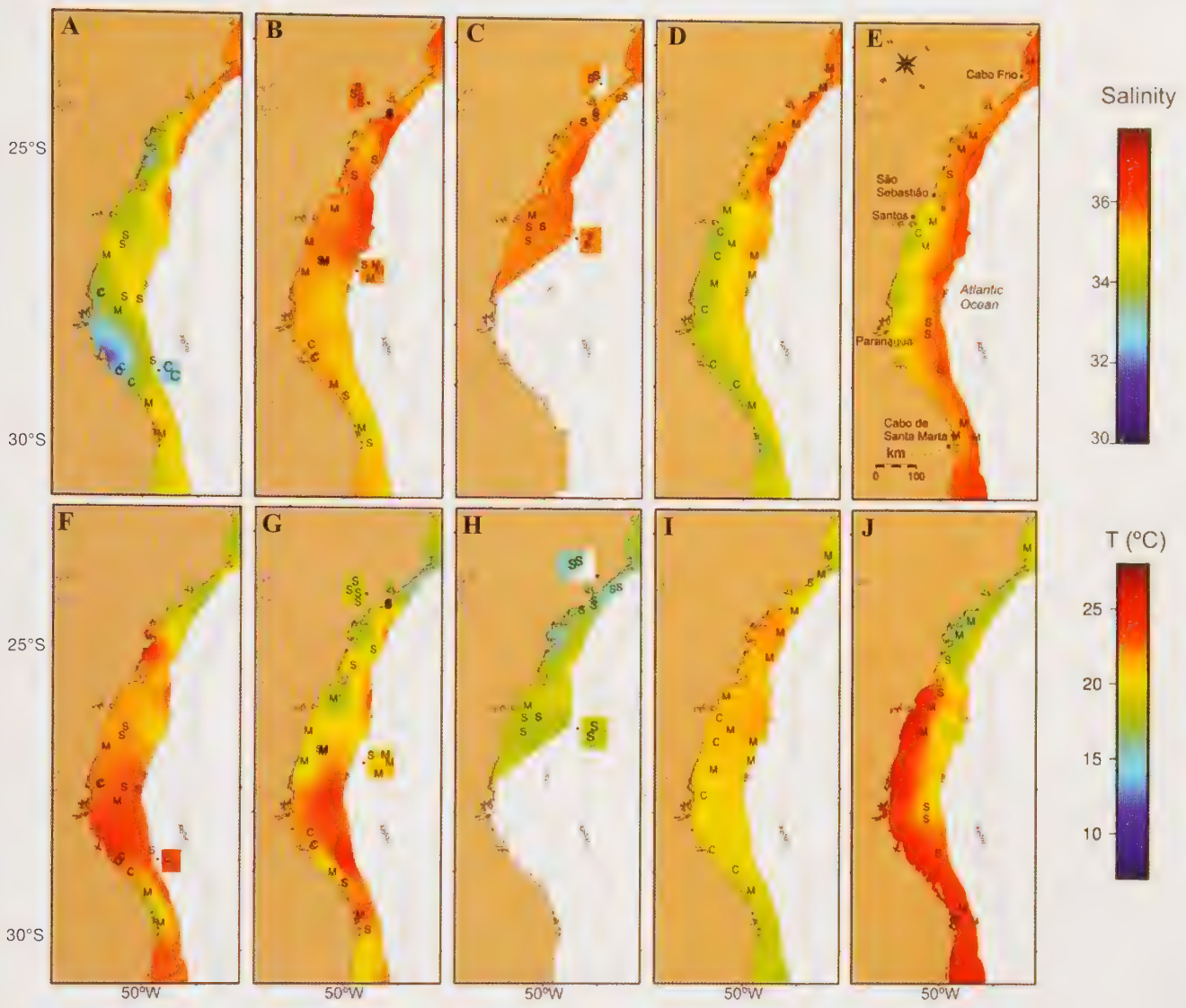

Figure 1

Maps of salinity and temperature (T) values collected at the mean depth of the fish aggregations at the water column and the locations of each midwater tow of each of 5 cruises of the Program ECOSAR (translates from Portuguese as "Prospecting to investigate sardine biomass by acoustic methods") in the southeastern Brazilian Bight off southeastern Brazil: (**A**) and (**F**) ECOSAR III (18 November–2 December 1995), (**B**) and (**G**) ECOSAR IV (20 January–2 February 2008), (**C**) and (**H**) ECOSAR V (8–24 November 2008), (**D**) and (**I**) ECOSAR VI (22 September–8 October 2009), and (**E**) and (**J**) ECOSAR VII (3–22 March 2010). Tows are codified according to the water masses in which it was accomplished: Coastal Water (C), South Atlantic Central Water (S), and Mixed Water (M), an area of mixing of water masses. For the range and mean of depths for these cruises, see Table 3. Because these maps show mean depths, depths of some tows may have fluctuated around the mean; therefore, there should be cases where the code of the water mass of tow and the temperature and salinity gradient do not correspond. Zoomed-in images are provided to show points of overlapping tows.

ary upwelling ecosystems (Lopes et al., 2006b). These hotspots are driven by substantial nutrients from oceanographic features, such as the Subtropical Shelf Front, the Rio de La Plata plume, the Patagonian tidal front, and coastal upwellings (Bisbal, 1995; Ciotti et al., 2014).

The coastline of southeastern Brazil (the northern sector of SSAS) from Cabo Frio (22°52′S) to Cabo de Santa Marta Grande (28°40′S) forms the southeastern Brazilian Bight (SBB) (Fig. 1). Three water masses occur frequently in the SBB: the high-salinity and nutrient-rich South Atlantic Central Water (SACW) (temperature [T] <18.5°C, salinity [S]=35.3–36.0); the warm nutrient-poor Tropical Water (T>18.5°C, S>36.0); and the low-salinity mesotrophic Coastal Water (CW; T≥18.5°C, S=34.0–35.3); the latitudinal and bathymet-

ric locations of these water masses change seasonally (Castro and Miranda, 1998; Ciotti et al., 2014). Like a typical subtropical shelf ecosystem, the SBB exhibits a strong seasonal signal of stratification (Castro, 2014) and pelagic fertilization (Lopes et al., 2006a).

In autumn and winter, the increased frequency and strength of southwest winds (i.e., downwelling-favorable winds) due to recurrent passages of atmospheric frontal systems (Ciotti et al., 2014) favor strong vertical homogeneity, the distance of ~86 km of the SACW from shore, the predominance of the CW and Tropical Water on the SBB, and, eventually, the northward displacement of the low-salinity and nutrient-rich Rio de La Plata plume up to the southern part of the SBB (Ciotti et al., 2014). In contrast, in spring and summer, both the prevailing northeast winds (Ciotti et al., 2014) and the higher frequency of cyclonic meanders of the Brazil Current (Campos et al., 1995) favor cross-shelf SACW intrusions toward the coast. Also in spring and summer, continental runoff generally is higher than that during other seasons, and increased runoff may make the CW expand offshore and occur nearer the ocean surface on the SBB (Lopes et al., 2006a). Such processes lead to strong vertical and geographic variability in temperature and salinity because of the presence of 2 markedly different water masses (CW and SACW) in the spring and summer (Castro, 2014; Ciotti et al., 2014; Fig. 1). In spite of this stratification, the interface zones between the CW, the SACW, and the offshore Tropical Water, in association with natural localized mixing, produce a Mixed Water (M) mass (Castro, 2014).

This spring–summer oceanographic structure (Castro, 2014) increases oceanic fertilization, pelagic productivity (Lopes et al., 2006a), and water column stability, and all such conditions synergistically enhance the larval survival of many fish species that spawn at this time, including important commercial species, such as the Brazilian sardinella (*Sardinella brasiliensis*) (Katsuragawa et al., 2006). Therefore, it is expected that the structure of the pelagic fish assemblage would respond to these typical spring–summer water masses and to their spatial variability.

The SBB produces approximately 50% of Brazil's marine landings (MPA[1]), and the Brazilian sardinella is the main species landed (UNIVALI[2]). Despite the ecological and economic importance of the SBB, our understanding of the ecological patterns of its shallow (depths <100 m) pelagic aggregations is still fairly limited because of 1) the limited number of surveys with pelagic trawls in comparison with other sampling gears, such as bottom trawls (e.g., Rocha and Rossi-Wongtschowski, 1998; Rossi-Wongtschowski et al., 2008)—a situation that is a general one for the whole SSAS (e.g., Haimovici et al., 1994; Jaureguizar et al., 2006), and 2) the focus of most pelagic trawl surveys on a single species (e.g., Brazilian sardinella; Johannesson[3]; Rijavec and Amaral[4]; Castello et al., 1991). These biases limit our understanding of the functioning of this large regional-scale (<1000 km) ecosystem and its changes due to climate changes and fisheries, therefore limiting our ability to implement strong EBFM.

During the Program of Assessment of the Sustainable Potential of the Living Resources in the Exclusive Economic Zone (REVIZEE), acoustic surveys and pelagic trawls were conducted off the SBB at depths >100 m (Madureira et al., 2005; Soares et al., 2005). Between 1995 and 2010, this sampling procedure was adopted to sample pelagic aggregations and the oceanographic environment in the SBB at depths <100 m during 7 cruises for the Program ECOSAR (abbreviation translated as: Prospecting to investigate sardine biomass by acoustic methods). The checklist of species from all of these cruises (Rossi-Wongtschowski et al., 2014) and the pattern of species abundance for ECOSAR II and III cruises (Soares et al., 2005) are already available.

In this study, we synthesized the data of ECOSAR III–VII cruises conducted in spring and summer 1) to provide an overall description of the species composition and abundance of the fish aggregations in the SBB during the spring and summer and 2) to investigate how these aggregations respond to the typical spring–summer water masses (CW, SACW, and M) and to a set of environmental and spatial covariates to such water masses.

Materials and methods

Sampling procedures

Fish and oceanographic data for this study were obtained in the spring or summer between 1995 and 2010 during the ECOSAR III, IV, V, VI and VII cruises on board the RV *Atlântico Sul* of the Federal University of Rio Grande. The search for fish aggregations was conducted over a pre-established grid during the day and night, at a mean speed of 5.1 m/s (10 knots), over a period lasting from 12 to 18 days. A grid of parallel transects was used, with a distance of 37 km between them. The grid spanned from the Cabo Frio (Rio de Janeiro, north limit) to Cabo de Santa Marta (Santa Catarina, south limit) (Fig. 1) and included depths from 20 to 102

[1] MPA (Ministério da Pesca e Aquicultura). 2011. Boletim estatístico da pesca e aquicultura 2011, 59 p. MPA, Brasilia, Brazil. [Available at website.]

[2] UNIVALI (Universidade do Vale do Itajaí). 2011. Boletim estatístico da pesca industrial de Santa Catarina—Ano 2010, 59 p. Centro de Ciência tecnológicas da Terra e do Mar, UNIVALI, Itajaí, Brazil. [Available at website.]

[3] Johannesson, K. A. 1975. Relatório preliminar das observações acústicas quantitativas sobre tamanho e distribuição dos recursos de peixes pelágicos ao largo da costa sul do Brasil. Programa de Pesquisa e Desenvolvimento Pesqueiro do Brasil Série Documentos Técnicos 10, 27 p.

[4] Rijavec, L., and J. C. Amaral. 1977. Distribuição e abundância de peixes pelágicos na costa sul e sudeste do Brasil: (resultados da pesquisa com ecointegrador) 2 cruzeiros. Programa de Pesquisa e Desenvolvimento Pesqueiro do Brasil Série Documentos Técnicos 24, 55 p.

m. Pre-established, fixed stations were determined on the grid to map the salinity and temperature patterns for the entire study area. To interpolate suitably among stations, the coverage level of the cruises was calculated as the ratio between the prospected distance, in kilometers, and the total area (Soares et al., 2005). The acoustic data were collected with a Simrad EK500[5] scientific split-beam echosounder (Simrad Fisheries, Lynnwood, WA) operating at 38 and 120 kHz. Such data were not used in this study and are available in Soares et al. (2005) and Madureira et al. (2005).

When schools were detected (during the day or night), the midwater net was deployed at the mean depth of the school. The tension and the length of the cables of the midwater net and the boat speed were changed frequently whenever the target reacted, and therefore the position of the net in the water column was correspondingly modified. The net performance and the mean depth of the net operation were measured with a Simrad FR500 probe (Trawl Eye system; Simrad Fisheries) located at the upper part of the net. The mean depth of net operation was considered the mean net depth between the beginning and the end of the haul (i.e., mean depth of the fish aggregation at the water column) and is referred to in this article as Z_a. The hauls were performed against the wind and current at, on average, speeds between 1.5 and 2 m/s (3 and 4 knots) for a period of time depending on the size and reaction of the schools. Boat speed was measured in relation to the sea bottom. For more details on the determination of grid sizes, sampling methods, and procedures of fisheries operations, see Soares et al. (2005) and Madureira et al. (2005).

A net designed especially for fishing small pelagic fish was used. It had a squared opening (sides of 15 m) and mesh of 400 mm between knots in the wings and square. The mesh gradually decreased from 50 mm in the tunnel to 20 mm in the bag, which was covered internally by a panel of mesh. The net was kept open by 2 doors (Suberkrub type) of 4 m^2 (3 m×1.35 m), weighing approximately 380 kg each.

The salinity and temperature were measured with a conductivity, temperature, and depth (CTD) profiler: SBE 19 SeaCAT (Sea-Bird Electronics Inc., Bellevue, WA) during the ECOSAR III cruise and Ocean Seven 316 CTD (IDRONAUT S.r.l, Brugherio, Italy) during the ECOSAR IV–VII cruises. Measurements were taken at each 5-m depth during the ECOSAR III cruise and at each 1-m depth during the other cruises.

During the ECOSAR IV, V, VI, and VII cruises, the local depth and geographic positions were taken at the beginning and at the end of the hauls. For the ECOSAR III cruise, only the geographic position and the local depth at the beginning of the haul were taken. For all cruises, the duration of tow (Δt in seconds) was taken. Because of a technical problem, the mean tow speed (vt in meters per second) for all tows was available only for ECOSAR III cruise.

The catch of each haul was weighed, and a random subsample was taken and frozen on board when large hauls were captured (>500 individuals). In this case, the weight of each species was estimated on the basis of their proportions in the subsample. Benthic and demersal species typically found on the seafloor were infrequently caught when the bottom of the net reached the seafloor, and they were found in low abundance. Because this net was not designed specifically to sample such fish, abundance estimates for these species may have been biased. Therefore, they were not considered in this study. The taxonomic identification guides used are listed in Rossi-Wongtschowski et al. (2014). Vouchers were stored at the Zoology Museum of the University of São Paulo. Rossi-Wongtschowski et al. (2014) provided a complete list of species, including the records from the benthic and demersal species, records from hauls not considered in the study discussed in this article (see below), and records from purse seine operations concurrently operated with a midwater net during some trawls.

Analysis procedures

Abundance estimates and classification of fish samples

Fish biomass was the abundance metric, and values of fish biomass were standardized to a volume (cubic meters) for all hauls to incorporate the differences in tow distance and duration (Harding et al., 2011). The volume of water was calculated as follows: distance of haul (D in meters)×area of the opening of the net (268 m^2). In the ECOSAR IV, V, VI, and VII cruises, D was calculated by using loxodromic lines based on the latitude and longitude at the beginning and at the end of the hauls (Freire and Vasconcellos, 2011). Because we did not have these geographic variables for the ECOSAR III cruise, D was estimated on the basis of vt as $D=vt\times\Delta t$.

We used the salinity and temperature values that were estimated through interpolation from the records of the nearest neighboring stations at the same depth of tow. Interpolations were conducted with nominal kriging, a geostatistical procedure that weights values collected at surveyed points according to a covariance function to predict a value for an unmeasured location, by using GeoR (Ribeiro and Diggle[6]; Diggle and Ribeiro, 2007) in R software, vers. 3.1.0 (R Core Team, 2014). Because of technical issues during the ECOSAR V cruise, salinity and temperature were not regularly measured along the grid (Fig. 1). As a result of this lack of data, we removed fish samples from the southern SBB.

The fish samples from the 78 tows considered in this study were not equally distributed over the entire length of the SBB (Fig. 1) or over the cruises and water

[5] Mention of trade names or commercial companies is for identification purposes only and does not imply endorsement by National Marine Fisheries Service, NOAA.

[6] Ribeiro, P. J., Jr., and P. J. Diggle. 2001. GeoR: a package for geostatistical analysis. R News 1(2):15–18. [Available at website.]

Table 1

Number of tows per water mass for each of 5 cruises (III–VII) of the Program ECOSAR (translates from Portuguese as "Prospecting to investigate sardine biomass by acoustic methods"). The water masses included the South Atlantic Central Water (SACW), Coastal Water (CW), and Mixed Water (M).

	Cruise				
Water mass	III	IV	V	VI	VII
SACW	5	9	10	1	5
CW	6	3	0	5	1
M	4	8	2	11	8
Total	15	20	12	17	14

masses (Table 1) because of the different selections of samples, operational constraints, weather conditions, and other aims of the surveys. Nevertheless, fish sampling covered the entire length of the SBB in most of the cruises (Fig. 1).

The water mass, either SACW or CW, in which each tow was carried out was identified on the basis of the mean temperature and salinity recorded at the mean depth of tow. Any record of salinity or temperature outside the usual bounds for these water masses may be indicative of mixing processes among SACW, CW, or Tropical Water; therefore, the water mass for such records was classified as M.

Species composition and abundance The frequency of abundance (biomass) for each species for each cruise (%B), total frequency of abundance for all cruises ($\%B_T$), and total frequency of occurrence (% FO_T; i.e., the number of occurrences of the species in relation to the total 78 tows) was calculated to infer the characteristics of the structure of the fish aggregations and assemblages.

The effect of water masses on the fish assemblage structure After we assigned each of the tows to one of the water masses (CW, SACW, and M), the following procedures were performed to construct the response biomass matrix: 1) species occurring in <3% of tows were removed from the data set because they may have added noise rather than information to the statistical solutions (Legendre and Legendre, 1998) and 2) the abundance data were first transformed in order to scale reduction due to high species-specific abundance variability among fish samples. As a result, the resulting matrix contained 78 tows and 36 species.

A nonparametric, permutational multivariate analysis of variance (PERMANOVA; Anderson et al., 2008) was used to test for differences in fish assemblages among water masses (factor fixed, with 3 levels: CW, SACW, M) and among the cruises (factor random, with 5 levels: ECOSAR III, IV, V, VI, VII cruises). In brief, PERMANOVA (analogous to multivariate analysis of variance [MANOVA]) is a routine that calculates the pseudo-*F* statistic for testing the response of variables (the response biomass similarity matrix) to factors in an analysis of variance experimental design on the basis of any resemblance measure. Unlike tests where multinormality is assumed (e.g., MANOVA), PERMANOVA obtains the significance of the test statistic by permutation. Therefore, this routine was quite suitable for our data that were not normally distributed (Anderson et al., 2008).

Because our design was unbalanced (Table 1), we used type-I sums of squares to conduct the partitioning the variability of the total species data. A potential problem in an unbalanced design is that the order in which the terms of the main PERMANOVA model are inserted into the analysis may affect the result because the terms are not independent of one another. Therefore, we changed the order of main-effect terms and verified how this different change in order affected the results (Anderson et al., 2008). Terms of the main model with negative components of variation were taken as probably having zero variance and, for that reason, were eliminated from the analyses and the data were re-analyzed (Fletcher and Underwood, 2002). A post-hoc permutational *t*-test from the PERMANOVA routine was then applied to compare levels of the fixed factor (water mass) when it was significant.

The method of PERMANOVA is sensitive to differences in within-group dispersions. A significant result for a given factor for PERMANOVA could signify that the groups differ in their location in multivariate space, in their dispersion in it, or a combination of the 2 (Anderson et al., 2008). Therefore, we used the permutational analysis of multivariate homogeneity of dispersions (PERMDISP), which is a distance-based test of homogeneity of multivariate within-group dispersions among groups of a single factor. A significant result of PERMANOVA and a nonsignificant effect of PERMDISP indicate that there is a genuine difference in location among the groups in the multivariate space (i.e., that there is a significant effect of factor). The PERMANOVA and PERMDISP routines were based on the Bray–Curtis similarity index and their significance on 9999 permutations.

Similarity percentages analysis (SIMPER) was applied with a cumulative contribution cutoff level of 90% to determine which species contributed to differences in fish assemblage structure among the water masses (Clarke and Warwick, 2001).

These analyses were performed with the software PRIMER 6, vers. 6.1.11, with the add-on package PERMANOVA+, vers. 1.0.1 (PRIMER-E Ltd., Ivybridge, UK).

The effect of environmental and spatial factors on the fish assemblage structure We assessed the relationship between the variability in the fish assemblage structure and the oceanographic and spatial variables (Table 2). This analysis was based on 2 matrices. The first matrix

Table 2

Means, ranges, and measurement sources of oceanographic and spatial factors sampled during ECOSAR IV–VII cruises and used as explanatory variables in the analysis conducted with the distance-based nonparametric linear modeling (available in DistLM in the PERMANOVA+ add-on for the software PRIMER 6). Eventual transformations before regression also are provided. Standard deviations (SDs) of the means are provided in parentheses. x=variable; na=not applicable; Z=local depth; Z_a=mean depth of the fish aggregation at the water column; CTD=conductivity, temperature, and depth.

Variable	Mean (SD)	Range	Source	Transformation
Latitude (°)	na	22.6–28.6	GPS	
Longitude (°)	na	41.7–48.6	GPS	
Distance from shore (km)	31.7 (28.5)	1.0–132.0	Satellite	$\ln(x+1)$
Z local (m)	47 (20)	20–102	Echosounder	
Z bottom (m)[1]	10 (14)	0–53	Echosounder	$\ln(x+1)$
Za (m)	24 (14)	11–84	Echosounder	$\ln(x+1)$
Chlorophyll-a (mg/m^3)[2]	2.06 (2.00)	0.30–6.30	Satellite	
Bottom salinity	35.38 (0.60)	33.80–36.00	CTD profiler	$\sqrt{x}$
Surface salinity	34.58 (1.68)	28.70–36.60	CTD profiler	$\ln(x+1)$
Bottom temperature (T°C)	17.90 (3.06)	12.90–26.00	CTD profiler	
Surface temperature (T°C)	23.47 (2.07)	18.70–28.60	CTD profiler	

[1]Distance from the seafloor to the bottom of the net.
[2]Satellite-derived data for surface levels of chlorophyll-a averaged over the period of the cruise were taken from the Moderate Resolution Imaging Spectroradiometer (MODIS) data set available from NASA. Available from website, accessed April 2015). Data are available with 8-day temporal resolution and 4-km spatial resolution. Therefore, we used data averaged over the period of the cruise.

was the same response matrix used in PERMANOVA, but it was reduced to 63 tows and 31 species because 1) the data from the ECOSAR III cruise were not considered because we did not have satellite chlorophyll-a data available for the period of this cruise, and 2) species occurring in <3% of the tows of the resulting matrix were excluded. The second matrix was one of environmental and spatial variables (matrix of predictors), containing 63 samples and 11 variables (Table 2). The abundance data of the response biomass matrix were previously transformed to scale reduction.

This removal of data from the ECOSAR III cruise did not affect the relation between the conclusions drawn from the results of PERMANOVA and SIMPER and those drawn from the analyses described below. This relation was not affected because we obtained practically the same results (not shown) in repeating the PERMANOVA and SIMPER analyses without the data from the ECOSAR III cruise.

The relationship between species and their environment was assessed by using the distance-based, nonparametric linear modeling available in DistLM (Anderson et al., 2008) in the PERMANOVA+ add-on (vers. 1.0.1) for the software PRIMER 6, vers. 6.1.11. This routine fits predictor variables (matrix of predictors) to a set of response variables (the response biomass similarity matrix) on the basis of any resemblance measure (Anderson et al., 2008). Unlike the multivariate regressions where multinormality is assumed, this routine tests the null hypothesis of a no species–environment relationship through permutation (Anderson et al., 2008), making it quite suitable for our data that were not normally distributed. Moreover, the flexibility of the routine to run on any resemblance measure allowed the use of the Bray–Curtis index (Anderson et al., 2008), which best described the distribution of species abundance in our data (Legendre and Legendre, 1998; Clarke and Warwick, 2001). The significance of test results was based on 9999 permutations.

To meet the assumption of linearity of model, (Anderson et al., 2008), before running DistLM, we checked for outliers and skewness in draftsman plots among the predictors, transforming them when necessary (Table 1; Legendre and Legendre, 1998). We also removed one redundant predictor when correlated (Pearson's correlation coefficient [r]) at $r \geq 0.70$ (Dormman et al., 2013) with another one. We used information criteria to choose the most parsimonious model, in other words, the simplest model (the one with the lowest number of predictors) with enough suitable explanatory power (Burnham and Anderson, 2002). We based our selection on both the corrected Akaike information criterion (AIC_c) and the Bayesian information criterion (BIC) (Burnham and Anderson, 2002). The model selection procedure *best*, available in the software PRIMER 6, provided the 20 best models. Balancing the severity of the BIC with the flexibility of the AICc to include variables in models has been shown to be a robust selection procedure (for more details, see Anderson et al., 2008). The following steps were conducted to select a model: the number of variables in the model was defined as the number of variables most frequently found among

Table 3

Minimum (Min), maximum (Max), and mean depth (Z_a) of the fish aggregations at the water column and the distance from shore for ECOSAR III–VII cruises. Standard deviations (SDs) of the means are presented in parentheses

	Z_a (m)			Distance from shore (km)		
Cruise	Min	Max	Mean (SD)	Min	Max	Mean (SD)
III	7.5	60	24.4 (14.6)	4.0	113.8	38.9 (35.5)
IV	11	55	20.6 (10.3)	2.6	51.7	22.9 (16.6)
V	13	84	32.6 (22.4)	2.8	78.0	27.7 (25.0)
VI	12	34	19.6 (6.1)	1.0	132.2	38.7 (38.6)
VII	12	58	29.0 (14.7)	4.2	100.2	38.5 (30.2)

the 20 most parsimonious models according to both criteria. Then, that model was chosen that had the lowest BIC value among those models with the number of variables defined above (Anderson et al., 2008).

The influence of the predictor variables of the selected model on the variation in fish assemblage structure was visually assessed by the constrained ordination distance-based redundancy analysis (dbRDA) (Anderson et al., 2008). Vectors on dbRDA ordination determine the strength and direction of the relationship between the predictors and the ordination axes. The length of the vectors was set proportionally to r, and their direction indicated the direction of the greatest increase in the variable. To explore the relationship between species and predictors, both species and predictor variable vectors were shown on the ordination. Only species showing a Spearman correlation coefficient ($|r_{SP}|$) ≥0.2 (Willis and Anderson, 2003) with one or more axes were displayed.

The pattern of species association We performed a cluster analysis 1) to detect potential groupings of species on the basis of their frequency of co-occurrence and 2) to explore the relation of these groupings with the significant predictors, plotting the groupings on the dbRDA ordination. Therefore, we used the same response matrix as that which we used for DistLM, reducing the number of species to include only those species contributing to (arbitrarily) 93% of the relative total frequency of occurrence. The data were transformed into presence and absence, and an R-mode cluster was constructed on the basis of a matrix of similarities with the Ochiai algorithm (Podani, 2000) and distances calculated by group-average sorting. The species groupings were arbitrarily defined at a cutoff level of 20% similarity.

Results

Abiotic variables

Fish sampling sites were in areas of the SBB at depths from 20 to 103 m (mean per cruise: 46.5 m [standard deviation (SD) 20.9]). The tows were, on average, located from 22.9 to 38.8 km offshore, with the nearest tow at 1 km from the shore and the farthest tow at 132 km (Fig. 1, Table 3). The values for Z_a ranged from 19 m to 32 m, with the shallowest aggregation at 7.5 m (ECOSAR III cruise) and the deepest aggregation at 84 m (ECOSAR V cruise) (Table 3). During most tows (60.5%), the net was hauled more than 3 m above the bottom (with a mean distance of 16.4 m [SD 14.4]) from the bottom of the net to the seafloor, and, during 6 tows (7.7% of all tows), the net was hauled from 1 to 3 m from the bottom. The net reached the bottom in 32% of the hauls.

The number of fish samples taken in each water mass varied among the ECOSAR cruises (Fig. 2). Of the 78 fish samples taken during the cruises, 43% were collected in SACW, 32% were captured in M, and 24% were taken in CW (Fig. 2).

Species composition and abundance

In the valid samples used in this study, 43 species from 23 families were recorded (Table 4). Carangidae was the most speciose family (9 species), followed by Engraulidae (5 species). The Argentine anchoita (*Engraulis anchoita* [Engraulidae]), rough scad (*Trachurus lathami* [Carangidae]), Atlantic cutlassfish (*Trichiurus lepturus*), Brazilian sardinella, and flying gurnard (*Dactylopterus volitans*) were the most abundant species (70% of the total biomass sampled). These 5 species, together with the Atlantic chub mackerel (*Scomber colias* [Scombridae]), gray triggerfish (*Balistes capriscus* [Balistidae]), American coastal pellona (*Pellona harroweri* [Pristigasteridae]), piquitinga anchovy (*Anchoa tricolor* [Engraulidae]), and harvestfish (*Peprilus paru* [Stromateidae]), accounted for 91% of the total biomass sampled (Table 4). The predatory Atlantic cutlassfish was the most common species in the sampled aggregations (Table 4).

Large schools of Argentine anchoita and rough scad dominated the biomass of the aggregations and were moderately common during the ECOSAR cruises (FO_T=~ 41% and 26%, respectively; Table 4). This find-

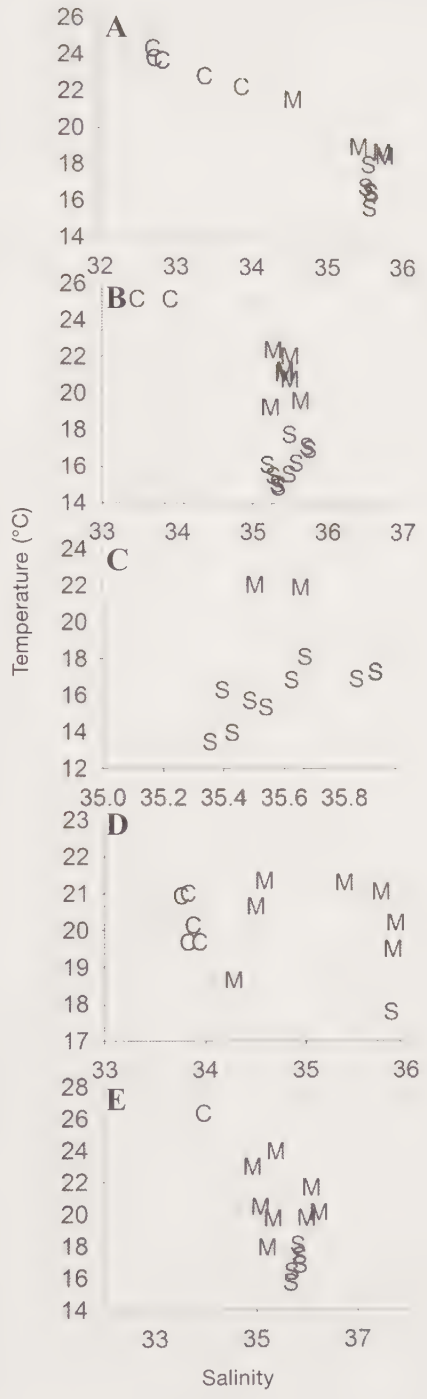

Figure 2

Plots of mean temperature versus mean salinity used for identification of the water masses at the mean depth where the tows were conducted during the spring–summer ECOSAR cruises: (**A**) III, (**B**) IV, (**C**) V, (**D**) VI, and (**E**) VII. The water masses are Coastal Water (C), South Atlantic Central Water (S), and Mixed Water (M)

ing indicates a wide distribution and persistency over the SBB and over the years of this study (1995–2010). The Atlantic cutlassfish and Brazilian sardinella, also abundant, displayed high frequency in the aggregations over the years (FO_T=70% and 51%, respectively), also indicating wide distribution and persistency (Table 4). Large schools of the flying gurnard were relatively common in aggregations from 4 cruises, IV–VII (i.e., from 2008 through 2010), having been captured principally (68% of 25 tows) at midwater depths (>3 m above the bottom) and secondarily (32%) on the bottom (<3 m). Large schools of the Atlantic chub mackerel (~3 metric tons [t], cruise IV), gray triggerfish (~0.7 t, cruise III), American coastal pellona (~0.6 t, cruise VI), and bluefish (*Pomatomus saltatrix*; ~ 0.2 t, cruise V) were dominant in aggregations during only one cruise (Table 4). The other species showed both low abundance and low frequency (Table 4), reflecting either association with dominant species or scattered, low-biomass groupings.

The effect of water masses on fish assemblage structure

We found significant differences in the structure of fish assemblages among the water masses, but not among the ECOSAR cruises (Table 5). This result was not affected by changes in the order of insertion of terms of the PERMANOVA model (Table 5). Moreover, this significant result was due to the location (which indicated difference) of the fish assemblage structure of each water mass in multivariate space rather than to differences in the dispersion within assemblages of each cruise (PERMDISP, $F_{1,76}$=4.16, P>0.05). The post-hoc permutational t-test revealed that the assemblage structure of SACW differed significantly from those of CW and M (SACW×CW: t=14.12, P=0.013; SACW×M: t=14.79, P=0.003), but the assemblage structures of the remaining 2 water masses did not differ significantly (CW×M: t=0.94, P>0.05). Consequently, the data of CW and M were grouped together before SIMPER analysis was begun.

The main species responsible for the difference in assemblage structure between the SACW and the combination of CW and M (CW+M)—the species that cumulatively accounted for ~75% of the difference—were the Argentine anchoita, Atlantic cutlassfish, rough scad, piquitinga anchovy, and white snake mackerel (*Thyrsitops lepidopoides*), all of which were most abundant in SACW, and the Brazilian sardinella, flying gurnard, false pilchard (*Harengula clupeola*), American coastal pellona, and Atlantic thread herring (*Ophistonema oglinum*), all of which were most abundant in CW+M (Table 6).

Patterns of species association

The resulting cluster for identifying species associations (Fig. 3) indicates the existence of 3 groups of species: group A, formed principally (70% of species sampled) by species that were most abundant in the SACW (e.g., the Argentine anchoita, Atlantic cutlassfish, and

Table 4

Frequency of abundance for each ECOSAR cruise (biomass; $\%B$), total frequency of abundance ($\%B_t$), and total frequency of occurrence (FO_T) of the species sampled during the spring–summer ECOSAR cruise series from 1995 (III) to 2010 (VII). For each species, the scientific names, families, cumulative total frequency of abundance ($\%B_{tcum}$), and total biomass (weight×10^5kg×m^{-3}) of each cruise are shown. An end ask (–) indicates B<0.1%.

Common name	Family	Species	Cruise ($\%B$)					$\%B_t$	$\%B_{tcum}$	FO_T
			III	IV	V	VI	VII			
Argentine anchoita	Engraulidae	*Engraulis anchoita*	35.4	32.8	39.0	23.1	12.0	25.7	25.7	41.3
Rough scad	Carangidae	*Trachurus lathami*	9.1	7.3	24.3	6.8	27.8	15.6	41.3	26.1
Atlantic cutlassfish	Trichiuridae	*Trichiurus lepturus*	5.0	7.5	5.7	8.1	15.2	9.3	50.6	58.7
Brazilian sardinella	Clupeidae	*Sardinella brasiliensis*	2.4	2.2	6.1	20.0	11.8	9.3	59.9	40.2
Flying gurnard	Dactylopteridae	*Dactylopterus volitans*	–	5.7	6.8	15.2	12.5	9.1	69.0	26.1
Atlantic chub mackerel	Scombridae	*Scomber colias*		33.8	0.3			8.4	77.4	9.8
Gray triggerfish	Balistidae	*Balistes capriscus*	29.8	0.2	0.4		0.3	3.9	81.4	7.6
American coastal pellona	Pristigasteridae	*Pellona harroweri*	4.4	–		14.7		3.6	85.0	12.0
Piquitinga anchovy	Engraulidae	*Anchoa tricolor*	1.7	–	0.5		10.1	3.3	88.3	8.7
Harvestfish	Stromateidae	*Peprilus paru*	1.0	0.2	0.2	1.0	7.5	2.6	90.9	19.6
Bluefish	Pomatomidae	*Pomatomus saltatrix*	–	–	12.1	0.1		1.5	92.4	8.7
False pilchard	Clupeidae	*Harengula clupeola*	2.7	1.0	0.5	3.8		1.5	93.9	22.8
Atlantic thread herring	Clupeidae	*Opisthonema oglinum*	0.3	1.8		3.0		1.1	94.9	13.0
Atlantic moonfish	Carangidae	*Selene setapinnis*	0.4	2.5		0.1	0.8	0.9	95.9	13.0
White snake mackerel	Gemplidae	*Thyrsitops lepidopoides*	0.1	0.7	0.8	1.5	0.2	0.7	96.5	23.9
Marini's anchovy	Engraulidae	*Anchoa marinii*	3.9	0.8				0.7	97.2	6.5
Atlantic bumper	Carangidae	*Chloroscombrus chrysurus*	0.1	1.2	0.8	0.5	0.4	0.6	97.8	20.7
Castin leatherjacket	Carangidae	*Oligoplites saliens*	1.1	1.3		0.6	–	0.6	98.4	20.7
Lookdown	Carangidae	*Selene vomer*	1.0	–			0.8	0.3	98.8	14.1
Argentine hake	Merlucciidae	*Merluccius hubbsi*			1.8			0.2	99.0	1.1
Dogtooth herring	Pristigasteridae	*Chirocentrodon bleekerianus*	0.3	–		0.7		0.2	99.2	10.9
Guachanche	Sphyraenidae	*Sphyraena guachancho*	0.8		0.1	0.1		0.1	99.3	9.8
Great pompano	Carangidae	*Trachinutus goodei*	–	0.5				0.1	99.5	2.2
Planehead filefish	Monacantidae	*Stephanolepis hispidus*		–			0.4	0.1	99.6	6.5
Atlantic spadefish	Ephippidae	*Chaetodipterus faber*	0.3	0.1				0.1	99.6	2.2
Longfinger anchovy	Engraulidae	*Anchoa filifera*				0.2		0.0	99.7	2.2
Plata pompano	Carangidae	*Trachinotus marginatus*		0.2				0.0	99.7	1.1
Red cornetfish	Fistulariidae	*Fistularia petimba*		–	0.3			0.0	99.8	2.2
Atlantic bonito	Scombridae	*Sarda sarda*				0.2		0.0	99.8	2.2
Silver-rag	Ariommatidae	*Ariomma bondi*				0.2		0.0	99.9	2.2
Great barracuda	Sphyraenidae	*Sphyraena barracuda*		0.2				0.0	99.9	4.3
Brown burrfish	Diodontidae	*Chilomycterus spinosus*	–	–	0.1		0.1	0.0	99.9	7.6
Queen tiggerfish	Balistidae	*Balistes vetula*	0.1					0.0	99.9	2.2
Bluntnose jack	Carangidae	*Hemicaranx amblyrhynchus*		0.1				0.0	99.9	1.1
Tome barracuda	Sphyraenidae	*Sphyraena tome*	–			–		0.0	99.9	2.2
Serra	Scombridae	*Scomberomorus brasiliensis*	0.1					0.0	99.9	1.1
Vermilion snapper	Lutjanidae	*Rhomboplites aurorubens*	0.1					0.0	99.9	1.1
Keelcheek bass	Acropomatidae	*Synagrops spinosus*	–					0.0	99.9	2.2
Brazilian sharpnose shark	Carcharhinidae	*Rhizoprionodon lalandii*	–					0.0	99.9	1.1
Buckler dory	Zeidae	*Zenopsis conchifer*		–				0.0	99.9	1.1
Bigeye scad	Carangidae	*Selar crumenophthalmus*		–				0.0	99.9	1.1
Broadband anchovy	Engraulidae	*Anchoviella lepidentostole*		–				0.0	99.9	1.1
Antenna codlet	Bregmacerotidae	*Bragmaceros atlanticus*	–					0.0	100.0	2.2
Total biomass			18.7	37.2	18.5	31.4	44.3			

Table 5

Results of permutational multivariate analysis of variance to test for differences in fish assemblage structure among water masses (WM) and the ECOSAR III–VII cruises. Because of the unbalanced design, we used type-I sums of squares and tested the effect of one factor *given* the effect of another. The variance component of the interaction term was negative in both cases; therefore, it was pooled, and the data were re-analyzed. Significant *P*-values are presented in bold. SS=sum of squares; MS=mean sum of squares.

Source of variation	df	SS	MS	Pseudo-*F*	*P*
WM, cruise | WM					
WM	2	12,570	6285.2	14.29	**0.0325**
Cruise	4	19,442	4860.4	1.14	0.1827
Pooled	71	3.04×10^9	4282.2		
Total	77	3.36×10^9			
Cruise, WM | cruise					
Cruise	4	17,633	4408.1	10.29	0.3861
WM	2	14,380	7189.8	1.68	**0.0067**
Pooled	71	3.04×10^9	4282.2		
Total	77	3.36×10^9			

Table 6

Summary of the analysis of similarity percentages to identify the most important species in distinguishing the assemblage that had, on average, higher biomass in the South Atlantic Central Water (SACW) than that of the assemblage that had, on average, higher biomass in the combination of the Coastal Water and Mixed Water (CW+M). Data used in this analysis were collected from the ECOSAR III–VII cruises. Abundance was measured as the mean (untransformed) value of biomass (weight$\times10^5$kg$\times$m^{-3}). The average Bray–Curtis dissimilarity values between SACW and CW+M (Diss.), the contributions to between-group dissimilarities (Contrib%), and the standard deviations (SD) of Bray–Curtis dissimilarities are presented. Higher Diss. and SD values indicate that the contribution of the species to the dissimilarity between the SACW and CW+M was reasonably consistent across all pairs of samples in the 2 groups. Only species that cumulatively contributed ~90% to dissimilarity are shown.

	Abundance				
Species	SAWC	CW+M	Diss.	SD	Contrib%
Argentine anchoita	14.0	4.0	17.7	0.8	20.3
Atlantic cutlassfish	4.1	2.0	12.4	0.9	14.2
Rough scad	4.5	4.4	9.8	0.6	11.2
Brazilian sardinella	1.9	3.4	6.7	0.8	7.7
Flying gurnard	0.1	4.8	6.1	0.4	7.0
False pilchard	0.1	0.8	3.5	0.6	4.0
American coastal pellona	0.2	1.9	3.3	0.4	3.8
Atlantic thread herring	0.0	0.7	2.4	0.4	2.8
Castin leatherjacket	0.2	0.3	2.4	0.4	2.7
Atlantic bumper	0.1	0.3	2.2	0.4	2.5
Piquitinga anchovy	1.9	0.1	2.2	0.3	2.5
Harvestfish	0.1	1.2	2.2	0.4	2.5
Atlantic moonfish	0.8	0.0	2.1	0.4	2.5
White snake mackerel	0.3	0.2	2.0	0.6	2.3
Gray triggerfish	0.1	1.9	1.7	0.3	1.9
Atlantic chub mackerel	8.0	0.0	1.5	0.3	1.7
Marini's anchovy	0.1	0.1	1.4	0.3	1.3
Bluefish	0.8	0.0	0.9	0.2	1.0
Great barracuda	0.1	0.0	0.9	0.1	1.0

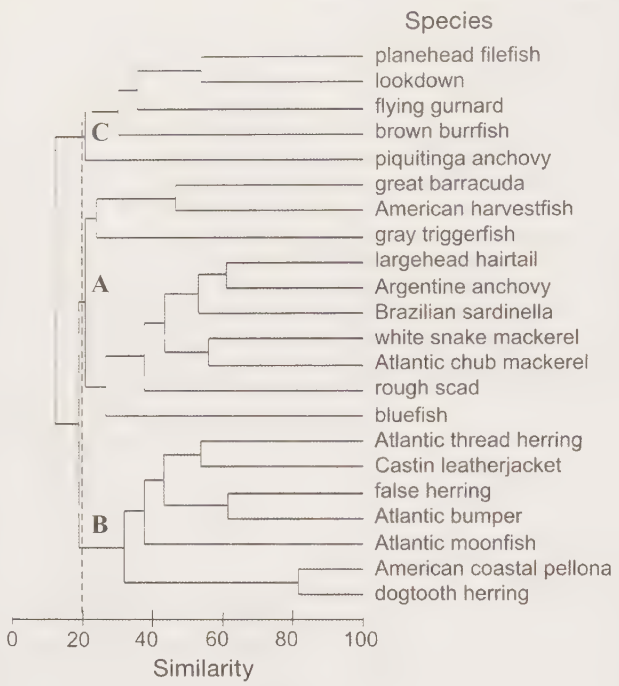

Figure 3

Resulting cluster determined with the Ochiai similarity index matrix and used to assess the pattern of co-occurrence of the main fish species (those species that totaled 93% of the relative total frequency of occurrence) sampled in the spring–summer ECOSAR IV–VII cruises. The species groupings (i.e., groups A, B, and C) were arbitrarily defined at a cutoff level of 20% similarity.

Table 7

Summary of results from analysis, conducted with the distance-based, nonparametric linear modeling (available in DistLM in the PERMANOVA+ add-on for the software PRIMER 6) of the relationship between multivariate structure of pelagic fish assemblages and oceanographic and spatial variables sampled during spring–summer ECOSAR IV–VII cruises in the southeastern Brazilian Bight. Data from these cruises (63 tows) were pooled because there was no interannual effect on the assemblage structure. The spatial variables were distance from shore (DS) and mean depth of the aggregation in the water column (Z_a). Models selected by the Bayesian information criterion and Akaike information criterion. Cumul.=cumulative percentage of the variability of the fish assemblage structure explained by the model. SS=sum of squares.

Variable	SS	Pseudo-*F*	*P*-values	Cumul. (%)
Z_a	7771.2	1.818	0.0190	3.0
DS	9323.6	2.263	0.0036	7.0

rough scad) and were principally responsible for the differentiation of the SACW assemblage structure from the CW+M assemblage structure (Table 6); group B, formed mostly (85% of species sampled) by species that were more abundant in the CW+M (e.g., the false pilchard, American coastal pellona, Atlantic thread herring, and castin leatherjacket [*Oligoplites saliens*]) and were relevant for distinguishing the assemblage structures of CW+M and SACW (Table 5); and group C, a mixed grouping, composed of no-diagnostic species in SIMPER (Table 6) and of those species that were diagnostically abundant in either the CW+M (e.g., flying gurnard) or the SACW (e.g., the piquitinga anchovy) assemblage.

The effect of environmental and spatial factors on fish assemblage structure

Because there was no significant variation in fish assemblage structure among the ECOSAR cruises (Table 5), data from all cruises were pooled to produce only one model for assessing the relationship between the variability in the assemblage structure and the oceanographic and spatial variables. The most parsimonious model was formed of 2 spatial variables: distance from shore and Z_a (Table 7). These variables explained 7% of total variation in fish assemblage structure. The resulting pattern among samples that was revealed on the constrained dbRDA ordination for this model (Fig. 4) indicates 2 clear gradients of shifts in the assemblage structure related to such variables. The vector of groupings of species (Fig. 3) on these gradients (Fig. 4) revealed 2 principal tendencies: 1) an increase in abundance of SACW-associated species with increasing Z_a and a decreasing distance from shore and 2) an increase in abundance of species associated with CW+M with decreasing Z_a and an increasing distance from shore.

Discussion

Our findings reveal that the pelagic aggregations of fishes over the SBB shelf were dominated by highly abundant mid-trophic-level schooling species in association with predatory fishes (of which the Atlantic cutlassfish was the most representative). That result is consistent with the shelf pattern typically observed worldwide, including in the California Current (Litz et al., 2014), Colombia (Duarte and García, 2004), Humboldt Current (Fablet et al., 2012), Southern Brazil (Soares et al., 2005), and Benguela (Pecquerie et al., 2004). In our study, the biomass of the aggregations was dominated by Argentine anchoita, followed by rough scad, Atlantic chub mackerel, American coastal pellona, Brazilian sardinella, flying gurnard, and Atlantic cutlassfish, all of which may play a key role in the pelagic ecosystem of the SBB.

Such patterns of dominance and aggregations were consistent with those previously found for the

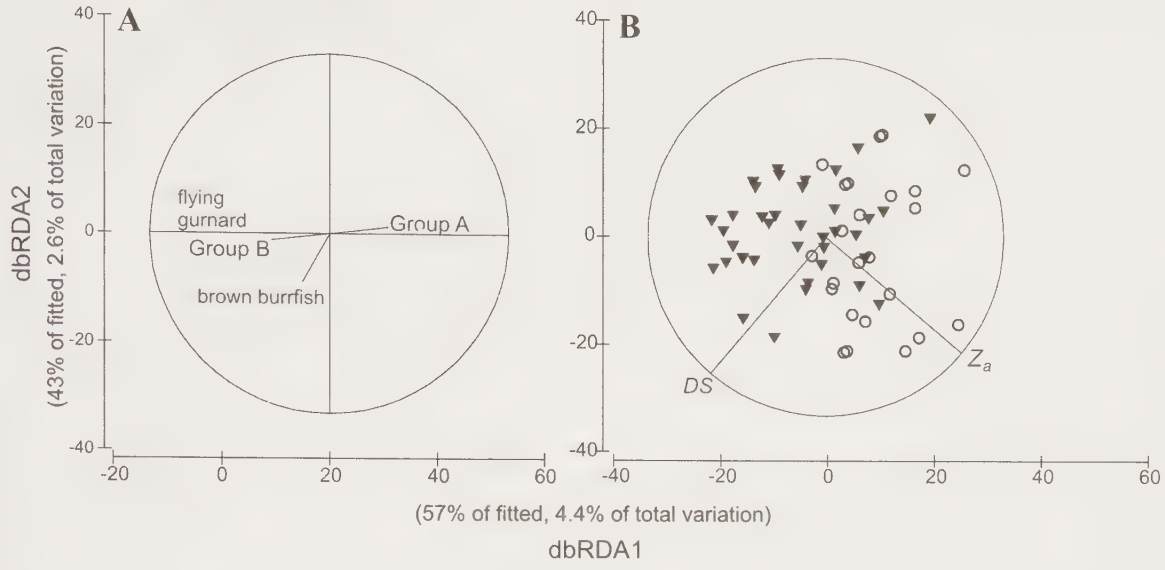

Figure 4

The first 2 axes from the distance-based redundancy analysis (dbRDA) that correlate the pelagic fish assemblage data collected during the spring–summer ECOSAR IV–VII cruises with (**A**) the species groups or species and (**B**) the explanatory variables (from the fitted model). *DS*=distance from shore, Z_a=mean depth of the fish aggregation. Data from ECOSAR IV–VII cruises (63 tows) are pooled because there was no interannual effect on the assemblages. Samples were taken either from the South Atlantic Central Water (circles) or from the combination of the Coastal Water and Mixed Water (triangles). Group A and B were defined in cluster analyses (Fig. 3) and showed a Spearman correlation coefficient $|r_{SP}| \geq 0.2$ with the axes. Group C species did not show clear association with a particular water mass; therefore, only those Group C species with correlations ≥0.2 with either axis are plotted. Percentage explained by the axis (fitted) and total variation explained by the model are provided on the axes.

SBB and other areas of the SSAS. The Argentine anchoita forms large schools and is the dominant species in standing stocks of pelagic fishes and larval assemblages in the inner SBB (depths <100 m; this study; Katsuragawa et al., 2006), outer SBB (depths >100 m; Madureira et al., 2005), southern Brazilian shelf (Mello et al., 1992; Castello, 1998; Madureira et al., 2005), and coastal waters of Argentina (Hansen et al., 2001), supporting the idea that it is a keystone species of the SSAS (Bisbal, 1995; Castello, 1998; Hansen et al., 2001). Catches by industrial purse-seine fleets or during previous scientific surveys indicate that large schools of rough scad and Atlantic chub mackerel are common from the SBB to northern Argentina (Mello et al., 1992; Haimovici e al., 1994; Saccardo and Katsuragawa, 1995; Castro Hernández and Santana Ortega, 2000; Jaureguizar et al., 2006). The rough scad constitutes up to 85% of the standing stock of carangid larvae in the SBB (Katuragawa et al., 2006). Large bycatches of American coastal pellona and Atlantic cutlassfish are common in bottom trawl fisheries in the SBB (e.g., Paiva-Filho and Schmiegelow, 1986; Bernardes Júnior et al., 2011). The Brazilian sardinella is the most abundant fish in industrial purse-seine catches in the SBB (Vasconcellos and Gasalla, 2001), where its larvae are widely distributed (Katsuragawa et al., 2006).

The massive schools of flying gurnard juveniles detected in the water column were an uncommon and previously unreported phenomenon because this fish, which is morphologically adapted for living on soft bottoms (i.e., it has a relatively dorsoventrally flattened body and thoracic-placed pelvic fins to "walk" and forage over substrate; Sazima and Grossman, 2005), usually is captured in somewhat smaller numbers (generally <1% of the total catch; e.g., Wood et al., 2009) or is observed in small groupings (of approximately 30–50 individuals) foraging on soft bottoms (Sazima and Grossman, 2005). Shoaling and crowding behavior has been reported for related species (e.g., the Oriental flying gurnard [*Dactyloptena orientalis*]; Noble, 1966) on the bottom but not for such species in the pelagic habit. It has been speculated that flying gurnard juveniles of such species cluster together in the water column to feed opportunistically on transitory and dense patches of zooplankton commonly present in spring and summer (Cordeiro[7]; Lopes et al., 2006b).

The aggregation structure in the SBB differed from the structure of aggregations in the pelagic zone off the

[7] Cordeiro, C. A. M. 2014. Personal commun. Departamento de Ciências do Mar, Univ. Federal de São Paulo, Santos, Brazil.

SBB (i.e., at depths >100 m) as characterized during the REVIZEE midwater trawl surveys (Soares et al., 2005). Aggregations at depths of approximately 100 m were composed mainly of Argentine anchoita (89% of the total catch), followed by American coastal pellona (7%), Atlantic cutlassfish (7%), white snake mackerel (7%), and rough scad (1%). Therefore, these aggregations were fairly similar to those in the SBB at depths <100 m. In depths of 100–200 m , there was a strong shift in species abundance, and the aggregations there were primarily composed of a mesopelagic lightfish species (*Maurolicus stehmani*) (60% of the total catch), together with the Argentine anchoita (18%), striped codlet (*Bregmaceros cantori*; 7%), and Atlantic cutlassfish (4%).

Over the shelf break of the SBB (at depths of 200–800 m), aggregations contained virtually no Clupeiformes (Soares et al., 2005) and consisted mostly of *M. stehmani* (96% of the total catch), which were associated with a few species (e.g., Atlantic cutlassfish, and the largescale lizardfish [*Saurida brasiliensis*]). Such a replacement of Clupeiformes by mesopelagic fishes in the SBB is a typical pelagic shelf–slope gradient worldwide (e.g., Brodeur et al., 2003).

The aggregations found in the SBB were different from those that were hydroacoustically detected in a similar depth range (<100 m) off the central and northeastern coasts of Brazil. In central Brazil, they were composed of massive schools of the balloonfish (*Diodon holocanthus* [Madureira et al., 2004]) or of multiple species of triggerfishes (i.e., the unicorn filefish (*Aluterus monoceros*), gray triggerfish, queen triggerfish [*Balistes vetula*], and ocean triggerfish [*Canthidermis sufflamen*]). In northeastern Brazil, they were many fewer in number, compared with aggregations in southeastern Brazil, and they were composed of Myctophidae and Bothidae and did not contain schools of Clupeiformes (Vaske et al.[8]). In addition to the differences in efforts and spatiotemporal scales of sampling, these differences between the aggregations found in our study and those reported for the northeastern Brazil are most likely related to the pronounced zoogeographical contrast in fish fauna between the northeastern and southeastern coasts of Brazil (Joyeux et al., 2001).

Most of the records for tows carried out in areas identified as M most likely represented areas of mixing between CW and SACW, instead of between CW or SACW and Tropical Water. Tows conducted in M were carried out near the shoreline (mean distance: 37.2 km [32.6]), where the influences of CW and SACW are stronger than that of Tropical Water, which is located farther offshore (~80 km from the shoreline) during spring and summer (Castro, 2014).

Our results reveal that there were 2 groupings of species that showed high occurrence and attained the highest biomass in specific water masses in the SBB in the spring–summer season: 1) the grouping that was strongly related to SACW and was composed mostly of Argentine anchoita, Atlantic cutlassfish, rough scad, piquitinga anchovy, white snake mackerel, and Atlantic chub mackerel and 2) the grouping that was formed mostly by Brazilian sardinella, flying gurnard, false pilchard, American coastal pellona, Atlantic thread herring, castin leatherjacket, and Atlantic bumper (*Chloroscombrus chrysurus*) and was strongly associated with CW and areas of mixing between CW and SACW.

The peak in biomass of each grouping followed the variation in location of their preferred water masses in relation to depth in the water column and distance from shore. The biomass of SACW-related assemblages reached its peak in deeper (Fig. 4) nearshore areas, and the biomass of CW+M-related assemblages reached its peak in waters farther offshore (Fig. 4), more surface layers. Such a pattern is consistent with the spring–summer, complex hydrography of the SBB, and this hydrography generates spatial variations in temperature and salinity. Cyclonic eddies and meanders of the Brazil Current on the SBB are stronger in the spring and summer (Campos et al., 1995). Additionally, in this season, the large-scale high-pressure center in the South Atlantic makes winds blow from the northeast, resulting in stronger wind stress along the shore that leads to a surface offshore Ekman transport (Rodrigues and Lorenzetti, 2001). Both processes result in wide intrusion of the SACW frontal zone toward the inshore zones and in its persistence in deeper waters of the SBB just below the CW (Campos et al., 1995). Such a setting is more conspicuous near the shore between Cabo Frio and São Sebastião Island (Ciotti et al., 2014). Additionally, in the spring and summer, increased continental runoff may cause the CW to expand offshore and nearer the ocean surface on the SBB (Lopes et al., 2006a).

The consistent association of groups of species to specific water masses supports evidence that their life cycles are intimately tied to the typical water masses in the spring and summer at the SBB (Katsuragawa et al., 2006). Most of these species have a marked spawning activity in the spring and summer in the area (Katsuragawa et al., 2006), when the availability of planktonic food and the standing stock were at their highest levels (Lopes et al., 2006b). The growth of pelagic fish larvae occurs at a higher rate in specific temperature ranges, and those ranges differ among species (e.g., Matsuura, 1998). Therefore, this observed fidelity to habitat (water mass) may ensure suitable food supply within optimal temperature conditions for higher larval growth, survival, and recruitment, in turn, ensuring reproductive success (Matsuura, 1998; Jablonski and Legey, 2004). For example, the body condition of larvae of Argentine anchoita was highest in the SACW upwellings (Clemmesen et al., 1997). Results from studies based on observational data (Matsuura, 1998; Jablonski and Legey, 2004) and simulated data (Dias et al.,

[8] Vaske, T., Jr., R. .P. Lessa, A. Monteiro, J. L. Bezerra, Jr, A. C. B. Ribeiro, L. Yokota, K. C. Moura, K. Lopez, and J. P. Firmino. 2005. Programa de Prospecção Acústica do Nordeste do Brasil (Levantamento da fauna com rede de meia água). REVIZEE Relatório Final, 54 p.

2014) have indicated that the reproductive activity and larval growth rates of Brazilian sardinella were higher at higher temperatures (~21–27°C) of CW in the SBB.

Although some species, such as the flying gurnard, Brazilian sardinella, and piquitinga anchovy, have been more abundant in a specific water mass, they co-occurred more frequently with species that were more abundant in another water mass. For example, although the Brazilian sardinella was more abundant in CW+M, it occurred more frequently with species more abundant in SACW. This result reveals that the species show a high flexibility with environmental variability and that their abundance patterns are characterized by gradients (instead of fixed points) that follow the environmental gradient defined from one water mass through another.

This study had 3 limitations. First, the number of fish samples from different water masses was not balanced within each survey and among the ECOSAR cruises; this difference in sampling may be one of the reasons for the lack of significant differences in fish structure among the different cruises (i.e., different years) and along the latitudes.

Second, although our large data set ensured a general overview of the species composition and abundance of pelagic fish aggregations in the SBB, we understand that our data set may be biased with regard to estimates of these attributes for the whole SBB pelagic nekton (i.e., the pool of organisms both inside and outside aggregations) because 1) it is unclear whether the adopted spatial scale for sampling best represented the variance in the biomass of populations because there was no previous study to inform it, 2) sampling randomness was not adopted, and 3) many pelagic large fast-swimming predators, such as sharks, the dolphinfish (*Coryphaena hippurus*), and the skipjack tuna (*Katsuwonus pelamis*), were poorly represented or not captured; despite being common in SBB aggregations (Rossi-Wongtschowski et al., 2014), such predators were not susceptible to midwater trawls (Brodeur et al., 2005). Therefore, it is strongly recommended that a future study should be based on information that helps to specify the best sampling spatial scale, on multiple sampling gear, and on a sampling design balanced in relation to cruises, latitudes, and water masses.

Third, although significant, the effect of the spatial variation of water masses explained little (7%) of the total variation in fish assemblage structure. The large body of undetermined effects in the data may result from important but unconsidered factors for recruitment success, for maintenance of stock size, and ultimately for spatiotemporal distribution of assemblages, such as turbulence, currents (Thomson et al., 1992), zooplankton availability, abundance, and productivity (Longhurst and Pauly, 2007), and especially the age of a population and its reproductive structure (Fablet et al., 2012; Carvalho and Castello, 2013; Dias et al., 2014).

Satellite-derived data for surface levels of chlorophyll-*a* during the periods of this study, used as a proxy for phytoplankton abundance, did not show significant effect on fish assemblage structure and therefore contributed to the large body of undetermined effects. For future studies, we recommended that phytoplankton be measured concomitantly with the tows, at the same depth of tow or as close as possible. Such simultaneous measurements should also be valid for other food resources, such as zooplankton. This concurrent measurement of phytoplankton would increase the possibility of detecting the recurrent and structuring role of plankton on pelagic assemblages of fishes (Longhurst and Pauly, 2007), of which the bulk of species are planktivorous. Other potential causes for this lack of significant effect are 1) that the spatial resolution of chlorophyll-*a* measurement may have been low and incompatible with the spatial scale of tows or 2) that fish populations may have a delayed response to phytoplankton and subsequent zooplankton peaks (Litz et al., 2014).

In conclusion, small pelagic fish populations dominated the multispecific aggregations over the SBB in spring and summer, and the spatiotemporal variability of the aggregations fitted well with the spring–summer, hydrographically complex structure of the SBB. Two species groupings were reliably linked to either the CW+M or the SACW. Such conclusions may support the adoption of an EBFM for the SBB, which has been heavily affected by fishing and activities related to oil and gas extraction.

For conservation purposes, for example, the mapping of the species assemblages in SBB water masses through remote sensing may be a useful indicator of the spatial variability of pelagic fish assemblages. The identification of areas with high density of Argentine anchoita will be particularly important for managing the potential, near-future exploitation of the SBB stocks of this species, stocks that are in almost-virginal condition (Madureira et al., 2009). The management of this stock will deserve particular attention because the Argentine anchoita population of the SBB exhibits a lower individual growth rate and a higher natural mortality rate than does the population that inhabits the southern Brazilian shelf (Carvalho and Castello, 2013). To better understand and forecast human-induced impacts in the SBB, an effective EBFM is needed and should include future efforts 1) to accurately estimate pelagic fish biomass and identify pelagic trophic groups to model food-web dynamics and 2) to investigate the relationship of fish assemblages and population structure and dynamics with water masses, physical forcings, and distribution of food availability to improve the predictability of multispecies multivariate models.

Acknowledgments

We are especially grateful to the Brazilian Institute of Environment and Renewable Natural Resources for funding the cruises for this study, and we thank the officers and crew of the ship *Atlântico Sul*, the staff

of the Fishing and Hydroacoustic Technology Laboratory, Federal University of Rio Grande, and the staff of the Laboratory of Growth and Ichthyology, Oceanography Institute of the University of São Paulo, for on-board work during cruises. We also thank D. Sasaki for producing the maps, M. Rodrigues da Costa, and A. Vaz dos Santos for their constructive contributions to an early manuscript version of this article, and 3 referees for their great contributions for improving the manuscript.

Literature cited

Anderson, M. J., R. N. Gorley, and K. R. Clarke.
2008. PERMANOVA for PRIMER: guide to software and statistical methods, 214 p. PRIMER–E Ltd., Plymouth, UK.

Bernardes Júnior, J. J., J. L. Rodrigues Filho, J. O. Branco, and J. R. Verani.
2011. Spatiotemporal variations of the ichthyofaunal structure accompanying the seabob shrimp, *Xiphopenaeus kroyeri* (Crustacea: Penaeidae), fishery in important fishery areas of the Santa Catarina shore, Brazil. Zoologia 28:151–164.

Bisbal, G. A.
1995. The Southeast South American shelf large marine ecosystem: evolution and components. Mar. Policy 19:21–38.

Brodeur, R. D., J. P. Fisher, R. L. Emmett, C. A. Morgan, and E. Casillas.
2005. Species composition and community structure of pelagic nekton off Oregon and Washington under variable oceanographic conditions. Mar. Ecol. Prog. Ser. 298:41–57.

Brodeur, R. D., W. G. Pearcy, and S. Ralston.
2003. Abundance and distribution patterns of nekton and micronekton in the northern California Current transition zone. J. Oceanogr. 59:415–434.

Burnham, K. P., and D. R. Anderson.
2002. Model selection and multimodel inference: a practical information-theoretic approach, 2nd ed., 488 p. Springer-Verlag, New York.

Campos, E. J. D., J. E. Gonçalves, and Y. Ikeda.
1995. Water mass characteristics and geostrophic circulation in the South Brazil Bight: summer of 1991. J. Geophys. Res., C 100:18537–18550.

Carvalho, F. M., and J. P. Castello.
2013. Argentine anchovy (*Engraulis anchoita*) stock identification and incipient exploitation in southern Brazil. Lat. Am. J. Aquat. Res. 41:820 – 827.

Castello, J. P., R. P. Habiaga, J. C. Amaral, and I Lima Jr.
1991. Prospecção hidroacústica e avaliação da biomassa de sardinha e anchoita, na região sudeste do Brasil (Outubro/novembro de 1998). Publ. Esp. Inst. Oceanogr. 8:15–29.

Castello, J. P.
1998. Teleósteos pelágicos. *In* Os ecossistemas costeiro e marinho do extremo sul do Brasil (U. Selliger, C. Odebrect, and J. P. Castello eds.). p. 137–143. Editora Ecoscientia, Rio Grande, Brazil.

Castro, B. M.
2014. Summer/winter stratification variability in the central part of the South Brazil Bight. Cont. Shelf Res. 89:15–23.

Castro, B. M., and L. B. Miranda.
1998. Physical oceanography of the western Atlantic continental shelf located between 4°N and 34°S coastal segment (4°W). *In* The Sea, vol. 11 (A. R. Robinson and K. H. Brink, eds.), p. 209–251. John Wiley & Sons, New York.

Castro Hernández, J. J., and A. T. Santana Ortega.
2000. Synopsis of biological data on the chub mackerel (*Scomber japonicus* Houttuyn, 1782). FAO Fish. Synop. 157, 77 p. FAO, Rome.

Ciotti, A. M., M. Mahiques, and O. O. Möller.
2014. The meridional gradients of the S-SE Brazilian continental shelf: introduction to the special volume. Cont. Shelf Res. 89:1–4.

Clarke, K. R., and R. M. Warwick.
2001. Change in marine communities: an approach to statistical analysis and interpretation, 2nd ed., 172 p. PRIMER-E, Plymouth, UK.

Clemmesen, C. M., R. P. Sánchez, and C. L. B. Rossi-Wongtschowski.
1997. A regional comparison of nutritional condition of SW Atlantic anchovy larvae (*Engraulis anchoita*) based on RNA/DNA ratios. Arch. Fish. Mar. Res. 45:17–43.

Cury, P., A. Bakun, R. J. M. Crawford, A. Jarre, R. A. Quiñones, L. J. Shannon, and H. M. Verheye.
2000. Small pelagics in upwelling systems: patterns of interaction and structural changes in "wasp-waist" ecosystems. ICES J Mar. Sci. 57:603–618.

Curtin, R., and R. Prellezo.
2010. Understanding marine ecosystem based management: a literature review. Mar. Policy 34:821–830.

Dias, D. F., L. P. Pezzi, D. F. M. Gherardi, and R. Camargo.
2014. Modeling the spawning strategies and larval survival of the Brazilian sardine (*Sardinella brasiliensis*). Prog. Oceanogr. 123:38–53.

Diggle, P. J., and P. J. Ribeiro.
2007. Model-based geostatistics, 232 p. Springer-Verlag, New York.

Dormann, C. F., J. Elith, S. Bacher, C. Buchmann, G. Carl, G. Carré, J. R. G. Marquéz, B. Gruber, B. Lafourcade, P. J. Leitão, T. Münkemüller, C. McClean, P. E. Osborne, B. Reineking, B. Schröder, A. K. Skidmore, D. Zurell, and S. Lautenbach.
2013. Collinearity: a review of methods to deal with it and a simulation study evaluating their performance. Ecography 36:27–46.

Duarte, L. O., and C. B. García.
2004. Trophic role of small pelagic fishes in a tropical upwelling ecosystem. Ecol. Model. 172:323–338.

Fablet, R., P. Gay, S. Peraltilla, C. Peña, R. Castillo, and A. Bertrand.
2012. Bags-of-Features for fish school cluster characterization in pelagic ecosystems: application to the discrimination of juvenile and adult anchovy (*Engraulis ringens*) clusters off Peru. Can. J. Fish. Aquat. Sci. 69:1329–1339.

Fletcher, D. J., and A. J. Underwood.
2002. How to cope with negative estimates of components of variance in ecological field studies. J. Exp. Mar. Biol. Ecol. 273:89–95.

Freire, R. R., and J. C. P. Vasconcellos.
2011. Cálculo de área de poligonais geodésicas ou loxodrômicas sobre o elipsóide do sistema geodésico WGS-84. Rev. Bras. Cartog. 63:555–563.

Haimovici, M., A. S. Martins, J. L. Figueiredo, and P. C. Vieira.
1994. Demersal bony fish of the outer shelf and upper slope of the southern Brazil subtropical convergence ecosystem. Mar. Ecol. Prog. Ser. 108:59–77.

Hansen, J. E., P. Martos, and A. Madirolas.
2001. Relationship between spatial distribution of the Patagonian stock of Argentine anchovy, *Engraulis anchoita*, and sea temperatures during late spring to early summer. Fish. Oceanogr. 10:193–206.

Harding, J. A., A. J. Ammann, and R. B. MacFarlane.
2011. Regional and seasonal patterns of epipelagic fish assemblages from the central California Current. Fish. Bull. 109:261–281.

Jablonski, S., and L. F. L. Legey.
2004. Quantifying environmental effects on the recruitment of the Brazilian sardine (*Sardinella brasiliensis*), 1977–1993. Sci. Mar. 68:385–398.

Jaureguizar, A. J., R. Menni, C. Lasta, and R. Guerrero.
2006. Fish assemblages of the northern Argentine coastal system: spatial patterns and their temporal variations. Fish. Oceanogr. 15:326–344.

Joyeux, J. C., S. R. Floeter, C. E. L. Ferreira, and J. L. Gasparini.
2001. Biogeography of tropical reef fish: the South Atlantic puzzle. J. Biogeogr. 28:831–841.

Katsuragawa, M., J. H. Muelbert, and J. F. Dias.
2006. O ictioplâncton na região entre o Cabo de São Tomé (RJ) e o Chuí (RS). *In* O ambiente oceanografico da plataforma continental e do talude na região sudeste-sul do Brasil (C. L. D. B. Rossi-Wongtschowski and L. S.-P. Madureira, eds.), p. 350–446. Edusp, São Paulo., Brazil.

Legendre, P., and L. Legendre.
1998. Numerical ecology, 2nd ed., 852 p. Elsevier Science BV, Amsterdam.

Litz, M. N. C., R. L. Emmett, P. J. Bentley, A. M. Claiborne, and C. Barceló.
2014. Biotic and abiotic factors influencing forage fish and pelagic nekton community in the Columbia River plume (USA) throughout the upwelling season 1999–2009. ICES J Mar. Sci. 71:5–18

Longhurst, A. R., and D. Pauly.
2007. Ecologia dos oceanos tropicais, 424 p. Edusp, São Paulo, Brazil.

Lopes, R. M., M. Katsuragawa, J. F. Dias, M. A. Montú, J. H. Muelbert, C. Gorri, and F. P. Brandini.
2006b. Zooplankton and ichthyoplankton distribution on the southern Brazilian shelf: an overview. Sci. Mar. 70:189–202.

Lopes, R. M., M. A. Montú, C. Gorri, E. Muxagata, L. Miyashita, and L. P. Oliveira.
2006a. O zooplâncton marinho da região entre o Cabo de São Tomé (RJ) e o Chuí (RS). *In* O ambiente oceanografico da plataforma continental e do talude na região sudeste-sul do Brasil (C. L. D. B. Rossi-Wongtschowski and L. S. Madureira, eds.), p. 265–358. Edusp, São Paulo, Brazil.

Madureira, L. S. P., J. P. Castello, C. Prentice-Hernández, M. I. Queiroz, M. L. Espírito Santo, W. H. Ruiz, P. R. Abdallah, J. E. Hansen, M. I Bertolotti, E. Manca, M. I. Yeannes, N. Avdalov, and F. Amorín.
2009. Current and potential alternative food uses of the Argentine anchoita (*Engraulis anchoita*) in Argentina, Uruguay and Brazil. *In* Fish as feed inputs for aquaculture: practices, sustainability and implications (M. R. Hasan and M. Halwart, eds.), p. 269–287. FAO Fish. Aquacult. Tech. Pap. 518. FAO, Rome.

Madureira, L. S.-P., R. G. P. Habiaga, A. Gonçalves, A. B. Greig, A. C. Duvoisin, C. F. Soares; I. Y. Fuse, F. G. Caldeira, L. R. Carvalho; S. C. Weigert, P. A. Saldo, and C. S. Ferreira.
2004. Prospecção de recursos pelágicos por método hidroacústico na plataforma, talude e região oceânica da costa Central do Brasil. Série Documentos REVIZEE: Score Sul, 56 p. Instituto Oceanográfico—USP, São Paulo, Brazil.

Madureira, L. S. P., M. C. Vasconcellos, S. C. Weigert, R. P. Habiaga, M. Pinho, C. S. Ferreira, A. C. Duvoisin, C. F. Soares, and M. A. Bruno.
2005. Distribuição, abundância e interações ambientais de espécies pelágicas na região sudeste e sul do Brasil, entre Cabo de São Tomé (RJ) e o Chuí (RS). *In* Prospecção de recursos pesqueiros pelágicos na Zona Econômica Exclusiva da região sudeste-sul do Brasil: hidroacústica e biomassas (L. S. P. Madureira and C. L. D. B. Rossi-Wongtschowski, eds.), p. 63–131. Instituto Oceanográfico—USP, São Paulo, Brazil.

Matsuura, Y.
1998. Brazilian sardine (*Sardinella brasiliensis*) spawning in the southeast Brazilian Bight over the period 1976–1993. Rev. Bras. Oceanogr. 46:33–43.

Mello, R. M., J. P. Castello, and K. M. F. Freire.
1992. Asociación de espécies pelágicas marinas en el sur de Brasil durante invierno y primavera. Frente Mar., Sec. A, 11: 63–69.

Möllmann, C., C. Folke, M. Edwards, and A. Conversi.
2015. Marine regime shifts around the globe: theory, drivers and impacts. Phil. Trans. R. Soc. B. 370:1–5.

Noble, A.
1966. Note on the food of flying gurnard, *Dactyloptena orientalis* (Cuvier). J. Mar. Biol. Assoc. India. 8(2):368–369.

Paiva-Filho, A. M., and J. M. M. Schmiegelow.
1986. Estudo sobre a ictiofauna acompanhante da pesca do camarão sete-barbas (*Xyphopenaeus kroyeri*) nas proximidades da Baía de Santos—SP. I.—Aspectos quantitativos. Bol. Inst. Oceanogr. 34:79–85.

Pecquerie L., L. Drapeau, P. Fréon, J. C. Coetzee, R. W. Leslie, and M. H. Griffiths.
2004. Distribution patterns of key fish species of the southern Benguela ecosystem: an approach combining fishery-dependent and fishery-independent data. Afr. J. Mar. Sci. 26:115–139.

Podani, J.
2000. Introduction to the exploration of multivariate biological data, 407 p. Backhuys Publishers, Leiden, Netherlands.

R Core Team.
2014. R: a language and environment for statistical computing. R Foundation for Statistical Computing, Vienna, Austria. [Available at website, accessed April 2014.]

Rocha, G. R. A., and C. L D. B. Rossi-Wongtschowski.
1998. Demersal fish community on the inner shelf of Ubatuba, Southeastern Brazil. Rev. Bras. Oceanogr. 46:93–109.

Rodrigues, R. R., and J. A. Lorenzetti.
2001. A numerical study of the effects of bottom topography and coastline geometry on the southeast Brazilian coastal upwelling. Cont. Shelf Res. 21:371–394.

Rossi-Wongtschowski, C. L. D. B., E. Y. Muto, and L.S.H. Soares.
2008. Ictiofauna. *In* Oceanografia de um ecossistema subtropical: plataforma de São Sebastião, SP (A.M.S. P. Vanin, ed.), p. 381–404. Edusp, São Paulo, Brazil.

Rossi-Wongtschowski, C. L. D. B., A. M. Vaz-dos-Santos, and C. C. Siliprandi.
2014. Checklist of the marine fishes collected during hydroacoustic surveys in the southeastern Brazilian Bight from 1995 to 2010. Arq. Zool. 45:73–88.

Saccardo, S. A., and M. Katsuragawa.
1995. Biology of the rough scad *Trachurus lathami*, on the southeastern coast of Brazil. Sci. Mar. 59:265–277.

Sazima, C., and A. Grossman.
2005. A non-digging zoobenthivorous fish attracts two opportunistic predatory fish associates. Neotrop. Ichthyol. 3:445–448.

Soares, C. F., L. S. P. Madureira, L. P. Habiaga, L. D. Laurino, C. S. Ferreira, and S. C. Weigert.
2005. Caracterização dos ecotipos detectados durante os cruzeiros de prospecção pesqueira acústica entre Cabo de São Tomé (RJ) e Chuí (RS). *In* Prospecção de recursos pesqueiros pelágicos na Zona Econômica Exclusiva da região sudeste-sul do Brasil: hidroacústica e biomassas (L. S. P. Madureira and C. L. D. B. Rossi-Wongtschowski, eds.), p. 17–61. Instituto Oceanográfico—USP, São Paulo, Brazil.

Speckman, S. G., J. F. Piatt, C. V. Minte-Vera, and J. K. Parrish.
2005. Parallel structure among environmental gradients and three trophic levels in a subartic estuary. Prog. Oceanogr. 66:25–65.

Thomson K. A., W. J. Ingraham, M. C. Healey, P. H. LeBlond, C. Groot, and C. G. Healey.
1992. The influence of ocean currents on latitude of landfall and migration speed of sockeye salmon returning to the Fraser River. Fish. Oceanogr. 1:163–179.

Vasconcellos, M. C., and M. A. Gasalla.
2001. Fisheries catches and the carrying capacity of marine ecosystems in southern Brazil. Fish. Res. 50:279–295.

Willis, T. J., and M. J. Anderson.
2003. Structure of cryptic reef fish assemblages: relationships with habitat characteristics and predator density. Mar. Ecol. Progr. Ser. 257:209–221.

Wood, A. J. M., J. S. Collie, and J. A. Hare.
2009. A comparison between warm-water fish assemblages of Narragansett Bay and those of Long Island Sound waters. Fish. Bull. 107:89–100.

NOAA
National Marine
Fisheries Service

Fishery Bulletin
established 1881

Spencer F. Baird
First U.S. Commissioner
of Fisheries and founder
of *Fishery Bulletin*

Trends in biomass of coral reef fishes, derived from shore-based creel surveys in Guam

Mariska Weijerman (contact author)[1,2]
Ivor Williams[3]
Jay Gutierrez[4]
Shanna Grafeld[5]
Brent Tibbatts[4]
Gerry Davis[6]

Email address for contact author: mariska.weijerman@noaa.gov

[1] Joint Institute for Marine and Atmospheric Research
School for Ocean and Earth Science and Technology
University of Hawaii at Manoa
Marine Science Building 312
1000 Pope Road
Honolulu, Hawaii 96822

[2] Environmental System Analysis Group
Wageningen University
P.O. Box 47
6700 AA Wageningen, Netherlands

[3] Coral Reef Ecosystem Program
Ecosystem Sciences Division
Pacific Islands Fisheries Science Center
National Mariner Fisheries Service, NOAA
1845 Wasp Boulevard, Building 176
Honolulu, Hawaii 96818

[4] Division of Aquatic and Wildlife Resources
Guam Department of Agriculture
163 Dairy Road
Mangilao, Guam 96913

[5] Department of Natural Resources and Environmental Management
University of Hawaii at Manoa
1910 East-West Road
Sherman Laboratory 101
Honolulu, Hawaii 96822

[6] Habitat Conservation Division
Pacific Islands Regional Office
National Marine Fisheries Service, NOAA
1845 Wasp Boulevard, Building 176
Honolulu, Hawaii 96818

Abstract—Coral reef fisheries have a cultural, economic, and ecological importance and sustain the societal well-being of many coastal communities. However, the complexities of the multigear, multispecies fisheries that target coral reef species pose challenges for fisheries management. We focus on the Guam shore-based coral reef fishery 1) to evaluate the characteristics of the past and recent fishery in terms of catch composition and effort per gear type and 2) to reconstruct the reef-fish population in shallow (depths ≤30 m) water during 1985–2012. To accomplish this, we used the results from a detailed creel survey conducted by the Guam Division of Aquatic and Wildlife Resources. The total estimated effort has stayed more or less stable; however, the estimated total catch has dropped from an annual mean of 100 metric tons (t) during the period 1985–1990 to 37 t during the period 2007–2012. Catch per unit of effort (CPUE) declined for most gear types between the 2 time periods. Reconstruction of historical targeted fish biomass, based on CPUE, showed a general decrease in biomass from 1985 to 2012. Biomass quickly dropped to about half of the 1985 values, then leveled off for a decade before declining again beginning in 2003 and continuing through 2012.

Manuscript submitted: 30 April 2015.
Manuscript accepted: 2 March 2016.
Fish. Bull. 114:237–256 (2016).
Online publication date: 18 March 2016.
doi: 10.7755/FB.114.2.9

The views and opinions expressed or implied in this article are those of the author (or authors) and do not necessarily reflect the position of the National Marine Fisheries Service, NOAA.

Coral reef fishing is an important activity for the social and economic welfare of many coastal communities (Dalzell et al., 1996; Moberg and Folke, 1999). Both commercial and recreational fishing provides jobs, and fishing expenditures generate millions of dollars in sales revenues and value-added benefits to the states and territories of the United States that have coral reefs (Craig, 2008). Healthy fish stocks also support marine recreational activities, such as scuba diving (Parsons and Thur, 2008). Furthermore, in many Pacific islands, coral reef fisheries serve vital nonmarket functions, such as building social and community networks, perpetuating fishing traditions, and providing food for local communities (Dalzell et al., 1996; Plagányi et al., 2013; Zeller et al., 2015).

Despite their socio-economic importance, reef-associated fisheries have received relatively little attention, especially when compared with pelagic fisheries (Sadovy, 2005), and comprehensive data for reef fisheries are often lacking (Warren-Rhodes et al., 2003; Houk et al., 2012). Furthermore, reef fisheries are particularly challenging to assess because they typically are more complex than pelagic fisheries (Dalzell, 1996). Generally, multiple gear types are used in reef fisheries, and each gear type has its own selectivity and targets multiple species, resulting in overlaps in the composition of the landings of reef fisheries (Dalzell, 1996; McClanahan and Cinner, 2008). A global

comparative study of reef-fish landings and their ecological footprint concluded that 55% of coral reef fisheries in 49 island countries were unsustainable, on the basis of the difference between actual reef-fish landings and an annual coral reef maximum sustainable yield value of 5 metric tons (t)/km^2 (Newton et al., 2007). A more recent study in just the western Pacific Ocean found a decline in catches of artisanal fisheries in most Pacific countries (Zeller et al., 2015). The potential, and evidently current, widespread overexploitation of reef fisheries highlights the need for proper management of these resources.

We focused our study on trends in catch and effort of the reef-fish fishery of Guam, which is the largest island in Micronesia and the most southerly island of the Mariana Archipelago in the western Pacific Ocean. As in many other Pacific islands, fish have been important sources of food since the first human settlements (Hensley and Sherwood, 1993). From prehistoric to recent times, there have been at least 52 different fishing methods used on Guam (Kerr[1]), and some of these traditional practices, such as the seasonal harvest of bigeye scad (*Selar crumenopthalmus*), fishing with surround nets, and throw- or cast-net fishing, are all still in use (Hensley and Sherwood, 1993). Modern fishing of reef fishes on Guam is best considered a recreational or subsistence fishery, and pelagic fisheries dominate the commercial landings there (Allen and Bartram[2]). A study of households (van Beukering et al.[3]) conducted in 2007 reported that 35–45% of respondents were active fishermen and that 28% of the fish consumed were caught by family members or friends (the 400 respondents in this study included the main ethnic and socioeconomic groups in Guam). Fish make up an especially important source of food for large cultural events, such as baptisms, weddings, and village fiestas (Pinhey et al., 2006).

Apart from their cultural and socioeconomic significance, reef-fish populations can play an important role in enhancing the resilience of reef ecosystems (i.e., the capacity of reef ecosystems to sustain and recover from a human-induced disturbance). For example, abundant and diverse assemblages of herbivorous fishes are effective at reducing algal biomass and at opening up space for settlement of coral recruits (McClanahan, 1997; Mumby et al., 2007a; Mumby and Harborne, 2010; Graham et al., 2011, 2013; Mumby et al., 2013).

Unlike many other countries and territories with coral reefs, Guam has long-term (>50 years) data for its coral reef fishery that have been obtained from creel surveys conducted by the Division of Aquatic and Wildlife Resources (DAWR), Guam Department of Agriculture. This creel survey program provides information on overall harvest and catch per unit of effort (CPUE). In the mid-1980s, DAWR adapted their existing creel survey program to better reflect changes in fishing practices. This survey program now encompasses an offshore *boat-based* fishery and an inshore *shore-based* fishery. The boat-based fishery focuses mainly on trolling for pelagic species and bottom fishing for species of commercial value in deepwater (depths >30 m), and the shore-based fishery targets reef fish in shallow-water (depths ≤30 m) primarily for recreational, subsistence, and cultural reasons (Appendix 1).

Previous analysis of these creel survey data indicated that Guam has a low fishery yield compared with other Pacific islands (Dalzell, 1996). A more recent study concluded that there had been an 86–94% decline in recreational fish catches over the previous 50 years (Zeller et al., 2007, 2015). Other studies in Guam have documented a similar decreasing trend in both the numbers of fish landed and the mean size at capture (Myers, 1993; McIlwain and Taylor[4]; Lindfield et al., 2014). Hensley and Sherwood (1993) conducted a comprehensive analysis of just the shore-based fishery in Guam from 1982 through 1991. Their main conclusions were that the fishery had changed because of the implementation of more modern fishing techniques and a switch from a traditional economic system (barter, catch what you eat) to a more western one (dollar based, sell for profit) and that these changes led to more pressure on reef resources and to overharvesting the most frequently targeted species.

The perception that reef-fish stocks in Guam are depleted has been corroborated by a recent large-scale study based on visual-survey data; this study concluded that reef-fish biomass around Guam was 66% below what would be expected in the absence of human perturbations (Williams et al., 2015). Other studies with visual-survey data have noted the relative scarcity of large-bodied fishes around Guam and other populated islands in the Mariana Archipelago, compared with the lightly or unpopulated islands in this archipelago (Richards et al., 2011; Williams et al., 2011). A paucity of large fishes often is indicative of overfishing (Friedlander and DeMartini, 2002; Fenner, 2014).

Although these studies reflect the declining trend in catch and a depletion of the reef-fish biomass at Guam and provide evidence of the effects of fishing on the life history of some taxa (e.g., parrotfishes [*Chlorurus* spp., *Scarus* spp.]; Taylor and Choat, 2014), time series for the total biomass of reef-fish populations and changes in the composition of reef-fish catches have not been

[1] Kerr, A. M. 2011. Fishing methods of the Mariana Islands, Micronesia. Univ. Guam Mar. Lab. Tech. Rep. 132, 44 p. [Available at website.]

[2] Allen, S., and P. Bartram. 2008. Guam as a fishing community. NOAA Pacific Islands Fish. Sci. Cent. Admin. Rep. H-08-01, 61 p. [Available at website.]

[3] van Beukering, P. (ed.), W. Haider, M. Longland, H. Cesar, J. Sablan, S. Shjegstad, B. Beardmore, Y. Liu, G. O. Garces. 2007. The economic value of Guam's coral reefs. Univ. Guam Mar. Lab. Tech. Rep. 116, 102 p. [Available at website.]

[4] McIlwain, J. L., and B. M. Taylor. 2009. Parrotfish population dynamics from the Marianas Islands, with a description of the demographic and reproductive characteristics of *Chlorurus sordidus*: final report to the Western Pacific Regional Fishery Management Council, 61 p. Univ. Guam Mar. Lab., Mangilao, Guam. [Available at website]

quantified. These potential declines in fish populations reduce overall biomass, reproductive potential, and ecosystem function (Taylor et al., 2012; Mumby et al, 2013; Williams et al., 2015). We aimed to improve our understanding of the effects of this socially and culturally important fishery, using the shore-based creel data 1) to compare catch composition in the early years (1985–2000) with the composition in the recent years (2007–2012) and 2) to reconstruct trends in the population biomass of functional groups of reef-fish species over the period 1985–2012 by using recent visual-survey data as a relative index.

Materials and methods

Fishery data source: creel surveys

The creel surveys conducted around Guam by the DAWR included 2 distinct fisheries: the shore-based fishery and the boat-based fishery. This division of the data and the terms used to describe its 2 parts are widely used in Guam, including among fishery management agencies; therefore, we used them in our study. It is important to note that the shore-based fishery includes fishing from boats when boats are launched from shore (Appendix 1). The shore-based fishery differs from the boat-based fishery in several key aspects. In general, larger boats are used in the boat-based fishery, which primarily targets pelagic or bottomfish species, and predominantly is a commercial fishery. However, the boat-based fishery landings also include a substantial amount of reef fishes (Appendix 1). We chose not to include boat-based fishery results in our study for 2 reasons. First, boat-based fishing effort is recorded in trip hours, and shore-based fishing effort is recorded in gear hours; therefore, it was difficult to generate CPUE for just the fishing of reef fishes with the boat-based fishery to include in our analysis (Appendix 1 Figure 1). Second, trends in the catch from spearfishing in the boat- and shore-based fisheries are very consistent, indicating that, at least for reef-fish species, these trends reflect changes that are common among the targeted stocks (Appendix 1 Figure 2).

Categorization of species into functional groups

We analyzed records in the catch database of the shore-based component of the creel survey program for Guam (DAWR data obtained from a database maintained by the Western Pacific Fisheries Information Network [WPacFIN[5]], NOAA Pacific Islands Fisheries Science Center [PIFSC]). A total of 580 species or families appeared in the records. For some taxa, there were very little data; therefore, we grouped data of all taxa on the basis of their taxonomy, ecological function, and importance to fisheries, as shown in Table 1.

Collection of catch and effort data

The shore-based surveys of the DAWR creel survey program are designed to collect information on effort and catch for all shore-based fishing activities (Hensley and Sherwood, 1993; Zeller et al., 2007). There are 2 parts in the shore-based fishery: 1) visual surveys to establish the number of people participating in fishing activities (which are called *participation surveys*) and to collect data on the type of fishing activities observed (effort data) and 2) interviews of a sample of fishermen to collect data on the duration of fishing activities and numbers and sizes of fish caught (catch and effort data). Effort was recorded as hours fished per gear type (gear hour) and catch was recorded as the number and weights of fish caught per hour fished per gear type (Oram et al.[6]). Data from restricted areas (Appendix 2) were collected during aerial surveys conducted on the same 2 days that the participation surveys took place (Oram et al.[6]).

Catch values for the shore-based fishery are provided on a voluntary basis by fishermen to creel surveyors. Effort primarily is based on the visual surveys of fisherman participating in fishing activities, with details about the actual hours of fishing coming from interviews. When conducting surveys, DAWR staff attempt to interview fishermen for each type of gear observed during the participation surveys (Appendix 3 Table 1). However, interviewers are not always able to collect information on all types of gear. For example, since 2005, many spear fishermen have refused to participate in the creel surveys (Lindfield et al., 2014). Consequently, the number of snorkel-spear interviews has declined from an average of 30 per year in 1985–90 to an average below 8 interviews per year during 2007–2012 (Appendix 3 Table 1), and this decline is unfortunate because counts of observations made during participation surveys indicate that spearfishing represents one of the most used fishing method of the shore-based fishery in terms of effort (Bak[7]). Because collecting data on CPUE for most of the taxa and for most of the gears was difficult and infrequent, results dependent on the CPUE statistics were grouped at the family taxon level and are best considered as relative measures.

Estimates of total catch, total effort, and catch per unit of effort

The staff of the PIFSC program WPacFIN who collaborates with the DAWR, use an expansion algorithm

[5] WPacFIN (Western Pacific Fishery Information Network). 2013. Guam shore-based creel survey. NOAA Pacific Islands Fish. Sci. Cent., Honolulu, HI. [Metadata available at website.]

[6] Oram, R., T. Flores Jr., B. Tibbatts, J. Gutierrez, J. P. Gesner, S. Wusstig, A. Regis, D. Hamm, M. Quach, and P. Tao. In press. Guam shore-based creel survey. NOAA Pac. Islands Fish. Sci. Cent. Admin. Rep., 25 p.

[7] Bak, S. 2012. Evaluation of creel survey program in the western Pacific region (Guam, CNMI, and American Samoa), 58 p. Unpubl. report prepared for the Western Pacific Regional Fishery Management Council, Honolulu, HI 96813.

Table 1

Categorization of functional groups, based on taxonomy, ecological function, or importance to fisheries, used in our study of trends of fish biomass in data from shore-based creel surveys conducted around Guam during 1985–2012

Functional group name	Description and notes	Example species
Bait fishes	Sardine-like species that periodically come to nearshore waters in large numbers	*Selar crumenophthalmus*, *Ellochelon vaigiensis*, *Gerres longirostris*, *Crenimugil crenilabis*
Invertebrates	The top shell (*Tectus niloticus*) was the dominant component in the total catch of invertebrates as a result of very high landings of this single species of 30 t in 1985 and 16 t in 1991	Crabs, lobsters, sea cucumbers, mollusks, octopuses, urchins, and clams
Nonreef-fish species	Species that are pelagic, deepwater, freshwater, or associated with sandy bottoms	Tuna, deepwater snappers (e.g., *Etelis coruscans*), *Kuhlia rupestris*
Macroalgae Planktivores	Fish species that feed on particles from water column	Soldierfishes (Holocentridae), some unicornfishes (e.g., *Naso annulatus*), chromises (*Chromis* spp.), cardinalfishes (*Apogon* spp.)
Coral-consuming fishes	Fish species that feed primarily on corals	Mostly butterflyfishes (*Chaetodon* spp.)
Detritivores	Fish species that feed primarily on detritus	Surgeonfishes (*Ctenochaetus* spp.)
Invertebrate-consuming fishes	Fish species that feed on invertebrates, separated into exploited species and lightly or nonexploited species	Exploited: emperors (*Lethrinus* spp.), snappers (*Lutjanus* spp.), goatfishes (Mullidae), wrasses (*Cheilinus* spp.); lightly or nonexploited: porcupinefishes (*Diodon* spp.), filefishes (*Aluterus* spp.)
Herbivore-browsers	Fish species that browse on plants, separated into exploited species and lightly or nonexploited species	Exploited: sea chubs (*Kyphosus* spp.), rabbitfishes (*Siganus* spp.), unicornfishes (e.g., *Naso unicornis*); lightly or nonexploited: milkfish (*Chanos chanos*)
Herbivore-grazers	Fish species that graze on plants, separated into exploited species and lightly or non-exploited species	Exploited: surgeonfishes (*Acanthurus* spp.); lightly or nonexploited: sergeants (*Abudefduf* spp.)
Herbivore-scrapers	Fish species that feed on plants and scrape hard substrate (including corals); all exploited species	Small-bodied parrotfishes (e.g., most species of *Scarus*, *Chlorurus sordidus*)
Herbivore-excavators	Fish species that feed on plants and excavate hard substrate (including corals); all exploited species	Large-bodied parrotfishes (e.g., most species of *Chlorurus*, *Scarus rubroviolaceus*)
Humphead parrotfish	An exploited species	*Bolbometopon muricatum*
Humphead wrasse	An exploited species	*Cheilinus undulates*
Benthic piscivores	Fish species that feed primarily on other fishes and are mostly resident to a reef area separated into exploited species and lightly or nonexploited species	Exploited: groupers (*Epinephelus* spp.); lightly or nonexploited: morays (*Gymnothorax* spp.)
Mid-water piscivores	Fish species that feed primarily on other fishes and are benthopelagic, all exploited species	Leatherjacket (*Scomberoides* sp.), needlefishes (Belonidae), reef cornetfish (*Fistularia commersonii*)
Roving piscivores	Fish that feed primarily on other fishes and rove on reefs; all exploited species	Jacks (Carangidae), barracudas (*Sphyraena* spp.)
Rays	All exploited species	Stingrays (Myliobatiformes)
Sharks	All exploited species	Reef-associated sharks (e.g., blacktip reef shark [*Carcharhinus melanopterus*], grey reef shark [*C. amblyrhynchos*], and whitetip reef shark [*Triaenodon obesus*])

to extrapolate results of the interviews of a sample of fishermen from shore-based surveys to estimates of island-wide catch and effort (Bak[7]). For comparisons of the fishery characteristics of the late 1980s with those of recent years, we used these WPacFIN estimates of aggregate effort and catch to examine possible shifts in fishing activities and catch composition. We somewhat arbitrarily chose to pool across 6-year periods to represent the *early* and *recent* periods of fishery data. It was important to pool across multiple years to increase the amount of data available, especially for the recent period (2007–2012); data were pooled also because of large interannual variability.

Fishery-independent surveys: calculation of biomass

In 2011, scientists of the Coral Reef Ecosystem Program of the NOAA Pacific Islands Fisheries Science Center conducted an intensive, short-term stationary-point-count survey (133 sample sites) of shallow (depths ≤30 m), hard-bottom coral reef areas around Guam. The methods used in this survey are described in detail in Williams et al. (2012) and briefly outlined here. Data of fish abundance and size distribution came from random visual surveys stratified into 3 depth ranges (<6 m, 6–18 m, and 18–30 m). Because roving apex predators, such as sharks (Carcharhinidae) and jacks (Carangidae), are generally not well sampled by divers in small-area surveys, information on abundance and size distribution of species of roving apex predators came from broad-scale towed-diver surveys conducted around Guam in 2007, 2009, and 2011 by the Coral Reef Ecosystem Program (Richards et al., 2011).

Length estimates of fishes from visual censuses were converted to weight by using allometric length–weight conversion:

$$W = a^{*}TL^{b}, \quad (1)$$

where a and b = constants;
TL = total length in millimeters; and
W = wet weight in grams.

Length–weight parameters came from Taylor,[8] Taylor et al. (2012), Taylor and Choat (2014), FishBase (Froese and Pauly[9]), and Nadon et al. (2015). In cases where length–weight information did not exist for a given species, parameters from congeners were used.

For each taxon, trophic classification was based on diet information, largely from FishBase. Using biomass density from the diver surveys and known areas of habitat from GIS maps, which were adapted within the Coral Reef Ecosystem Program from other GIS products (NCCOS[10]), we estimated biomass per functional group and for all fishes combined; these estimates were minimum values because cryptic and nocturnal fishes generally are undercounted by daytime visual surveys.

Estimation of catchability and reconstruction of historical fish biomass

A reconstructed time series of reef-fish biomass can be estimated from a CPUE time series and gear-specific catchability coefficients (Haddon, 2001). Generally, it is assumed that catch rates are linearly related to stock biomass and that the catchability coefficient is constant (Haddon, 2001). For the reconstruction in our study, we estimated the relationship between CPUE (as a proxy for relative biomass) and fish population biomass by incorporating a fishery-independent estimate of biomass in 2011, as described in the previous section. This approach requires that the CPUE data come from a representative sample, where the catch was taken in a consistent way by one or more fishing methods. The CPUE data used in this study had limitations, namely that the CPUE data for taxa infrequently encountered by any gear type in the DAWR creel surveys were not reliable; infrequently encountered taxa included many reef fishes, although the CPUE data have been shown to be reliable for some of the jacks (Bak Hospital[11]). Because of these limitations, in addressing federal management by means of annual catch limits, the CPUE time series available from the creel surveys were rejected for reef-fish stock assessments (Sabater and Kleiber, 2014). However, in this study, we were interested not in absolute abundance or stock size but in temporal trends of fish populations and relative differences between the late 1980s and recent years, and these data are suitable for that purpose.

In the shore-based surveys, 9 gear types were differentiated (Table 2). The gear type *hooks-and-gaffs* was used almost entirely to catch octopus (98% of hook-and-gaff landings for the period 1985–2012), and the type *other methods* included gears used in gleaning for invertebrates and algae (60% and 16% of total landings per respective gear type; WPacFIN[5]) (Hensley and Sherwood, 1993). Therefore, for the historical reconstruction of reef-fish biomass, we excluded catch and effort data for the gear types hooks-and-gaffs and other methods from analyses. We also excluded catch and effort data for the gear type cast nets from estimation of reconstructed reef-fish biomass because cast nets were used primarily to catch juvenile fishes (i.e., rabbitfishes [*Siganus* spp.], goatfishes [Mullidae], and

[8] Taylor, B. 2012. Personal commun. James Cook University, Townsville, Queensland 4811, Australia.

[9] Froese, R., and D. Pauly (eds.). 2015. FishBase, vers. 10/2015. [World Wide Web electronic publication; available at website, accessed March 2015.]

[10] NCCOS (National Centers for Coastal Ocean Science). 2005. National Centers for Coastal Ocean Science, Shallow-Water Benthic Habitats of American Samoa, Guam, and the Commonwealth of the Northern Mariana Islands (CD-ROM). Silver Spring, MD. [Metadata available at website]

[11] Bak Hospital, S. 2015. Western Pacific creel survey program data summary and analysis: Guam, the Commonwealth of the Northern Mariana Islands, and American Samoa. NOAA Pac. Islands Fish. Sci. Cent. Admin. Rep. H-15-06C, 194 p. [Available from Pac. Islands Fish. Sci. Cent., Natl. Mar. Fish. Serv., NOAA, 1845 Wasp Blvd., Bldg. 176, Honolulu, HI 96818.]

Table 2

Annual mean fishing effort, catch, and catch per unit of effort (CPUE), by gear type, in Guam during the 2 periods 1985–1990 and 2007–2012. Data were collected during shore-based creel surveys conducted by the Guam Division of Aquatic and Wildlife Resources and expanded by the Western Pacific Fisheries Information Network of the NOAA Pacific Islands Fisheries Science Center. Catch and effort values are based on expanded data and exclude nonreef-associated fishes (e.g., pelagic, freshwater, and intertidal fish species). Values of CPUE (with standard errors [SEs] in parentheses) are based on unexpanded interview data (not on a ratio of tabled catch and effort). *P*-values are from the Welch's 2-sample *t*-test (which allowed unequal variances), in which CPUE was compared between the 2 time periods. NA represents cases when less than 3 interviews per year per gear type were available (see Appendix 3 Table 1). Effort is given in gear hours (gh), and catch is given in kilograms.

	1985–1990			2007–2012			
Gear type	Mean effort (gh) (% of total)	Mean catch (kg)	CPUE (SE) (kg/gh)	Mean effort (gh) (% of total)	Mean catch (kg)	CPUE (SE) (kg/gh)	*P*-value
Hook and line	127,219 (58.5%)	22,464	0.15 (0.02)	145,309 (70.6%)	17,828	0.08 (0.02)	0.015
Cast net	31,913 (14.7%)	15,88	00.36 (0.04)	29,555 (14.4%)	4,108	0.10 (0.02)	<0.001
Gill net	22,647 (10.4%)	28,259	1.25 (0.11)	10,918 (5.3%)	9,807	0.56 (0.18)	0.01
Surround net	1470 (0.7%)	4128	1.36 (0.67)	552 (0.3%)	555	0.67 (0.08)	NA
Snorkel spear[1]	18,453 (2.9%)	16,507	0.76 (0.15)	11,736 (5.7%)	2,137	0.19 (0.06)	0.013
Scuba spear[1]	1553 (0.7%)	988	0.75 (0.10)	155 (0.1%)	58	0.34 (0.04)	NA
Hooks and gaffs	6396 (2.9%)	2228	0.30 (0.05)	5554 (2.7%)	2,139	0.36 (0.16)	NA
Drag net	901 (0.4%)	1377	1.18 (0.53)	141 (0.1%)	133	0.97 (0.35)	NA
Other gear	6868 (3.2%)	8454	0.55 (0.29)	1930 (0.9%)	181	0.07 (0.01)	0.10
Total	217,420	100,285		205,850	36,945		

[1]Catch and effort values for 2007–2012 are underestimated because most spear fishermen refused to participate in interviews after 2005 (Lindfield et al., 2014).

jacks) that can be hyper-abundant in shallow, sandy bays that were not part of the sampling domain for the fishery-independent visual surveys from which we took data. Appendix 4 shows the number of times each of the exploited fish groups defined in Table 1 were caught by fishermen interviewed for the creel survey program; data were broken out by gear type and pooled into 3-year time periods.

During the interviews for the creel surveys, fishing is reported per region per day type (i.e., weekday or weekend days; for a map of the regions used for creel surveys, see Appendix 2 Figure). Therefore, we first compared annual average CPUE by region and day type, using a Welch 2-sample *t*-test for cases in which we had at least 6 years of CPUE data with at least 3 observations per year (Appendix 3 Table 2). On the basis of the results of these tests (Appendix 5), we decided to aggregate CPUE data over regions and day types for subsequent analyses. Even with such treatment, for some gear types, interview data were sparse, especially for surround net fishing, scuba spearfishing, and drag-net fishing (Appendix 3 Figure). Moreover, for drag-net fishing and scuba spearfishing, some values were missing. We calculated CPUE for missing data as the average of the 3 previous years (Appendix 3 Table 2).

We based our reconstruction of historical relative fish biomass on the assumption that CPUE (I), itself expressed as catch (C) divided by effort (E), is linearly related to biomass (B) in year t:

$$C_t/E_t = I_t = q * B_t. \quad (2)$$

We further assumed that the gear-specific catchability coefficient (q) was constant. Therefore, although catchability varies depending on the experience of the fisherman and other factors, we assumed that there is no overall change in catchability through time. We also assumed that the observational errors of CPUE were lognormal, were multiplicative, and had constant variance. Although these conditions are unlikely—given the small extent of actual interview data for many taxa and strata, with the resulting high incidence of zeros and Poisson-like distributions with outliers—these assumptions were adopted to allow a simple approximation. If there are n years in an analysis, the best estimate of the constant q is the geometric average of the time series of ratios of CPUE and biomass (I_t/B_t), and it can be calculated with the following equation (Haddon, 2001):

$$q = e^{\frac{1}{n}\sum \mathrm{Ln}\left(\frac{I_t}{B_t}\right)}. \quad (3)$$

This method is well established for pelagic fisheries (Haddon, 2001), and we further assumed that it is applicable for the complex reef fishery when we parsed out catches and effort by gear type. We used the fishery-dependent statistics to estimate CPUE per gear type per year and fishery-independent data to estimate biomass (as detailed previously). However, we had reliable biomass estimates only for 2011. Because we required an n

of at least 3, we assumed that the mean biomass was the same between 2010 and 2012 and equivalent to that derived from the stationary-point-count surveys conducted in 2011. For each gear type, we derived smoothed estimates of q in accordance with Equation 3, with an n of 3, I equal to the gear-specific annual CPUE values for 2010–2012, and B equal to the summed biomass of functional groups exploited by the gear type. Information on which functional groups to include in the summed biomass was derived from the catch composition of total landings for 1985–2012. Functional groups that composed more than 10% of the catch per gear type were included: for example, over this time span, 23% of the targeted browsers (e.g., unicornfishes [*Naso* spp.]), 12% of the target grazers (most surgeonfishes [*Acanthurus* spp.]), and 37% of the roving piscivores (e.g., jacks) were caught by gill-net fishing; therefore, we added the estimates of biomass from the visual surveys for those 3 groups for the calculation of q for gill-net fishing.

To reconstruct the annual total biomass for the period 1985–2012, we divided the gear-specific CPUE for each year by the estimated gear-specific catchability q, using Equation 2 rewritten as $B_t=I_t/q$. Within each year, we then calculated the reconstructed biomass for each functional group by multiplying the annual total biomass estimate by the species composition observed in 2011. For example, in 1985, the total biomass was estimated at 10,025 t, and excavators (large-bodied parrotfishes [e.g. *Chlorurus* spp.]) composed 1.3% of the species composition in 2011; given those values, the biomass of excavators in 1985 was estimated at 130 t (10,025×0.013). Therefore, the results of this analysis indicate trends in relative fish stock size over time, with the assumption of constant catchabilities and species composition.

Results

Past and recent periods: comparing total catch, effort, and catch per unit of effort

Hook-and-line was the most commonly used gear type, accounting for 59% of total estimated annual effort in 1985–1990 (past) and 71% of total estimated annual effort in 2007–2012 (recent) (Table 2). Cast nets were the second most often used gear type, accounting for ~14% of total annual estimated effort in both time periods. Effort for all other gear types was reported less frequently in recent years than during the earlier time period, and declines in effort between the time periods ranged from 16% for drag net fishing to 87% for hook-and-gaff fishing (Table 2). The decline in effort for those other gears was balanced by a 14% increase in effort for hook-and-line fishing, resulting in an estimated total fishing effort that was similar in the 2 time periods: an annual mean of 217,420 gear hours for 1985–1990 in contrast to an annual mean of 205,850 gear hours for 2007–2012.

Reported catch was considerably higher during the period 1985–1990, with an estimated mean annual total catch of 100 t, compared with an average of 37 t in the period 2007–2012 (Fig. 1, Table 2). The most noteworthy difference between the 2 time periods was a 74% decrease in the catch for cast net fishing despite little change in effort and a 21% decrease in the catch from hook-and-line fishing despite a 14% increase in effort. The largest decline in catch was for spearfishing: reported catch of snorkel spearfishing and scuba spearfishing dropped by 87% and 94%, respectively (with reported effort declining by 36% and 90%, respectively). However, the observed decline in estimated spearfishing effort and landings is certainly related to the refusal of some spear fishermen to participate in creel surveys since around 2005 (Lindfield et al., 2014).

Based on the total landings for the shore-based fishery and the use of 95 km^2 as the reef area at depths of 0–30 m around Guam (determined with the adapted habitat maps of hard- and soft-bottom habitats), annual yields dropped from 1.30 t/km^2 during 1985–1990 to 0.58 t/km^2 during 2007–2012. For reef-associated fishes (i.e., excluding pelagic fishes, invertebrates, and non-reef-associated species), annual yield was 1.59 t/km^2 and 0.74 t/km^2, respectively, and 71 km^2 were used as the reef area for hard-bottom habitat at depths of 0–30 m around Guam (determined with one of the adapted habitat maps).

Hook-and-line fishing was assumed to be the most reliable data source because hook and line gear was the dominant gear type in the catch and effort records. On the basis of the fishery data for this gear type only, landings showed no clear trend over time, albeit with large annual fluctuations (Fig. 2A). However, landings of species other than bait fishes (e.g., bigeye scad [*Selar crumenophthalmus*]) showed a downward trend (Fig. 2A). The mean annual CPUE, based on the unexpanded interview data, for hook-and-line fishing varied because of the interannual fluctuation in bait fish landings, but the overall mean CPUE decreased 49% between the 2 time periods, from an annual mean of 0.15 kg/gear hour (standard error [SE] 0.02) for 1985–1990 to 0.08 kg/gear hour (SE 0.02) for 2007–2012 (Table 2, Fig. 2B).

CPUE was also significantly lower in the recent time period for gill net fishing and snorkel spearfishing, compared with levels in the past. The only gear type for which CPUE did not significantly decrease (P=0.1) was the gear type *other methods* (i.e., reef gleaning), although CPUE for that type trended downward (Table 2). For the remaining gear types, there was not enough information to statistically compare differences between the time periods (annual number of interviews was less than 3); however, for all gear types, except hooks-and-gaffs, mean CPUE was lower in the recent time period and the overall trend showed a decline in CPUE (Appendix 3 Figure).

Species composition of landings

In most years, combined landings of browsers (predominantly unicornfishes and rabbitfishes) and invertebrate

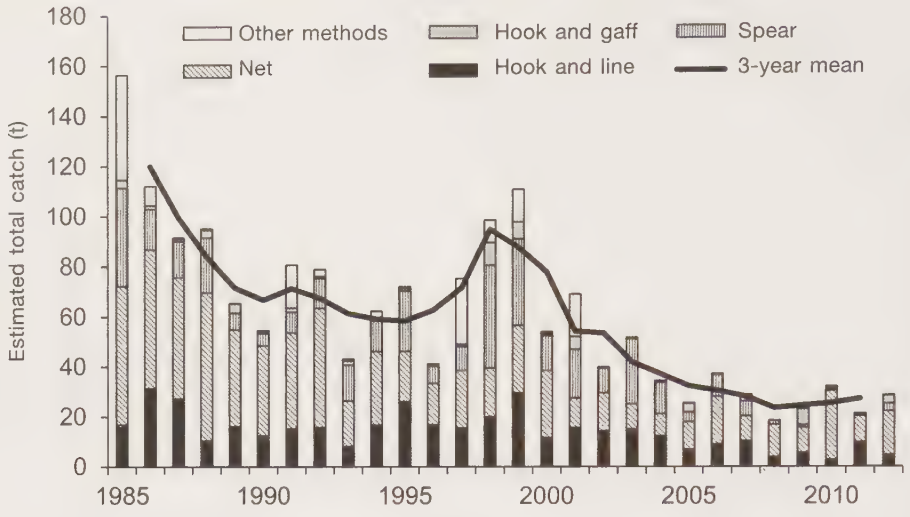

Figure 1

Time series of shore-based fishery landings in Guam for the period 1985–2012 in metric tons (t) per gear type based on expanded data provided by the Western Pacific Fisheries Information Network of the NOAA Pacific Islands Fisheries Science Center. Landings of pelagic bait fishes are excluded from the catches for hook-and-line fishing. Net fishing includes fishing with a cast net, gill net, surround net, and drag net, and spear fishing includes fishing with both scuba and snorkel spear. The gear type of the category "other methods" includes gears used in gleaning invertebrates and algae. The black line represents the 3-year mean of the catches summed over all gear types.

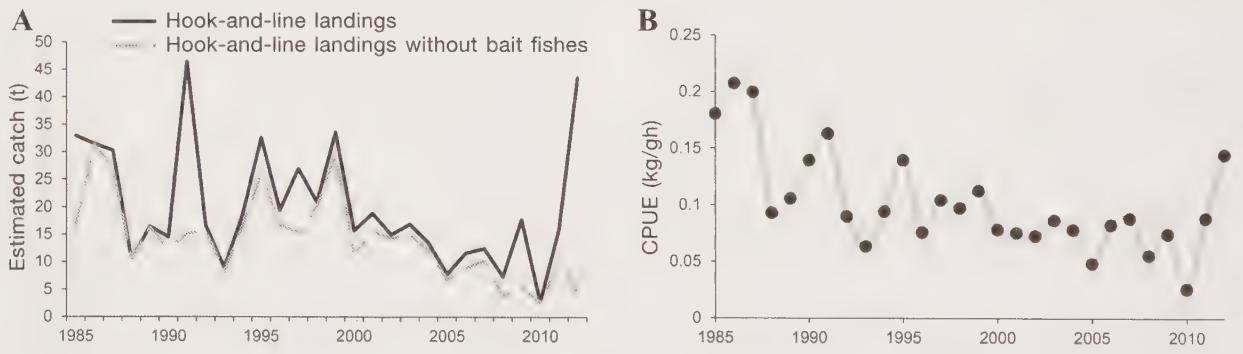

Figure 2

Around Guam for the period 1985–2012, time series (**A**) of landings for the shore-based hook-and-line fishery based on expanded data provided by the Western Pacific Fisheries Information Network of the NOAA Pacific Islands Fisheries Science Center and (**B**) of hook-and-line catch per unit of effort (CPUE) based on data from shore-based creel surveys conducted by the Guam Division of Aquatic and Wildlife Resources. Landings of pelagic bait fishes were excluded from data represented by the gray dashed line in graph A. Values of CPUE are given in kilograms per gear hour (gh).

feeders (predominantly goatfishes and emperors [*Lethrinus* spp.]) made up >40% of the total catch (Table 3). In comparison with catch data from the late 1980s, data for 2007–2012 showed a shift from the largest group being target browsers to the largest group being pelagic bait fishes. In general, the relative contribution of bait fishes increased over time, with bait fishes making up as much as 72.6% of the total catch (in 2012). The humphead parrotfish (*Bolbometopon muricatum*) was reported only in catches in 1985, and the humphead wrasse (*Cheilinus undulatus*) was reported in, on average, 0.4% of the catches during the period 1985–1990 but dropped to <0.1% of catches during the period 2007–2012. Roving piscivores, on the other

Table 3

Relative contributions of functional groups to the total catch per year, based on data collected during shore-based creel surveys conducted by the Guam Division of Aquatic and Wildlife Resources and expanded by the Western Pacific Fisheries Information Network of the NOAA Pacific Islands Fisheries Science Center. All values are percentages. Numbers in italic type indicate a contribution >15% to the annual total catch. The functional groups are described in Table 1.

Functional group	1985	1986	1987	1988	1989	1990	1991	1992	1993	1994	1995	1996	1997	1998	1999	2000
Bait fishes	*16.4*	6.8	7.2	9.1	9.8	*15.8*	*42.2*	12.0	9.9	10.1	13.9	10.7	*23.6*	3.7	6.5	*16.5*
Invertebrates	*22.0*	4.4	3.1	3.6	6.8	5.1	12.2	6.0	8.9	9.2	4.8	2.8	12.8	*15.4*	9.2	6.1
Nonreef-associated fishes	1.8	5.2	7.9	2.1	0.8	1.8	0 5	1.8	2.8	2.5	1.6	0.8	2.5	5.3	2.4	2.0
Macroalgae	3.2	3.2	0.1	0.1	0.0	0.0	0.5	0.1	0.3	0.8	0.3	0.0	11.6	3.4	6.6	0.1
Invertebrate-consuming fishes	*15.1*	*20.3*	*19.7*	*24.1*	*27.4*	*19.0*	9.5	*21.8*	*23.8*	*18.4*	*19.8*	*22.6*	13.8	*18.9*	12.5	*19.5*
Planktivorous fishes	1.9	0.7	1.1	0.7	2.2	1.5	0.6	1.2	5.2	1.8	2.2	2.5	1.4	3.0	1.1	2.0
Coral-consuming fishes	0.0	0.0	0.0	0.0	0.0	0.0	0.0	0.0	0.0	0.0	0.0	0.0	0.0	0.0	0.1	0.6
Detritivorous fishes	0.1	0.2	0.0	0.0	0.0	0.0	0.0	0.1	0.2	0.4	0.3	0.1	0.1	0.2	0.1	0.3
Browsers	*22.4*	*30.8*	*39.0*	*40.4*	*34.5*	*26.3*	*16.0*	*35.8*	*17.0*	*29.4*	*35.0*	*36.2*	*19.6*	*30.7*	*29.0*	*30.5*
Grazers	3.9	3.9	9.3	8.8	7.7	12.3	3.9	9.6	7.4	6.3	7.6	10.6	4.4	4.4	4.4	7.8
Scrapers	1.3	1.2	0.5	1.1	0.2	0.5	2.5	1.7	2.2	2.2	1.7	1.7	1.6	1.5	4.3	1.6
Excavators	1.8	0.0	0.0	0.2	0.0	0.5	0.9	0.9	0.8	0.7	1.6	1.0	0.4	2.7	1.2	0.8
Humphead parrotfish	0.2	0.0	0.0	0.0	0.0	0.0	0.0	0.0	0.0	0.0	0.0	0.0	0.0	0.0	0.0	0.0
Humphead wrasse	0.3	0.1	0.2	0.6	1.1	0.1	0.0	0.0	0.0	0.0	0.0	0.5	0.0	0.0	0.0	0.1
Benthic piscivores	1.7	2.5	5.2	2.2	1.1	5.4	2.6	3.2	8.1	4.5	4.5	2.3	2.4	4.0	4.4	5.4
Mid-water piscivores	3.0	3.0	0.0	1.6	3.0	2.8	1.6	1.1	2.2	3.2	2.1	2.2	0.2	0.5	3.4	1.3
Roving piscivores	4.7	3.3	6.8	5.2	4.8	8.9	7.1	4.3	9.6	3.6	3.3	5.9	5.4	6.0	10.5	5.4
Rays	0.0	0.1	0.0	0.2	0.4	0.0	0.0	0.0	0.0	0.0	0.0	0.0	0.0	0.1	0.0	0.0
Sharks	0.0	14.2	0.0	0.0	0.0	0.0	0.0	0.4	1.6	7.0	1.4	0.1	0.4	0.2	4.2	0.1

	2001	2002	2003	2004	2005	2006	2007	2008	2009	2010	2011	2012
Bait fishes	8.3	5.5	5.9	6.0	10.7	11.2	10.4	*21.1*	*47.5*	3.4	*30.1*	*72.6*
Invertebrates	*17.4*	3.8	14.4	6.9	*20.1*	5.5	7.8	2.2	13.7	2.9	1.0	4.8
Nonreef-associated fishes	1.9	1.2	5.5	13.1	3.5	2.2	0.4	2.3	2.6	5.0	0.6	2.8
Macroalgae	10.3	0.3	0.2	0.1	0.0	0.1	0.1	0.1	0.1	0.3	0.1	0.0
Invertebrate-consuming fishes	*19.7*	*20.8*	*17.8*	10.0	*20.5*	10.8	*16.2*	7.9	6.5	10.2	*15.3*	6.1
Planktivorous fishes	0.8	1.0	0.9	3.2	0.5	0.7	0.3	0.6	1.4	1.0	0.2	0.2
Coral-consuming fishes	0.2	0.0	0.0	0.0	0.0	0.0	0.0	0.1	0.0	0.0	0.0	3.9
Detritivores	2.2	0.0	0.0	0.0	0.1	0.3	2.7	0.0	0.0	0.0	0.0	0.0
Browsers	*16.8*	*35.0*	*26.1*	*22.4*	12.1	*35.9*	*25.7*	*21.1*	7.4	*46.1*	10.3	2.9
Grazers	5.1	5.6	10.3	9.8	8.2	8.4	5.5	8.7	6.9	*20.3*	6.8	0.3
Scrapers	0.6	1.1	3.4	0.9	2.1	2.6	0.9	4.8	0.6	1.3	1.7	0.5
Excavators	0.7	1.0	3.5	1.4	0.5	0.3	0.1	0.4	0.2	0.1	0.6	0.0
Humphead parrotfish	0.0	0.0	0.0	0.0	0.0	0.0	0.0	0.0	0.0	0.0	0.0	0.0
Humphead wrasse	0.0	0.0	0.2	0.0	0.0	0.1	0.4	0.0	0.0	0.0	0.0	0.1
Benthic piscivores	2.3	6.1	3.1	4.0	3.5	5.4	6.4	2.2	1.2	0.5	0.8	0.5
Mid-water piscivores	2.9	1.3	1.0	2.8	0.8	0.9	0.2	1.8	0.6	0.9	1.6	0.0
Roving piscivores	10.1	13.6	6.0	*19.4*	*17.2*	9.2	*22.9*	*24.2*	11.3	8.1	*30.9*	5.2
Rays	0.0	0.0	0.0	0.0	0.0	2.0	0.0	0.0	0.0	0.0	0.0	0.0
Sharks	0.7	3.5	1.8	0.0	0.3	4.3	0.1	2.4	0.0	0.0	0.0	0.0

hand, increased on average from 5.6% to 17.1% of the catch over the same time periods. The available data do not include information on fish size; therefore, it is not clear whether this increase was a result of increases in the seasonal fishery for juvenile jacks or in catches of mature jacks. However, because the gear types that target juveniles—hook-and-line and cast net—had increased catches and because catches by gill net, which does not target juvenile jacks, dropped by half, it appears that the increase in catch of roving piscivores was likely due to an increased catch of juveniles.

Reconstruction of fish biomass by functional group

Results from initial analysis of unexpanded data, from the interviews as part of the shore-based surveys, indicate that only for the CPUE for hook-and-line fishing in regions 1 and 2 on the eastern coast of Guam (for a map of the regions used in creel surveys, see Appendix 2 Figure) was there a difference ($P<0.05$) between day types (weekdays and weekend days), and there was no significant difference in CPUE between regions (Appendix 5). Therefore, to simplify analysis, we pooled

Table 4

Mean catch per unit of effort (CPUE), by gear type, determined from shore-based creel surveys conducted by the Guam Division of Aquatic and Wildlife Resources in 2010–2012 and estimated biomass of targeted species, by gear type, from visual surveys conducted by the Coral Reef Ecosystem Program of the NOAA Pacific Islands Fisheries Science Center in 2011. These values were used to calculate the catchability coefficient (q) for each gear type. Data for cast-net fishing were excluded from this analysis (see the *Materials and methods* section). gh=gear hour.

	CPUE (kg/gh)			Biomass	q
Gear type	2010	2011	2012	(t)	(/1000 gh)
Drag net	0.99	0.91	0.31	157	0.0042
Gill net	1.26	0.09	0.77	386	0.0012
Hook and line	0.03	0.09	0.14	324	0.0002
Scuba spear	0.37	0.40	0.24	544	0.0006
Snorkel spear	0.06	0.06	0.38	386	0.0003

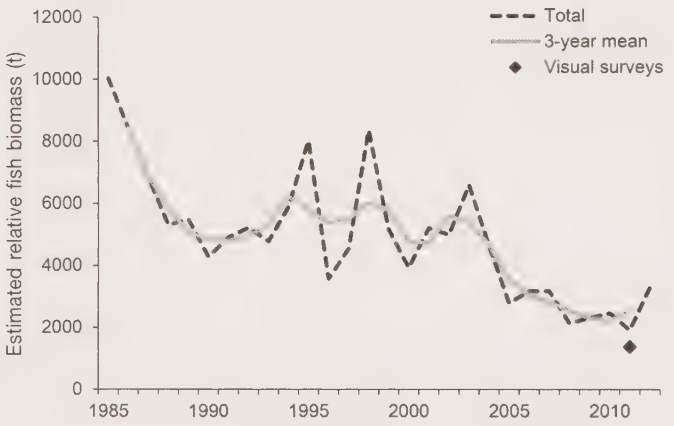

Figure 3

Reconstructed time series of total biomass of reef fishes in shore-based creel surveys conducted around Guam in 1985–2012 in relation to the estimate of total biomass from visual surveys conducted in 2011. The time series excludes pelagic species and bai tfishes and is based on annual catch composition per gear type with the assumption of a constant catchability coefficient for each gear type. The black diamond represents the estimated biomass for 2011 computed by multiplying biomass density (from surveys conducted by the Coral Reef Ecosystem Program of the NOAA Pacific Islands Fisheries Science Center) by the reef area (71 km^2) of hard-bottom habitats at depths of 0–30 m around Guam. The gray line indicates the 3-year mean of catches summed over all gear types.

the data up to the island level by combining both day types and all regions. With the estimated catchability coefficient of each gear type (Table 4), we reconstructed a time series for relative biomass (Fig. 3). There was a steep (almost 50%) downward trend in fish biomass from 1985 to around 1990. In the following decade, fish biomass leveled off but then declined again by about 2003 (Fig. 3).

On the basis of the reconstructed time series for total fish biomass (Fig. 3), we were able to estimate relative biomass of the functional groups targeted in the shore-based fisheries for reef fishes (Fig. 4). For the reconstructed biomass per functional group, species composition was assumed to have remained similar to the species composition observed during the visual surveys conducted in 2011 and, therefore, is an estimate of the true value.

Discussion

The fishery data used in this study show an overall reduction in catches in Guam that in turn indicates a general decline in reconstructed stock biomass from the late 1980s to recent years (Fig. 3)—a finding that is consistent with the results of fishery-independent surveys that show significant depletion of shallow-water reef-fish populations and large fishes around Guam (Richards et al., 2011; Williams et al., 2011, 2015). Parrotfishes were caught by hook-and-line fishing (33%) and by spearfishing (40%), and lower landings were reported in recent years. Assuming there have been no increases in recruitment and that the size composition of the catch reflects the size structure of the population, this decline in catches indicates a reduction in adult biomass and reproductive potential of the stock (Birkeland and Dayton, 2005). The decline in reconstructed biomass of parrotfishes and other herbivores (Fig. 4) observed in our study is also of some ecological concern. Herbivorous fishes play a critical role in maintaining benthic algal communities in states that are conducive for coral growth and recruitment (Mumby et al., 2007a; McClanahan, 1997), and herbivory is particularly important in promoting coral recovery after disturbances, such as hurricanes and bleaching events (Mumby et al., 2007b; Edwards et al., 2011; Graham et al., 2013). Therefore, declines in local parrotfish biomass may indicate that reefs surrounding Guam are less resilient to such events.

Estimated CPUE and catches for all gear types were substantially lower during the recent period (2007–2012) than they were during the period 1985–1990 (Table 2). Because CPUE estimates for the hook-and-line fishery in our earliest period (0.15 kg/gear hour for 1985–1990; Table 2) are considerably lower than the estimates recorded in Guam during the early 1980s (0.55 kg/gear hour; Katnik, 1982, cited in Dalzell et al., 1996), it seems likely that the evident downward trends in

CPUE and catch began before the first period for which we have creel data (before 1985). Fishery yields of reef fishes around Guam also have been low compared with previously published global yields for coral reef fisheries—annual levels that ranged from 0.2 to 44.0 t/km^2 (Dalzell, 1996). These global values are, however, confounded by differences in species groupings and effort reported for different locations around the world, as well as by the different assumptions about habitats included in area calculations. Still, our results clearly show that the downward trend in catch and CPUE, a pattern that earlier studies already noted (Hensley and Sherwood, 1993; Myers, 1993), has continued, and another study has reported that declines in catch started at least 50 years ago (Zeller et al., 2015).

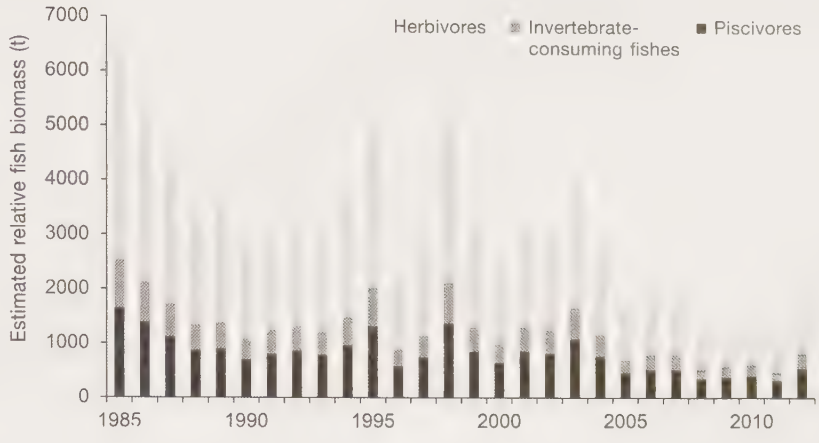

Figure 4

Reconstruction of relative biomass for 3 trophic groups for the period 1985–2012 based on a constant gear catchability coefficient per gear type and the reconstructed biomass determined with catch-per-unit-of-effort data from shore-based creel surveys conducted by the Guam Division of Aquatic and Wildlife Resources and with estimates of biomass, derived from the fishery-independent surveys conducted in 2011, for the functional groups targeted in shore-based creel surveys. Piscivores include mid-water piscivores (e.g., barracudas), benthic piscivores (e.g., groupers), and roving piscivores (e.g., jacks); invertebrate-consuming species include target species of this category; and herbivores include grazers (e.g., surgeonfishes), browsers (e.g., unicornfishes), scrapers (small-bodied parrotfishes), and excavators (large-bodied parrotfishes).

Declines in catch are not restricted to Guam. A recent synthesis of domestic catch reconstruction for 25 Pacific island countries and territories from 1950 to 2010 showed that, at 60% of those localities, peak catch occurred before 2000 and that in only one location did the peak catch occur after 2010 (Zeller et al., 2015). Also noteworthy is the shift in catch composition, where the majority of the landings in recent years comprises lower-valued species, such as the bigeye scad (*Selar crumenophthalmus*). This change in catch composition could be a result of the large pulses in bait fish populations, but it could also indicate a change in composition of the fish community. A similar change in catch composition was found in an analysis of landings by spear fishermen (Lindfield et al., 2014). Scuba spearfishing around Guam was associated not only with a decline in the size of parrotfishes caught but also with a shift from a dominance of large parrotfishes to a mixed assemblage with increasing proportions of surgeonfishes. This shift in community structure and a possible loss in biodiversity could lead to altered ecosystem functioning. Shifts in community structure and an altered ecosystem functioning have been observed in Kiritimati, where, in comparison with an unfished location (Palmyra Atoll), apex predators were relatively smaller, had a shorter life span, and were less abundant and prey fishes were larger but not more abundant (Ruttenberg et al., 2011). In a global analysis of reef fish surveys, Mora et al. (2011) found a strong link between ecosystem functioning and biodiversity, the latter of which is negatively influenced by human populations through overexploitation or the loss or degradation of habitats. Effective efforts to conserve biodiversity should, therefore, include the preservation of the functional roles that species perform (Brown and Mumby, 2014).

Although we are confident that our results provide a good indication of trends in CPUE and in the derived relative fish biomass, our study has several limitations. Calculating the CPUE for a multispecies, multigear reef fishery is not straight forward. Among other issues, many factors influence the decisions that fishermen make about when and where to fish and which gear to use. Consequently, there are undocumented changes in selectivity or catchability of specific gear types over different temporal and spatial scales. Accounting for all of these dependent decisions of fishermen was beyond the scope of our study; however, there was no quantitative or anecdotal information that documented any systematic changes in those decisions over the time period for which we have data. Also, too little creel data are available for some gear types, such as cast nets, and for spearfishing, and that lack of data clearly limits the scope by which the WPacFIN-expanded data can fully represent the total catch and effort.

Additionally, the assumption that the species composition has stayed the same between 1985 and 2012 is also unlikely to be true because the catch composition did change. Fishing affects the species composition of piscivores (e.g., sharks and jacks), and large fishes are often the first ones to disappear from catch records (Friedlander and DeMartini, 2002; Fenner, 2014). We

recognize that it is important to be cautious in interpreting the results of our analysis of data from the creel survey program for Guam. However, the lack of alternative survey or fishery information over extended time periods makes it important that these data are used to their fullest extent.

The findings from our analysis of the data from shore-based creel surveys, given the above caveats, indicate a decline in relative biomass of reef-fish populations and a shift in community structure since the start (1985) of our study period. Our results are broadly in agreement with the findings of a number of previous studies that have focused on catches from boat- and shore-based fisheries in Guam (Hensley and Sherwood, 1993; Myers, 1993; Dalzell, 1996; Zeller et al., 2007, 2015), as well as with results of studies of local fish abundance and size distributions (Richards et al., 2011; Houk et al., 2012; Lindfield et al., 2014). Because fishing for reef fishes is an important social and cultural activity for fishermen and their families in Guam, the decline over recent decades in the biomass of stocks of shallow-water coral reef fishes is a cause for concern.

Acknowledgments

Funding for the senior author and S. Grafeld was obtained from the NOAA Coral Reef Conservation Program. We would like to acknowledge the staff at the Division of Aquatic and Wildlife Resources, Guam Department of Agriculture, for data collection and the following people at the NOAA Pacific Islands Fisheries Science Center: K. Low, M. Quack, and P. Tao for extracting and helping to interpret data, M. Nadon for advice on data analyses, and C. Boggs and J. Wetherall for their valuable comments on the draft manuscript.

Literature cited

Birkeland, C., and P. K. Dayton.
2005. The importance in fishery management of leaving the big ones. Trends Ecol. Evol. 20:356–358.

Brown, C. J., and P. J. Mumby.
2014. Trade-offs between fisheries and the conservation of ecosystem function are defined by management strategy. Front. Ecol. Environ. 12:324–329.

Craig, R. K.
2008. Coral reefs, fishing, and tourism: tensions in U.S. ocean law and policy reform. Stanford Environ. Law J. 27:3–41.

Dalzell, P.
1996. Catch rates, selectivity and yields of reef fishing. *In* Reef fisheries (N. V. C. Polunin and C. M. Roberts, eds.), p. 161–192. Springer Science+Media, Dordrecht, Netherlands.

Dalzell, P., T. J. H. Adams, and N. V. C. Polunin.
1996. Coastal fisheries in the Pacific islands. Oceanogr. Mar. Biol. Annu. Rev. 34:395–531.

Edwards, H. J., I. A. Elliott, C. M. Eakin, A. Irikawa, J. S. Madin, M. McField, J. A. Morgan, R. Van Woesik, and P. J. Mumby.
2011. How much time can herbivore protection buy for coral reefs under realistic regimes of hurricanes and coral bleaching? Global Change Biol. 17:2033–2048.

Fenner, D.
2014. Fishing down the largest coral reef fish species. Mar. Poll. Bull. 84:9–16.

Friedlander, A. M., and E. E. DeMartini.
2002. Contrasts in density, size, and biomass of reef fishes between the northwestern and the main Hawaiian islands: the effects of fishing down apex predators. Mar. Ecol. Prog. Ser. 230:253–264.

Graham, N. A. J., D. R. Bellwood, J. E. Cinner, T. P. Hughes, A. V. Norström, and M. Nyström.
2013. Managing resilience to reverse phase shifts in coral reefs. Front. Ecol. Environ. 11:541–548.

Graham, N. A. J., P. Chabanet, R. D. Evans, S. Jennings, Y. Letourneur, M. A. MacNeil, T. R. McClanahan, M. C. Öhman, N. V. C. Polunin, and S. K. Wilson.
2011. Extinction vulnerability of coral reef fishes. Ecol. Lett. 14:341–348.

Haddon, M.
2001. Modelling and quantitative methods in fisheries, rev. print., 406 p. Chapman and Hall, Boca Raton, FL.

Hensley, R. A., and T. S. Sherwood.
1993. An overview of Guam's inshore fisheries. Mar. Fish. Rev. 55(2):129–138.

Houk, P., K. Rhodes, J. Cuetos-Bueno, S. Lindfield, V. Fread, and J. L. McIlwain.
2012. Commercial coral-reef fisheries across Micronesia: a need for improving management. Coral Reefs 31:13–26.

Lindfield, S. J., J. L. McIlwain, and E. S. Harvey.
2014. Depth refuge and the impacts of SCUBA spearfishing on coral reef fishes. PLoS ONE 9(3):e92628.

McClanahan, T. R.
1997. Primary succession of coral-reef algae: differing patters on fished versus unfished reefs. J. Exp. Mar. Biol. Ecol. 218:77–102.

McClanahan, T. R., and J. E. Cinner.
2008. A framework for adaptive gear and ecosystem-based management in the artisanal coral reef fishery of Papua New Guinea. Aquat. Conserv.: Mar. Freshw. Ecosyst. 18:493–507.

Moberg, F., and C. Folke.
1999. Ecological goods and services of coral reef ecosystems. Ecol. Econ. 29:215–233.

Mora, C., O. Aburto-Oropeza, A. A. Bocos, P. M. Ayotte, S. Banks, A. G. Bauman, M. Beger, S. Bessudo, D. J. Booth, E. Brokovich, et al.
2011. Global human footprint on the linkage between biodiversity and ecosystem functioning in reef fishes. PLoS Biol. 9(4):e1000606.

Mumby, P. J., S. Bejarano, Y. Golbuu, R. S. Steneck, S. N. Arnold, R. van Woesik, and A. M. Friedlander.
2013. Empirical relationships among resilience indicators on Micronesian reefs. Coral Reefs 32:213–236.

Mumby, P. J., and A. R. Harborne.
2010. Marine reserves enhance the recovery of corals on Caribbean reefs. PLoS ONE 5(1):e8657.

Mumby, P. J., A. R. Harborne, J. Williams, C. V. Kappel, D. R. Brumbaugh, F. Micheli, K. E. Holmes, C. P. Dahlgren, C. B. Paris, and P. G. Blackwell.
2007a. Trophic cascade facilitates coral recruitment

in a marine reserve. Proc. Natl. Acad. Sci. U.S.A. 104:8362–8367.

Mumby, P. J., A. Hastings, and H. J. Edwards.
2007b. Thresholds and the resilience of Caribbean coral reefs. Nature 450:98–101.

Myers, R. F.
1993. Guam's small-boat-based fisheries. Mar. Fish. Rev. 55(2):117–128.

Nadon, M. O., J. S. Ault, I. D. Williams, S. G. Smith, and G. T. DiNardo.
2015. Length-based assessment of coral reef fish populations in the main and Northwestern Hawaiian Islands. PLoS ONE 10(8):e0133960.

Newton, K., I. M. Côté, G. M. Pilling, S. Jennings, and N. K. Dulvy.
2007. Current and future sustainability of island coral reef fisheries. Curr. Biol. 17:655–658.

Parsons, G. R., and S. M. Thur.
2008. Valuing changes in the quality of coral reef ecosystems: a stated preference study of SCUBA diving in the Bonaire National Marine Park. Environ. Resour. Econ. 40:593–608.

Pinhey, T. K., D. H. Rubinstein, and S. M. Vaughn.
2006. Fishing and fiestas in Guam: an exploratory note on the reinforcement of cultural traditions. Pacific Studies 29:74–82.

Plagányi, É. E., I. van Putten, T. Hutton, R. A. Deng, D. Dennis, S. Pascoe, T. Skewes, and R. A. Campbell.
2013. Integrating indigenous livelihood and lifestyle objectives in managing a natural resource. Proc. Natl. Acad. Sci. 110:3639–3644.

Richards, B. L., I. D. Williams, M. O. Nadon, and B. J. Zgliczynski.
2011. A towed-diver survey method for mesoscale fishery-independent assessment of large-bodied reef fishes. Bull. Mar. Sci. 87:55–74.

Ruttenberg, B. I., S. L. Hamilton, S. M. Walsh, M. K. Donovan, A. Friedlander, E. DeMartini, E. Sala, and S. A. Sandin.
2011. Predator-induced demographic shifts in coral reef fish assemblages. PLoS ONE 6(6):e21062.

Sabater, M., and P. Kleiber.
2014. Augmented catch-MSY approach to fishery management in coral-associated fisheries. *In* Interrelationships between corals and fisheries (S. A. Bortone, ed.), p. 199–218. CRC Press, Boca Raton, FL.

Sadovy, Y.
2005. Trouble on the reef: the imperative for managing vulnerable and valuable fisheries. Fish Fish. 6:167–185.

Taylor, B. M., and J. H. Choat.
2014. Comparative demography of commercially important parrotfish species from Micronesia. J. Fish Biol. 84:383–402.

Taylor, B. M., J. L. McIlwain, and A. M. Kerr.
2012. Marine reserves and reproductive biomass: a case study of a heavily targeted reef fish. PLoS ONE 7(6):e39599.

Warren-Rhodes, K., Y. Sadovy, and H. Cesar.
2003. Marine ecosystem appropriation in the Indo-Pacific: a case study of the live reef fish food trade. Ambio 32:481–488.

Williams, I. D., J. K. Baum, A. Heenan, K. M. Hanson, M. O. Nadon, and R. E. Brainard.
2015. Human, oceanographic and habitat drivers of central and western Pacific coral reef fish assemblages. PLoS ONE 10(4):e0120516.

Williams, I. D., B. L. Richards, S. A. Sandin, J. K. Baum, R. E. Schroeder, M. O. Nadon, B. Zgliczynski, P. Craig, J. L. McIlwain, and R. E. Brainard.
2011. Differences in reef fish assemblages between populated and remote reefs spanning multiple archipelagos across the central and western Pacific. J. Mar. Biol. 2011:Article ID 826234.

Williams, I., J. Zamzow, K. Lino, M. Ferguson, and E. Donham.
2012. Status of coral reef fish assemblages and benthic condition around Guam: a report based on underwater visual surveys in Guam and the Mariana Archipelago, April–June 2011. NOAA Tech. Memo. NMFS-PIFSC-33, 22 p.

Zeller D, S. Harper, K. Zylich, and D. Pauly.
2015. Synthesis of underreported small-scale fisheries catch in Pacific-island waters. Coral Reefs 34:25–39.

Zeller, D., S. Booth, G. Davis, and D. Pauly.
2007. Re-estimation of small-scale fishery catches for U.S. flag-associated island areas in the western Pacific: the last 50 years. Fish. Bull. 105:266–277.

Appendix 1

Boat-based and shore-based creel survey data

Data on both boat- and shore-based fisheries are collected during creel surveys conducted by staff of the Guam Division of Aquatic and Wildlife Resources (DAWR). Boat-based fisheries are focused mainly on trolling for pelagic species and bottom fishing for deepwater (depths >30 m) species for commercial reasons, and shore-based fisheries target shallow-water reef fishes for recreational or cultural reasons. Landings of fishes associated with shallow (depths ≤30 m) reefs—the focus of this study—accounted for 26% of the total catch of fishes for the boat-based fishery from 1985 through 2012 (based on data from the DAWR boat-based creel surveys). In the last 3 years for which complete data are available (2010–2012), average annual catches of reef fishes from shore-based fisheries were 63 metric tons (t), of which reef fish composed 43.5% and bigeye scad (*Selar crumenopthalmus*) made up 50.2% (Appendix 1 Table). During the same time period, average annual catches from boat-based fisheries were 359 t, pelagic fishes accounted for 76.4% of the catch composition, and reef fishes accounted for 13.1%.

Although landings of reef fishes from shore-based fishing activities accounted for just 37% of the total (boat-based and shore-based combined) reef-fish landings, the shallow-reef fish populations exploited in the shore-based fishery potentially are very important for subsistence or cultural reasons. Data from interviews from the shore-based fishery of the DAWR creel survey program revealed that only one fisherman sold the catch, on one occasion, during the period from 1985 through 2012. Because boat-based fisheries account for a large amount of reef fish catches, we first determined whether the trend in catches of just the shore-based fisheries was comparable with the trend in catches from the boat-based fisheries of reef fishes and, if so, whether the trend would be representative of the catches of coral reef fish.

The majority of the reef fishes captured in the boat-based fisheries were caught by spearfishing with snorkel and scuba (Appendix 1 Fig. 1), gear types used in both boat-based and shore-based fisheries. We visually compared the difference in trends of the standardized values of catches between boat-based and shore-based spearfishing (Appendix 1 Fig. 2). A Comparison of these trends from both fisheries indicates that only in about the first 4 years did values differ by 2–4 units but, beginning in 1988, values were very similar between the fisheries, leading us to conclude that the trends in catches reflect common changes in the target stocks as well.

Appendix 1 Table

Composition of catches from the boat-based and shore-based components of the creel survey conducted in Guam during 2010–2012. Other=invertebrates and unknown species. Data came from the Guam Division of Aquatic and Wildlife Resources and the Western Pacific Fisheries Information Network of the NOAA Pacific Islands Fisheries Science Center.

	Boat-based fishery		Shore-based fishery	
Species	Portion of catch (%)	Average annual catch (kg)	Portion of catch (%)	Average annual catch (kg)
Reef fishes	13.1	47,021	43.5	27,465
Pelagic fishes	76.4	274,129	0.6	395
Bottom fishes	3.3	11,729	0.0	5
Bigeye scad	6.9	24,754	50.2	31,714
Other	0.3	947	5.7	3614
Total	100.0	358,579	100.0	63,193

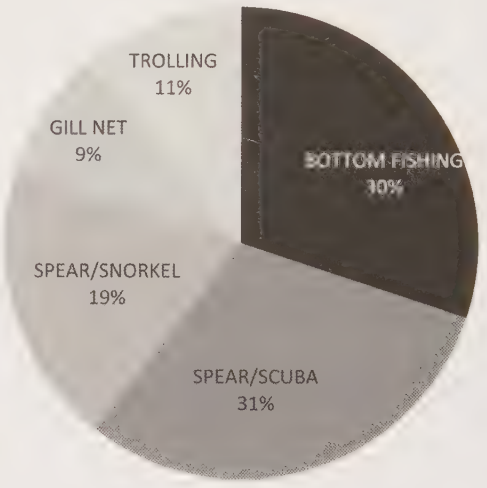

Appendix 1 Figure 1

Composition of the 5 gear types used most in boat-based fisheries to catch reef fishes (representing 98% of reef fish catches) during 2000–2005, based on data from the Guam Division of Aquatic and Wildlife Resources and the Western Pacific Fisheries Information Network of the NOAA Pacific Islands Fisheries Science Center.

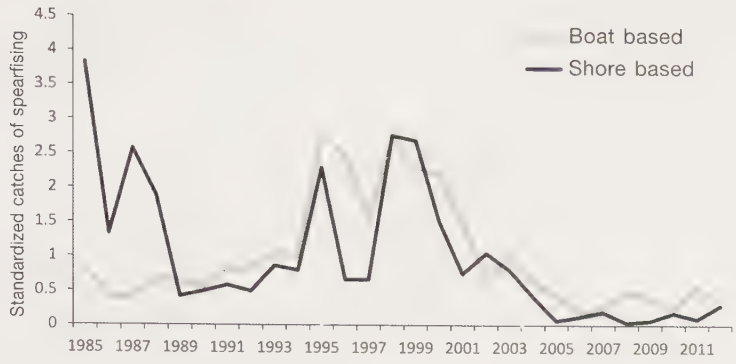

Appendix 1 Figure 2

Comparison of standardized catches of reef fishes between boat-based (gray line) and shore-based (black line) spearfishing during 1985–2012, based on data from the Guam Division of Aquatic and Wildlife Resources and the Western Pacific Fisheries Information Network of the NOAA Pacific Islands Fisheries Science Center.

Appendix 2

Shore-based creel surveys

For reporting purposes of the shore-based fishery of the creel survey program of the Guam Division of Aquatic and Wildlife Resources, Guam has been divided into 93 fishing sites that are grouped into 4 coastal regions (Appendix 2 Figure):

- Region 1 consists of the northwestern portion of Guam from Gun Beach to Adelup (sites 1–11)
- Region 2 consists of the southwestern portion of Guam from Adelup to Agat (sites 12–34, excluding inaccessible sites 35–41)
- Region 3 consists of the central-eastern to southern portion of Guam from Pago Bay to Merizo (sites 42–71, excluding inaccessible sites 57–60)
- Region 4 consists of the northern part of Guam, and access is restricted there because of a military base (sites 72–93)

The staff of the Western Pacific Fisheries Information Network (WPacFIN), NOAA Pacific Islands Fisheries Science Center, provides assistance with fishery statistics to partners at the Guam Division of Aquatic and Wildlife Resources and has developed an expansion algorithm to extrapolate results of the shore-based creel surveys into estimates of island-wide catch and effort. The shore-based creel surveys have 2 parts, interviews of a sample of fishermen and surveys where fishing activities were observed and recorded (participation surveys). Staff of the WPacFIN estimated annual fishing effort (measured in gear hours) per gear type per region by multiplying the total number of gear hours fished, from observations in the participation survey, by 2 correction factors 1) the ratio of the number of days in a year to the total number of scheduled survey days and 2) the number of available fishing hours in the morning and in the evening (Bak, footnote 1 in the main text). Staff of the WPacFIN estimated total annual catch per gear per region as the product of total annual effort and the gear- and region-specific average catch per unit effort (CPUE), the latter derived within each stratum as total sampled catch divided by total sampled effort. The estimated total catch per species within each stratum was calculated by multiplying aggregate annual catch by the ratio of that particular species in the catch from the interviews (Bak[12]). Missing CPUE data was substituted with a moving average of the previous 10 years of CPUE data.

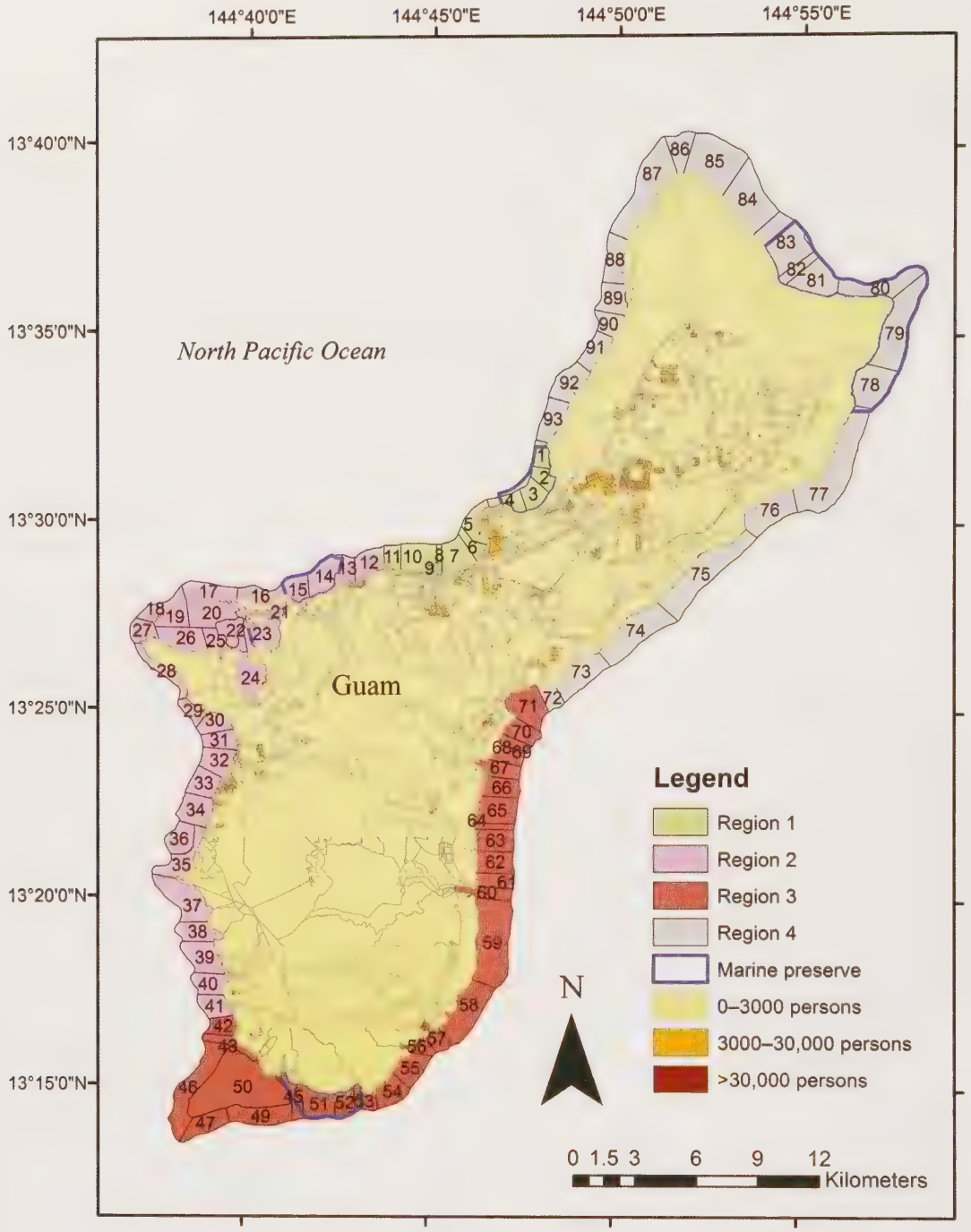

Appendix 2 Figure

Map of the fishery regions and sites around Guam where data were collected during shore-based creel surveys conducted by the Guam Division of Aquatic and Wildlife Resources (DAWR), based on a GIS shapefile of fishery sites from the DAWR.

Appendix 3

Interviews and catch per unit of effort

Appendix 3 Table 1

Number of interviews conducted as part of shore-based creel surveys conducted around Guam, per gear type per year. For some gear types in some years, the total number of interviews was between 1 and 4 or <5.

	1985	1986	1987	1988	1989	1990	1991	1992	1993	1994	1995	1996	1997	1998	1999
Hook and line	53	46	32	38	45	59	63	66	61	83	78	76	87	84	85
Gill net	38	34	28	28	25	41	35	40	33	36	49	31	50	48	51
Surround net	7	<5	<5	5	0	<5	0	<5	0	<5	<5	0	0	0	0
Snorkel spear	35	20	21	18	14	14	15	16	14	36	21	20	25	34	49
Scuba spear	<5	<5	0	<5	<5	<5	<5	<5	<5	<5	9	<5	<5	<5	<5
Drag net	8	9	8	<5	<5	5	7	7	6	<5	5	<5	<5	<5	10

	2000	2001	2002	2003	2004	2005	2006	2007	2008	2009	2010	2011	2012
Hook and line	86	86	60	78	61	60	65	61	64	62	57	48	45
Gill net	41	31	28	16	15	13	13	11	12	6	13	12	9
Surround net	0	0	0	<5	<5	0	<5	<5	<5	0	<5	<5	0
Snorkel spear	28	27	19	14	10	8	9	5	6	5	7	<5	11
Scuba spear	<5	<5	<5	<5	0	0	0	0	0	0	<5	0	0
Drag net	4	<5	0	0	0	<5	<5	0	0	0	0	0	0

Appendix 3 Table 2

Annual values of catch per unit of effort around Guam, by gear type and year, calculated by the Western Pacific Fisheries Information Network, NOAA Pacific Islands Fisheries Science Center, from data collected during shore-based creel surveys. Values in bold are the mean of the 3 previous years for values that were missing in the survey-data..

	1985	1986	1987	1988	1989	1990	1991	1992	1993	1994	1995	1996	1997	1998	1999
Hook and line	0.18	0.21	0.20	0.09	0.11	0.14	0.16	0.09	0.06	0.09	0.14	0.08	0.10	0.10	0.11
Gill net	1.19	1.16	1.11	1.76	1.08	1.18	0.94	0.85	0.45	0.64	0.61	0.48	0.49	0.29	0.51
Surround net	1.79	3.07	0.48	1.19	0.72	0.93	0.93	0.93	0.37	2.14	0.65	0.65	0.51	0.51	0.93
Snorkel spear	1.50	0.87	0.71	0.58	0.49	0.43	0.53	0.72	0.92	0.88	0.82	0.49	0.73	1.73	0.87
Scuba spear	1.25	**1.25**	1.25	0.53	0.89	0.34	0.40	0.32	0.34	0.34	2.04	0.32	0.34	0.64	0.29
Drag net	1.11	1.23	0.95	0.20	2.66	0.91	2.06	2.96	0.91	2.11	1.54	**1.52**	1.42	1.83	1.66

	2000	2001	2002	2003	2004	2005	2006	2007	2008	2009	2010	2011	2012
Hook and line	0.08	0.08	0.07	0.09	0.08	0.05	0.08	0.09	0.06	0.07	0.03	0.09	0.14
Gill net	0.62	0.50	0.46	0.35	0.25	0.66	0.18	0.45	0.63	0.15	1.26	0.09	0.77
Surround net	0.65	0.93	0.65	0.37	0.93	0.93	0.65	0.65	0.51	0.93	0.51	0.93	0.51
Snorkel spear	0.64	0.91	0.91	1.49	0.74	0.29	0.47	0.40	0.12	0.12	0.06	0.06	0.38
Scuba spear	0.32	0.40	0.40	0.24	0.40	0.34	0.32	0.40	**0.35**	**0.35**	**0.37**	0.40	0.24
Drag net	0.31	1.21	0.91	**0.81**	2.11	0.31	**1.08**	0.31	**0.56**	2.11	**0.99**	0.91	0.31

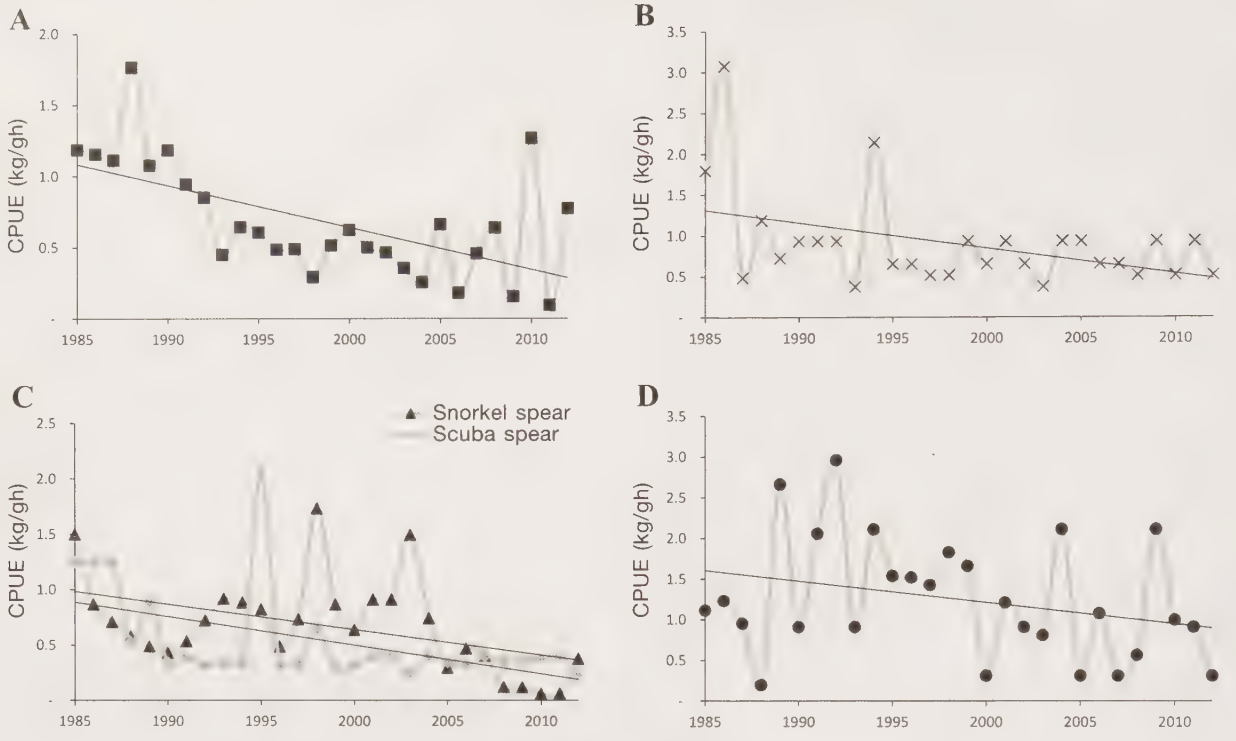

Appendix 3 Figure

Values of catch per unit of effort (CPUE) around Guam during 1985–2012 for (**A**) gill net fishing, (**B**) surround net fishing, (**C**) snorkel and scuba spearfishing, and (**D**) drag net fishing. The black lines indicate the linear trend line. gh=gear hour.

Appendix 4

Number of times landings included each functional group

The tables in this appendix provide the number of times that a functional group, as defined in Table 1 in the main text, was recorded from landings data for 3-year periods from interviews of shore-based creel surveys conducted around Guam from 1985 through 2012. Data are provided over 3-year periods to preserve the confidentiality of the identities of fishermen. Blank cells indicate that no interview took place in that period.

Appendix 4 Table

	Drag net	Gill net	Hook and line	Scuba spear	Snorkel spear	Surround net
Scrapers (small-bodied parrotfishes)						
1985–1987	0	10	2	4	61	2
1988–1990	0	7	0	0	18	0
1991–1993	0	39	3	1	18	0
1994–1996	0	34	5	6	53	5
1997–1999	1	54	8	5	120	
2000–2002	0	16	7	6	39	0
2003–2005	0	7	1	3	20	0
2006–2008	0	4	2		14	0
2009–2011		3	0	2	5	0
2012–2013		3	0		8	0

Table continued

Appendix 4 Table *continued*

	Drag net	Gill net	Hook and line	Scuba spear	Snorkel spear	Surround net
Excavators (large-bodied parrotfishes)						
1985–1987	0	3	0	0	24	0
1988–1990	0	2	0	0	7	0
1991–1993	0	8	2	4	8	0
1994–1996	0	4	3	7	21	0
1997–1999	0	6	6	5	39	
2000–2002	0	1	2	2	25	0
2003–2005	0	1	4	1	4	0
2006–2008	0	1	2		1	0
2009–2011		0	2	0	3	0
2012–2013		0	0		3	0
Target browsers (e.g., unicornfishes, rabbitfishes)						
1985–1987	11	92	68	10	198	24
1988–1990	6	112	85	1	137	2
1991–1993	2	104	116	4	46	4
1994–1996	3	80	114	20	129	4
1997–1999	10	145	138	12	229	
2000–2002	5	102	127	6	145	0
2003–2005	0	28	47	7	51	2
2006–2008	1	28	39		30	1
2009–2011		23	24	1	20	2
2012–2013		8	9		19	0
Target grazers (e.g., surgeonfishes)						
1985–1987	1	67	18	2	80	5
1988–1990	2	90	14	0	72	2
1991–1993	0	76	34	3	36	2
1994–1996	0	76	28	9	84	2
1997–1999	2	119	19	6	133	
2000–2002	0	64	21	4	77	0
2003–2005	0	25	26	1	29	1
2006–2008	0	17	17		16	1
2009–2011		10	9	0	8	3
2012–2013		4	5		9	0
Target invertebrate-consuming fishes (e.g., emperors, goatfishes, snappers)						
1985–1987	60	258	46	2	151	32
1988–1990	23	274	85	1	79	3
1991–1993	44	337	203	6	62	2
1994–1996	18	329	259	12	181	7
1997–1999	64	469	329	3	307	
2000–2002	14	305	255	13	163	0
2003–2005	1	77	136	8	47	4
2006–2008	1	29	117		28	0
2009–2011		48	71	1	16	3
2012–2013		33	29		29	0
Target benthic piscivores (e.g., groupers)						
1985–1987	1	10	8	1	31	1
1988–1990	0	39	33	1	32	0
1991–1993	0	55	93	2	26	1
1994–1996	0	22	61	3	47	2
1997–1999	0	32	68	1	71	
2000–2002	0	24	72	2	40	0
2003–2005	0	4	66	2	13	0
2006–2008	0	4	46		10	0
2009–2011		2	17	0	2	1
2012–2013		2	6		6	0

Table continued

Appendix 4 Table *continued*

	Drag net	Gill net	Hook and line	Scuba spear	Snorkel spear	Surround net
Mid-water piscivores (e.g., needlefishes, Heller's barracuda [*Sphyraena helleri*])						
1985–1987	13	16	17	1	4	7
1988–1990	6	9	25	0	1	0
1991–1993	6	22	25	0	4	0
1994–1996	4	20	29	0	6	1
1997–1999	12	25	25	0	19	
2000–2002	2	5	25	0	10	0
2003–2005	2	4	23	0	4	0
2006–2008	2	4	7		2	0
2009–2011		5	14	0	1	1
2012–2013		3	0		3	0
Roving piscivores (e.g., jacks)						
1985–1987	27	76	71	1	9	5
1988–1990	13	84	78	1	3	5
1991–1993	9	63	139	0	5	0
1994–1996	11	73	234	0	3	1
1997–1999	14	98	303	0	3	
2000–2002	6	66	236	0	5	0
2003–2005	0	20	189	1	3	1
2006–2008	0	10	190		1	2
2009–2011		19	132	0	1	0
2012–2013		13	89		1	0

Appendix 5

Comparison of catch per unit of effort between day types

Results from analysis in this study revealed a significant difference between weekday and weekend hook-and-line fishing in regions 1 and 2 (for location of these regions, see Appendix 1, Fig. 1). Comparisons of catch per unit of effort (CPUE) per day type for all regions combined and the gear types cast net, gill net, and snorkel spear did not show a significant difference ($P \geq 0.05$) between weekday and weekend fishing. There were not enough data to compare weekday and weekend CPUE for the remaining gear types.

Appendix 5 Table

Comparison of catch per unit of effort (CPUE) per gear type between day types (weekday and weekend) with a Welch 2-sample t-test (which allows for unequal variances) and between regions with analysis of variance (ANOVA) for the hook-and-line fishery around Guam. Values are means (and standard deviations [SD]) during 1985–2012. Region 0 is the combination of regions 1, 2, 3 and 4. Values of CPUE are given in kilograms per gear hour.

		Mean CPUE (SD)		Welch 2-sample *t*-test		ANOVA		
Gear type	Region	Weekday	Weekend	*P*	*n*	Mean CPUE	*P*	*n*
Hook and line	1	0.12 (0.09)	0.07 (0.05)	0.02	28	0.09 (0.06)	0.37	28
	2	0.10 (0.07)	0.07 (0.04)	0.04	28	0.09 (0.05)		
	3	0.12 (0.08)	0.09 (0.05)	0.10	28	0.11 (0.05)		
Cast net	0	0.25 (0.18)	0.22 (0.14)	0.45	28			
Gill net	0	0.65 (0.47)	0.71 (0.47)	0.62	28			
Snorkel spear	0	0.75 (0.57)	0.59 (0.37)	0.23	28			

Fishery Bulletin

Guidelines for authors

Contributions published in *Fishery Bulletin* describe original research in marine fishery science, fishery engineering and economics, as well as the areas of marine environmental and ecological sciences (including modeling). Preference will be given to manuscripts that examine processes and underlying patterns. Descriptive reports, surveys, and observational papers may occasionally be published but should appeal to an audience outside the locale in which the study was conducted.

Although all contributions are subject to peer review, responsibility for the contents of papers rests upon the authors and not on the editor or publisher. *Submission of an article implies that the article is original and is not being considered for publication elsewhere.*

Plagiarism and double publication are considered serious breaches of publication ethics. To verify the originality of the research in papers and to identify possible previous publication, manuscripts may be screened with plagiarism-detection software.

Manuscripts must be written in English; authors whose native language is not English are strongly advised to have their manuscripts checked by English-speaking colleagues before submission.

Once a paper has been accepted for publication, online publication takes approximately 3 weeks.

Types of manuscripts accepted by the journal

Articles

Articles generally range from 20 to 30 double-spaced typed pages (12-point font) and describe an original contribution to fisheries science, engineering, or economics. Tables and figures are not included in this page count, but the number of figures should not exceed one figure for every four pages of text. Articles contain the following divisions: **abstract, introduction, methods, results, and discussion.**

Short communications

Short communications are generally less than 20 double spaced typed pages (12-point font) and, like articles, describe an original contribution to fisheries science. They follow the same format as that for articles: **abstract, introduction, results and discussion, but the results and discussion sections may be combined**. Short communications are distinguished from full articles in that they report a noteworthy new observation or discovery—such as the first report of a new species, a unique finding, condition, or event that expands our knowledge of fisheries science, engineering or economics—and do not require a lengthy discussion.

Companion articles

Companion articles are presented together and published together as a scientific contribution. Both articles address a closely related topic and may be articles that result from a workshop or conference. They must be submitted to the journal at the same time.

Review articles

Review articles generally range from 40 to 60 double-spaced typed pages (12-point font) and address a timely topic that is relevant to all aspects of fisheries science. They should be forward thinking and address novel views or interpretations of information that encourage new avenues of research. They can be reviews based on the outcome from thematic workshops, or contributions by groups of authors who want to focus on a particular topic, or a contribution by an individual who chooses to review a research theme of broad interest to the fisheries science community. **A review article will include an abstract, but the format of the article *per se* will be up to the authors**. Please contact the Scientific Editor to discuss your ideas regarding a review article before embarking on such a project.

Preparation of manuscript

Title page should include authors' full names, mailing addresses, and the senior author's e-mail address.

Abstract should be limited to 200 words (one-half typed page), state the main scope of the research, and emphasize the authors conclusions and relevant findings. Do not review the methods of the study or list the contents of the paper. Because abstracts are circulated by abstracting agencies, it is important that they represent the research clearly and concisely.

General text must be typed in 12-point Times New Roman font throughout. A brief introduction should convey the broad significance of the paper; the remainder of the paper should be divided into the following sections: Materials and methods, Results, Discussion, and Acknowledgments. Headings within each section must be short, reflect a logical sequence, and follow the rules of subdivision (i.e., there can be no subdivision without at least two subheadings). The entire text should be intelligible to interdisciplinary readers; therefore, all acronyms, abbreviations, and technical terms should be written out in full the first time they are mentioned. Abbreviations should be used sparingly because they are not carried over to indexing databases and slow readability for those readers outside a discipline. They should never be used for the main subject (species, method) of a paper.

For general style, follow the U.S. *Government Printing Office Style Manual* (2008) [available at website] and *Scientific Style and Format: the CSE Manual for Authors, Editors, and Publishers* (2014, 8th ed.) published by the Council of Science Editors. For scientific nomenclature, use the current edition of the American Fisheries Society's *Common and Scientific Names of Fishes from the United States, Canada, and Mexico* and its companion volumes (*Decapod Crustaceans, Mollusks, Cnidaria and Ctenophora*, and *World Fishes Important to North Americans*). For species not found in the above mentioned AFS publications and for more recent changes in nomenclature, use the Integrated Taxonomic Information System (ITIS) (available at website), or, secondarily, the California Academy of Sciences *Catalog* of *Fishes* (available at website) for species names not included in ITIS. Common (vernacular) names of species should be lowercase. Citations must be given of taxonomic references used for the identification of specimens. For example, "Fishes were identified according to Collette and Klein-MacPhee (2002); sponges were identified according to Stone et al. (2011)."

Dates should be written as follows: 11 November 2000. Measurements should be expressed in metric units, e.g., 58 metric tons (t); if other units of measurement are used, please make this fact explicit to the reader. Use numerals, not words, to express whole and decimal numbers in the general text, tables, and figure captions (except at the beginning of a sentence). For example: We considered 3 hypotheses. We collected 7 samples in this location. Use American spelling. Refrain from using the shorthand slash (/), an ambiguous symbol, in the general text.

Word usage and grammar that may be useful are the following:

- *Aging* For our journal the word *aging* is used to mean both age determination and the aging process (senescence). The author should make clear which meaning is intended where ambiguity may arise.

- *Fish and fishes* For papers on taxonomy and biodiversity, the plural of *fish* is *fishes,* by convention. In all other instances, the plural is *fish.*
  Examples:
  The fishes of Puget Sound [biodiversity is indicated];
  The number of fish caught that season [no emphasis on biodiversity];
  The fish were caught in trawl nets [no emphasis on biodiversity].
  The same logic applies to the use of the words *crab* and *crabs, squid* and *squids,* etc.

- *Sex* For the meaning of male and female, use the word *sex*, not *gender.*

- *Participles* As adjectives, participles must modify a specific noun or pronoun and make sense with that noun or pronoun.
  Incorrect:
  Using the recruitment model, estimates of age-1 recruitment were determined. [Estimates did not use the recruitment model.]
  Correct:
  Using the recruitment model, we determined age-1 estimates of recruitment. [The participle now modifies the word *we,* i.e., those who were using the model.]
  Incorrect:
  Based on the collected data, we concluded that the mortality rate for these fish had increased. [*We* were not based on the collected data.]
  Correct:
  We concluded on the basis of the collected data that the mortality rate for these fish had increased. [Eliminate the participle and replace it with an adverbial phrase.]

Equations and mathematical symbols should be set from a standard mathematical program (MathType) and tool (Equation Editor in MS Word). LaTex is acceptable for more advanced computations. For mathematical symbols in the general text (α, χ^2, π, $\pm$, etc.), use the symbols provided by the MS Word program and italicize all variables, except those variables represented by Greek letters. Do not use photo mode when creating these symbols in the general text.

Number equations (if there are more than 1) for future reference by scientists; place the number within parentheses at the end of the first line of the equation.

Literature cited section comprises published works and those accepted for publication in peer-reviewed journals (in press). Follow the name and year system for citation format in the "Literature cited" section (that is to say, citations should be listed alphabetically by the authors' last names, and then by year if there is more than one citation with the same authorship. A list of abbreviations for citing journal names can be found at website.

Authors are responsible for the accuracy and completeness of all citations. Literature citation format: Author (last name, followed by first-name initials). Year. Title of article. Abbreviated title of the journal in which it was published. Always include number of pages. For a sequence of citations in the general text, list chronologically: (Smith, 1932: Green. 1947; Smith and Jones, 1985).

Digital object identifier (doi) code ensures that a publication has a permanent location online. Doi code should be included at the end of citations of published literature. Authors are responsible for submitting accurate doi codes. Faulty codes will be deleted at the page-proof stage.

Cite all software, special equipment, and chemical solutions used in the study within parentheses in the general text: e.g., SAS, vers. 6.03 (SAS Inst., Inc., Cary, NC).

Footnotes are used for all documents that have not been formally peer reviewed and for observations and personal communications. These types of references should be cited sparingly in manuscripts submitted to the journal.

All reference documents, administrative reports, internal reports, progress reports, project reports, contract reports, personal observations, personal communications, unpublished data, manuscripts in review, and council meeting notes are footnoted in 9 pt font and placed at the bottom of the page on which they are first cited. Footnote format is the same as that for formal literature citations. A link to the online source (e.g., [http://www/..... , accessed July 2007.]), or the mailing address of the agency or department holding the document, should be provided so that readers may obtain a copy of the document.

Tables are often overused in scientific papers; it is seldom necessary to present all the data associated with a study. Tables should not be excessive in size and must be cited in numerical order in the text. Headings should be short but ample enough to allow the table to be intelligible on its own.

All abbreviations and unusual symbols must be explained in the table legend. Other incidental comments may be footnoted with italic numeral footnote markers. Use asterisks only to indicate significance in statistical data. Do not type table legends on a separate page; place them above the table data. *Do not submit tables in photo mode.*

- Notate probability with a capital, italic *P*.
- Provide a zero before all decimal points for values less than one (e.g., 0.07).
- Round all values to 2 decimal points.
- Use a comma in numbers of five digits or more (e.g., 13,000 but 3000).

Figures must be cited in numerical order in the text. Graphics should aid in the comprehension of the text, but they should be limited to presenting patterns rather than raw data. Figures should not exceed one figure for every four pages of text and must be labeled with the number of the figure. Place labels **A, B, C,** etc. within the upper left area of graphs and photos. Avoid placing labels vertically (except for the y axis).

Figure legends should explain all symbols and abbreviations seen in the figure and should be double-spaced on a separate page at the end of the manuscript.

Line art and halftone figures should be submitted as pdf files with >800 dpi and >300 dpi, respectively. Color is allowed in figures to show morphological differences among species (for species identification), to show stain reactions, and to show gradations in temperature contours within maps. Color is discouraged in graphs, and for the few instances where color may be allowed, the use of color will be determined by the Managing Editor. Approved color figures should be submitted as TIFF or JPG files in CMYK format.

- Capitalize the first letter of the first word in all labels within figures.
- Do not use overly large font sizes in maps and for units of measurements along axes in graphs.
- Do not use bold fonts or bold lines in figures.
- Do not place outline rules around graphs.
- Place a North arrow and label degrees latitude and longitude (e.g., 170°E) in all maps.
- Use symbols, shadings, or patterns (not clip art) in maps and graphs.

Supplementary materials that are considered essential, but are too large or impractical for inclusion in a paper (e.g., metadata, figures, tables, videos, websites), may be provided at the end of an article. These materials are subject to the editorial standards of the journal. A URL to the supplementary material and a brief explanation for including such material should be sent at the time of initial submission of the paper to the journal.

- **Metadata, figures, tables** should be submitted in standard digital format (Word docx, pdf) and should be cited in the general text as (Suppl. Table, Suppl. Fig., etc.).
- **Websites** should be cited as (Suppl. website) in the general text and be made available with doi code (if possible) at the end of the article.
- **Videos** must not be larger than 30 MB to allow a swift technical response for viewing the video. Authors should consider whether a short video uniquely captures what text alone cannot capture for the understanding of a process or behavior under examination in the article. Supply an online link to the location of the video (e.g., YouTube).

Copyright law does not apply to *Fishery Bulletin,* which falls within the public domain. However, if an author reproduces any part of an article from *Fishery Bulletin*, reference to source is considered correct form (e.g., Source: Fish. Bull. 97:105).

Failure to follow these guidelines and failure to correspond with editors in a timely manner will delay publication of a manuscript.

Submission of manuscript

Submit manuscript online at the ScholarOne website. Commerce Department authors should submit papers under a completed NOAA Form 25-700. For further details on electronic submission, please contact the Associate Editor, Kathryn Dennis, at

kathryn.dennis@noaa.gov

When requested, the text and tables should be submitted in Word format. Figures should be sent as separate PDF files (preferred), TIFF files, or JPG files. Send a copy of figures in the original software if conversion to any of these formats yields a degraded version of the figure.

Questions? If you have questions regarding these guidelines, please contact the Managing Editor, Sharyn Matriotti, at

sharyn.matriotti@noaa.gov

Questions regarding manuscripts under review should be addressed to Kathryn Dennis, Associate Editor.

Fishery Bulletin

Subscription form

Superintendent of Documents **Publications** Order Form

*5178

☐ YES, please send me the following publications:

____ Subscriptions to *Fishery Bulletin*
for $32.00 per year ($44.80 foreign)

The total cost of my order is $ _____ . Prices include regular domestic postage and handling and are subject to change.

_____
(Company or Personal Name) (Please type or print)

_____
(Additional address/attention line)

_____
(Street address)

_____
(City, State, ZIP Code)

_____
(Daytime phone including area code)

_____
(Purchase Order No.)

Charge your order. IT'S EASY!

VISA

MasterCard

Please Choose Method of Payment:

☐ Check payable to the Superintendent of Documents
☐ GPO Deposit Account ☐☐☐☐☐☐☐–☐
☐ VISA or MasterCard Account
☐☐☐☐☐☐☐☐☐☐☐☐☐☐☐☐
☐☐☐☐ (Credit card expiration date)

To fax your orders (202) 512-2104

_____
(Authorizing Signature)

Mail to: Superintendent of Documents
P.O. Box 979050, St. Louis, Missouri 63197
Tel. no. (U.S. callers): 866-512-1800
Tel. no. (International callers): 1-202-512-1800

Thank you for your order!

Also available online at
http://bookstore.gpo.gov/actions/GetPublication.do?stocknumber=703-023-00000-2
email: ContactCenter@gpo.gov